

Some pages of this thesis may have been removed for copyright restrictions.

If you have discovered material in Aston Research Explorer which is unlawful e.g. breaches copyright, (either yours or that of a third party) or any other law, including but not limited to those relating to patent, trademark, confidentiality, data protection, obscenity, defamation, libel, then please read our [Takedown policy](#) and contact the service immediately (openaccess@aston.ac.uk)

Aston University

16th August, 2017

Engineering yeast for G protein-coupled receptor functional studies: pharmacological characterisation of adrenergic receptors

Lina Mikaliunaite

Doctor of Philosophy

© Lina Mikaliunaite 2017 asserts her moral right to be identified as the author of this thesis.

This copy of the thesis has been supplied on condition that anyone who consults it is understood to recognise that its copyright rests with its author and that no quotation from the thesis and no information derived from it may be published without appropriate permission or acknowledgement.

Abstract

G protein-coupled receptors (GPCRs) are membrane proteins responsible for myriad physiological functions. Around a third of drugs on the market already target GPCRs. However, the emphasis on developing GPCR assays to screen compound libraries for potential GPCR-interacting drugs is still very strong. One such cell-based assay was developed at GlaxoSmithKline (GSK) by Dowell and Brown [1, 2]. This assay uses a cheap, rapidly growing unicellular organism – baker's yeast. In this organism the pheromone signalling pathway is one of only two GPCR-activated pathways. Yeast engineering done at GSK in 2000 produced MMY strains lacking the native yeast Ste2 GPCR and other key proteins, together with the integration of chimeric yeast/mammalian G protein alpha subunits thereby allowing mammalian GPCRs to couple to the yeast signalling machinery [2]. A significant limitation of the assay has been that some pharmacologically-important receptors cannot be tested using the current MMY strains and protocols. The aim of this study was to optimise the functional expression of adrenergic receptors that had previously been difficult to express and/or characterise pharmacologically in these yeast strains. The work described here examined both the MMY strains themselves and the expression constructs, asking the question how these features might contribute to a robust assay readout for two GPCR classes; the α - and β -adrenoceptors. The origin of the instability of some of the MMY strains was traced to the experimental strategy originally used to delete the *URA3* marker gene and a stable MMY strain was generated as a proof-of-principle. A systematic comparison between different expression vector designs identified that the addition of the mating factor α (MF- α) leader sequence to the amino-terminus of the β_1 - and β_2 -adrenoceptors is required to produce a pharmacological response in the yeast assay. Notably, this permitted reproducible functional expression of the β_2 -adrenoceptor, which had not been previously possible at GSK, despite being published in the scientific literature. These improvements allowed for the pharmacological characterisation of a panel of interacting β -AR ligands, yielding data that has shed new light on ligand bias. Finally, a cholesterol-expressing yeast engineering strategy was designed to specifically investigate the role of plasma membrane composition in GPCR functional studies. The insights gained from the experiments described in this thesis should allow for improved testing of other GPCRs in the drug development pipeline.

I would like to dedicate this thesis to my husband Arturas. For believing in me, for supporting me from the beginning – I am forever grateful.

Thank you.

Acknowledgements

I would first of all like to thank my supervisors Professor Roslyn Bill and Dr Simon Dowell. For your support, for encouragement, for opportunities to learn and develop – I am very grateful. I would also like to thank past and present group members at Aston University – Dr Stephanie Cartwright, Dr Michelle Clare, Dr Marvin Dilworth, Dr Pinar Karagoz, Ravneet Kaur, Anjana Patel, and Dr Sarah Routledge. Thank you for your moral and practical support – I have truly enjoyed working with all of you. I would like to thank Simran Lallie and Hannah Jones who were brave enough to join my bench side as my placement students. I would also like to thank Dr John Simms and Dr Andrew Brown for helping me navigate the uncharted waters of pharmacology.

Lastly, I would like to thank BBSRC and GlaxoSmithKline for funding this project and giving me the opportunity to experience working in industry. Thank you Dr Simon Dowell, my supervisor at GSK, for making the necessary arrangements and supporting me on my placement.

Table of Contents

Abstract	1
Acknowledgements.....	3
Abbreviations	7
List of Figures and Tables	9
Chapter 1 - Introduction	12
1.1. G protein coupled receptors	12
1.1.1. The structure.....	12
1.1.2. Mechanism of function	14
1.2. An overview of approaches to study GPCRs	14
1.2.1. Radioligand binding assays	15
1.2.2. Second messenger assays	15
1.3. Hijacking the yeast pheromone pathway	17
1.3.1. General introduction to <i>Saccharomyces cerevisiae</i> mating.....	17
1.3.2. Signal initiation.....	19
1.3.3. Downstream signalling cascade and their effectors	19
1.3.4. Down-regulation of the pheromone pathway.....	20
1.3.5. Physiological response to pheromone stimulation.....	21
1.3.6. Summary of MMY strains.....	22
1.4. GPCR research in yeast	22
1.4.1. General introduction.....	22
1.4.2. An overview of GPCR expression optimisation in yeast	23
1.4.3. The beginning of GPCR research in yeast	24
1.4.4. Notable functional GPCR studies in yeast.....	24
1.4.5. Lipid role in GPCR functionality – the future direction	25
1.5. The signalling of β -adrenoceptors	27
1.5.1. Catecholamine binding site.....	28
1.5.2. Transitioning between the inactive (R) and active (R*) states and coupling to $G\alpha_s$	30
1.6. Project aims and objectives	31
Chapter 2 – Materials and Methods	33
2.1. Materials	33
2.1.1. Yeast strains, growth and maintenance.....	33
2.1.2. FD-glu GPCR functional assay medium, reagents, ligands.....	36
2.1.3. Molecular biology.....	40
2.1.4. Western blot reagents and consumables	47
2.2. Methods.....	50
2.2.1. Yeast strains, growth and maintenance.....	50
2.2.2. FD-glu GPCR assay set-up and conditions.....	52

2.2.3.	Data collection and analysis.....	53
2.2.4.	Molecular Biology	54
2.2.5.	Membrane isolation and western blotting procedures.....	61
Chapter 3 –	Optimisation of the yeast functional GPCR assay	64
3.1.	Introduction	64
3.2.	Effects of 3-amino triazole on reporter signal strength.....	65
3.3.	Substrate concentration effects on the signal	69
3.4.	Instrument-dependent signal dynamic range.....	70
3.5.	Experimental variation.....	73
3.6.	Compound screening on α_{2A} -AR and α_{2B} -AR in yeast.....	74
3.7.	The parameter-dependent variations of the functional GPCR assay in yeast – what to expect and how to interpret the data.....	76
Chapter 4 –	The functional expression of adrenoceptors β_1 and β_2 in MMY strains	78
4.1.	Introduction	78
4.2.	Episomal p426GPD plasmids for the expression of β_1 -AR and β_2 -AR	79
4.2.1.	The construction of p426GPD-(MF α /Ste2)-ADRB1 and p426GPD-(MF α /Ste2)-ADRB2.....	79
4.2.2.	The transformation of MMY 12-28 strains with p426GPD episomal plasmids.....	82
4.2.3.	Overview of the pre-screening strategy for the identification of functional colonies ..	84
4.2.4.	Episomal plasmid screening results	86
4.2.5.	Summary of episomal plasmid screening results.....	90
4.3.	Integrative p306GPD plasmids for the expression of β_1 -AR and β_2 -AR	91
4.3.1.	The construction of the p306GPD-(MF α)-ADRB1 and p306GPD-(MF α)-ADRB2 plasmids	91
4.3.2.	The transformation of MMY12-24 yeast with the p306GPD plasmids and the functional colony selection	93
4.3.3.	Summary of integrated plasmid screening results	97
4.4.	Western blot analysis of protein expression patterns of the β_1 -AR and β_2 -AR	97
4.4.1.	β_1 -AR expression in the MMY15 (G α_s) strain	98
4.4.2.	β_2 -AR expression in the MMY15 (G α_s) strain	101
4.4.3.	Summary of western blot analysis of β_1 -AR and β_2 -AR expression in MMY yeast	104
Chapter 5 –	The pharmacological characterisation of adrenoceptors β_1 and β_2 in yeast.....	105
5.1.	Introduction	105
5.2.	Ligand selection and experimental set-up.....	105
5.3.	Pharmacological characterisation of the β_1 -AR in MMY strains	107
5.3.1.	Agonist assay.....	107
5.3.2.	Antagonist assay	111
5.4.	Pharmacological characterisation of the β_2 -AR in MMY strains	115
5.4.1.	Agonist assay.....	115

5.4.2. Antagonist assay	119
5.5. Comparison of signalling pathways for β_1 -AR and β_2 -AR in yeast	124
5.6. Comparison of the functional yeast assay for GPCRs against other assays in a high-throughput screening setting.....	127
5.7. Chapter summary.....	131
Chapter 6 – The engineering of <i>Saccharomyces cerevisiae</i> strains	132
6.1. Introduction	132
6.2. The engineering of <i>ura3</i> Δ MMY11 strain.....	133
6.2.1. <i>Saccharomyces cerevisiae</i> strain MMY12-28 counter-selection with 5-FOA.....	133
6.2.2. Design of genomic PCR test for the detection of tr <i>URA3</i> and fl <i>URA3</i> genotypes	136
6.2.3. The deletion of the full length <i>URA3</i> gene.....	137
6.3. The engineering of cholesterol biosynthesis pathway in <i>S. cerevisiae</i> MMY strains.....	138
6.3.1. The design of <i>erg5</i> Δ ::DHCR24 and <i>erg6</i> Δ ::DHCR7 integration cassettes.....	140
6.3.2. The engineering of pAUR135- <i>erg5</i> -DHCR24- <i>erg5-cys1t</i> and pAUR135- <i>erg6</i> -DHCR7- <i>erg6-cys1t</i> plasmids.....	142
6.3.3. The selection of the MMY11 <i>erg5</i> Δ ::DHCR24 strain	148
6.3.4. Future work.....	150
Chapter 7 – Discussion and future work.....	151
7.1. MMY yeast are a powerful tool for GPCR drug discovery.....	151
7.2. A comparison of episomal and integrative plasmid functional expression systems – which is better?.....	152
7.3. Protein expression level and functional expression of the β -adrenoceptors.....	153
7.4. Fixing the uracil selection marker deletion in the MMY yeast strains.....	154
7.5. Pharmacology of β_1 -AR and β_2 -AR – the Devil is in the (structural) details	156
7.6. Thesis summary.....	157
References.....	158
Appendix A – G α protein sequence alignment	163
Appendix B – Vector and plasmid maps	165
.....	172
Appendix C – compound structures.....	176
Appendix D – supplementary compound profiling data.....	182
.....	187
Appendix E – Assay correlation data.....	188
Appendix F – Publications arising from this thesis.....	190

Abbreviations

3-AT – 3-amino triazole

5-FOA – 5-fluoroorotic acid

AbA – aureobasidin A

AC – adenylate cyclase

ADRA2A – gene for adrenoceptor α_{2A}

ADRA2B – gene for adrenoceptor α_{2B}

ADRB1 – gene for adrenoceptor β_1

ADRB2 – gene for adrenoceptor β_2

AUR1C – resistance to aureobasidin A

ATCC – American type culture collection

β_1 -AR – adrenoceptor β_1

β_2 -AR – adrenoceptor β_2

BCA – bichinchonic acid

BSA – bovine serum albumin

bp – base pair

cAMP – cyclic adenosine monophosphate

CEN-ARS – centromere autonomously replicating sequence

chG α – chimeric G α subunit

CHO-K1 – Chinese hamster ovary cell line K1

DAG – 1,2-diacylglycerol

DMSO – dimethyl sulfoxide

EFC – enzyme fragment complementation

EDTA – ethylenediaminetetraacetic acid

ELISA – enzyme-linked immunosorbent assay

FD-glu – fluorescein di- β -D-glucopyranoside

GPCR – G protein-coupled receptor

GDP – guanosine diphosphate

GPD – glyceraldehyde-3-phosphate dehydrogenase

GRK – G protein-coupled receptor kinase

GSK – GlaxoSmithKline

GTP – guanosine triphosphate

HA – human influenza hemagglutinin

HEPES – 4-(2-hydroxyethyl)-1-piperazineethanesulfonic acid

HRP – horseradish peroxidase

IP3-DAG – inositol-1,4,5-triphosphate 1,2-diacylglycerol

IUPHAR – International Union of Basic and Clinical Pharmacology

LB – Luria Bertani (broth)

LBA – Luria Bertani ampicillin

LiAc – lithium acetate

MAPK – mitogen activated kinase

MCS – multiple cloning site

MFA α – mating factor α

NEB – New England Biolabs

PBS – phosphate buffered saline

PIC – protease inhibitor cocktail

PLC – phospholipase C

PCR – polymerase chain reaction

PEG – polyethylene glycol

PVDF – polyvinylidene difluoride

RFU – relative fluorescence units

RGS – regulator of G protein signalling

RT – room temperature

SEM – standard error of means

SDS – sodium dodecyl sulfate

SOB – super optimal broth

TAE – tris-acetate-EDTA

TE – tris-EDTA

YNB – yeast nitrogen base

YPD – yeast extract-peptone-dextrose (medium)

WHAUL – tryptophan (W), histidine (H), alanine (A), uracil (U), leucine (L)

List of Figures and Tables

Figures and table are presented sequentially within each chapter. Tables are highlighted in bold text.

Chapter 1

Figure 1.1 The general structure of a G protein-coupled receptor

Figure 1.2 Working principles of commercially available cAMP assays

Figure 1.3 Schematic representation of yeast pheromone response pathway

Figure 1.4 Modified pheromone signalling pathway in MMY yeast strains.

Figure 1.5. The operational model developed by Black and colleagues.

Figure 1.6 Catecholamine binding pocket as shown in crystal structure of β_1 -AR.

Figure 1.7 C-terminal sequence alignment of different G α proteins including yeast Gpa1.

Chapter 2

Table 2.1 The summary of MMY yeast strain genotypes

Table 2.2 The panel of adrenoceptors α_2A and α_2B interacting compounds used in Chapter 3 experiments

Table 2.3 The panel of adrenoceptors β_1 and β_2 interacting compounds used in Chapter 6 experiments.

Table 2.4 The list of enzymes used for molecular biology

Figure 2.5 GeneRuler 1kb DNA ladder.

Table 2.6 List of primers

Table 2.7 List of vectors

Table 2.8 The list of PCR protocols

Chapter 3

Figure 3.1 The workflow of the yeast functional GPCR assay set up.

Figure 3.2 The inhibition of His3p by 3-amino triazole.

Figure 3.3 Effects of 3-AT on α_{2B} -AR receptor expressed in YIG153.

Figure 3.4 Effects of 3-AT on α_{2A} -AR receptor expressing YIG152.

Figure 3.5 Effects of increasing FD-glu substrate on the signal development and pEC₅₀ of brimonidine.

Figure 3.6 Variation of RFUs generated on different instruments in YIG152 strain.

Figure 3.7 Variation of RFUs generated on different instruments in YIG153 strain.

Figure 3.8 Experimental variation in β_1 -AR and β_2 -AR expressing strains.

Figure 3.9 Compound profiling on α_{2A} and α_{2B} receptors.

Chapter 4

Figure 4.1 Construction of p426GPD-ADRB1 and p426GPD-ADRB2.

Figure 4.2 Construction of the p426GPD-MF α -ADRB1 and p426GPD-MF α -ADRB2.

Figure 4.3 Construction of the p426GPD-Ste2L-ADRB1 and p426GPD-Ste2L-ADRB2.

Figure 4.4 MMY yeast transformation result.

Figure 4.5 The overview of colony selection strategy for the identification of functional expression of β_1 -AR and β_2 -AR in p426GPD vectors.

Figure 4.6 An example of a pre-screening experiment.

Table 4.7 Distribution of colonies pre-selected as potentially functional according to the strain and plasmid construct.

Table 4.8 Summary of episomal colony screening results.

Figure 4.9 The β_1 -AR expressing MMY strain responses to the isoprenaline stimulation.

Figure 4.10 The β_2 -AR expressing MMY strain responses to isoprenaline stimulation.

Figure 4.11 Construction of the p306GPD-ADRB1 and p306GPD-ADRB2.

Figure 4.12 Construction of the p306GPD-MF α -ADRB1 and p306GPD-MF α -ADRB2.

Figure 4.13 Transformation of the MMY15 with p306GPD vectors.

Figure 4.14. The β_1 -AR expressing MMY strain responses to the isoprenaline stimulation.

Figure 4.15. The β_2 -AR expressing MMY strain responses to the isoprenaline stimulation.

Figure 4.16 β_1 -AR protein expression in p426GPD vectors comparison with the functional data obtained from the FD-glu assay.

Figure 4.17 β_1 -AR protein expression in p306GPD vectors comparison with the functional data obtained from the FD-glu assay.

Figure 4.18 Transformation of MMY15 with p426GPD vectors.

Figure 4.19 β_2 -AR protein expression in p306GPD vectors comparison with the functional FD-glu assay results.

Figure 4.20 β_2 -AR protein expression in p306GPD vectors comparison with the functional FD-glu assay results.

Chapter 5

Table 5.1 List of β_1 -AR and β_2 -AR agonists and antagonists used in this study.

Figure 5.2 The summary of agonist assay results in β_1 -AR expressing MMY strains.

Table 5.3 Summary of pEC₅₀ and E_{max} values of β_1 -AR agonist assay in MMY strains.

Figure 5.4 Selected compound response on the β_1 -AR presented in all strains.

Figure 5.5 The summary of antagonist assay results in β_1 -AR expressing MMY strains.

Table 5.6 Summary of pIC₅₀ and E_{max} values of β_1 -AR antagonist assay in MMY strains.

Figure 5.7 Selected compound antagonism on the β_1 -AR presented in all strains.

Figure 5.8 The summary of agonist assay results in β_2 -AR expressing MMY strains.

Table 5.9 Summary of pEC_{50} and E_{max} values of β_1 -AR agonist assay in MMY strains.

Figure 5.10 Selected agonist responses on β_2 -AR expressing strains.

Figure 5.11 The summary of antagonist assay results in β_2 -AR expressing MMY strains.

Table 5.12 Summary of pIC_{50} and E_{max} values of β_2 -AR antagonist assay in MMY strains.

Figure 5.13 Selected antagonist responses on β_2 -AR expressing strains.

Figure 5.14 Summary of xamoterol (22) pharmacology on β -adrenoceptors in yeast.

Figure 5.15 Correlation plots of pEC_{50} and pIC_{50} values between those obtained in $G\alpha_S$ strain and other $chG\alpha$ strains.

Table 5.16 Pearson's correlation analysis of pEC_{50} and pIC_{50} values.

Figure 5.17 Yeast $G\alpha_S$ agonist ant antagonist assay correlation comparison with various cAMP assays in CHO cell background.

Table 5.18 Yeast $G\alpha_S$ agonist ant antagonist assay comparison with various cAMP assays in CHO cell background – correlation parameter analysis.

Table 5.19 Correlation matrix analysis of CHO cAMP assay produced pEC_{50} and pIC_{50} on β_1 -AR and β_2 -AR collected from GSK database.

Chapter 6

Table 6.1 Summary of 5-FOA selection results.

Figure 6.2 Selection for Ura⁻ phenotype with 5-FOA.

Figure 6.3 Optimisation of primers for *URA3* detection.

Figure 6.4 The detection of *fjURA3Δ* by genomic PCR.

Figure 6.5 The summary of key enzymes and their substrates for shifting the sterol synthesis from ergosterol to cholesterol in yeast.

Figure 6.6 An overview of the strategy for cholesterol pathway engineering in MMY yeast.

Figure 6.7 The schematic representation of the construction of p426GPD-ERG5.

Figure 6.8 The restriction digestion analysis of p426GPD-ERG5 and p426-ERG6 vectors.

Figure 6.9 Schematic representation of the 'gap repair' cloning of the p426GPD-erg5-DHCR24-cys1t-erg5 and p426-erg6-DHCR7-cys1t-erg6 vectors.

Figure 6.10 The selection of successfully ligated p426GPD-erg5-DHCR24-cys1t-erg5.

Figure 6.11 The selection of successfully ligated p426-erg6-DHCR7-cys1t-erg6.

Figure 6.12 The selection of successfully ligated pAUR135-erg5-DHCR24-cys1t-erg5 and pAUR135-erg6-DHCR7-cys1t-erg6.

Figure 6.13 PCR screening of the integration of pAUR135-erg5-DHCR24-cys1t-erg5 into MMY11_ura3Δ.

Figure 6.14 The selection of MMY11 erg5Δ::DHCR24 colonies.

Chapter 1 - Introduction

This project examines the use of a yeast-based assay system to study the functional expression of G protein-coupled receptors (GPCRs) for use in the drug discovery pipeline. The focus of the project was adrenoceptors, some of which had previously been difficult to characterise pharmacologically in this yeast system. The yeast strains used are named the MMY strains developed in 2000 at GlaxoSmithKline [2]. The work described in this thesis examines the MMY strains themselves and the GPCRs expression constructs, asking the question how an improved understanding of both would contribute to a robust assay readout for adrenoceptors. In this introduction, the importance of GPCR research to the drug discovery and the development of the MMY strains is described, following by a discussion of the limitations of the MMY-based assay and the consequent aims and objectives of the thesis project.

1.1. G protein coupled receptors

The G protein-coupled receptor family – the largest receptor family is comprised of around 800 members, a large proportion of which are of significant physiological and pharmacological importance. These membrane proteins are involved in a myriad of physiological functions in humans and are implicated in many diseases ranging from diabetes, cancer, cardiovascular diseases, inflammatory diseases such as asthma, hormonal disorders, narcotic substance abuse, and many others. Not surprisingly, around a third of all drugs on the market target G protein-coupled receptors (GPCRs). Despite this, the mechanism of majority of these drugs are poorly understood. For this reason a great effort is focused on understanding the relationship between the receptors' structure, downstream signalling effects on the cell's function and therapeutic effect. This subchapter will introduce the basic concepts of GPCRs and their mechanism of function. More detail on adrenergic-specific function is described in section 1.5.

1.1.1. The structure

Direct structural data on GPCRs were not available until 2000 when the first eukaryotic (bovine) GPCR crystal structure of the light sensing receptor rhodopsin was published [3]. The second high resolution structure of a GPCR was not published until seven years later and was a result of extensive crystal growth optimisation trials and sophisticated protein engineering which allowed Kobilka and colleagues to determine the β_2 adrenoceptor structure at 2.4 Å resolution [4]. However, the isolation and sequencing of rhodopsin and the β_2 adrenoceptor back in the mid-1980s had already hinted that the

clusters of hydrophobic amino acids made up the seven transmembrane helices and was then believed to be a common feature of many membrane proteins [5].

Our current knowledge confirms that the GPCRs are large transmembrane receptors composed of seven alpha-helices, an extracellular N-terminus and three extracellular loops, a cytosolic or intracellular C-terminus and three intracellular loops (**Figure 1.1**) [6]. The extracellular domain is facing outside of the cell and is often the site for ligand binding, especially for larger molecules [6]. The

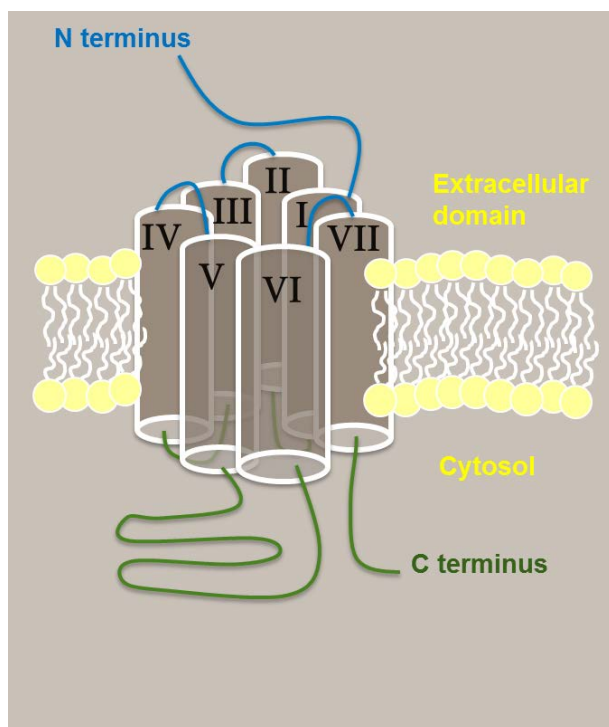


Figure 1.1 The general structure of a G protein-coupled receptor. The large protein is comprised of seven membrane-spanning helices, 3 extracellular loops together with an extracellular N terminus, and 3 intracellular loops and the C terminus in the cytosol. The intracellular domain binds to G proteins, arrestins and other proteins in the case of a mammalian GPCRs. The endogenous or synthetic ligands, neurotransmitters or hormones bind at the extracellular domain.

intracellular domain, and the third loop in particular, are important for receptor coupling to the G protein complex $G\alpha\beta\gamma$ [6] and also for interaction with other proteins of mostly regulatory nature, such as GPCR kinases and arrestins [7].

The other important entity of the GPCR signalling mechanism is the G protein complex composed of sub-units $G\alpha$, $G\beta$, and $G\gamma$. When the receptor is inactive, the G protein trimer sits anchored to the membrane through a fatty acid chain and only couples to the receptor when it is activated. A more detailed mechanism of activation and signalling is explained in the next section and section 1.5 in a context of β -adrenoceptors. The specificity of G protein coupling to a receptor and activation of different effectors is determined by the $G\alpha$ subtype, of which there are four main classes – G_s , G_i , $G_{q/11}$, and G_{12} . The main effectors of $G\alpha_s$ and $G\beta\gamma$ are adenylyate cyclase (**AC**), phospholipase C (**PLC**), ion channels, Rho A/Rho kinase, and MAP kinase. The $G\alpha$ sub-unit can either activate or inhibit them.

1.1.2. Mechanism of function

GPCRs are important in human physiology because they allow the cell to respond to signals coming from the external environment and induce physiological changes in response. These receptors achieve this by translating that signal into an internal message, often amplifying it. Upon the conformational changes, caused by an external stimulus, GPCRs couple to the G protein trimer in turn causing the α subunit to exchange its bound GDP into GTP [7]. This exchange causes further conformational changes on the $G\alpha$ subunit which dissociates from the $G\beta\gamma$ subunit. Both entities then associate with their target proteins, which are mentioned in the previous section, activating them and generating further amplification of the message via second messengers, such as cyclic adenosine monophosphate (cAMP), diacylglycerol (DAG), and inositol-1,4,5-trisphosphate (IP_3) [6, 7]. The $G\alpha$ association with its target also causes hydrolysis of GTP into GDP, inactivating $G\alpha$. Inactivated $G\alpha$ re-associates with $G\beta\gamma$ [6]. The external signal that is capable of inducing conformational changes can be a neurotransmitter, hormone, neuropeptide, or other small molecules such as purines, prostanoids, cannabinoids and others [6]. Conformation changes can also be induced by protease mediated cleavage of the N terminus or conformational changes of covalently bound ligand, such as retinal bound to rhodopsin, one of the earliest models of GPCR structure [3, 6].

1.2. An overview of approaches to study GPCRs

The yeast chimeric $G\alpha$ proteins allow the investigation of different mammalian GPCR coupling to $G\alpha$ proteins in the single cell background, with the same output – the measurement of growth, and presumably the same number of receptors. However, in mammalian cells the $G\alpha$ protein coupling dictate which signalling pathways are modulated and therefore assessment is made by monitoring the change in the effector protein activity upregulation or downregulation. The effectors often produce second messengers to amplify the signal. For this reason the outputs are different too, ranging from calcium or cyclic AMP quantification to cytoskeleton re-arrangement. This sub-chapter will review these assays because it is important to understand how these assays work in order to explain any discrepancies in pharmacological parameters generated in mammalian cell assays vs the yeast assay data.

1.2.1. Radioligand binding assays

The radio-labelled ligand binding assays were developed based on work described Yalow and Berson in 1959 [8] and are used for assessing parameters such as affinity of a ligand to a receptor, receptor density in tissue, cellular or membrane preparations [9]. The assay involves the binding of a radio-labelled compound to GPCR receptors. Affinities of ligands can be compared by performing a competition binding assay where a fixed concentration of a known radioligand is applied along with increasing concentrations of an unlabelled ligand. The non-specific binding has to be determined (using a competitive unlabelled ligand at high concentrations), as the ligand will bind to other sites within membrane and assay tubes [9]. The common problem with this assay is that often agonist binding to GPCRs will display biphasic curves that do not fit theoretical competition binding curve model with a Hill coefficient of unity. To overcome this, GTP can be added to stabilise receptor conformation and in turn agonist's affinity to the receptor [9]. However, GTP will lock the $G\alpha$ subunit in the active conformation, which has low affinity for the receptor. The agonist has a higher affinity for the $G\alpha$ -bound (inactive) receptor, and therefore adding GTP can diminish the signal for the agonist assay. Allosteric ligands also potentially pose a problem to a lot of GPCR work, as they are able to bind to other sites and make a ternary complex with a competitor ligand. The radio-labelled ligand assays require optimisation of assay incubation time and temperature, buffer composition, as well as cell type-dependent culturing and receptor expression conditions. The radio-isotope label has been increasingly replaced by a fluorescent label as it is much safer [10]. However, it does pose some issues such as: a) the adaptability of the fluorescent tag to a smaller molecules without affecting its pharmacological properties; b) determining binding-specific fluorescence from background and unspecific binding fluorescence; c) fluorophore's sensitivity to pH and other environment properties.

Although binding and competitive binding assays are fairly old techniques and do not give information about receptor interaction with the signalling pathways, nor there is a linear relationship between binding saturation and maximum cellular response, the techniques are still widely used especially determining whether the protein is folded when expressed in recombinant production host and for quantification of total receptor level (expressed as saturation of binding sites) [11-13].

1.2.2. Second messenger assays

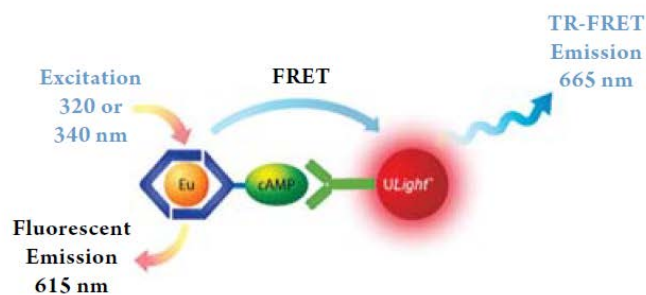
Another type of GPCR assay uses the second messenger, generated by GPCR activation events, as a functional measure of ligand efficacy on the receptor. Upregulation or downregulation of cyclic adenosine monophosphate (cAMP), inositol trisphosphate (IP_3), calcium ions (Ca^{2+}), or mitogen-activated protein kinases (MAPKs) depend on the subtype of $G\alpha$ that is coupled to the activated

receptor, therefore, unlike in yeast, $G\alpha$ is the main determinant of which second messenger is regulated [14].

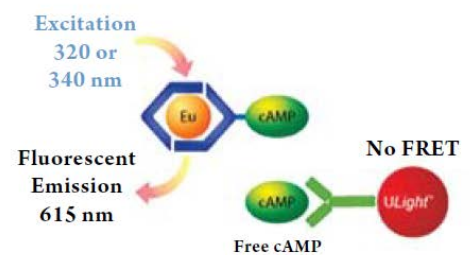
There are several ways in which changes in second messenger can be determined. For example, cAMP can be measured by competitive binding between radiolabelled cAMP and cellular cAMP binding in immunoassays that report quantities of bound cAMP by inversely proportional colorimetric or fluorescent change [14]. Several commercial assays are available for measuring cAMP in a cell lysate, for example Lance and AlphaScreen (Perkin Elmer) which are also based on competitive binding of the cellular molecule with a fluorophore-conjugated or biotinylated version of that molecule (cAMP or IP_3) and measurement of FRET (**Figure 1.2 [A]**) [15]. Another method for detection of cAMP uses enzyme

A

In the absence of free cAMP

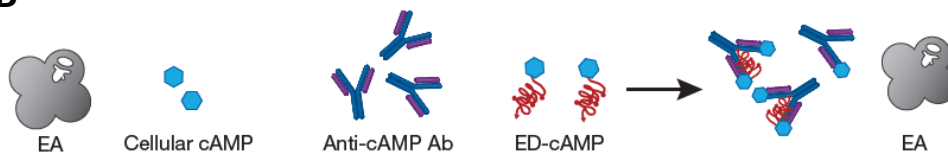


In the presence of free cAMP



B

Low Levels of Cellular cAMP



High Levels of Cellular cAMP

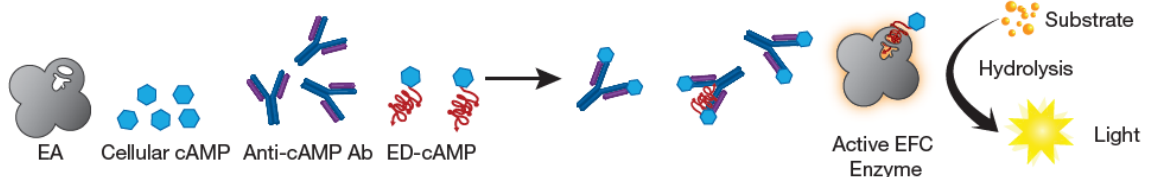


Figure 1.2 Working principles of commercially available cAMP assays. The cAMP second messenger is measured competitive binding between cellular cAMP and engineered cAMP to either contain a fluorophore **[A]** or an enzyme fragment **[B]**. The later technique requires engineered cell lines but can be measured in whole cells. The diagrams were taken from PerkinElmer and DiscoverX product literature [14, 15].

fragment complementation technology where cAMP is labelled with a fragment enzyme which competes with cellular unlabelled cAMP and under high cellular cAMP produces a chemiluminescence signal (**Figure 1.2 [B]**) [16].

Calcium ions are measured by either UV light based ratiometric indicator techniques, or visible light fluorescence indicators. The activated ERK1/2, which is a MAPK, can result from $G\beta\gamma$ signalling as well

as $G_{i/o}$ and G_s , making it a useful indicator when a particular $G\alpha$ is unknown or when wider coverage of receptors or agonists is desired. However, ERK1/2 can also be activated by other non-GPCR regulated pathways. This can be tested by applying pertussis toxin which specifically blocks $G\alpha_i$ and has no effect on ERK1/2 activation by other pathways. ERK1/2 can be detected using conventional protein detection techniques such as Western Blotting or ELISA as specific antibodies are available commercially [14].

The quantification of second messenger assays are attractive because they measure physiological response in the cell and can inform on the potency and efficacy of the drug. The second messenger assays can also be adapted for larger automated screening studies. However, they should be used in conjunction with drug binding studies, because functional assays do not inform us on the affinity of the drug. All the mentioned parameters are important in determining a drug's suitability for clinical application.

1.3. Hijacking the yeast pheromone pathway

Yeast as a single-celled organism is very independent and unlike mammalian cells does not have a great need for cell-to-cell communication. The exception to this is the pheromone mating pathway. Together with the Gpr1-mediated glucose sensing pathway these two pathways are the only two GPCR signalling pathways known in yeast. The pheromone pathway has been the focus of extensive genetic engineering with the aim of producing a tool for functional studies of human GPCRs. This pathway was discovered and characterised in 1980s and is unique to pheromone signalling, unlike the glucose sensing pathway, which is a more complex process in yeast and therefore less amenable to functional pathway engineering (both reviewed in [17]).

This review will focus on different stages of pheromone signalling through the native GPCRs Ste2/Ste3, outlining genetic modifications that were introduced in the generation of the MMY strains used in this project and their physiological effects on the host. The MMY strains have been used to assay human GPCRs; the limitations in their use are discussed later (**section 1.6**).

1.3.1. General introduction to *Saccharomyces cerevisiae* mating

Yeast *S. cerevisiae* are able to mate with opposing partners, of which there are two genotypes – $MATa$, which secrete a-pheromone (also called mating factor a), and $MAT\alpha$, which secrete the α -pheromone (alternatively mating factor alpha) [18, 19]. The Ste2 receptor on the plasma membrane of $MATa$ cells is responsive to the α -pheromone (encoded by *MF(ALPHA)1* and *MF(ALPHA)2* genes) [20, 21]; similarly, $MAT\alpha$ is activated by the a-pheromone (*MFA1*, *MFA2*) [22, 23] binding to Ste3 [19]. As in

mammalian cells, the G protein complex is composed of three G proteins - $G\alpha$ (encoded by *GPA1*), $G\beta$ (*STE4*), and $G\gamma$ (*STE18*). These GPCR signalling mechanism components are unique in this organism

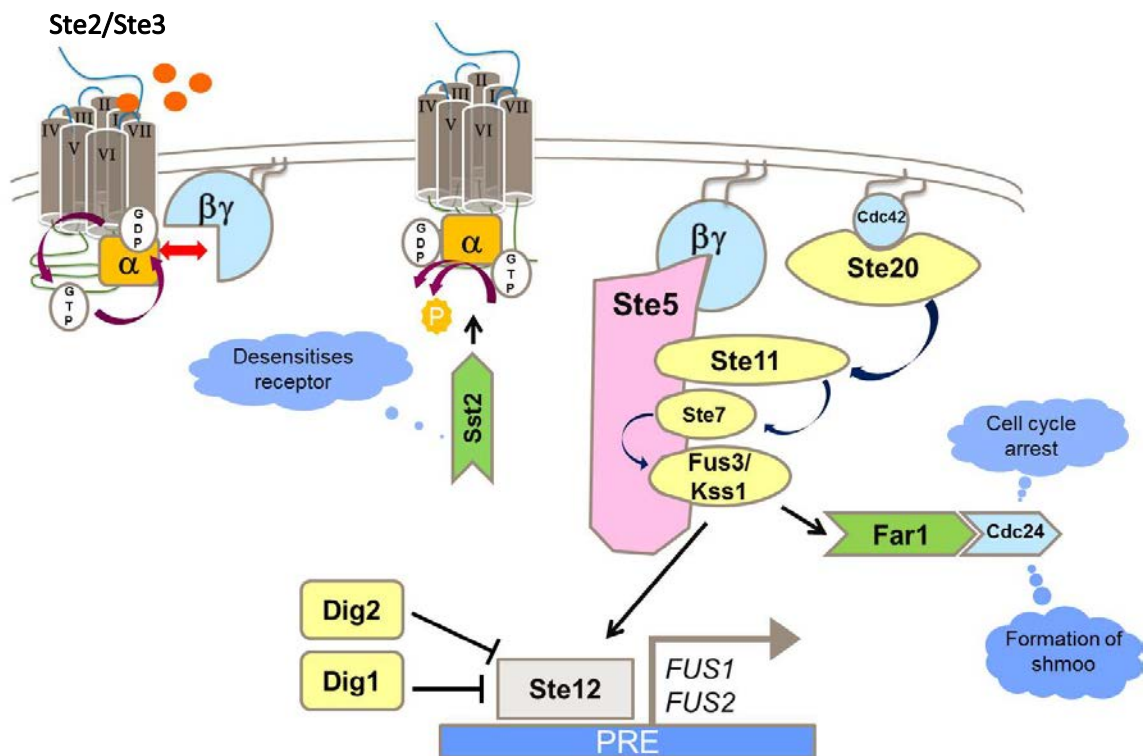


Figure 1.3 Schematic representation of yeast pheromone response pathway. Upon binding of the pheromone (orange circles) conformational changes in the receptor activate the $G\alpha$ subunit (encoded by *GPA1*) permitting GDP to be exchanged into GTP. This action releases the $G\beta\gamma$ subunit (encoded by *STE4* and *STE18*) which then activates target proteins Ste20 and Ste11, as a result bringing them in close proximity to each other. Ste11, anchored by Ste5 which acts as a scaffold for other mitogen-activated protein kinases, is then phosphorylated by Ste20. This initiates a further activation cascade of kinases Ste7, Fus3 and Kss1. The latter two activate their targets Far1 and Ste12 both of which have significant roles in preparing yeast cells for mating. Transcription factor Ste12 binds to the pheromone response element (PRE) on the promoters of mating genes, including *FUS1* and *FUS2*. Ste12 is inhibited by regulators Dig1 and Dig2. Negative feedback regulator Sst2 accelerates GTP hydrolysis on $G\alpha$ returning it into rest state and re-coupling with $G\beta\gamma$. The signalling is then terminated.

because no other pathways are activated via this route. It has therefore been a good pathway in which to study and dissect the principles of cell signalling [24]. Signalling through the pheromone pathway induces the expression of a number of mating genes and several physiological changes occur to prepare the cell to mate with a cell of opposing mating type. The mating generally occurs during stress conditions and increases the cell's chance of survival.

To prevent any spontaneous signalling or competition for the $G\alpha$ subunit with the mammalian GPCR, the native Ste2 was deleted in the MMY strains, which are the subject of this thesis.

1.3.2. Signal initiation

The sequences of both **a**-pheromone (YIIKGVFWDPAC) and α -pheromone (WHWLQLKPGQPMY) are available; however, because the latter is easier to purify or synthesise, it is usually the *MAT α* cells that are treated with the α -pheromone [24]. Upon binding of the pheromone to the receptor, the changes in receptor conformation allow the $G\alpha$ subunit to catalyse the exchange of GDP to GTP, which in turn releases the $G\beta\gamma$ subunit. Although the $G\alpha$ subunit has other than regulatory roles, the main signalling cascade in yeast continues via the $G\beta\gamma$ subunit.

Mammalian receptors generally cannot effectively couple to yeast G-proteins. A number of groups have worked on engineering modified variants of $G\alpha$ and $G\beta\gamma$ that would complete a functional signalling mechanism with mammalian GPCRs [1, 25]. The crystal structure of the G protein trimer mapped out a large N-terminal region crucial for $G\alpha$ - $G\beta\gamma$ binding as well as several other residues in the Switch region (where GDP is exchanged to GTP) that made also contacts, and finally the C-terminus which was important for receptor coupling, structured as an α helix [26]. The $G\alpha$ - $G\beta\gamma$ interaction needs to be fully functional because, if $G\alpha$ is unable to release $G\beta\gamma$, then signalling will not proceed even if the receptor is stimulated with an appropriate ligand. If association of the two entities is not adequate, a high background will result. The engineering work carried out at GSK revealed that the most efficient $G\alpha$ -Gpa1 chimeras were those in which 5 amino acids at the C-terminus of Gpa1 were replaced with 5 amino acids of the mammalian $G\alpha$ s [1]. Eleven chimeric $G\alpha$ -Gpa1p were constructed and introduced into MMY strains [1, 2].

1.3.3. Downstream signalling cascade and their effectors

The $G\gamma$ subunit anchors the dimer to the membrane via lipid groups while $G\beta$ binds to the effectors Ste5/Ste11 complex, Ste20, and Far1/Cdc24 complex.

The key effect of $G\beta\gamma$ disassociation is firstly the recruitment of the elements and kinases of the signalling cascade to the plasma membrane where they can take their action on one another (**Figure 1.3**). For example, the Far1/Cdc24 activates Cdc42, and in turn GTP-bound Cdc42 activates Ste20. The Ste20 protein is brought closer to Ste11 and is then able to phosphorylate and activate Ste11, which in turn activates other kinases Ste7, Kss1 and Fus3. The latter two kinases are thought to phosphorylate transcription factor Ste12 which regulate the transcription of mating genes by binding to the pheromone response elements within the promoter region and recruiting transcription machinery. Dig1 and Dig2 are involved in repression of Ste12 and are also phosphorylated by Fus3 when their suppression of Ste12 is not needed.

The activated Fus3 kinase acts on various targets within the cell and is important in many aspects of mating process. One of the processes, induced by Fus3 phosphorylation of Far1, induces the formation of the mating projection which changes the cell's morphology to a pear-like shaped structure called a 'shmoo'. Far1 also mediates cell cycle arrest in G1 phase [27]. Studies have shown that Far1, although required for the formation of 'shmoo' and induction of the cell arrest, is not essential in other pheromone signalling pathway branches which also involve Cdc24 [28]. Furthermore, deletion of *FAR1* was shown to increase agonist-induced signalling of mammalian GPCR SSTR2 expressed via the pheromone pathway in yeast [25]. *FAR1* was also deleted in the MMY yeast (**Figure 1.4**)

These processes are reviewed in detail in [24, 29].

1.3.4. Down-regulation of the pheromone pathway

Receptor internalisation and recycling has been known to occur in yeast for several decades, but only recently it was described how several α -arrestins down-regulate the pheromone receptor Ste2. The first α -arrestin, Ldb19, was shown to regulate basal Ste2 levels, most likely as part of the quality control of missfolded protein. Rod1 was shown to initiate the internalisation of pheromone-bound Ste2 receptor. An orthologue of Rod1 – Rog3 – inhibited pheromone signalling via Rsp5 independent manner; authors suggest that Rog3 might be physically blocking the Gpa1 ($G\alpha$ subunit) [30]. Rod1 is thought to be able to promote receptor endocytosis and destruction via ubiquitination by E3 ligase Rsp5 and Rsp-independent pathways [31]. Rsp5 function is inhibited by kinases Snf1 and Ypk1 which are upregulated during stress conditions to favour cell mating and enhance survival. It is thought that phosphorylation of Rod1 promotes its disassociation from the Ste2. Although no Ste2-Rod1 crystal structure is available, the α -arrestin Rod1 is proposed to interact with Ste2 in a similar way as visual and β -arrestins interact with their cognate receptors in mammalian cells [31].

Another mechanism for desensitisation of the pheromone signalling has been defined early in the pheromone research. The Sst2, a member of RGS family, accelerates GTP hydrolysis to GDP on $G\alpha$ subunit by approximately 20-fold, making the G protein trimer reform into the inactivated state, that way negatively regulating the signalling cascade. Sst2 is closely associated with Gpa1, therefore its proximity also provides rapid response to activation of Gpa1 to prevent its spontaneous disassociation from the $G\beta\gamma$ subunit. Deletion of Sst2 greatly enhances the stimulation intensity which is beneficial for measuring agonist activity on human GPCRs in the MMY yeast.

1.3.5. Physiological response to pheromone stimulation

As a result of Ste2 or Ste3 GPCR stimulation and pheromone-induced signalling pathways, the cell cycle is arrested in the G1 phase, the expression of around 200 genes, many of which have other roles outside pheromone signalling pathway, begins, cytoskeleton proteins and sphingolipid rafts rearrange to form mating projections towards the opposing pheromone mating partner [19, 32]. The cells conjugate at the projections, fuse their plasma membranes and later both nuclei and the diploid zygote cell forms. The cell will divide meiotically or mitotically depending on the environment conditions, as outlined earlier [18]. Once the changes are initiated there is no need for further pathway stimulation via the pheromone receptor which is desensitised as outlined in 1.3.4. The diploid cells that form do not respond to the pheromone at all.

The laboratory strains are usually a homogenous population of either mating type and therefore unable to form diploids; the MMY strains used in this project are *MATa*. Nevertheless, the cell cycle arrest and other physiological responses associated with preparation for mating are unfavourable for functional or structural studies of GPCRs and therefore the yeast has been engineered to grow continuously.

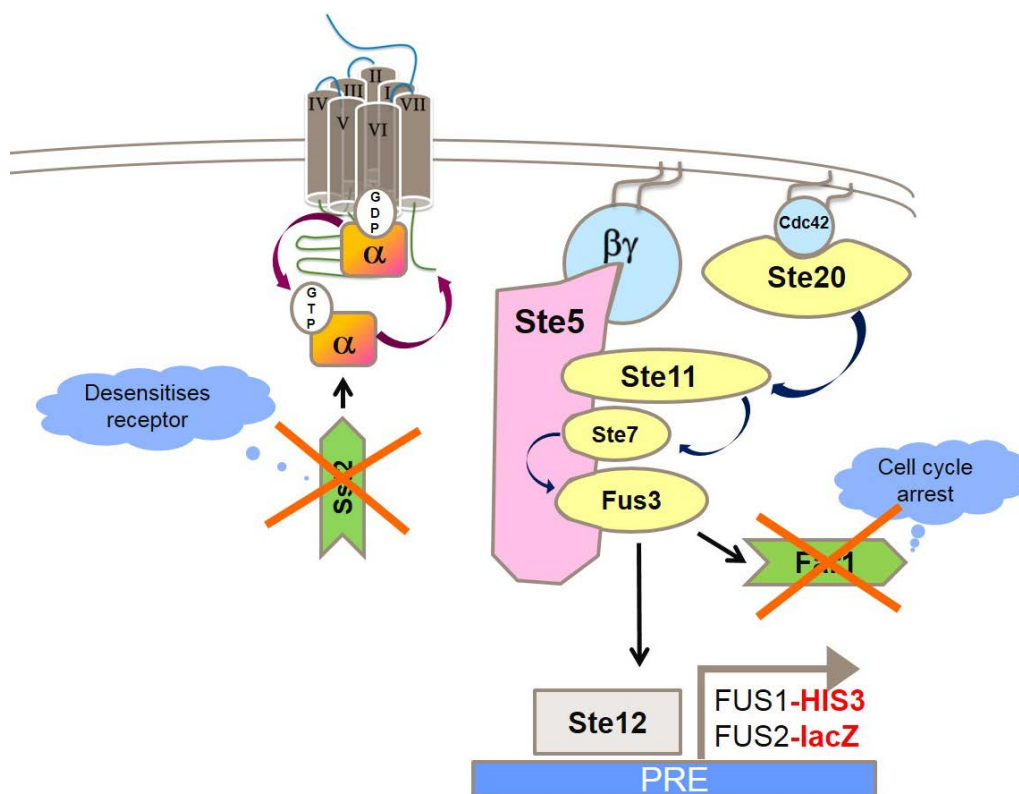


Figure 1.4 Modified pheromone signalling pathway in MMY yeast strains. The deletions of *SST2* and *FAR1* prevent the desensitisation of the pathway and cell cycle arrest in G1 phase as well as other morphological changes in the cell. Two reporter genes – *HIS3* and *lacZ* have been introduced under the regulation of *FUS1* and *FUS2* promoters respectively. Native *STE2* receptor gene has also been deleted to prevent any sequestration of Gαβγ trimer. The Gpa1 (a Gα) was also replaced by chimeric Gpa1-Gα proteins to allow coupling to human GPCRS.

1.3.6. Summary of MMY strains

In summary, *SST2*, *STE2* and *FAR1* genes have been deleted in the MMY strains to allow human GPCR-mediated pheromone signalling pathway continuous activation. Instead of inducing cell changes in preparation for mating, this signalling promotes cell growth in the absence of histidine or the expression of lacZ reporter gene under the *FUS2* promoter. Because of deletion of *SST2* the pathway is not rapidly desensitised which allows accumulation of the signal to detectable levels in a ligand concentration-dependent manner. The full genotypes of MMY strains can be found in **Table 2.1**.

These changes greatly improved the sensitivity of this functional coupling detection. However, central to this interaction is the engineered chimeric Gpa1-G α proteins, referred from now on as **chG α s**. As reviewed by Dowell and Brown [1] several Gpa1-human G α chimeric protein combinations have been described by different groups, together with the crystal structure of the G protein trimer mapping out the interactions between the receptor, G α protein to which it couples and G $\beta\gamma$ complex which activates the signalling cascade in yeast. The N-terminus helix of the G α appeared to have most contacts with the G $\beta\gamma$ dimer but other residues, such as S229 and A348 have been shown to be important too. Interestingly the replacement of only 5 amino acids at the Gpa1 C-terminus had conferred greater coupling efficiency to mammalian GPCRs when compared with a larger Gpa1 C-terminal sequence replacements with the mammalian G α protein sequences made by Kang *et al* [1, 2, 33]. These chG α proteins also demonstrated receptor coupling specificities comparable to those observed in mammalian G α proteins. A Gpa1 in which 5 C-terminal amino acids were deleted without replacement failed to couple to Ste2 or mammalian GPCR, indicating that these amino acids are essential for coupling to the receptor [2].

1.4. GPCR research in yeast

1.4.1. General introduction

The pheromone pathway has attracted a lot of research interest as outlined in the previous section. There are several reasons for this. Firstly, yeast has a reputation as a good model system to study basic cellular mechanisms such as cell cycle and was also attractive for studying cell signalling. The availability of research and genetic engineering tools has also contributed to this and so did the sequencing of *Saccharomyces cerevisiae* genome in 1996 [34].

Secondly, the increasing interest in GPCR research has prompted researchers to look for recombinant production hosts. To obtain naturally occurring GPCRs is difficult because of low abundance in native cells and sample heterogeneity, making it difficult to study receptor functionality or obtain crystal

structures. Yeast has been favoured in this respect due to easy and cheap growth, comparable to that of *Escherichia coli*, but with superior protein processing machinery and post-translational modification mechanisms. The trafficking of proteins is also more similar to mammalian cells in yeast. Bacteria lack these properties and therefore more complex proteins, such as GPCRs, are easier to express and study in yeast.

GPCR research, and membrane protein research in the wider context, has proven to be successful in yeast at large and continues to grow to this date. Several membrane structures have been solved using yeast – mainly *Saccharomyces cerevisiae* and *Pichia pastoris* – including Adenosine A_{2A} [35]. However, there are still many obstacles to overcome when expressing membrane proteins in recombinant protein production hosts, such as different glycosylation patterns [36]. The lipid role in membrane protein function has also gained more interest recently and with more tools available yeast has provided to be useful in this respect as well. This review will outline the technological developments relevant to GPCR research in yeast.

1.4.2. An overview of GPCR expression optimisation in yeast

Although yeast are very good at producing recombinant protein in high yield once the protein expression is optimised, the level of optimisation can vary greatly depending on the protein and other factors relating to the host. The first variable to be selected is usually the host itself. When the goal of the study is to obtain protein for structural studies, *Pichia pastoris* is usually the host of choice for its ability to grow to high densities and therefore higher production yields [37, 38]. However, *Saccharomyces cerevisiae* is better researched and adapted to genetic manipulation, and is often selected if the protein production in *P. pastoris* is troublesome. The functional GPCR studies which do not necessarily require high production yield are also carried out in *S. cerevisiae* because of genetic tools available. The construction of the MMY strains was no exception.

The strain background also has to be considered as there are myriad of wild-type and engineered strains available. The most popular backgrounds are various deletion strains. For example, if further engineering is desired, the deletions or mutations in selectable marker genes are advantageous; if protein degradation is an issue, a protease deficient strains are often chosen.

Several growth conditions can be optimised to increase production yield and quality, for example temperature and medium composition, such as addition of a ligand, DMSO or other supplements [38].

The need for a signal to direct the mammalian GPCR through the correct expression pathways and eventually trafficking to the plasma membrane was recognised early on. The reason behind using a yeast secretion signals was that the mammalian protein signals may not be recognised in a foreign

host. To use amino-terminal sequences of either Ste2 receptor or the mating factor α (MF α), also referred as the α pheromone, was an intuitive choice because the mammalian GPCR would be expected to go through the same translation pathway as the native GPCR. The amino-terminal sequence of the Ste2 receptor was used either as replacement or as a fusion protein [12, 39, 40]. However, Ste2 leader sequence did not always produced a clear advantage over a wild type construct [12]. The MF α from *S. cerevisiae*, on the other hand, is routinely used in *S. cerevisiae*, *P. pastoris* and *S. pombe* expression vector designs and are also included in standard commercial vectors such as pPICZ α .

1.4.3. The beginning of GPCR research in yeast

The first reported successful signalling of a mammalian GPCR in yeast was published in 1990 by King *et al.* [39]. In this study β_2 -AR was co-expressed with rat G α_5 subunit under strong promoters *GAL1* and *CUP1* respectively in *gpa1 Δ* cells and was shown to induce physiological changes associated with the pheromone signalling pathway activation upon agonist stimulation and blocked by an antagonist. The N-terminus of β_2 -AR was replaced with the Ste2 N-terminus to increase the receptor's expression to the plasma membrane (presumably) in *S. cerevisiae* and *S. pombe* [39, 40]. A patent was filed and granted based on this work [41], however some groups in academia and industry have struggled to replicate this work (GSK archive). The Strain 8c used in original work is not publicly available and the experiments in W301-1A strain failed to show dose-dependent response to isoprenaline. As shown in published work, the full length mammalian G α s do not provide enough contacts for efficient G α sequestration of yeast G $\beta\gamma$ (reviewed in [1]).

In summary, β_2 -AR has been expressed in *Saccharomyces cerevisiae* [39], *Schizosaccharomyces pombe* [40], and *Pichia pastoris* [42] but functional studies and application for high-throughput screening have not been successful.

1.4.4. Notable functional GPCR studies in yeast

Since the engineering of MMY strains and protocol development many GPCRs have been tested and compared to mammalian cell assays at GSK. The targets included well known GPCRs as well as orphan GPCRs. Examples include adenosine A $_{2A}$, cannabinoid receptors CB $_1$ and CB $_2$, Melatonin ML $_{1B}$, 5-HT $_{1A}$, 5-HT $_{1D}$, somatostatin sst $_2$ and sst $_5$, P2Y $_1$, P2Y $_2$, GPR55, FFA2, GPR41, GPR43 and many others [2, 43-45]. The stability of the yeast assay has been demonstrated on cannabinoid receptors which produced consistent pEC $_{50}$ values over several years [46].

In addition to the functional studies and screening programmes developed for GPCRs in yeast at GSK, several other groups used the engineered yeast for functional studies and have described several novel aspects of GPCR biology. The adenosine A₁ receptor was assessed for its coupling to three different signalling pathways when stimulated with two agonists R-PIA and VCP-189 [47]. The rat muscarinic M₃ receptor was shown to couple to 3 out of 5 strains tested, representing the coupling of the M₃ to G proteins consistent with coupling described in mammalian cells [48]. The actions of agonist carbachol and antagonists atropine, scopolamine, and pirenzepine were also assessed. The antagonists displayed a range of modulation on M₃ from inverse agonist, to neutral antagonist and a weak agonist in different MMY strains. The findings were confirmed in mammalian cell assays, albeit different ligand potencies. A novel action of the aforementioned ligands on chimeric G α_{12} strain has shown that the yeast system can be useful in determining signalling bias of ligands [48].

Other notable GPCR studies in engineered yeast has been published on family B GPCRs. For example GLP-1 receptor involved in diabetes was shown to have comparable pharmacology in yeast with that in mammalian cells. The yeast assay was used to show GLP-1 coupling to both G α_s and G α_{i1} . Furthermore, several natural and synthesised ligands indicated preferential induction of coupling to G α_{i1} with the exception of liraglutide, a GLP-1 mimetic, and also some allosteric modulators displayed reduced efficacy in the G α_{i1} strain. Both these observations provide more insight into mechanisms of adverse symptoms associated with the therapeutic use of these ligands [49]. Another case study involving CLR and accessory RAMP proteins showed bias towards coupling to certain G α strains depending on the bound ligand. This is an interesting example showing how yeast can further our understanding of pharmacology in complex systems where two recombinant proteins may need to be co-expressed [50].

1.4.5. Lipid role in GPCR functionality – the future direction

The first crystal structure of β_2 -AR has reported a presence of lipids, including cholesterol, packed in between the receptors [4]. However, long before the structural evidence emerged it was postulated that cholesterol plays a role in GPCR signalling. Cholesterol can have direct effects through binding to residues on the receptor and indirect effects by changing the properties of the surrounding membrane environment. For example cholesterol can change the thickness of lipid bilayer and affect lipid bilayer curvature stress [51, 52].

Overall, the cholesterol binding sites, and therefore conformational effects on the receptor, are receptor-dependent although they tend to be at the hydrophobic residues. The cholesterol

concentration-dependent effects have been shown on β_2 -AR and serotonin $1A$ receptor by simulations, affecting its dimerisation in terms of plasticity and flexibility of dimer conformation as well as stability of dimer interactions [51, 53]. In the absence of cholesterol the dimer conformation of serotonin $1A$ receptor was more rigid and changed with increasing cholesterol concentrations. However, in very high concentrations of cholesterol less stable dimer formations were observed. This has physiological relevance since cells in different tissues vary in their cholesterol content, contributing to an explanation of age and tissue-dependent responses to various ligands. Similar simulations also showed the effects of cholesterol on dimerisation of chemokine receptor type 4 (CXCR4). Cholesterol was required to form correct symmetry of the dimers for functional activation of CXCR4 [54]. Similarly the helices involved in dimer formation of β_2 -AR changed upon increasing concentrations of cholesterol. In the absence of cholesterol the dimers formed between helices H4 and H5 and shifted towards H1 and H2 formation upon addition of cholesterol, which is likely have an effect on $G\alpha_s$ protein coupling because pocket formed by H3, H5 and H6 is important in this interaction as discussed later [53, 55].

Yeast also produce a similar sterol called ergosterol which is important in membrane protein function. Some effects of sterol are also thought to be a result of direct binding to membrane proteins and some effects of plasma membrane plasticity are also postulated. This has been shown by genetically modifying sterol synthesis pathway in yeast to produce cholesterol or ergosterol intermediates [56-59]. This was achieved by deleting *ERG6* and *ERG5* genes of ergosterol biosynthesis pathway and replacement with mammalian genes *DHCR7* and *DHCR24*. These gene products were identified as key enzymes that saturate the sterol intermediates at positions C-7 and C-24 in cholesterol but not in ergosterol synthesis, while Erg5 introduces double bond at position C-22 and Erg6 adds methyl group at position C-24 in ergosterol synthesis therefore also competes with Dhcr24 for the substrate.

The Tat2, a high affinity tryptophan permease, Can1, another amino acid permease which plays role in canavanine resistance, and Pdr12, an ABC transporter which can efflux weak amino acids under toxic accumulation in the plasma, were the subjects of the first study by Souza *et al.* [56]. For Tat2, cholesterol was an adequate replacement of native sterol for function comparable nearly to that of wild type strain levels, but ergosterol intermediates in *erg5/6 Δ* strain were not. On the other hand Pdr12 and Can1 had a strict preference for ergosterol and lost their functions when the synthesis pathway was disrupted. The methyl group at C-24 appeared to be required for Pdr12 function. All proteins investigated were localised to the plasma membrane in the presence of cholesterol suggesting the trafficking was not affected [56].

The second study investigated the native yeast GPCR – the Ste2. It was found that MF α retained potency on this receptor in both WT and cholesterol producing strain. However, the efficacy of it was lower in the latter group – the maximum response at 10^{-5} M MF α was around half of that observed in the WT yeast [58].

Another study investigated if mammalian recombinant protein production can be improved by engineering *P. pastoris* to produce cholesterol using the same genetic engineering strategy described above. The improvement of functional sodium-potassium pump production was apparent from just comparing the expression patterns on western blots. As previously mentioned, in ergosterol producing strains the maximum expression was at 8h post-induction, while in cholesterol strain the production increased over time, producing much higher yields over 72h post-induction. That was attributed to cholesterol interaction with the β subunit. This effect seems to stabilise the expression of the β subunit and the overall assembly of the $\beta_1\alpha_3$ dimer, whereas in ergosterol producing strains the β expression was poor, leading to the retention of both subunits in the ER and consequent degradation. The radio-ligand binding assay on intact cells confirmed that cholesterol-producing strain demonstrated 2.5 to 4-fold increase in binding sites compared to the wild type and protease deficient strains producing ergosterol [57].

The structural, functional and simulation studies clearly show that cholesterol is required for GPCR function and more details are emerging on individual receptors. Although it is possible to reconstitute a more native-like lipid environment during the purification of membrane proteins for structural studies, this work has implications for functional GPCR studies in whole cell.

1.5. The signalling of β -adrenoceptors

A great effort has been focused on determining signalling mechanisms of GPCRS at a molecular level in order to design better drugs. The β -adrenoceptors are archetypical class A GPCRs on which many structural and mechanistic functions of the GPCRs have been elucidated. The structural studies is quite a laborious process and has required some modification of the receptor, for example, replacement of highly motile domains with stabilising proteins or antibodies, or replacement of individual residues to increase thermostability. The number of crystal structures increased immensely from 2007 when β_2 -AR structure was reported [4] and although crystal structures give only snapshots of receptor's active or inactive state in the presence or absence of various ligands, combined with other functional studies the picture of how GPCRs bring about their function is becoming clearer.

The signal transduction through β -adrenoceptors can be divided into several stages: 1) binding of the ligand; 2) transition between inactive (R) and active (R*) states; 3) conformational change-induced coupling to the signalling molecules, 4) activation of effector proteins and regulation of second messenger cAMP. In the case of β_1 -AR and β_2 -AR it can be the G protein trimer or β -arrestin. The relationship between binding of a ligand and cellular response is not linear because the signal is amplified by cAMP and different cell types will respond to the same type of stimulation differently due to different receptor expression levels and other factors, such as lipids, enzymes etc.

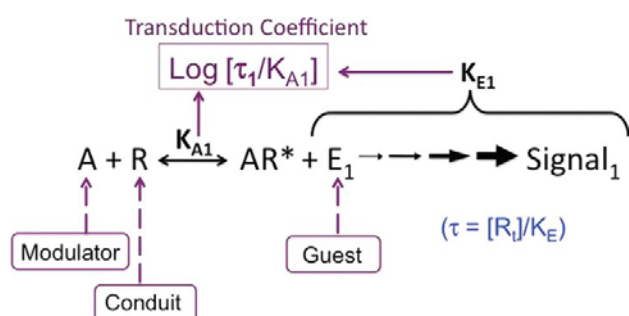


Figure 1.5. The operational model developed by Black and colleagues. Figure taken from paper by Kenakin *et al* [61]

To characterise this pharmacologically the operational model of ligand binding was developed by Black *et al* in 1985 [60, 61]. It describes the relationship between the agonist concentration and receptor binding, and subsequently, the amount of agonist-receptor complex and the response. In this model, the agonist is designated a modulator role and the conduit to the GPCR, while the signalling molecule, in case of β -ARs a G protein or a β -arrestin, is the guest protein denoted in E. Below an overview of structural of each of these stages is given.

This is important to bare this in mind when interpreting results of ligand activity on the same receptor in different assays and cell backgrounds, including the yeast. The advantages of assessing compound ability to induce coupling to different G α proteins in yeast is that the cellular background is uniform and that it lacks other interacting proteins. The significance of this is that cross-talk with signalling pathways in mammalian cells can make the interpretation of data challenging and can also lead to some discrepancies when comparing mammalian assay data to that of yeast.

As already mentioned in section 1.3.6 the MMY yeast G α subunit Gpa1 has been replaced with a chimeric G α proteins which contain 5 amino acids of human Gas at the C terminus to provide specificity and efficiency for human GPCR coupling to yeast signalling cascade. The sections below provide more detail on how the domains of β -adrenoceptors change upon binding to the ligands and how the receptor couples to the trimeric G protein.

1.5.1. Catecholamine binding site

The binding pocket of all adrenergic receptors is an archetypical class A GPCR binding pocket tucked inside the membrane segment of the receptor between the transmembrane helices. There are two main entities of the catecholamines – the catechol ring ‘head’ and ethanolamine ‘tail’. The catecholamine binding pocket is highly conserved at the residues that interact with the molecule, but the residues that move outside this region during the conformational transition to the active state are different.

Crystallographic studies have shown several important residues involved in ligand binding. **Ser**^{5.43} (5.43 according to the Ballesteros-Weinstein numbering system [62], S212 in β_1 -AR, S204 in β_2 -AR according to the protein sequence) on H5 (helix 5) formed a bridge between H5 and H6 via hydrogen bond with **Asn**^{6.55} (N310 in β_1 -AR, N293 in β_2 -AR). The rotational change allowing this occurred when **full agonist, partial agonist, or an inverse agonist** was bound, but not when antagonists was present in the binding pocket [63, 64].

Another closely located **Ser**^{5.46} (S215 in β_1 -AR, S207 in β_2 -AR) residue was bound directly to **full agonists**, via hydrogen bond to the catechol moiety 'head'. No other activity modulators, including partial agonists, interacted with this residue, which is what is thought to be crucial for full agonistic effect of a ligand [63]. **Ser**^{5.46} is also seen in a different rotational conformation when it's not bound to a full agonist.

The contraction of the binding pocket by 1Å [63] was also observed with **full and partial agonists** within the β_1 -AR binding pocket. This contraction is thought to be important in the activation process and the authors suggest that because antagonist molecules have a greater distance between the head group and amine group they are unable to make this contraction.

The **inverse agonists** bucindolol and carvedilol have a β -hydroxyl group between the head group and the secondary amine as a general structure, also characteristic of other antagonists. The β -hydroxyl forms a potential hydrogen bond with **Asn**^{7.39} on H7 (N329 in β_1 -AR) and the amine form a hydrogen bond with **Asp**^{3.32} on H3 (D121 in β_1 -AR) (**Figure 1.6**) [64]. However, their aromatic substituents at the amine ends make additional contacts in the extended ligand pocket to residues in helices 2, 3, 7, and ICL2 [64] which is different to other antagonists. The authors of the paper believe that this explains their ability to signal through non-G protein signalling pathways, mainly the β -arrestin signalling pathway, but the exact conformational changes of the receptors for this event are still unknown.

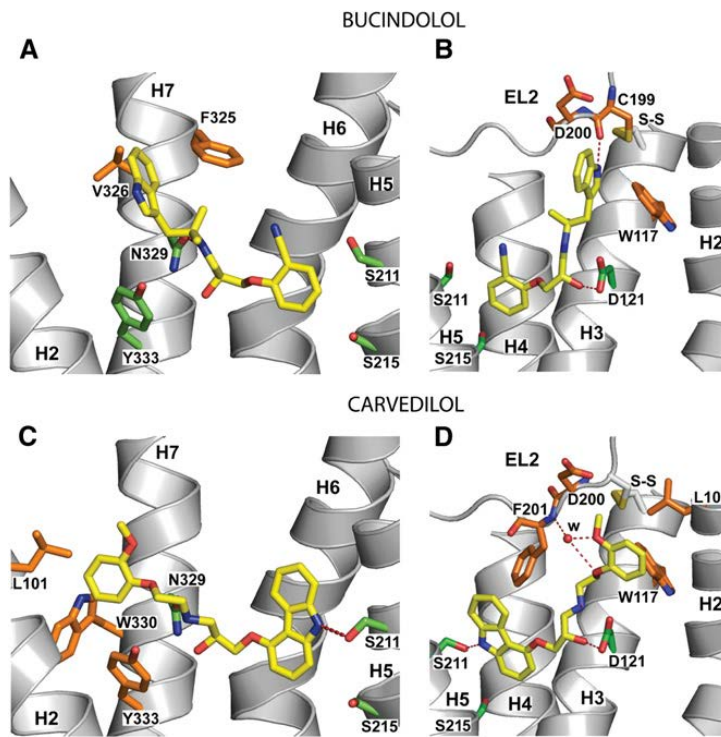


Figure 1.6 Catecholamine binding pocket as shown in crystal structure of β 1-AR. The stabilised turkey β 1-AR was co-crystallised with antagonist bucindolol [A], [B], and inverse agonist carvedilol [C], [D]. The key interacting residues are discussed in 1.5.1. Adapted from [64].

1.5.2. Transitioning between the inactive (R) and active (R*) states and coupling to $G\alpha_s$

The current understanding of GPCR-G protein trimer interaction is that an agonist bound receptor stabilises coupling to the G protein trimer and in turn bound $G\alpha$ stabilises the active conformation of the receptor increasing the receptor's affinity to the ligand [55, 65]. Crystal studies of β -adrenoceptors also showed that a large 14Å outward movement of intracellular portion of H6 was associated with receptor activation and binding of $G\alpha_s$ - $G\beta\gamma$ trimer [55]. Furthermore, the $G\alpha_s$ protein's C-terminal 5 α helix has been shown to insert into a pocket formed by intracellular portions of H3, H5, H6 and intracellular loop 2 (ICL2). Important residues of the 5 α helix of the $G\alpha_s$ protein include Tyr391, which is within the last 5 amino acid region of C-terminus and is present on the chimeric $G\alpha_s$ in MMY15 (Figure 1.7) [2, 55]. Additional contacts with Glu384 and Asp381, which is highly conserved residue on the 5 α helix of $G\alpha_s$ (Figure 1.7), are also shown in the structure, although not discussed in the paper [55]. The efficacy of agonists are thought to be determined by how well they are able to change the conformational state of the receptor and stabilise this pocket for $G\alpha_s$ coupling [65]. The formed complex allows the release of GDP from the $G\alpha$ switch pocket; the GTP binds to nucleotide-free $G\alpha$

which is then able to disassociate from G β γ and activate adenylate cyclase causing cAMP production as already mentioned in section 1.1.2.

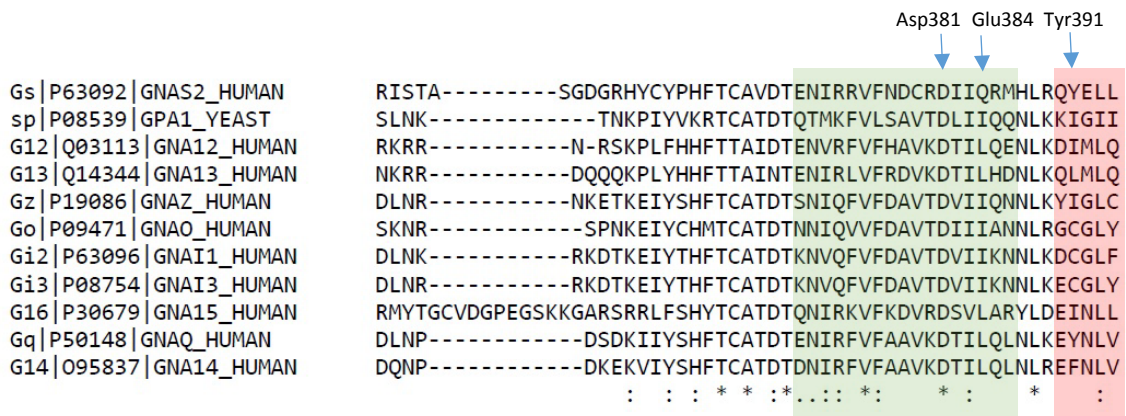


Figure 1.7 C-terminal sequence alignment of different G α proteins including yeast Gpa1. The green shading indicates 5 α helix, as mapped out in [26], which was shown to be central to GPCR-G protein trimer coupling [55]. The red shading indicates the C-terminal amino acids which were used to engineer chimeric G α s in MMY strains [2]. The blue arrows indicate important residues on G α s which were shown by crystallography studies to make contacts with the β_2 -AR [55].

1.6. Project aims and objectives

The yeast functional GPCR assay is an excellent tool in drug discovery for G protein-coupled receptors. However, not all GPCRs have been successfully adapted to this system due to low or absent functional expression. The aim of this study was to optimise the functional expression of adrenergic receptors that had previously been difficult to express and/or characterise pharmacologically in these yeast strains. Further understanding of the host's response to protein expression was sought after along this process.

This following objectives were set to achieve this:

- First of all, a set of experiments were performed in order to understand the assay parameters in well coupling α_{2A} and α_{2B} adrenoceptors. The objective was to establish what is a receptor dependent variable and how technical parameter optimisation can improve assay signal read out (Chapter 3).
- Secondly, a systematic comparison between different expression vector designs was performed to identify whether the addition of the mating factor α (MF- α) leader sequence to the amino-terminus of the β_1 - and β_2 -adrenoceptors is required to produce a pharmacological response in the yeast assay (Chapter 4).

- Thirdly, when the functional expression of the β -adrenoceptors was achieved, a pharmacological characterisation was performed to gain more insight into the signalling mechanisms of these receptors (Chapter 5)
- Lastly, to increase the number of pharmacological targets compatible with the yeast functional assay, strategies were designed to further engineer the host to provide a more native-like environment for the G protein coupled receptors (Chapter 6).

Chapter 2 – Materials and Methods

2.1. Materials

2.1.1. Yeast strains, growth and maintenance

2.1.1.1. MMY yeast strains

The yeast strains were obtained from the GSK archive BioCat [46] and are listed below.

Table 2.1 The summary of MMY yeast strain genotypes and phenotypes

Strain	Genotype	Corresponding human Gα subunit type	Signal transduction in human cells
W303-1A	MATa <i>his3 ade2 leu2 trp1 ura3 can1</i>		
MMY9	W303-1A <i>trp1 fus1::FUS1-HIS3 LEU2::FUS1-lacZ far1Δ::URA3 gpa1Δ::ADE2 sst2Δ::URA3 ura3::p140</i>		
MMY11	MMY9 <i>ste2Δ::G418^R</i>		
MMY12	MMY11 <i>TRP1::GPA1</i>		
MMY14	MMY11 <i>TRP1::Gpa1/Gα q(5)</i>	<i>q</i>	Activation of phospholipase C
MMY15	MMY11 <i>TRP1::Gpa1/Gα s(5)</i>	<i>s</i>	Activation of adenylate cyclase
MMY16	MMY11 <i>TRP1::Gpa1/Gα 16(5)</i>	<i>16</i>	Activation of phospholipase C
MMY19	MMY11 <i>TRP1::Gpa1/Gα 12(5)</i>	<i>12</i>	Activation of the Rho GTPases
MMY20	MMY11 <i>TRP1::Gpa1/Gα 13(5)</i>	<i>13</i>	Activation of the Rho GTPases
MMY21	MMY11 <i>TRP1::Gpa1/Gα 14(5)</i>	<i>14</i>	Activation of phospholipase C
MMY22	MMY11 <i>TRP1::Gpa1/Gα o(5)</i>	<i>o</i>	Inhibition of adenylate cyclase
MMY23	MMY11 <i>TRP1::Gpa1/Gα i1(5)</i>	<i>i1</i>	Inhibition of adenylate cyclase
MMY24	MMY11 <i>TRP1::Gpa1/Gα i3(5)</i>	<i>i3</i>	Inhibition of adenylate cyclase
MMY25	MMY11 <i>TRP1::Gpa1/Gα z(5)</i>	<i>z</i>	Inhibition of adenylate cyclase
MMY28	MMY11 <i>TRP1::Gpa1/Gα s(5)</i>	<i>s</i>	Activation of adenylate cyclase
YIG152	MMY25 <i>URA3::pRS306GPD-ADRA2A</i>	<i>z</i>	
YIG153	MMY20 <i>URA3::pRS306GPD-ADRA2B</i>	<i>13</i>	
Strain	Phenotype		
MMY9	Ade ⁺ , Trp ⁻ , Leu ⁺ , Ura ⁻ , His ⁺		
MMY11	Ade ⁺ , Trp ⁻ , Leu ⁺ , Ura ⁻ , His ⁺		
MMY12-28	Ade ⁺ , Trp ⁺ , Leu ⁺ , Ura ⁻ , His ⁻ (upon activation of GPCR becomes His ⁺)		

For the data presented in Chapter 3, the MMY strains with genome integrated *ADRA2A* or *ADRA2B* receptors were used. The *ADRA2A* was integrated into MMY25 (pRS306GPD-ADRA2A) and *ADRA2B*

was integrated into MMY20 (pRS306GPD-ADRA2B). The resulting strains were named YIG152 and YIG153 respectively; this nomenclature will be used from now on to describe these strains. The integrations were performed and validated earlier at GSK and were stored in the GSK's archive system BioCat (Cat# 118197 and 118198 respectively).

2.1.1.2. General

- Deionised water for all microbial work was obtained from a Millipore Elix Type 2 water purification system, unless stated otherwise.
- Higher purification grade MiliQ Ultrapure Synthesis A10 Type 1 water was used where stated.

2.1.1.3. Yeast extract-peptone-dextrose medium (YPD)

1% Bacto-yeast extract (Cat#212750, Difco), 2% Bacto-peptone (Cat#211677, Difco) were dissolved in water. For plates, 2% Difco granulated agar (Cat# 214530, Difco) was added. 40% D-glucose was added to a final concentration of 2% after the medium had been autoclaved at 121°C for 15min and cooled to less than 50°C. Media were stored at room temperature for short periods, for longer periods at 4°C. Plates were stored at 4°C.

40% glucose

D-glucose (Cat# G8270, Sigma-Aldirch) was dissolved in water to make a 40% solution, filter sterilized (0.2 mm pore size) and stored at 4°C.

2.1.1.4. 5-FOA/YPD medium

The 100x 5-FOA was diluted in warm YPD to 1x concentration to make 5-FOA/YPD medium.

100x 5-FOA

5-Fluoroorotic acid monohydrate (5-FOA) (Cat# PC4054, Apollo Scientific) was dissolved in DMSO at 2mg/mL for a 100x stock.

2.1.1.5. Complete synthetic WHAUL medium

WHAUL is a complete synthetic medium that was developed at GSK and is used to grow MMY yeast strains. It lacks tryptophan, histidine, adenine, uracil and leucine. The medium is composed of 1x WHAUL liquid at pH 5.5 or pH 7.0, 1x yeast nitrogen base (YNB), 2% glucose and sterile water. The medium is also supplemented with 1x histidine while the GPCR receptors are not being activated. 2% Difco granulated agar was added if plates were desired.

10x WHAUL liquid

L-arginine HCl (Cat# A5131, Sigma-Aldrich) – 205mg/L;
L-aspartic acid (Cat# A7219, Sigma-Aldrich) – 1023mg/L;
L-glutamic acid sodium salt (Cat# 37106, BDH Biochemicals) – 1023mg/L;
L-lysine (Cat# L5626, Sigma-Aldrich) – 307mg/L;
L-methionine (Cat# M9625, Sigma-Aldrich) – 205mg/L;
L-phenylalanine (Cat# P2126, Sigma-Aldrich) – 512mg/L;
L-serine (Cat# S4311, Sigma-Aldrich) – 3837mg/L;
L-threonine (Cat# 29578582, Molekula) – 2046mg/L;
L-tyrosine (Cat# T3754, Sigma-Aldrich) – 307mg/L;
L-valine (Cat# 11273495, Molekula).

The pH was adjusted as required with NaOH pellets.

10x YNB

6.7g yeast nitrogen base without amino acids and ammonium sulphate (Cat# 233520, Difco) was dissolved in 100mL MilliQ water, filter sterilized (0.2 mm pore size) and stored at 4°C.

100x Histidine

2mg/mL L-histidine monohydrochloride monohydrate (Cat# M49020584, Molekula) solution in MiliQ water, filter sterilized (0.2 mm pore size).

100x Uracil

2mg/mL L-uracil (Cat# M82294919, Molekula) solution in MiliQ water, filter sterilized (0.2 mm pore size).

100x Tryptophan

2mg/mL L-tryptophan (Cat# M56990934, Molekula) solution in MiliQ water, filter sterilized (0.2 mm pore size).

2.1.1.6. Yeast transformation reagents

1M LiAc

1M lithium acetate (Cat# L6883, Sigma-Aldrich), autoclaved and stored at room temperature.

50% PEG

50g PEG3350 (Cat# 88276, Fluka) were dissolved in distilled water to a final volume of 100 mL, autoclaved and stored at room temperature.

10x TE

0.1M Tris-HCl (pH 7.5), 0.01M EDTA.

LiAc-TE

5mL 1M LiAc, 5mL 10 x TE, 40mL H₂O.

LiAc-PEG-TE

5mL 1M LiAc, 5mL 10x TE, 40mL 50% PEG.

ssDNA

1mL aliquots of single-stranded DNA (Salmon Testes DNA; Cat# D1626 Sigma-Aldrich) were heated at 95°C for 10 min and placed on ice if not used immediately.

2.1.2. FD-glu GPCR functional assay medium, reagents, ligands

2.1.2.1. FD-glu GPCR assay medium

The FD-glu assay medium consisted of 1x WHAUL pH 7.0 liquid, 1x YNB, 1x BU salts pH 7.0, 2% glucose, 10-100µM FD-glu, 2-50mM 3-AT, water.

10x Buffering (BU) salts

46.5g Na₂HPO₄•2H₂O and 30g NaH₂PO₄ were dissolved in 995mL water, the pH adjusted to 7.0. This solution was used to buffer the assay medium as pH 7.0 is optimal for human GPCR receptors.

1M 3-AT

The powdered 3-AT was dissolved in water according to manufacturer's instructions, then aliquoted into 50mL falcon tubes. Stored at -20°C.

10mM FD-glu

5mg of fluorescein di- β -D-glucopyranoside (FD-glu) (Cat# F-2881, Life Technologies) powder were dissolved in 761.5 μ L of 100% DMSO (Cat# D2650, Sigma-Aldrich). Stored at -20°C.

Note 1: Protocols for preparing yeast culture media were taken from "G Protein-Coupled Receptors in Drug Discovery" (2009) **Chapter 15: Yeast Assays for G Protein-Coupled Receptors** by Simon J. Dowell and Andrew J. Brown [46].

2.1.2.2. FD-Glu GPCR assay plates and other consumables

Greiner black wall-clear bottom sterile 96-well plates (Cat# 655090, Greiner) and 384-well plates (Cat# 781090, Greiner) were used.

Breathe-Easy membrane (Cat# Z380059, Sigma-Aldrich) were used for sealing the plates.

2.1.2.3. FD-glu GPCR assay compounds

Different compound panels were obtained for experiments with the α 2-AR receptors and the β 1-AR receptors. All compounds tested at GSK were dissolved in 100% DMSO. The compounds from both panels were supplied pre-dispensed on black-walled clear bottom Greiner 384-well plates.

Table 2.2 The panel of adrenoceptors α_{2A} and α_{2B} interacting compounds used in Chapter 3 experiments. The compounds without the generic name are GSK proprietary compounds.

Compound ID	Generic /other name	Receptor interaction
C1	GSK Library C	Unknown
C2	GSK Library C	Unknown
C3	GSK Library C	Unknown
C4	GSK Library C	α_2 binder
C5	xylazine	α_2 partial agonist
C6	tizanidine	α_2 agonist
C7	GSK Library C	Unknown
C8	yohimbine	α_2 antagonist
C9	GSK Library C	Unknown
C10	GSK Library C	Unknown
C11	GSK Library C	Unknown
C12	mianserin	α_1 antagonist
C13	GSK Library C	α_2 agonist
C14	GSK Library C	α_2 agonist
C15	GSK Library C	α_2 agonist
C16	idazoxan	α_2 antagonist
C17	GSK Library C	α_2 agonist
C18	GSK Library C	α_2 agonist
C19	UK 14,304 (Brimonidine)	α_{2A} full agonist α_{2B} partial agonist
C20	GSK Library C	Unknown
C21	GSK Library C	α_2 binder
C22	octopamine	TA1 receptor agonist
C23	GSK Library C	α_2 agonist

Table 2.3 The panel of adrenoceptors β_1 and β_2 interacting compounds used in Chapter 6 experiments.Agonists

Compound ID	Generic name	Receptor interaction (from IUPHAR)
C21	orciprenaline	β_2 agonist
C22	xamoterol	β_1 partial agonist
C25	dobutamine	β_1 and β_2 partial agonist
C31	procaterol	β_2 agonist
C33	zinterol	β_2 agonist
C34	fenoterol	β_2 agonist
C36	terbutaline	β_2 partial agonist
C39	mirabegron	β_1 and β_2 agonist
C40	indacaterol	β_1 and β_2 agonist
C42	isoprenaline	β_1 and β_2 full agonist
C46	pindolol	β_1 and β_2 partial agonist

Antagonists

Compound ID	Generic name	Receptor interaction (from IUPHAR)
C20	levobetaxolol	β_1 and β_2 antagonist
C23	labetalol	β_1 and β_2 antagonist
C24	metoprolol	β_1 and β_2 antagonist
C26	nadolol	β_1 and β_2 antagonist
C27	propranolol	β_1 and β_2 antagonist
C28	alprenolol	β_2 antagonist
C29	sotalol	β_1 and β_2 antagonist
C30	carvedilol	β_1 and β_2 antagonist
C35	levobunolol	β_1 and β_2 antagonist
C37	esmolol	β_1 antagonist
C38	propafenone	β_1 and β_2 antagonist
C41	atenolol	β_1 and β_2 antagonist
C43	acebutolol	β_1 antagonist
C44	practolol	β_1 antagonist
C48	bupranolol	β_1 and β_2 antagonist
C49	betaxolol	β_1 and β_2 antagonist

The concentration of ligands ranged from 10mM to 169nM diluted in 3-fold dilutions, except β -AR compound panel which ranged from 10mM to 6nM.

For colony screening and assay optimisation at Aston brimonidine (UK 14,304) and isoprenaline were purchased from Sigma-Aldrich (cat# U104 and I6504 respectively). Brimonidine was dissolved in 100% DMSO. Isoprenaline was dissolved in water and supplemented with 1mM ascorbic acid to minimise degradation. 10mM stocks were aliquoted and stored at -20°C.

2.1.3. Molecular biology

2.1.3.1. Bacterial transformation

Escherichia coli strains

XL10-Gold Ultracompetent (Cat# 200315, Agilent) and XL1-Blue Competent (Cat# #200249, Agilent) *Escherichia coli* cells were available in the laboratory, and were prepared as chemically competent cells according to the protocol detailed section 2.2.3.1.

NEB® 5- α F'Iq Competent *E. coli* (High Efficiency) (Cat# C2992H, NEB) commercially prepared *E. coli* were used for the ligation of *ERG6* plasmids.

Luria Bertani (LB) +/- ampicillin (LBA)

20g/L of LB broth powder (Cat# I3022, Sigma-Aldrich), which contains 10g/L tryptone, 5 g/L yeast extract and 5 g/L NaCl, was dissolved in water. 15g/L of Difco granulated agar was added when making plates. For selection of transformed cells, the medium was supplemented with 100mg/L of ampicillin (LB-amp media).

Super optimal broth (SOB)

SOB medium was prepared by enriching LB medium with 186mg/L of KCl, 10mM MgCl₂, and 10mM MgSO₄. This medium was used for preparation of chemically competent *E. coli* cells [66].

Super optimal broth with catabolite repression (SOC)

The SOC medium was prepared by supplementing SOB medium with 2% glucose. This medium was used to recover heat-shocked *E. coli* cells during transformation experiments[66].

1x TB buffer

10mM HEPES, pH 6.7, 15mM CaCl₂, 55mM MnCl₂, 250mM KCl, MiliQ water.

The solution was filter sterilised and stored at 4°C when not in use.

Note 2: The materials for preparing chemically-competent *E. coli* cells were taken from the European Molecular Biology Laboratory (EMBL) website [66], Cloning methods section. The procedures and recipes were adopted from the original publication by Inoue et al. (1990), *Gene*, 96:23-28.

2.1.3.2. Cloning enzymes and other reagents

Enzymes

Table 2.4 The list of enzymes used for molecular biology

Name	Application	Manufacturer	Cat#	Buffer
<i>AvrII</i>	Restriction	Clontech	1022A	Buffer K
<i>BalI</i>	Restriction	Clontech	1009A	Ball buf.
<i>BamHI</i>	Restriction	Fermentas	ER0051	<i>BamHI</i>
<i>BshTI (AgeI)</i>	Restriction	Fermentas	ER1461	Orange
<i>EcoRI</i>	Restriction	Fermentas	ER0271	<i>EcoRI</i>
<i>HindIII</i>	Restriction	Fermentas	ER0501	Red
<i>NcoI</i>	Restriction	Fermentas	ER0571	Tango
<i>NdeI</i>	Restriction	Fermentas	ER0581	Orange
<i>NotI</i>	Restriction	Fermentas	ER0591	Orange
<i>PvuII</i>	Restriction	Fermentas	ER0631	Green
<i>SalI</i>	Restriction	Fermentas	ER0641	Orange
<i>SmaI</i>	Restriction	Fermentas	ER0661	Tango
<i>SpeI (BcuI)</i>	Restriction	Fermentas	ER1251	Tango
<i>Van91I</i>	Restriction	Fermentas	ER0711	Red
<i>XagI (EcoNI)</i>	Restriction	Fermentas	ER1301	Red
<i>XbaI</i>	Restriction	Fermentas	ER0681	Tango
<i>XhoI</i>	Restriction	Fermentas	ER0691	Red
FastAP	Phosphatase/cloning	Fermentas	EF0654	FastAP
Rapid ligation kit	Ligation/cloning	Fermentas	K1422	5x RL buf.
Gibson Assembly cloning kit	Ligation/cloning	NEB	E2611	

Note 3: Fermentas is part of Thermo Fisher Scientific group. The supplier of Fermentas enzymes is Fisher Scientific UK Ltd, Loughborough, United Kingdom.

Note 4: The Takara enzymes and vectors were obtained from Takara Bio USA, Inc., Saint-Germain-en-Laye, France.

DNA marker

GeneRuler DNA Ladder Mix, ready-to-use

GeneRuler 1kb DNA ladder (Cat# SM0331, Thermo Scientific) was used for the reference of DNA fragment size, pictured below:

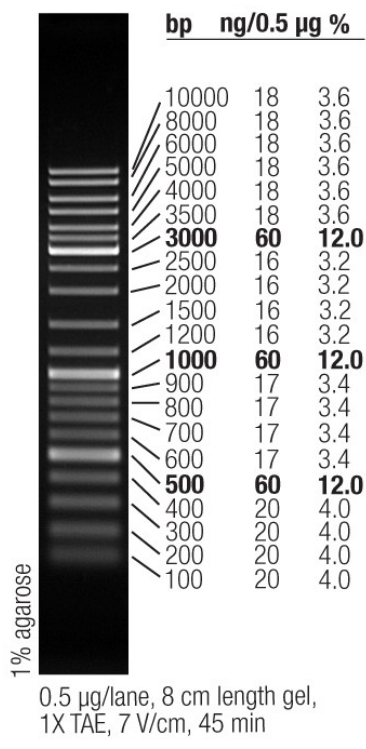


Figure 2.5 GeneRuler 1kb DNA ladder.

Tris-Acetic acid-EDTA buffer gel electrophoresis:

50x stock TAE: 40mM Tris-HCl, 20mM Acetate, 1mM EDTA.

1x working solution TAE: 20mL 50x TAE, 980mL water.

1% agarose: 1g agarose (Cat# A40702, AGTC Bioproducts) per 100mL of 1xTAE was heated in microwave to dissolve the powder. After the agarose cooled down, theRedSafe DNA stain (Cat# BT41003, Cambridge Bioscience) was added at 1µL per 10mL.

Plasmid releasing reagent for yeast plasmid isolation

2% Triton X-100, 1% SDS, 100mM NaCl, 10mM Tris-HCl (pH 8.0), 1mM Na₂-EDTA.

2.1.3.3. Polymerase chain reaction (PCR)

PCR reactions

0.5µL of Herculase II fusion DNA polymerase (Cat# 600675, Agilent) was used per 25µL PCR reaction, with 1x Herculase II reaction buffer 0.2mM dNTPs (Cat# 18427-013, Invitrogen), 250nM of Forward and Reverse primer. For b1_for_1 and b1_rev_1 primers 10% DMSO (Cat# D2650, Sigma-Aldrich) was also added. For amplification from the plasmid, 29ng DNA template was used. For genomic detection – between 100-250ng of gDNA was used. The composition of the reaction was determined based on the manufacturer's recommendations.

Primers

All primers were synthesised by Invitrogen, in Paisley, United Kingdom (part of Thermo Fisher Scientific Ltd).

Table 2.6 List of primers

For p426GPD plasmids						
Name	Gene	Application	Sequence from 5' to 3'	Direction	Optimised Annealing Temp	PCR Protocol
b1_For_1	ADRB1	Cloning	AAAAAAGGATCCCACCATGGGCGGGGGTG	For	65° C	1
b1_Rev_1	ADRB1	Cloning	AAAAAAGGATCCCTACACCTTGGATTCCGAGGCG	Rev		
b1_For_2	ADRB1	Cloning	AAAAAAGAATTACCATGGGCGGGGGTGCTC	For	65° C	1
b1_Rev_2	ADRB1	Cloning	AAAAAAGTCGACCTACACCTTGGATTCCGAGGC	Rev		
b2_For_1	ADRB2	Cloning	AAAAAAGAATTACCATGGGGCAACCCGGGAACG	For	65° C	1
b2_Rev_1	ADRB2	Cloning	AAAAAAGTCGACTTATAGCAGTGAGTCATTTGTAC	Rev		
Primer 7	ADRB1	Sequencing	CAATGACACACAGGGTCTCG	Rev		
Primer 8	ADRB1	Sequencing	TCCTTCTTCTGCGAGCTGTG	For		
Primer 9	ADRB1	Sequencing	TCAAGACGCTGGGCATCATC	For		
Primer 10	ADRB2	Sequencing	CAGCACATCAATGGAAGTCC	Rev		
Primer 11	ADRB2	Sequencing	GACTTTTGGCACTTCTGGTG	For		
Primer 12	ADRB2	Sequencing	CTAACGCTTGAGGGCTTTG	Rev		
Primer 13	ADRB2	Sequencing	CATTGTGCATGTGATCCAGG	For		
For <i>ura3</i> deletion						
Name	Gene	Application	Sequence from 5' to 3'	Direction	Optimised Annealing Temp	PCR Protocol
1_URA3	URA3	Genomic detection	CCTAGTCCTGTTGCTGCCAA	Rev	60°C	2
2_URA3	URA3	Genomic detection	TTCCAGCCTGCTTTTCTGT	For		
5_YAP1	YAP1	Genomic control	TGTCAGGTGATGATGGCAGC	For	60°C	2
6_YAP1	YAP1	Genomic control	CCGAGATGGGTTTCTTGGGA	Rev		
For DHCR7/24 gene integration						
Name	Gene	Application	Sequence from 5' to 3'	Direction	Optimised Annealing Temp	PCR Protocol
3_ERG5	ERG5	Cloning	CCGCATTGACTTCGACGGAT	For	57°C	3
4_ERG5	ERG5	Cloning	GCTGTCATGCTCGCCTTCA	Rev		
3_ERG6	ERG6	Cloning	AAAAAAGagctcCCGATTTTGGGCAGTCTCT	For	60°C	3
4_ERG6	ERG6	Cloning	AAAAAAGaattcAATACTGGTCGTTTGCCACG	Rev		
Primer 24	erg5prom	Sequencing	GCATATAGACGCAGGTTTGG	Rev		
Primer 25	erg5prom	Sequencing	CGCTGCTGACAAAACATAGC	For		
Primer 26	DHCR24	Sequencing	CCACCAACAGTCAAATCATCC	Rev		
Primer 27	DHCR24	Sequencing	CTATTGGTTGGACATTGCCAG	For		
Primer 28	DHCR24	Sequencing	CGTCACCTTTTGGATGAACC	Rev		
Primer 29	DHCR24	Sequencing	CCAAATCAACCTGGTATGGT	For		
Primer 30	erg5term	Sequencing	TTCAGGAAACCAAGCTGGCAG	Rev		
Primer 31	erg6prom	Sequencing	GGATGCGTAAGGTCTTAAGAG	Rev		
Primer 32	erg6prom	Sequencing	TCGGTAAACGGAAGACTA	For		
Primer 33	DHCR7	Sequencing	GTAACAAAGTTGCGTCACC	Rev		
Primer 34	DHCR7	Sequencing	CCAATGTTCTATCTCACATCC	For		
Primer 35	DHCR7	Sequencing	GGGTTTGGTTGGTTACTACA	Rev		
Primer 36	DHCR7	Sequencing	GGGTTTGGTTGGTTACTACA	For		
Primer 37	erg6term	Sequencing	GAATTCGCTGTAGGGGAGCA	Rev		
Primer 38	ERG5	Sequencing	GACTTCTCCAGTAATTGGGTC	Rev		
Primer 39	erg5prom	Genomic detection	GGAGTCAGATCATCCAAATC	For	57°C	4
Primer 40	erg5term	Genomic detection	GTATCATCTACCGCTGCAT	Rev		
Primer 41	ERG6	Sequencing	GTTGCTTCTGGGAAGTTTGGG	Rev		
Primer 42	erg6prom	Genomic detection	CCTTCATCTCTCTCCTTACG	For	57°C	4
Primer 43	erg6term	Genomic detection	CACTTGCCGCTGTAGACAATAG	Rev		
Primer 44	AUR-1C	Sequencing	CGGACGAACGAGAACAGAAGT	Rev		

2.1.3.4. Vectors and plasmids

Both p426GPD and p306GPD vectors have a common backbone containing the following components [67]:

- A yeast *GPD* promoter, which in its genomic location induces the expression of the house keeping gene, glyceraldehyde 3-phosphate dehydrogenase;
- multiple cloning site (MCS);
- cytochrome C gene terminator sequence;
- *URA3* for nutrient selection;
- 2 micron yeast replication origin;
- *AmpR* for ampicillin resistance selection in *E. coli*.

Table 2.7 List of vectors

#	Name	Backbone	Size	What's inserted?	Other additions/tags	Cloning strategy
1	p426GPD	p426	6602 bp	MCS		Deposited from GSK
2	p426GPD-DEST-ADRB1	p426	8120 bp	<i>ADRB1</i>	Gateway sequences around <i>ADRB1</i>	Deposited from GSK
3	p426GPD-HA-ADRB2	p426	7990 bp	<i>ADRB2</i>	HA tag at 5' of <i>ADRB2</i>	Deposited from GSK
4	p426GPD-MF α	p426	6902 bp	MCS	MF α leader sequence	Deposited from GSK
5	p426GPD-STE2L	p426	6647 bp	MCS	Ste2p receptor leader sequence, 5' of MCS	Deposited from GSK
6	p426GPD-ADRB1	p426	8046 bp	<i>ADRB1</i>		Amplified from #2 using b1_for/rev_1 PCR primers with <i>Bam</i> HI sites at 5' 3' added, then digested, ligated
7	p426GPD-ADRB2	p426	7850 bp	<i>ADRB2</i>		From #3 cut and ligated using <i>Bam</i> HI into #1
8	p426GPD-MF α -ADRB1	p426	83332bp	<i>ADRB1</i>	MF α leader sequence 5' of <i>ADRB1</i> , in frame	Cut from #6 at <i>Bam</i> HI, purify, cut with <i>Nco</i> I. #4 double-cut with <i>Bam</i> HI and <i>Nco</i> I. Then ligated.
9	p426GPD-MF α -ADRB2	p426	8140 pb	<i>ADRB2</i>	MF α leader sequence 5' of <i>ADRB2</i> , in frame	Cut from #7 at <i>Nco</i> I, purify, cut with <i>Bam</i> HI. #5 double cut with <i>Bam</i> HI and <i>Nco</i> I. Then ligated
10	p426GPD-STE2L-ADRB1	p426	8063 bp	<i>ADRB1</i>	Ste2L leader sequence 5' of <i>ADRB1</i> , in frame	Amplified from #2 using b1_for/rev_2 PCR primers with <i>Eco</i> RI at 5' and <i>Sa</i> II at 3' added. Then digested, ligated
11	p426GPD-STE2L-ADRB2	p426	7898 bp	<i>ADRB2</i>	Ste2L leader sequence 5' of <i>ADRB2</i> , in frame	Amplified from #2 using b2_for/rev_1 PCR primers with <i>Eco</i> RI and <i>Sa</i> I sites at 5' 3' added, then digested, ligated
12	p306GPD	p306	5266 bp	MCS		Deposited from GSK

13	p306GPD-ADRB1	p306	6710 BP	<i>ADRB1</i>		Cut from #6 and ligate into #12 at <i>Spe I</i> + <i>Hind III</i> sites
14	p306GPD-ADRB2	p306	6514 bp	<i>ADRB2</i>		Cut from #7 and ligate into #12 at <i>Spe I</i> + <i>Sal I</i>
15	p306GPD-MF α -ADRB1	p306	6970 bp	<i>ADRB1</i> with MF α	MF α leader sequence	Cut from #8 and ligate into #12 at <i>Spe I</i> + <i>Hind III</i>
16	p306GPD-MF α -ADRB2	p306	6778 bp	<i>ADRB2</i> with MF α	MF α leader sequence	Cut from #9 and ligate into #12 at <i>Spe I</i> + <i>Hind III</i>
17	p426GPD-ERG5	p426	9224 bp	<i>ERG5</i>	<i>ERG5</i> with 5' and 3' flanking sequences	Amplified with 3_ERG5 and 4_ERG5, then digested with <i>Eco RI</i> and inserted into #1
18	p426-ERG6	p426	8420 bp	<i>ERG6</i>	<i>ERG6</i> with 5' and 3' flanking sequences	Amplified with 3_ERG6 and 4_ERG6, then digested with <i>Sac I</i> and <i>Eco RI</i> and inserted into #1
19	pUC57-DHCR24	pUC57	4601 bp	<i>DHCR24</i>		Synthesised by GenScript
20	pUC57-DHCR7	pUC57	4886 bp	<i>DHCR7</i>		Synthesised by GenScript
21	p426GPD-erg5-DHCR24-cys1t-erg5	p426	9441 bp	<i>DHCR24</i>	<i>DHCR24</i> reading frame replacing <i>ERG5</i>	Yeast gap repair
22	p426GPD-erg6-DHCR7-cys1t-erg6	p426	8960 bp	<i>DHCR7</i>	<i>DHCR7</i> reading frame replacing <i>ERG6</i>	Gibson assembly
23	pAUR135	pAUR135	6074 bp		Aureobasidin A resistance	Purchased
24	pAUR135-erg5-DHCR24-cys1t-erg5	pAUR135	8885 bp	<i>erg5-DHCR24</i>	Aureobasidin A resistance	Cut from #21 at <i>EcoRI</i> and inserted into #23
25	pAUR135-erg6-DHCR7-cys1t-erg6	pAUR135	9117 bp	<i>erg6-DHCR7</i>	Aureobasidin A resistance	Cut from #22 at <i>SacI</i> and <i>EcoRI</i> and inserted into #23
26	pJL164		8400 bp		<i>ura3</i> Δ cassette	purchased
27	p140	pUC19	3364 bp	Truncated <i>ura3</i>	<i>Sta1</i> and <i>EcoRV</i> fragment cut out of <i>URA3</i> coding region	Deposited from GSK

2.1.3.5. DNA purification and isolation

- QIAquick PCR Purification Kit (Cat# 28104, Qiagen) and Wizard® SV Gel and PCR Clean-Up System (Cat# A9282, Promega) were used to purify the DNA from the PCR and restriction digestion reactions.
- QIAquick Gel Extraction Kit (Cat# 28704, Qiagen) was used to purify the DNA from agarose gel.
- QIAGEN Plasmid Maxi Kit (Cat# 12162, Qiagen), QIAGEN Plasmid Mini Kit (Cat# 12123, Qiagen), and GeneJET Plasmid Miniprep Kit (Cat# K0503, Thermo Scientific) were used to isolate plasmid DNA from *E. coli* strains.
- Thermo Scientific™ Pierce™ Yeast DNA Extraction Kit (Cat# 10473985, Thermo Scientific) was used to isolate genomic yeast DNA for colony screening.

Phenol-chloroform DNA extraction reagents

Phenol: chloroform: isoamyl alcohol mixture (Cat# 77617, Sigma-Aldrich)

Absolute and 70% ethanol (Cat# E/0665DF/17, Fisher Chemical)

3M Sodium Acetate (Cat# S2889, Sigma-Aldrich)

Thermo Scientific™ Glycogen, molecular biology grade (Cat# 11883933)

2.1.4. Western blot reagents and consumables

2.1.4.1. Membrane isolation reagents and buffers

Breaking buffer, pH 7.4

50mM Na₂HPO₄, 2mM EDTA (pH 7.4), 100mM NaCl, 5% glycerol

Buffer 'A' pH 7.0

20mM HEPES, 50mM NaCl, 10% glycerol

Membrane resuspension buffer

50mM Tris-HCl (pH 8.0), 150mM NaCl, 2mM EDTA

Glass beads

Acid-washed glass beads (Cat# G8772, Sigma-Aldrich).

Protease inhibitor cocktail (PIC)

A yeast specific protease inhibitor cocktail set IV (Cat# 539136, Merk-Millipore) was used.

BCA and cupric sulfate

Bicinchoninic acid solution (Cat# B9643, Sigma-Aldrich) and copper(II) sulfate solution (Cat# C2284, Sigma-Aldrich) were used for determining membrane protein concentration.

BSA standards

Bovine serum albumin (Cat# 82516, Sigma-Aldrich) was diluted at 0.8mg/mL, 0.6mg/mL, 0.4mg/mL and 0.2mg/mL in membrane resuspension buffer.

2.1.4.2. Acrylamide gels

Separating gel

4.4mL water, 3mL 1.5M Tris-HCl (pH 8.8), 3.8mL 30% Protogel acrylamide mix, 120µL 10% SDS, 40µL 20% ammonium persulfate, 9µL TEMED.

Stacking gel

1.3mL water, 3.1mL 0.5M Tris-HCl (pH 6.8), 0.7mL 30% Protogel acrylamide mix, 50µL 10% SDS, 20µL 20% ammonium persulfate, 5µL TEMED.

1.5M Tris-HCl (pH 8.8)

9.09g of Sigma 7-9[®] Tris-base (Cat# T1378, Sigma-Aldrich) dissolved in 50mL water, then pH adjusted to 8.8.

0.5mM Tris-HCl (pH 6.8)

3.94g of Trizma[®] hydrochloride (Cat# T5941, Sigma-Aldrich) dissolved in 50mL water, then pH adjusted to pH 6.8.

10% SDS

5g of SDS (Cat# L3771, Sigma-Aldrich) dissolved in water to a final volume of 50mL.

20% ammonium persulfate

The solution was freshly made before preparing gel solution. 200mg of powder (Cat# A9164, Sigma-Aldrich) were dissolved in 800µL of water.

30% acrylamide solution

Protogel is a pre-mixed 37:5:1 Acrylamide to Bisacrylamide stabilized solution (Cat# A2-0072, Geneflow).

TEMED (Cat# T9281, Sigma-Aldrich).

Pre-made gels

12% Mini-PROTEAN[®] TGX[™] Precast Protein Gels, 10-well gels (Cat# 4561044) and Novex 12% Tris-glycine gels (Cat# XP00122BOX, Invitrogen) were used.

2.1.4.3. Running buffers

For running acrylamide gels

10x Tris/Glycine/SDS buffer (Cat# B90032, Geneflow) was diluted in water to make 1x working concentration. An equivalent 1x Laemli running buffer: SDS-Tris-Glycine was made in-house at GSK and was used to run Novex gels.

For protein transfer onto the membrane

10x Tris/Glycine transfer buffer (Cat# B90056, Geneflow) was made to 1x working concentration with 20% methanol.

iBlot® Transfer Stack, PVDF, mini (Cat# IB401002, Invitrogen) stacks for dry blotting system was used at GSK.

2.1.4.4. Antibody binding and detection

Primary antibodies

Anti-beta 2 Adrenergic Receptor antibody (Cat# ab182136, Abcam)

Anti-beta 1 Adrenergic Receptor antibody (Cat# ab3442, Abcam)

Secondary antibody

Anti-rabbit IgG, HRP-linked Antibody (Cat# 7074S, Cell Signalling Technology)

PBS

PBS tablets (Cat# 1282-1680, Fisher Chemical), 1 per 100mL, were dissolved in water to give 1x PBS solution.

Milk-PBS

2.5g skimmed milk powder was dissolved in 50mL PBS

Tween wash buffer

2ml of Tween-20 (Cat# P9416, Sigma-Aldrich) was dissolved in 998mL to make 0.2% tween 20 in 1x PBS.

EZ-ECL substrate

SuperSignal™ West Dura Extended Duration Substrate (Thermo Scientific, Cat# 34076) and EZ-ECL Chemiluminescence Detection Kit for HRP (Cat# K1-0172, Geneflow) were used as HRP substrate for detection.

2.2. Methods

2.2.1. Yeast strains, growth and maintenance

2.2.1.1. General

- All incubations for yeast were carried out at 30°C, and for bacteria (*E. coli*) at 37°C both for growth on Petri plates and liquid culture. Liquid cultures, in addition, were shaken at 220 oscillations per minute. The capacity of glass or plastic flasks was 5x the volume of the culture medium to allow adequate aeration.
- Untransformed MMY strains were grown in YPD.
- Transformed yeast were grown in complete synthetic WHAUL medium at pH 5.5 (WHAUL-5.5) for general work and pH 7.0 (WHAUL-7.0) in FD-Glu assay conditions.

2.2.1.2. Yeast transformation

Yeast transformations were carried out as previously described (Dowell and Brown, 2009). Briefly, a single MMY colony was inoculated into 3mL YPD for MMY11 or WHAUL-5.5 + His + Ura for other MMY strains and grown overnight at 30°C with shaking at 220rpm. The next morning 500µL of the overnight culture were subcultured into 20mL of the same medium in a 100mL conical shake flask. After 4 hours of further growth, the cells were washed with 1 vol of sterile double distilled water, resuspended in 1mL of water and transferred into a 1.5mL eppendorf tube. The centrifugations for the washes were performed at 600g, 4min, room temperature. The pelleted cells were resuspended into 400µL of LiAc-TE buffer. 50µL of cell suspension was used per transformation, mixed with 300µL LiAc-PEG-TE, 5-25µL ssDNA and 1µg of DNA for test samples only. The mixtures were incubated at room temperature for 10min, then heat-shocked at 42°C. 100µL of the transformed cell mixture were plated onto WHAUL-5.5 + His plates. Colonies generally appeared after 42-72h.

2.2.1.3. Colony selection for *ura3Δ*

Day 1-2

The above described yeast transformation protocol was used with some modifications. After the cells were heat-shocked, instead of directly plating them on the selection plates, the yeast were grown for 2h at 30°C in 1mL 5-FOA/YPD to increase the selection stringency. After that, the cells were diluted with further 1mL of medium and then plated on 5-FOA/YPD plates, 100μL of the culture per plate.

Day 4

Plates were left to grow for 48h post-transformation until small-to-medium size colonies formed. Because a high number of colonies usually appeared on the plates, a number of colonies were picked and diluted to approximately 2.0×10^4 cells/mL and spread on fresh 5-FOA/YPD plates.

Day 5-6

When small colonies appeared, the plates were replica-plated onto a fresh 5-FOA/YPD and WHAUL+His+Trp-Ura (–Ura for short) plates.

Day 6-8

Colonies which appeared on the –Ura plates were selected for colony PCR (protocol 2).

A crude DNA extraction directly from colonies was done as follows:

Colonies were resuspended in 200μL of water to make a back-up colony on a fresh plate. Then, the cells were pelleted at 15,000rpm for 1min. Supernatant discarded. The pellets were resuspended in 100μL 1% SDS – 0.2M LiAc and incubated at 70°C for 5min. 300μL of absolute ethanol were then added and the suspensions were vortexed for 1min to break open the cells. The samples were centrifuged at 15,000rpm for 3min. Supernatant discarded. The pellets were washed with 1vol of 70% ethanol. Supernatant discarded. The pellets were resuspended in 100μL of water. The samples were briefly spun (~15s) at 15,000rpm to pellet the cellular debris. 1μL of this crude fresh extract was used for PCR.

2.2.2. FD-glu GPCR assay set-up and conditions

2.2.2.1. Assay set-up for ligand measuring induced yeast growth

Day 1

For preparation of the assay, a single colony of transformed yeast were inoculated into WHAUL-5.5 medium for overnight culturing at 30°C. For screening assays the colonies were inoculated into 200µL of culture in 96-well sterile plates, and grew to lower OD₆₀₀ than normal. For other assays 3mL of medium was used for the overnight culture.

Day 2

The assay set-up required several steps. Firstly, the ligand dilutions were dispensed (please see below). Secondly, the assay medium was prepared (2.1.2.1), and finally, the cell density from the overnight culture was measured and diluted into the assay medium to a final OD₆₀₀ of 0.02. The total volume per well in 96-well plate was 200µL, in 384-well it was 50µL. The prepared plates were sealed with Breathe-Easy membrane and incubated at 30°C for 18-48h.

Day 3 or 4

The final data were collected and analysed on the last day.

2.2.2.2. Ligand preparation

The GSK compounds

At GSK both panels of compounds were aliquoted into 384-well plates by an automated system. The compounds were dissolved in 100% DMSO and aliquoted in 0.5µL volumes in each well. The sealed plates were stored at 4°C for up to two months.

Compounds at Aston

Brimonidine, or UK 14, 304, was used as an agonist for α_{2A} -AR and α_{2B} -AR receptor stimulation studies at Aston. 5mg of brimonidine were dissolved in 1.712mL 100% DMSO to give concentration of 10mM. The stock solution was stored at -20°C.

Isoprenaline, or isoproterenol, was used as an agonist for β_1 -AR and β_2 -AR receptor stimulation studies at Aston. The isoprenaline powder was dissolved in water at concentration of stock solution at 10mM,

supplemented with 1mM of ascorbic acid (Cat# 92902, Sigma-Aldrich). 200 μ L aliquots were stored at -20°C for a single use.

For the 3-fold serial dilutions in 96-well plates, 200 μ L of 10mM solution were pipetted into well 1. 133 μ L of 100% DMSO were dispensed into wells 2-12. 66 μ L were drawn from well 1 and transferred into well 2. With a fresh tip, the contents of well 2 were mixed, then 66 μ L were drawn again and transferred into well 3. The procedure was repeated until well 12, in which only DMSO was present. 2 μ L of each dilution were transferred into the Greiner assay plate, which equalled 1% of the overall assay mix in the well. The same principle was applied to 384-well plates where 0.5 μ L of the ligand was mixed in the final assay volume of 50 μ L. The final concentrations ranged from 10mM to 169nM with no ligand in well 12.

2.2.3. Data collection and analysis

The fluorescence was read as relative fluorescence units (RFU) with an EnVision Multilabel plate reader (PerkinElmer) and SpectrafluorPlus (Tecan) at GSK and a Gemini GM fluorescence reader (Molecular Devices) a Mithras (Berthold) at Aston University. Where possible, data were normalised against the highest signal produced by brimonidine stimulation as the upper asymptote and the negative DMSO control as the lower asymptote. The pEC₅₀ and R² values were retrieved from a non-linear three parameter fit data analysis. All data simulations were performed with MS Excel and GraphPad Prism V.7.

One-way ANOVA was used to compare EC₅₀ values in Chapter 3.

For correlation analyses in Chapter 5 Pearson's correlation coefficient was calculated. Linear regression plots were plotted on the XY scatter to indicate the differences between slopes. The data for assay comparison in **Figure 5.18** and **Table 5.19** can be found in the **Appendix E**.

P values <0.05 were deemed to be significant.

GraphPad Prism was used to obtain all calculations.

2.2.4. Molecular Biology

2.2.3.1. Bacterial transformation

Preparation of competent *E. coli* cells

Frozen stocks of *E. coli* XL-BLUE were inoculated into 3mL LB for overnight growth at 37°C. 1.5mL of the overnight culture were sub-cultured into 250mL of SOB medium and grown at reduced temperature of 30°C until OD₆₀₀ reached 0.4. The cells were then chilled for 15min, pelleted at 6000rpm, 4°C, 10min. The cell pellet was resuspended in 50mL ice-cold TB buffer, then incubated on ice for 10min, and finally centrifuged at 6000rpm, 4°C, 10min. The resulting pellet was re-suspended in 9.3mL TB buffer with 0.7mL 100% DMSO. The cells were aliquoted in pre-chilled Eppendorf tubes and frozen at -80°C immediately.

All handling after culturing were done in the cold room, keeping the cells on ice-cold water at all times.

Heat shock transformation of competent *E. coli* cells

The cells were transformed with either ligated DNA or plasmid DNA by incubating a mixture of DNA and 50µL of thawed cells for 30min on ice, then heat-shocking the mixture at 42°C for 90s, and returning it back on the ice for 5min. The cells were recovered in SOC medium at 37°C for 1h. After this incubation, the cells were plated out on LBA plates and left to grow at 37°C overnight.

2.2.3.2. Cloning

General

Ultrapure water was obtained from a Type 1 Milli-Q Synthesis A10 water purification system and was used for all molecular biology work, except where water was supplied with other reagents, such as PCR and Ligation kits, and for making 1X TAE buffer. For the later, Type 2 deionised water from a Millipore Elix water purification system was used.

Ligations

Ligations were performed using a Rapid DNA Ligation Kit in accordance with manufacturer's guidelines. The insert/vector molar ratio was aimed to be 3:1. 5µL of the reaction were transformed into

chemically competent *E. coli*. 90% of the transformation reaction was plated out on LBA plates overnight.

FastAP Thermosensitive Alkaline Phosphatase was used to prevent the vector backbone from re-ligating. The phosphatase reactions were carried out as per manufacturer's instructions.

A control with no T4 ligase enzyme and with the 'backbone' only were set up alongside all ligations to test the ligation efficiency and for the ligated vector size comparison.

Standard digestion reactions

All reactions were performed at 37°C, except where advised otherwise in the manufacturer's instructions, for 2h in the buffers supplied. An excess of 5U of enzyme per 1µg of DNA was used.

Agarose gel electrophoresis

Agarose gel electrophoresis was performed in a MultiSub Horizontal gel electrophoresis system for 40-60 min at 80-100V.

Preparation of *ura3Δ* fragment

The pJL164 vector (Cat# 87471, ATCC) was digested with *SpeI* and *XhoI* enzymes to release the *ura3Δ* cassette of approximately 3000 bp. This fragment was separated from the backbone on the agarose gel, then purified. 1µg of the fragment was used per transformation as detailed in the standard yeast transformation protocol.

Yeast 'Gap repair'

The first step of the yeast gap repair procedure is yeast transformation with the fragments to be ligated. For this, the standard yeast transformation protocol was used (2.2.1.2). The second step was to extract the plasmids and transform them into *E. coli* because the yield of the yeast plasmid extraction is too low for any further analysis. The previously described release of plasmid from yeast was followed [68]. Briefly, a 1.4mL of overnight culture of selected colonies was pelleted, resuspended in 200µL of plasmid release reagent, 200µL phenol-chloroform, and 300µL of glass beads. The cell

mixture was vortexed for 2min, spun at 15,000rpm for 5 min to separate the organic and aqueous layers. 5µL of the aqueous layer was transformed into E. coli as described in section

2.2.3.3. Polymerase chain reaction protocols and equipment

Protocols

Table 2.8 The list of PCR protocols

Step	Protocol 1		Protocol 2		Protocol 3		Protocol 4	
	Temp., °C	Time, s	Temp., °C	Time, s	Temp., °C	Time, s	Temp., °C	Time, s
Initial denaturation	95	180	95	120	95	600	95	600
Denaturation	95	30	95	20	95	20	95	20
Primer annealing	65	30	60	20	57/60	20	57	20
Extension	72	120	72	30	72	90	72	360
Final extension	72	300	72	180	72	180	72	600

Steps 2-4 were repeated 34 times.

Primer design

- Primers were designed and selected based on ΔG (hairpin) and ΔG (dimer) energies, self-annealing and 3' annealing properties. The online Primer-Blast (<https://www.ncbi.nlm.nih.gov/tools/primer-blast/>) and NetPrimer (<http://www.premierbiosoft.com/netprimer/>) tools were used to design primers.
- Primers for sequencing the genes after ligation into new vectors were designed to cover the whole gene in around 300-400bp fragments. Forward and reverse primers were used, and were also designed to extend into 5' and 3' end flanking regions.
- All sequencing were carried out at GSK's in-house sequencing facilities.

2.2.3.4. Plasmid construction

All vector and plasmid maps can be found in the **Appendix B**.

p426GPD-ADRB1 plasmid

The *ADRB1* gene was amplified using b1_for_1 and b1_rev_1 primers (**Table 2.6**) using vector #2 as a DNA template. 10% DMSO was required in order to increase primer annealing temperature. Extensive optimisation of the PCR was performed, however multiple PCR products were unavoidable. To overcome this issue the PCR product was separated on 1.1% agarose-1x TAE gel for 70min at 90V.

Bands of nearly 1500bp size were well separated from other bands on the gel, making it easy to excise using a scalpel. The DNA was purified from the gel and digested with *Bam*HI. The DNA was then purified using the phenol-chloroform-ethanol extraction method. The digested and purified *ADRB1* gene fragment was ligated into p426GPD vector backbone which was also digested with *Bam*HI and dephosphorylated with FastAP in preparation for ligation.

*Bam*HI, *Sac*I and *Xma*I endonucleases were used to identify the correct orientation of the inserted fragment (see 4.1.1).

p426GPD-ADRB2 plasmid

The *ADRB2* gene located in plasmid #3 (**Table 2.7**) had *Bam*HI sites conveniently located at 5' and 3' ends of the gene. Therefore the plasmid was digested, separated on agarose gel and excised for purification. The p426GPD backbone was also digested with *Bam*HI, dephosphorylated with FastAP and purified.

*Bam*HI, *Sac*I, *Eco*NI + *Eco*RI endonucleases were used to determine the correct orientation of the inserted fragment (see 4.1.1).

p426GPD-MF α -ADRB1 plasmid

For the *ADRB1* gene to be inserted in p426GPD-MF α (#4, **Table 2.7**) in-frame with the pre-pro leader sequence upstream of the 5' end, restriction sites *Nco*I at the 5' end and *Bam*HI at the 3' end were used. The gene was cut out from the p426GPD-ADRB1 plasmid (#6, **Table 2.7**) in which two *Bam*HI sites exist – one at the 3' end of the *ADRB2* gene, and the second once at the 5' end, just 5bp upstream from the *Nco*I site. Therefore, the gene donor plasmid #6 was first digested with *Bam*HI, and then separated by standard gel electrophoresis. The lower band was purified from the gel and further digested with *Nco*I to give the correct 'sticky ends'. The p426GPD acceptor vector was digested with *Nco*I and *Bam*HI simultaneously. The ligated plasmid was analysed with a double *Nco*I + *Bam*HI digest to demonstrate the presence of the insert, and with a single *Bam*HI digest to show that only one *Bam*HI restriction site was present as predicted (**Figure 4.2**).

p426GPD-MF α -ADRB2 plasmid

The same design strategy was applied as for the p426GPD-MF α -ADRB1 plasmid; the gene was inserted into *NcoI* at the 5' end and *BamHI* at the 3' end. Similar procedures were followed, however the gene donor plasmid p426GPD-ADRB2 (#7, **Table 2.7**) had two restriction sites for both enzymes. Firstly, it was cut with *NcoI*, which produced two bands of the predicted sizes. The lower band was separated on an agarose gel and purified. The retrieved DNA was then subjected to *BamHI* digestion to give correct 'sticky ends'. The backbone p426GPD-MF α was treated as before. Again, the ligated plasmid was analysed with a double *NcoI* + *BamHI* digest to demonstrate the presence of the insert, and with a single *BamHI* digest to show that only one *BamHI* restriction site was present as predicted (**Figure 4.2**).

p426GPD-Ste2L-ADRB1

The *ADRB1* gene was amplified using b1_For_2 and b1_Rev_2 primers (**Table 2.6**) which introduced *EcoRI* and *Sall* restriction sites at the 5' and 3' of the gene, respectively. Similarly to b1_For_1 and b1_Rev_1, primer amplification required the addition of 10% DMSO. Multiple unspecific products were separated on a 1.1% agarose-1x TAE gel. The correct size band was cut out and purified, then subjected to double *EcoRI* + *Sall* digestion. The purified DNA fragment was ligated into a donor plasmid #5 (**Table 2.7**) which had an Ste2L leader sequence upstream from the *EcoRI* restriction site. Single and double *EcoRI* and *Sall* digestions were used to confirm the insertion of the *ADRB1* gene.

p426GPD-Ste2L-ADRB2

The *ADRB2* gene was also amplified using primers b2_For_1 and b2_Rev_1 (**Table 2.6**) in order to introduce *EcoRI* and *Sall* restriction sites. No gel separation of the PCR product was required and the DNA was purified for digestion directly. After the double digest with the mentioned enzymes, the gene was ligated into plasmid #5 (**Table 2.7**) similarly to the *ADRB1* plasmid described above.

p306GPD-ADRB1 plasmid

The p426GPD-ADRB1 plasmid #6 (**Table 2.7**) was digested with *SpeI* and *HindIII* and so was the p306GPD vector #12. The purified digested *ADRB1* DNA fragment was ligated into a dephosphorylated purified backbone.

p306GPD-ADRB2 plasmid

The p426GPD-ADRB2 plasmid #7 (**Table 2.7**) was digested with *SpeI* and *HindIII* and so was the p306GPD vector #12. The purified digested *ADRB2* DNA fragment was ligated into a dephosphorylated purified backbone.

p306GPD-MF α -ADRB1 plasmid

The p426GPD-MF α -ADRB1 plasmid #8 (**Table 2.7**) was digested with *SpeI* and *HindIII* and so was the p306GPD vector #12. The purified digested *ADRB1* DNA fragment was ligated into a dephosphorylated purified backbone.

p306GPD-MF α -ADRB2 plasmid

The p426GPD-MF α -ADRB2 plasmid #9 (**Table 2.7**) was digested with *SpeI* and *HindIII* and so was the p306GPD vector #12. The purified digested *ADRB2* DNA fragment was ligated into a dephosphorylated purified backbone.

p426GPD-ERG5 plasmid

The 3_ERG5 and 4_ERG5 primers (**Table 2.6**) were used to amplify the *ERG5* gene and sequences flanking 5' and 3' ends. The PCR product was then digested with *EcoRI* to obtain a 2622 bp fragment which was then inserted into the p426GPD plasmid at the same restriction site to obtain p426GPD-ERG5. The *EcoRI* sites were endogenously present in the genomic sequence close to the primer annealing sites.

SacI restriction was used to determine the correct orientation of the inserted fragment.

p426-ERG6 plasmid

The 3_ERG6 and 4_ERG6 primers (**Table 2.6**) were used to amplify the *ERG6* gene and the sequences flanking 5' and 3' ends. No usable endogenous restriction sites were present therefore aforementioned primers were designed to include *SacI* restriction site 5' of the PCR product and *EcoRI* at the 3' end. These restriction sites were used to insert the fragment into p426GPD. In this process the GPD promoter was lost, however, the promoter was not required for this cloning strategy.

p426GPD-erg5-DHCR24-cys1t-erg5 plasmid

The *DHCR24* gene was synthesised by GenScript and supplied in the pUC57 vector. The gene was cut out at the *SacI* and *BamHI* sites at 5' and 3' ends respectively. The yeast 'gap repair' method was used to insert the gene into the p426GPD-ERG5 by homologous recombination, replacing the *ERG5* reading frame with *DHCR24*. The p426GPD-ERG5 was linearised with *BalI* which linearises the plasmid within *ERG5* prior to reaction set up. Correctly ligated clones were selected by *HindIII* digestion, which linearises the plasmid if the *DHCR24* gene is present while cutting it into 1376 and 7848 bp fragments if *ERG5* is present.

p426-erg6-DHCR7-cys1t-erg6 plasmid

The 'gap repair' method was not successful for this method, therefore an alternative Gibson Assembly method was used. For this, the p426-ERG6 plasmid was digested with *Van91I* and *AgeI* to cut out a large fragment from the *ERG6* region within the plasmid. The synthesised pUC57-DHCR7 plasmid was digested at *XbaI* and *SmaI* to release the *DHCR7* gene fragment. The purified DNAs were set up in a reaction according to manufacturer's instructions and later transformed into *E. coli* 5α F'lg strain.

The correctly-ligated colonies were identified using *BamHI*, *HindIII*, and *PvuII* enzymes which cut the *DHCR7* and *ERG6* gene-containing plasmids differently (see **Figure 6.7**)

pAUR135-erg5-DHCR24-cys1t-erg5 plasmid

The final plasmid for *DHCR24* integration into the *S. cerevisiae* genome, the integration cassette, consisting of *ERG5* upstream sequence (termed promoter), the *DHCR24* gene, *ERG5* downstream sequence and *CYS1* terminator sequence, was inserted into the MCS of pAUR135 vector at the *EcoRI* restriction site.

pAUR135-erg6-DHCR7-cys1t-erg6 plasmid

Similarly to the previous plasmid the integration cassette, consisting of *ERG6* upstream sequence (termed promoter), the *DHCR7* gene, *ERG6* downstream sequence and *CYS1* terminator sequence, was inserted into the MCS of pAUR135 at the *SacI* and *EcoRI* restriction sites.

2.2.3.5. DNA purification methods

The DNA cut from agarose gel was purified from the gel using Wizard® SV Gel and PCR Clean-Up System and QIAquick PCR Purification Kit were used to extract the DNA from agarose gel according to manufacturers' instructions.

The DNA from PCR or other liquid reactions was purified using the QIAquick PCR purification kit according to the instructions provided in the kit or the phenol-chloroform-ethanol extraction method detailed below.

Phenol-chloroform-ethanol extraction method

- The DNA was extracted with 1vol of Phenol-chloroform. The mixture was mixed and spun at high speed for 5min. The top layer of the biphasic mixture was collected and transferred into a new Eppendorf tube.
- 2vol of absolute ethanol were added as well as 1-2 μ L of glycogen and sodium acetate to make up concentration of 0.3M. The mixed solution was let to precipitate for a few minutes, and then spun it at high speed for 5-10 min.
- The final wash was done with a large volume (~500 μ L) of 70% ethanol which was again spun at high speed for 5min.
- The supernatant was removed completely, letting the pellet to dry for a couple of minutes.
- The pellet was re-suspended in a small volume of water.

2.2.5. Membrane isolation and western blotting procedures

2.2.4.1. Membrane isolation

Yeast cultures were grown in 50mL WHAUL-5.5 + His (+ Ura for untransformed samples) until OD₆₀₀ of 2.0-2.5, pelleted at 600g for 4min, room temperature, and resuspended in 1mL buffer 'A'. The cell suspension was transferred into breaking tubes and again pelleted to remove the buffer. Next, the pellet was resuspended in 500 μ L of breaking buffer, from which point the samples were kept on ice at all times. 1mL of acid-washed beads was added along with PIC at 1:500 dilution. The cells were disrupted in TissueLyser LT (Qiagen) for 10min at 50 oscillations per second. The lysate transferred into a fresh Eppendorf tube and spun at 15,000rpm for 15min to separate the membranes from cellular debris and the beads. Final ultra-high speed centrifugation at 66,000rpm was carried out for 60min

during which all membranes were pelleted. The supernatant was removed. The membranes were left to soak in 100µL membrane resuspension buffer overnight at 4°C.

The concentration of total protein was determined the next date using the BCA assay (see below).

2.2.4.2. BCA assay for membrane protein concentration

BCA and cupric sulfate were mixed at 50:1 ratio. BSA standards were added at 20µL into 180µL of the assay mix. 5µL of test samples were mixed with 15µL of membrane resuspension buffer and then with 180µL of BCA assay mix. The standards and test samples were incubated at 37°C for 10min and then measured at 562nm. The standard curve was plotted from the standard measurement to determine $y = mx + b$ where x was the protein concentration and y the absorbance at 562nm.

2.2.4.3. Sample preparation

35-70µg of total yeast membranes, isolated from a range of *ADRB1* and *ADRB2* receptor expressing yeast, were incubated with reducing SDS sample buffer and membrane resuspension buffer on ice for 1h before loading on the gel.

2.2.4.4. Acrylamide gels

To make the gel, the reagents were mixed in the order as listed in the recipe (2.1.5.1). The separating gel was made first and left to set for 20 min. Then, the stacking gel was prepared.

Both in-house made and pre-made gels were run at 130V for around 60-100min until the blue dye reached the bottom.

2.2.4.5. Protein transfer

Proteins from the acrylamide gel were transferred onto a nitrocellulose membrane sandwiched between filter paper sheets, immersed in transfer buffer and an ice pack for 50 min at 100V.

For dry transfer, the proteins were transferred onto a PVDF membrane using iBlot dry transfer system from Invitrogen for 7min on setting P3.

2.2.4.6. Antibody directed detection of β 1-AR and β 2-AR

The membrane was blocked in milk-PBS for 1h before adding the primary antibody at 1:5000 dilution. The primary antibody was added and incubated over-night at 4°C. The unbound antibody was washed off with Tween wash buffer in 3x 5min washes. The secondary HRP conjugated antibody was agitated in milk-PBS for 1h at 1:5000 dilution and after washed as before.

The chemiluminescence signal was detected after the 3min incubation with the HRP substrate. GeneSnap software was used to acquire the images from the Syngene G:Box equipment.

Chapter 3 – Optimisation of the yeast functional GPCR assay

3.1. Introduction

The yeast functional GPCR assay for functional studies of G protein-coupled receptors (GPCRs) has been designed for the high-throughput screening of compound libraries for potential GPCR-interacting molecules. As with most high-throughput technologies, there are parameters that can be adjusted for a particular target, in this case a different GPCR. Because this assay is live cell-based, it is particularly amenable. Nevertheless, it is essential that the assay is reproducible with particular conditions to allow a reliable interpretation of the results. This chapter overviews the conditions and parameters that were tested using two strains – MMY25 with integrated p306GPD-ADRA2A plasmid and MMY20 with integrated p306GPD-ADRA2B plasmid, termed YIG152 and YIG153 respectively. These strains express recombinant adrenoceptors α_{2A} and α_{2B} respectively. Finally, the concluding results illustrate the effect of varying assay parameters on the readout and apparent pharmacology.

The summary of assay conditions discussed in this chapter:

- Stringency of background growth control with 3-AT
- Substrate concentration effects on the signal
- Instrument dependent signal dynamic range
- Experiment-to-experiment variability

Figure 3.1 The workflow of the yeast functional GPCR assay set up. The assay generally takes three days from inoculation to data collection. Key steps and components are noted.



3.2. Effects of 3-amino triazole on reporter signal strength

The 3-amino triazole (3-AT) is used in this assay to control the unspecific background signal by inhibiting the *HIS3* gene product which has a key role in histidine synthesis. Generally in other systems where this reporter gene is used, the stringency of background inhibition can be adjusted by titrating the concentration of 3-AT [69]. To investigate whether the same applies to our assay system and to what extent, concentrations of 3-AT ranging from 2 to 50mM were tested in YIG152 (α_{2A} -AR) and YIG153 (α_{2B} -AR).

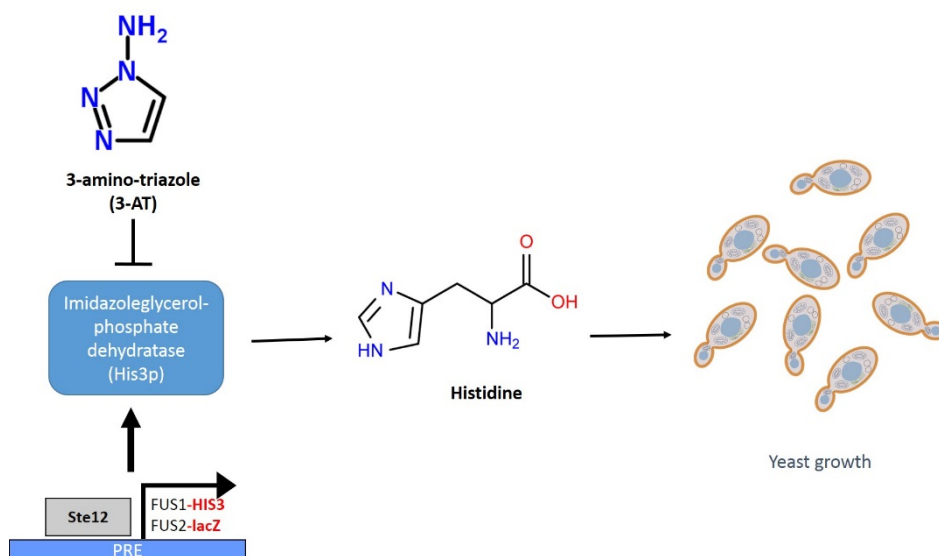


Figure 3.2 The inhibition of His3p by 3-amino triazole. 3-AT has been used to control the background growth by inhibiting the activity of imidazoleglycerol phosphate dehydratase, a product of *HIS3* gene which is often used as a reporter gene including the MMY yeast assay for functional GPCR studies.

Figure 3.3 summarises the results of 3-AT titration on the α_{2B} receptor. The results combine data from two experiments carried out at the same conditions with 3-AT concentration as a single variable. Results are presented as relative fluorescence units (RFU) against log compound concentration in molar units. The background reporter expression is much higher in the YIG153 strain expressing α_{2B} -AR as compared to α_{2A} -AR. For example, at 2mM 3-AT **[A]**, regardless of compound concentration, the RFUs were very high and no concentration-response relationship was observable. At 5mM 3-AT **[B]** the fluorescence signal indicates an inhibition of the growth at lower compound 9 and 11 concentrations, however at a relatively low range of 50-140nM compound concentrations the signals plateaued. The pEC_{50} values for compounds 9 and 11 were generated using a non-linear three parameter fit, however, the concentration-response relationship appears to be too obscured by the high RFUs to judge whether those values are a true representation of the receptor stimulation. The 10mM 3-AT concentration lowered the unspecific yeast growth to allow the compound stimulation of the receptor

to produce more robust concentration-response curves for all three compounds [C] with a good fit, pEC₅₀ values, and a dynamic RFU range. At 20mM 3-AT [D] and [F] produced similar pEC₅₀ values for compounds 11 and 19, but a lower value for compound 9. The overall fluorescence also decreased by approximately 1x10⁶ RFUs indicating that the overall inhibition is more stringent. The same is true for 50mM 3-AT [E]: the RFUs reached only about 1.67x10⁶ at the highest E_{max} compared with 5.4x10⁶ RFUs observed at 10mM 3-AT.

Results presented in **Figure 3.4** show effects of three increasing concentrations of 3-AT on α_{2A} -AR receptor in YIG152, presented as relative fluorescence units (RFU) against log compound concentration in molar units. There was not much difference between the responses in the presence of 2mM (**Figure 3.4 [A]**) and 5mM [**B**] 3-AT in terms of fluorescence intensity and pEC₅₀ and E_{max} ([**D**] and [**E**]). The pEC₅₀ values were slightly lower at 5mM 3-AT [**D**]. At 10mM of 3-AT [**C**] there was a significant reduction in fluorescence, also reflected by the lower pEC₅₀ values. Compound 9 seemed to produce a stronger pathway activation in terms of His3 production to overcome the effects of the 3-AT inhibition compared with the other two compounds. Concentrations higher than 10mM 3-AT were not tested with this receptor, as a further reduction in signal would be expected.

Overall, 3-AT appeared to be a powerful modulator of His3 promoted cell growth and consequently the assay reporter signal. The inhibition required depends on the receptor type. The YIG152 yeast required less 3-AT to produce a desired signal window compared with the YIG153 which appears to have a high unspecific cell growth and required a more stringent background inhibition.

Out of the three compounds presented in section 3.2, compound 19 is commonly available under the generic name brimonidine or UK 14,304; the other two compounds are from the GSK compound library and therefore only available for testing on the GSK site. However, brimonidine as a previously characterised full α_{2A} -AR full agonist and α_{2B} -AR partial agonist was deemed to be a suitable control for further experiments on these receptors discussed in this chapter.

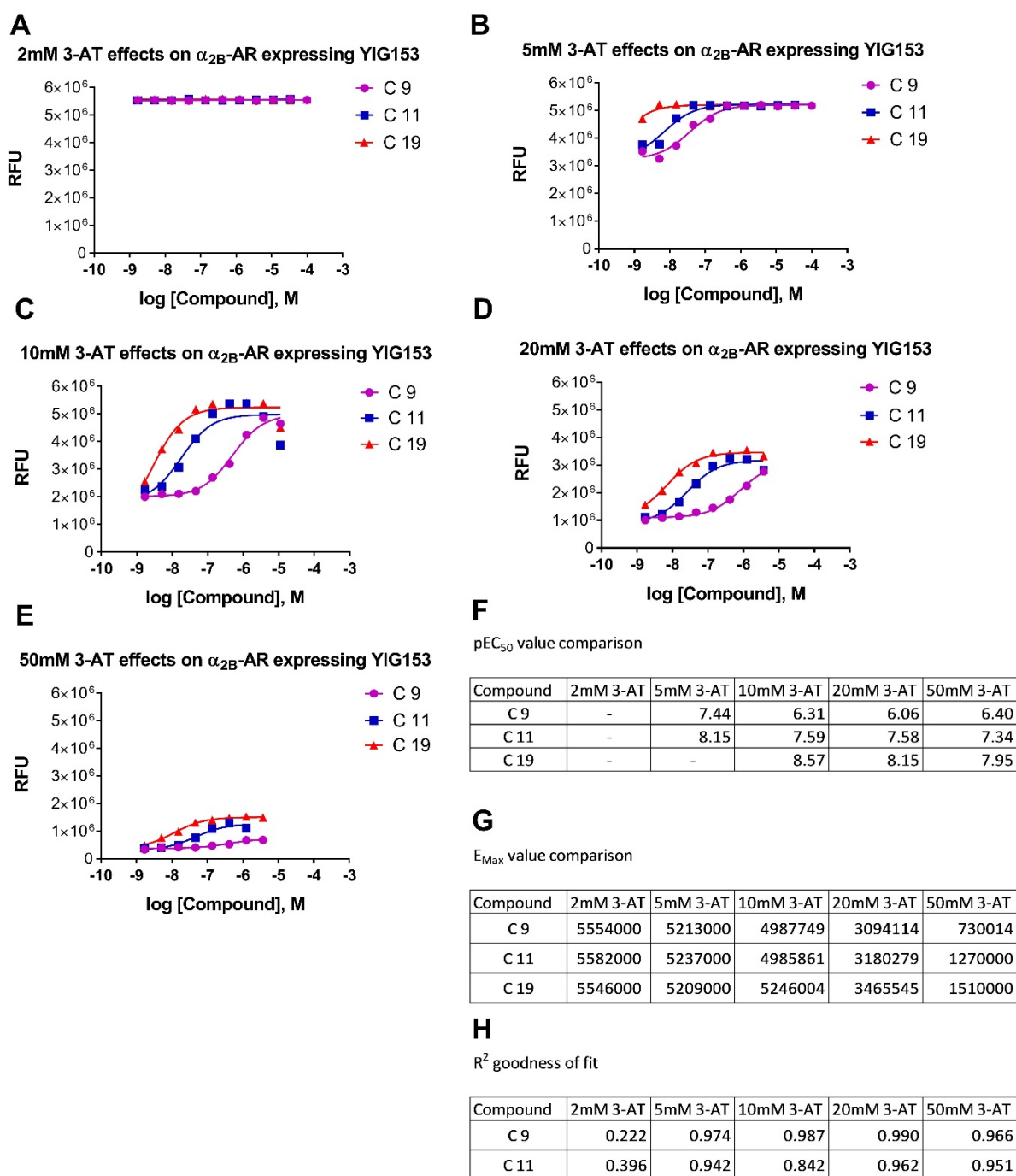


Figure 3.3 Effects of 3-AT on α_{2B} -AR receptor expressed in YIG153. The results are shown for fluorescence signal development on compounds 9, 11, and 19 with 2mM [A], 5mM [B], 10mM [C], 20mM [D], and 50mM [E] 3-AT. The pEC₅₀ values were obtained from a non-linear three parameter fit using GraphPad Prism, V6. Panels [A] and [B] indicate that 2mM and 5mM are not adequate to produce the concentration-response relationship expected for this receptor. Results in [C] show the widest signal window, while in [D] and [E] the inhibitory effect appears to be too strong and the positive signal is reduced along with the unspecific signal resulted from background growth. The pEC₅₀ values are summarised in [F], E_{max} in [G] and R² in [H]. For all the data in this figure n=1.

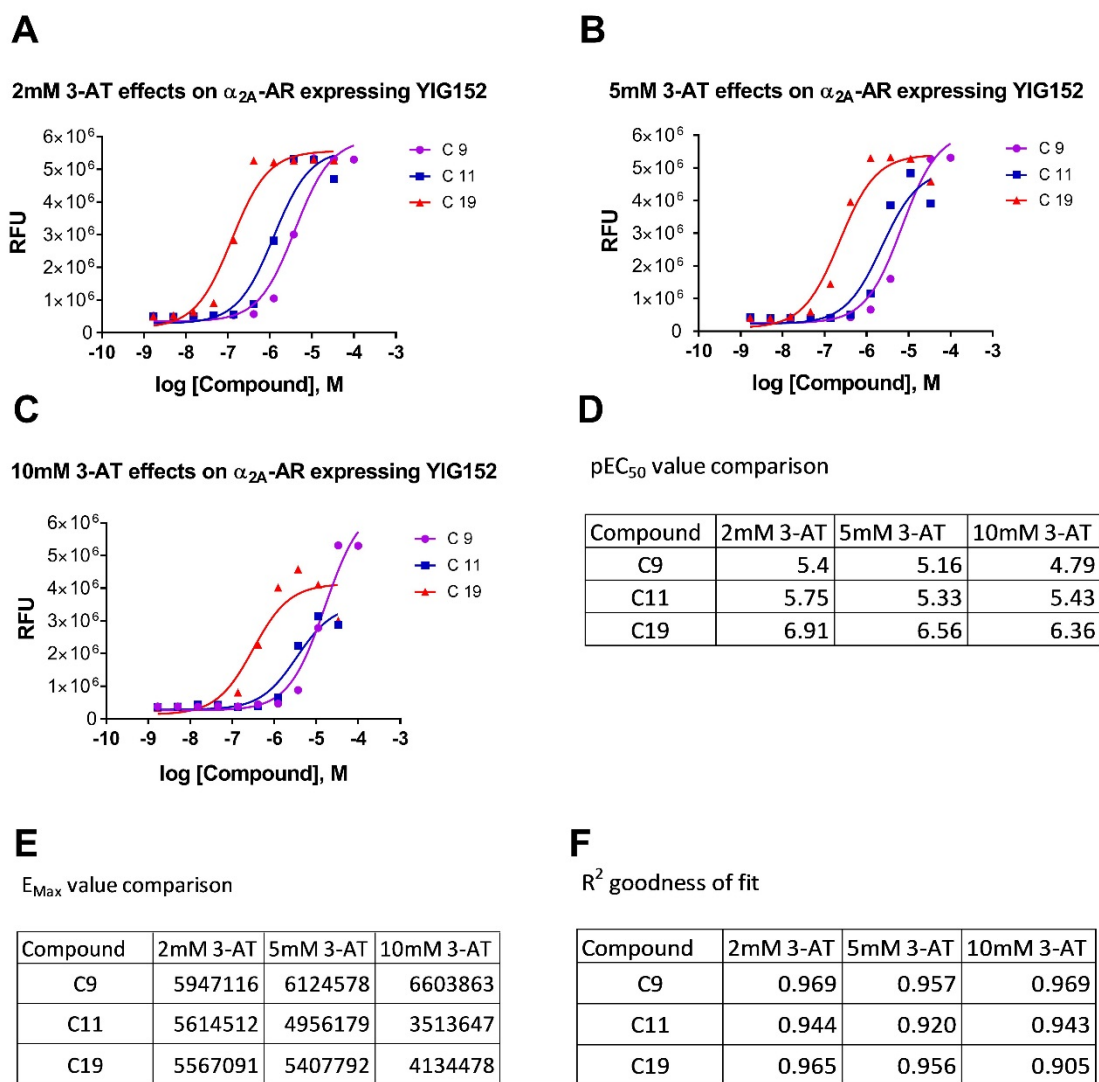


Figure 3.4 Effects of 3-AT on α_{2A} -AR receptor expressing YIG152. Compounds 9, 11, and 19 were incubated over the same period of 24h with an increasing 3-AT concentrations. In [A] the results at 2mM is shown, in [B] at 5mM, and in [C] at 10mM of 3AT. pEC₅₀ values did not change significantly and are summarised in the [D]. E_{max} values in [E] indicate that C9 was less affected by increasing 3-AT in terms of efficacy as compared to C11 or C19. R² [F] values indicate the goodness of data fit. n=1

3.3. Substrate concentration effects on the signal

Fluorescein di- β -D-glucopyranoside (FD-glu) is another important component of the assay mix. It acts as a substrate for the exoglucanase secreted in growing yeast cells, which use the enzyme to cleave off glucose from polysaccharides, and consequently upon cleavage releasing the fluorescein, the fluorescent molecule, from this conjugate. The concentration of FD-glu in the standard protocol is

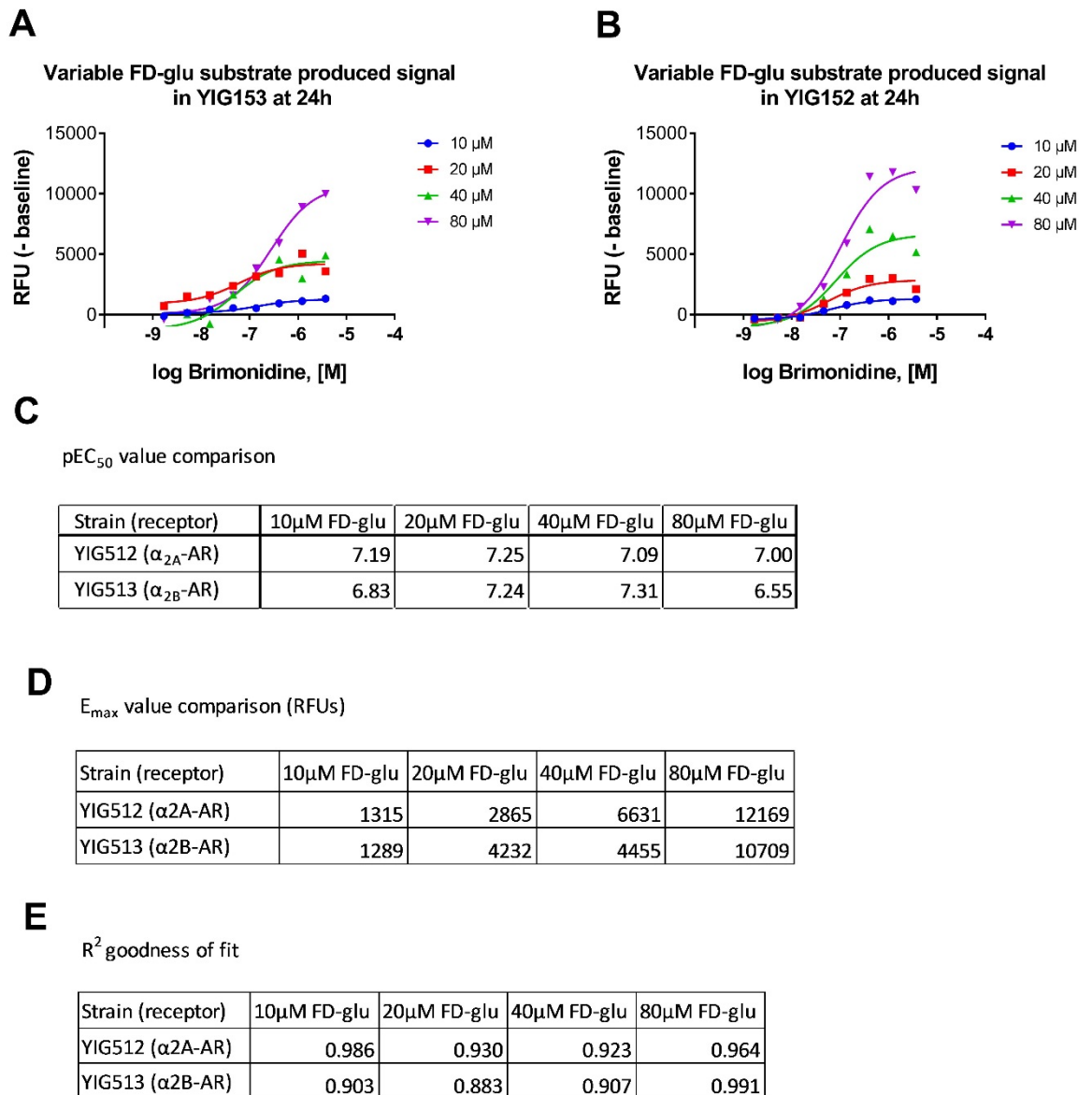


Figure 3.5 Effects of increasing FD-glu substrate on the signal development and pEC₅₀ of brimonidine. RFUs increase with FD-glu concentrations in YIG153 [A] and YIG152 [B]. 10 μ M (●) is the standard protocol concentration, but 20 μ M (■), 40 μ M (▲) and 80 μ M (▼) were also tested. Although 80 μ M FD-glu in the assay medium produced around a 10-fold increase in the RFU signal as compared to the starting 10 μ M concentration, the pEC₅₀ values did not increase significantly [C]. E_{max} [D] and R² [E] are also presented. The base line RFU was subtracted from the signal for a clearer representation of the stimulation-specific signal. n=1.

10 μ M. However, experiments were designed to assess how increasing the concentration of the substrate affected the output signal and the pharmacology of brimonidine on α_{2A} -AR and α_{2B} -AR. A range of 10-80 μ M of FD-glu in doubling increments was therefore tested and is presented in **Figure 3.5**.

Not surprisingly, with increasing substrate, the RFU values were higher in both experimental groups ([A] and [B]), 80 μ M of the substrate providing approximately a 10-fold increase in the signal window compared with the standard 10 μ M concentration. However, the pEC₅₀ values did not increase with the higher signal output, and did not vary significantly [C]. The maximum RFUs increased in both YIG152 and YIG153, although brimonidine is only partial agonist on α_{2B} -AR expressed in YIG153, suggesting that the additional substrate only increases the sensitivity of signal detection. Although the increase in the signal window might be beneficial for a weakly expressed and/or coupling receptor, the standard FD-glu concentration was adequate to produce the same pharmacological parameters as the higher concentrations of the substrate [C].

3.4. Instrument-dependent signal dynamic range

During the assay optimisation phase of the project it was noted that different instruments at GSK and Aston University produced a different scale of RFUs and their dynamic range. This was examined in order to assess whether it had an effect on interpreting the data. A side-by-side experiments with a range of 3-AT concentrations in YIG152 and YIG153 stimulated with brimonidine are presented in **Figures 3.6** and **3.7** respectively.

The first observation that can be drawn is that the three instruments used for the optimisation of the assay – EnVision (PerkinElmer), Gemini (Molecular Devices), and Mithras (Berthold) – generate a different magnitude of RFUs, which can be ranked in the following order:

1. EnVision (GSK) – 10⁶
2. Mithras (ASTON) – 10⁴ - 10⁵
3. Gemini (ASTON) – 10³

The extent of the signal window can be also ranked in a similar order, with the EnVision producing a 10-fold difference between the background RFU and E_{max} RFU on the YIG152 2mM 3-AT data, while Mithras and Gemini produce a 4-fold difference (deduced from **Figure 3.6** graphs [A], [B], [C]).

The other noticeable difference in **Figure 3.6** is that the E_{max} RFU drop substantially with increasing 3-AT concentrations, as recorded on the Mithras and Gemini instruments ([A] and [B]), while the RFUs obtained on the EnVision instrument [C] do not show such decrease in the E_{max}, ([D] and [F]) which indicates that this instrument is set for a different dynamic range (gain can be adjusted) than the other

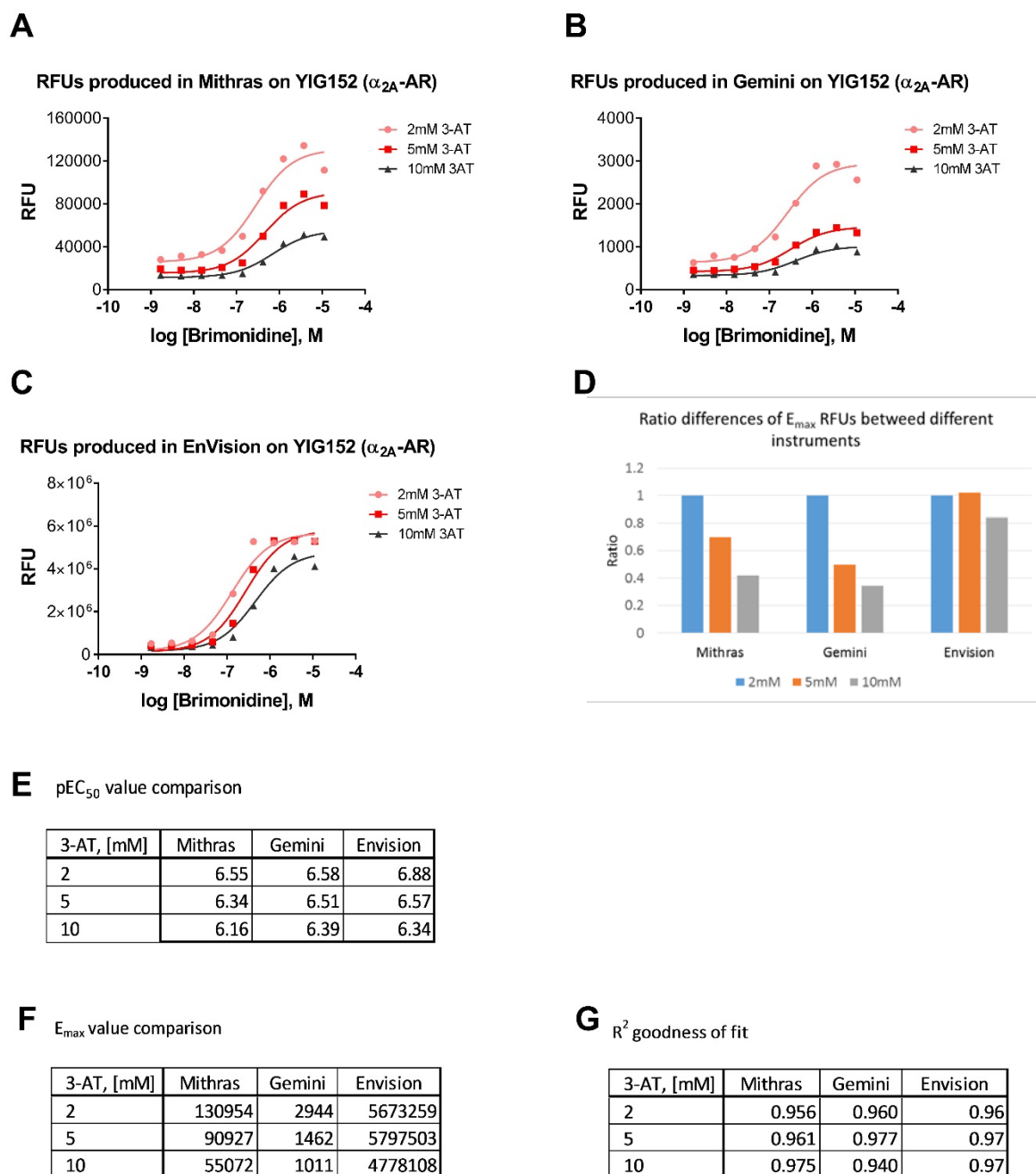


Figure 3.6 Variation of RFUs generated on different instruments in YIG152 strain. Three instruments were evaluated – Mithras [A], Gemini [B], and EnVision [C]. The EnVision data produced the greatest signal window between baseline and signal but showed little reduction in E_{max} RFU when 3-AT concentration was increased [C] and [D]. The Mithras – and Gemini – produced data showed a lower signal window, and a decrease in E_{max} RFU at 5mM and 10mM 3-AT as compared to the lower 2mM concentration, overall demonstrating how the RFU profiles can differ depending on which instrument is used [D] and [F]. The pEC_{50} values produced on different instruments did not differ significantly [E]. 3-AT induced largest drop of E_{max} RFUs on Gemini produced data while Mithras RFUs dropped proportionally [D]. The fit of the data for all experiments was $R^2 > 0.95$ [G]. $n=1$.

two instruments tested. The pEC_{50} values obtained with all three instruments, however, can still be averaged out with an acceptable variation [D], giving confidence in the robustness of the assay.

Interpreting the brimonidine-stimulated functional coupling of the α_{2B} -AR receptor in YIG153 is less straightforward. The signal window is smaller and is equal to an approximately 2-fold increase in all three instruments (**Figure 3.6**). As established in section 3.2, this strain has a higher unspecific background signal, but the smaller signal window can also be the result of a weaker stimulation, since brimonidine is only a partial α_{2B} -AR agonist, while it is a full α_{2A} -AR agonist. This could be investigated if both receptors were tested with dexmedetomidine or guanfacine, which are in reverse – full α_{2B} -AR agonists and a partial α_{2A} -AR agonists. Nevertheless, the high background growth at lower concentrations of the 3-AT, the brimonidine-specific RFU signal is obscured when measured using the EnVision, but is much clearer when the assay was measured on other instruments, indicating that not only did the assay condition play a role in this example, but also the instrument configuration has too.

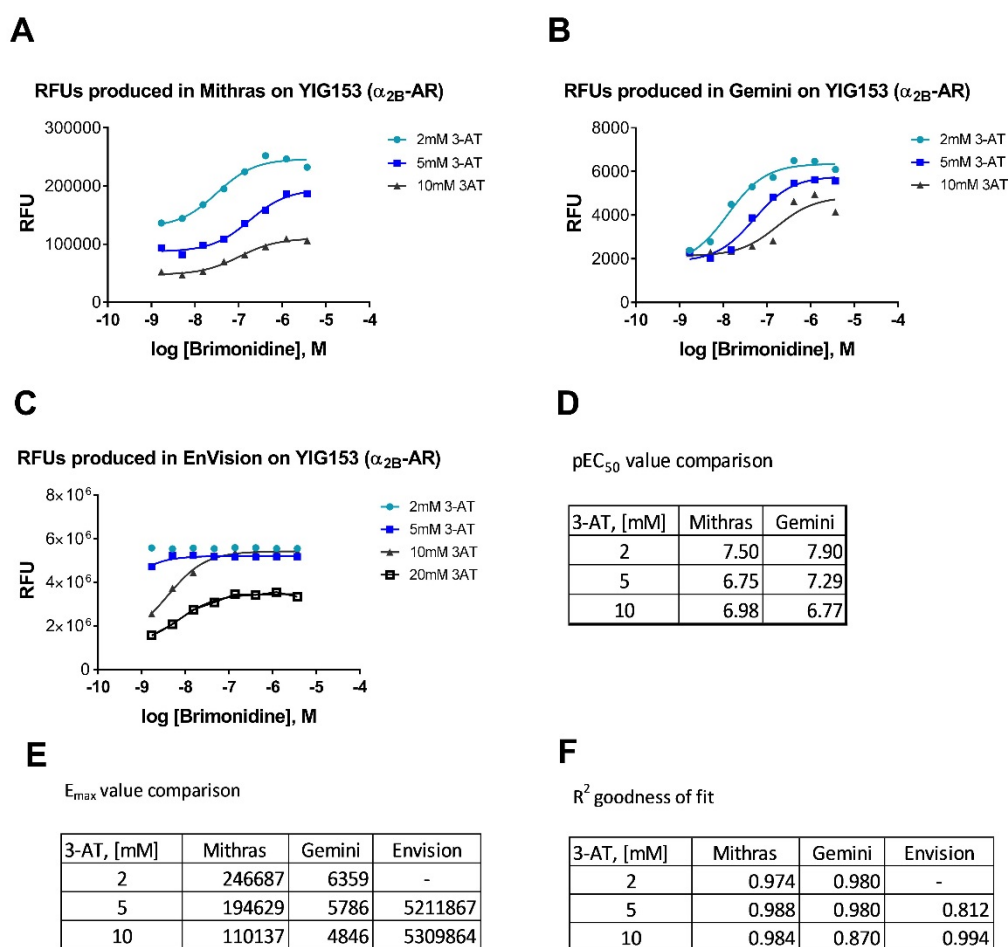


Figure 3.7 Variation of RFUs generated on different instruments in YIG153 strain. Similarly to figure 3.5 Mithras [A], Gemini [B], and EnVision [C] were evaluated in the strain expressing α_{2B} -AR. Because of the high background at low 3-AT concentrations, the EnVision generated data do not show a concentration-response relationship and therefore were not included in pEC₅₀ value analysis in [D]. The signal windows in all examples YIG153 are not as great as in the previous example, partly because the brimonidine is only a partial agonist of this receptor. E_{max} and R² values are shown in [E] and [F] respectively.

3.5. Experimental variation

Experimental variation is illustrated using a sample of data which are discussed in more detail in Chapter 5. These data were generated on the same instrument (SprectraFluor Plus, Tecan), therefore providing a more accurate representation of data variation that would be observed when setting up a drug screening project. The optimised β_1 -AR and β_2 -AR expression was assessed in various MMY strains carrying a different chimeric Gpa1-G α protein (please refer to the legends in **Figure 3.8** panels [A] and [B] or in [C]). Isoprenaline, or isoproterenol, is a well characterised, subtype non-selective β -AR full agonist, and was selected in this study as a control compound to which the data were normalised. The data were collected using the same conditions (please refer to the Methods section 2.2.2) but on different days with the aim to show experiment-to-experiment variation. The error bars on the data points in [A] and [B] indicate SEM. SEM of pEC₅₀ values are presented in [C]. Both indicators demonstrate that the experimental variation is reasonably low.

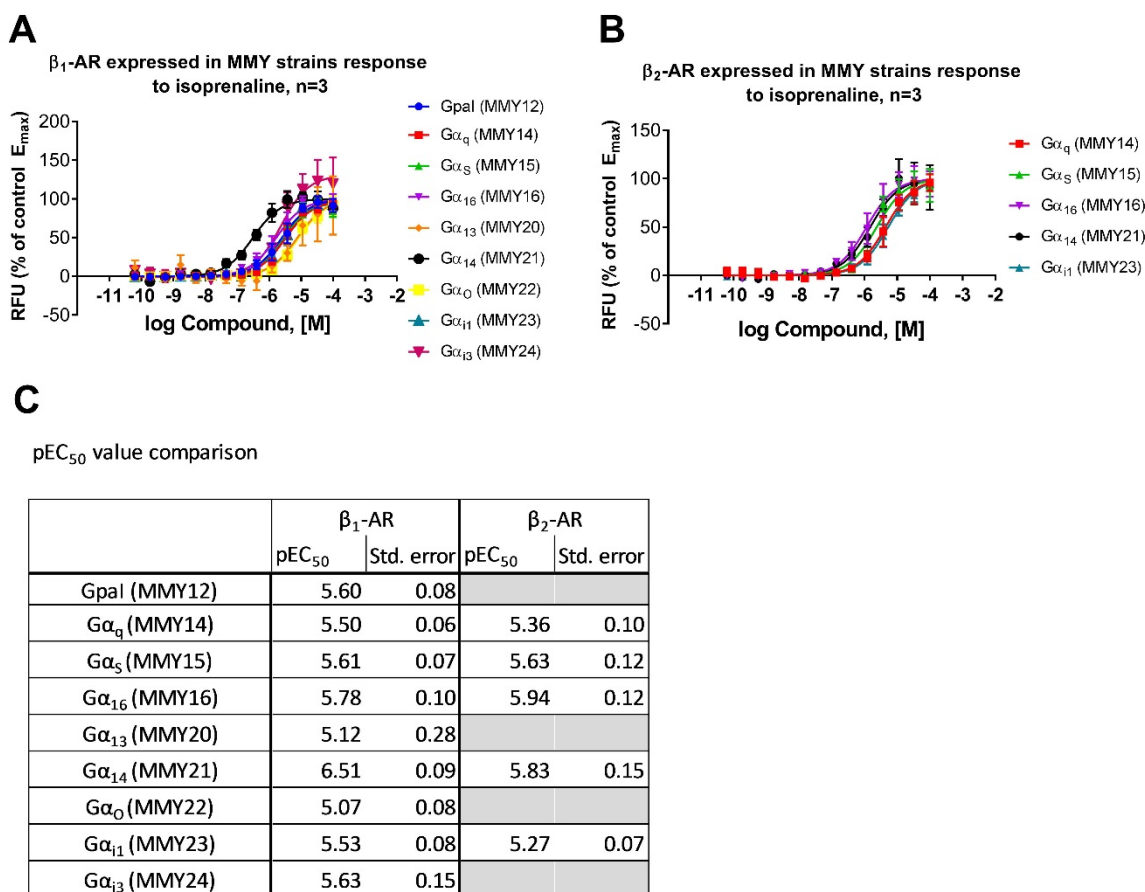


Figure 3.8 Experimental variation in β_1 -AR and β_2 -AR expressing strains. Isoprenaline stimulated responses in MMY strains expressing β_1 -AR [A] show acceptable error bars, expressed as the SEM, and similar pEC₅₀ values [C], with the exception of the G α_{14} (MMY21) strain. The β_2 -AR was found to couple to less strains and the error bars and the pEC₅₀ values are even less variable ([B] and [C]). The pEC₅₀ are expressed as a mean of 3 individual experiment values. The mean values and the SEM were obtained from the three-parameter curve fit model (Graphpad Prism, V7).

3.6. Compound screening on α_{2A} -AR and α_{2B} -AR in yeast

To demonstrate the utility of the yeast functional GPCR assay, a panel of 23 compounds of known and unknown activity on α adrenoceptors (see **Table 2.2**) were tested. The results at 2mM and 10mM of 3-AT are shown in **Figure 3.9** to illustrate the improvement after optimal 3-AT concentration was determined. The data shows that there are three potent α_{2A} agonists in this experiment (**[A]** and **[C]**). Three parameter non-linear fit analysis revealed pEC₅₀ values of 4.79, 5.46, and 6.34 for compounds 9, 11, and 19 respectively **[C]**. The remaining twenty compounds did not show significant effect on this receptor.

For the other receptor in this sub-family – α_{2B} – the profile appeared quite different (**[B]** and **[D]**). Nineteen compounds demonstrated strong to moderate agonistic effects at 10mM of 3-AT (**[D]**). Compound 22 shows a characteristic profile of a partial agonist. And finally, compounds 4, 8, and 21 appeared as inverse agonists and showed strong inhibition of growth and hence the fluorescent signal even at 2mM 3-AT which was generally too low to inhibit background growth to reveal agonistic effect of other ligands. In fact, compound 8 is yohimbine, a known α_2 antagonist [70]. Compounds 9, 11, and 19 showed potency as agonists on α_{2B} as well as on α_{2A} with pEC₅₀s of 6.48, 7.56, and 9.07 respectively (**[D]**).

Compound 19, which is generally known as UK 14,304 or brimonidine, is a potent α_2 agonist [71], which data presented in **Figure 3.9** confirm.

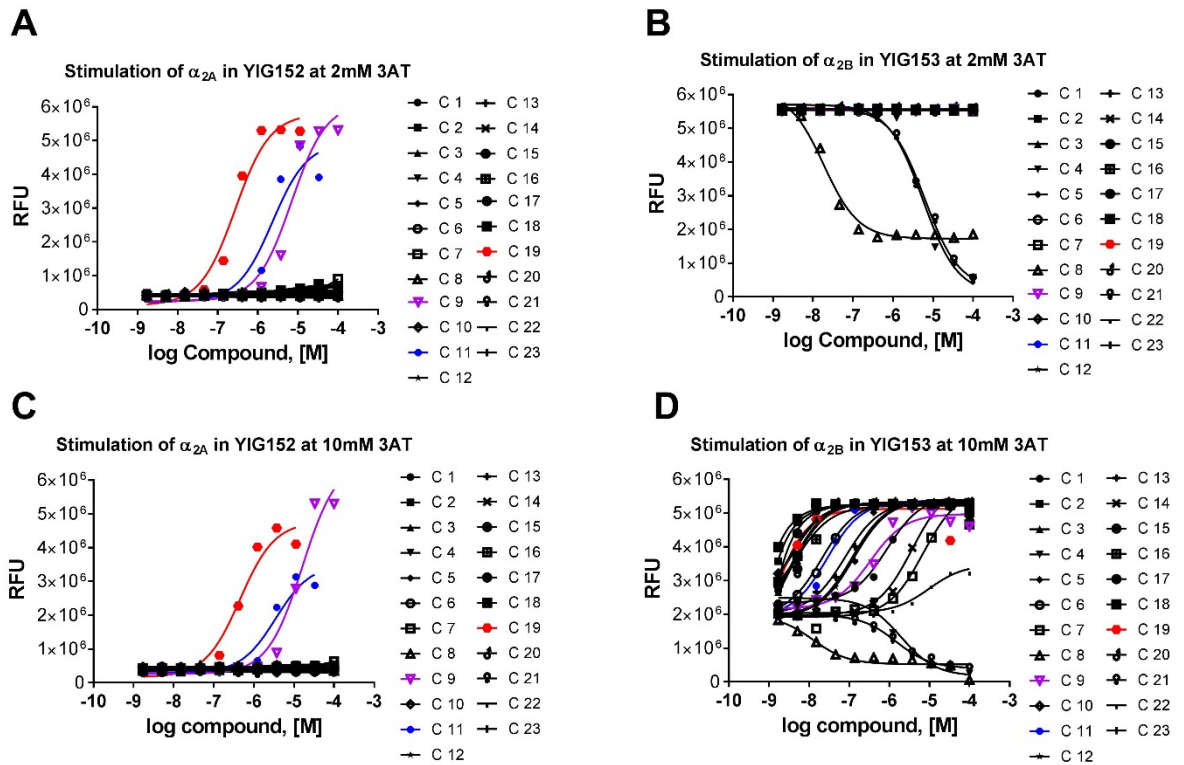


Figure 3.9 Compound profiling on α_{2A} and α_{2B} receptors. Results at 2mM [A] and 10mM [C] of 3-AT on α_{2A} receptor. The relative fluorescence units are plotted against log compound concentration in molar units. Compounds 9, 11, and 19 emerged as potent agonists of α_{2A} receptor. pEC₅₀ values for these compounds are 5.27, 5.74, and 6.59 respectively. Results at 2mM [B] and 10mM [D] of 3-AT on α_{2B} receptor. The majority of profiled compounds showed agonistic effect on the α_{2B} receptor with compounds 4, 8, 21, and 22 being an exception. Compounds 9, 11, and 19 appear to be potent agonists on the α_{2B} receptor, pEC₅₀ values of 6.34, 7.47, and 8.38 respectively. For all data in this figure n=1.

3.7. The parameter-dependent variations of the functional GPCR assay in yeast – what to expect and how to interpret the data

As with any pharmacological assay, it is important to establish which observations and changes can be attributed the interactions between the drug and the receptor, and which are the artefacts of the method. This chapter was aimed at establishing this in more detail than has been described in the past literature. In an industrial setting, the assay plate would be designed to include two controls: a positive – known full agonist, and a negative – a non-interacting molecule, each present in >8 wells, from which the 'Z' value is calculated. The purpose of these controls would be to build statistical significance in assay readiness, therefore the experimental variation associated with controls has to be well understood. The experiments described in 3.2 – 3.5 were aimed at understanding the behaviour of the positive control agonists, especially when attempting to express and characterise previously such as β_1 -AR and β_2 -AR receptors described in the later chapters. Some of the experiments were designed to confirm the observations previously made by colleagues at GSK, and some resulted from experience at the Aston University.

What was quickly apparent is that 3-AT is a powerful inhibitor of His3-induced growth, which in some strains results from a high unspecific expression of the *HIS3* gene. This could be explained by the activation of the *STE12* promoter by other factors than the G $\beta\gamma$ activated signalling cascade [72], although this effect would likely be consistent between the strains. Another important aspect of signalling fidelity is ratios of the G α and G $\beta\gamma$ subunits; lower G α ratio leaves uncoupled G $\beta\gamma$, weakly activating the signalling cascade, while higher ratio sequesters the G $\beta\gamma$ reducing the signal. During the last stage of the MMY strain engineering the chG α proteins were introduced last and possibly integrated with a different copy numbers, however chG α protein expression levels have been shown to be very similar [2]. Nevertheless, it was observed at GSK that some strains always produce higher background, indicating that it is the strain background rather than the GPCR that will determine high unspecific RFU signal in the assay.

Although this phenomenon can be controlled with variation of the 3-AT concentrations very effectively, what the 3-AT is less able to produce is a wider signal window, that is a difference between basal RFU and the maximum (E_{max}) RFU. If the ability of the agonist to keep the receptor in the active conformation is weak, as could be the case in α_{2B} -AR examples presented in **Figures 3.3** and **3.7**, then the increased 3-AT concentration not only inhibits the unspecific but also the signalling cascade-activated expression of His3 (**Figure 3.3 [C], [D], [E]**). The increased substrate FD-glu can somewhat increase the signal window (**Figure 3.5**) but it is a less desirable solution. If the control agonist is only able to produce several-fold signal induction, a pharmacology study of other modulators, such as potent partial agonists, would be difficult and perhaps even misleading, because in a small signal window lower efficacy may not be detected. Finding a more suitable control would be a better

solution, or look into other ways to improve the expression of the GPCR, which is discussed in results chapter 4. This is not always achievable because the pharmacology of GPCRs is a complex phenomenon and the role of the expression host are important, which is discussed further in this thesis.

The final conclusion of this chapter is that the assay parameters can be adjusted to fine tune the best signal window, but a robust expression of the receptor is required. The illustration of this principle is the fact that even sub-optimal conditions (such as high 3-AT, lower substrate concentrations, less sensitive instrument obtained RFUs) were able to demonstrate a similar potency of the full agonists brimonidine on the α_{2A} -AR expressing YIG152 as compared to the potency obtained at optimal conditions. It also shows that the functional yeast FD-glu assay is a robust method for assessing the pharmacology of the GPCR interacting molecules.

Chapter 4 – The functional expression of adrenoceptors β_1 and β_2 in MMY strains

4.1. Introduction

The adrenoceptors α_{2A} and α_{2B} expressed in the MMY yeast have been demonstrated in the previous chapter to facilitate a potential drug candidate high-throughput screening. Another sub-class of the adrenoceptors β_1 -AR and β_2 -AR are also drug targets for asthma, obstructive pulmonary disease, hypertension and other diseases. However these receptors were not successfully expressed in MMY strains at GSK in the past. The aim of this chapter is therefore is to investigate the different expression methods in the pursuit of functional expression of these two receptors.

There are generally two methods for introducing recombinant genes for protein production in yeast – the first one relies on the gene being integrated in a specific locus together with transcription initiation elements upstream of the reading frame. In the second method, the genetic design of the expression cassette may be the same but the plasmid, in which these elements are constructed, is able to replicate independently from the genetic DNA in a form of the circular plasmid. Both methods have been tested and presented in this chapter. Furthermore, different leader sequences, or cell surface expression signals, have been described in the literature that have various effects on membrane protein expression and localisation. In order to identify the best plasmid construct for the functional expression of adrenoceptors β_1 and β_2 Ste2 receptor N terminal and the mating factor α leader sequences (MF α) were tested.

The episomal p426GPD plasmid transformant screening results indicate leader sequence and receptor dependent effects. Potentially coupling MMY strains - $G\alpha_s$, $G\alpha_q$, $G\alpha_{14}$ and Gpa1 (native yeast $G\alpha$) – were identified for β_1 -AR receptor. However, all β_2 -AR transformants seem to have lost any coupling over time. For this reason the functional expression of both receptors was tested using integrating p306GPD plasmids which is discussed in **section 4.2**. A major finding of this chapter is that the functional expression of β_2 -AR was finally achieved. Both receptors β_1 -AR and β_2 -AR remained stably expressed over time, allowing for further pharmacological characterisation for the first time in the MMY yeast strains. The **section 4.3** compares to the protein expression differences between these different expression systems. It was found that non-functional colonies did not express the β -adrenoceptor but further work is needed to investigate what it means in terms of cellular response and receptor localisation.

4.2. Episomal p426GPD plasmids for the expression of β_1 -AR and β_2 -AR

Episomal expression plasmids are a useful tool in identifying the best coupling in chG α strains for individual receptor in MMY strains because they are maintained at high copy number [73] in the cell and when a strong constitutive promoter, such as GPD, is used the expression of the gene of interest is usually very efficient [73]. Furthermore, the 2 micron origin of replication present in the plasmid allows it to propagate independently and genomic integration is not required, increasing the success of the yeast transformation. The p426GPD series vectors were used in this work with and without additional leader sequences, such as MF α and Ste2p secretion signals, upstream from 5' end of the gene of interest.

4.2.1. The construction of p426GPD-(MF α /Ste2)-ADRB1 and p426GPD-(MF α /Ste2)-ADRB2

Three variants of p426GPD were used to construct episomal expression plasmids – p426GPD (standard with no leader sequence), p426GPD-MF α , and p426GPD-Ste2L. The latter two contain secretion signal for protein translocation into the plasma membrane. The ADRB1 and ADRB2 genes were inserted into the MCS using conventional molecular biology tools. The strategy for each plasmid type is described below and the detailed procedures can be found in the Methods and Materials section and **Appendix B**.

'The standard' p426GPD-ADRB1/ -ADRB2 expression constructs

The ADRB1 (1434bp) and ADRB2 (1242bp) genes were inserted into the p426GPD vector (6602bp) using the *Bam*HI endonuclease site. The ADRB1 gene was obtained by PCR amplification from the p426GPD-DEST-ADRB1 plasmid template and the ADRB2 was cut out from the p426GPD-HA-ADRB2 plasmid (both these plasmids were constructed in GSK). The reason behind constructing these plasmids was to compare the receptors' expression without any additional sequences, such as the 'Gateway' cloning sequences and the HA tag. Several endonuclease digestions were performed to select for plasmids with a ligated insert, and, because the *Bam*HI digested gene fragments were able to insert in the correct or the reversed order, correct orientation of the insert was tested too:

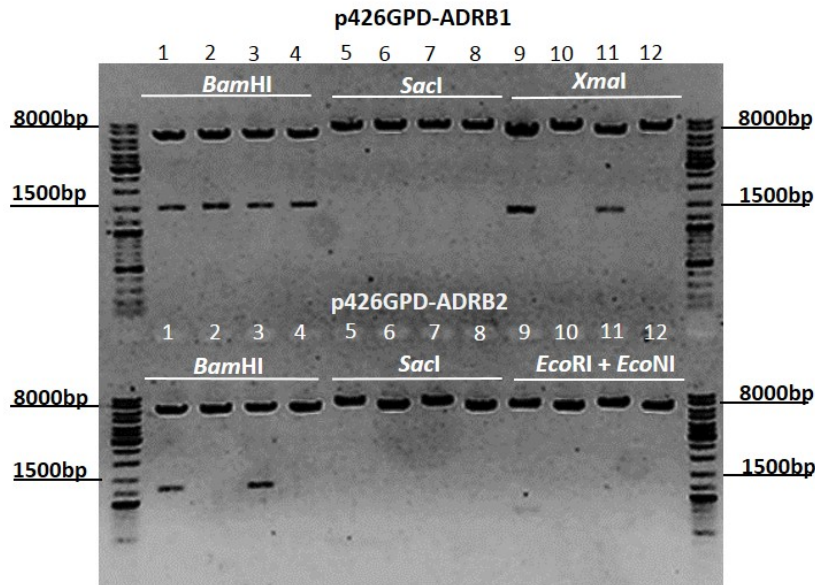


Figure 4.1 Construction of p426GPD-ADRB1 and p426GPD-ADRB2. The top panel depicts the results of p426GPD-ADRB1 selected clones that were digested with *Bam*HI (lanes 1-4), *Sac*I (lanes 5-8) and *Xma*I (lanes 9-12). Although lanes 1-8 show that all plasmids had the insert, lanes 9 and 11 show an additional band of around 1200bp, indicating that the gene in these plasmids has been inserted in a reversed orientation. Therefore only clones 2 and 4 (lanes 10 and 12) have the correctly inserted gene. In the bottom panel p426GPD-ADRB2 digestion results are shown. In this case only clones 1 and 3 had a gene inserted as demonstrated by the *Bam*HI (lanes 13 and 15) and *Sac*I (lanes 17 and 19) digestion patterns. However, clone 1 when digested with *Eco*RI and *Eco*NI double digestion (lane 21) revealed an additional band of around 700bp which indicates a reverted orientation. Clone 3 (lane 23) has however, produced the correct size bands and was selected as a positive ligation result for this plasmid.

p426GPD-ADRB1

- 1) *Bam*HI: 2 fragments 1444bp + 6602bp;
- 2) *Sac*I: 1 fragment – 8046bp if insert is present, 6602bp if no insert;
- 3) *Xma*I: 2 fragments – 171bp + 7875bp if correct insertion, 1285bp + 6761bp if reverse orientation.

p426GPD-ADRB2

- 1) *Bam*HI: 2 fragments 1248bp and 6602bp;
- 2) *Sac*I: 1 fragment – 7850bp if insert is present, 6602bp if no insert;
- 3) *Eco*NI + *Eco*RI: 2 fragments – 525bp + 7325bp if correct insertion, 756bp + 7094bp if reverse orientation.

The correct plasmid constructs were successfully identified; the results of this are depicted in **Figure 4.1**.

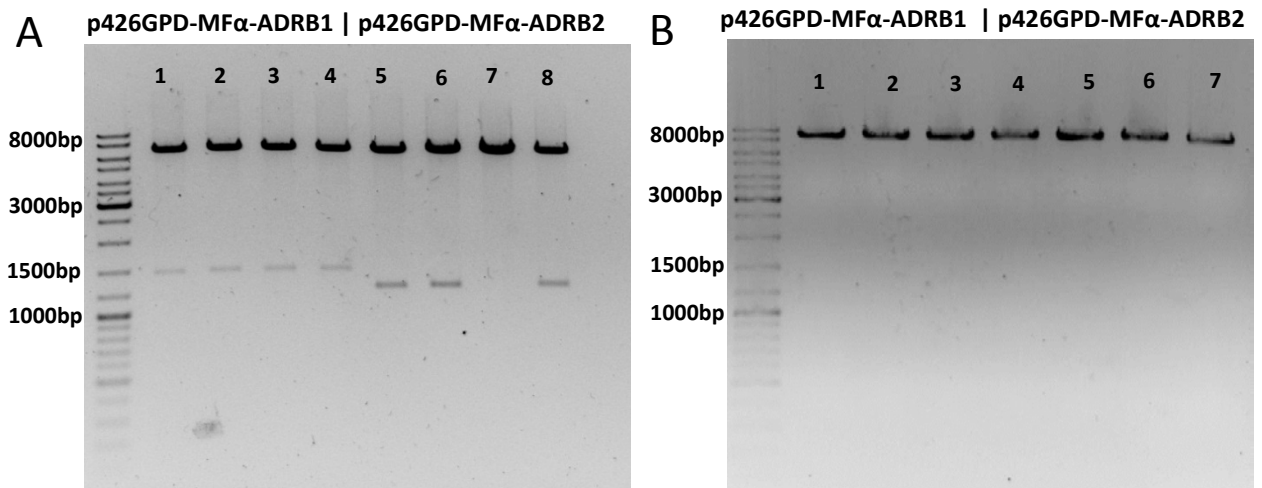


Figure 4.2 Construction of the p426GPD-MFα-ADRB1 and p426GPD-MFα-ADRB2. Two restriction analyses were performed with [A] *NcoI* and *BamHI* enzymes, lanes 1-4 on the *ADRB1* construct and lanes 5-8 on the *ADRB2* construct, revealing that only *ADRB2* plasmid clone 3 (lane 7) did not have the insert. [B] The restriction with *BamHI* confirmed that in all 7 selected plasmids, the *ADRB1* construct in lanes 1-4 and the *ADRB2* construct in lanes 5-7, the second *BamHI* restriction site at the 5' end present in the donor vector has been deleted, as the enzyme is shown to cut only once. The small MFα leader sequence fragment has been inserted just downstream from the GPD promoter in both vectors. The constructs were designed so that upon activation via the GPD promoter the MFα leader and β₁-AR or β₂-AR would be translated as one protein with a short linker between the two subunits.

The mating factor α p426GPD-MFα-ADRB1 / -ADRB2 expression constructs

The second set of plasmids depicted in **Figure 4.2** was designed to have a 242bp fragment of mating factor α sequence linked to the 5' end of the gene. This fragment was already present in the parental vector designated p426GPD-MFα. Just as the 'standard' empty p426GPD, this vector has also a GPD promoter upstream of the MFα leader sequence, then a MCS for a convenient insertion of desired genes, and the *CYC1* terminator downstream. The insertion of the *ADRB1* and *ADRB2* genes into the p426GPD-MFα was carried out using the *NcoI* endonuclease site at the 5' end of the gene and *BamHI* at the 3' end for both of the genes. Digesting the parental plasmid and the p426GPD-ADRB1/ADRB2 plasmid, from which the genes of interest were obtained, with these enzymes resulted in the compatible ends at the correct orientation, therefore only the presence of the fragment was sufficient for confirming that the right construct was obtained following the ligation procedure.

The Ste2 pre-pro leader sequence containing p426GPD-Ste2L-ADRB1 /-ADRB2 expression constructs

Similarly to the p426GPD-MFα vector, the p426GPD-Ste2L has a 39bp leader sequence upstream from the MCS. The PCR amplified *ADRB1* and *ADRB2* genes were inserted into this parental vector at the *EcoRI* site at the 5' end and the *Sall* at the 3' of the gene. The resulting predicted plasmid maps are

available in the **Appendix B**. One clone of each plasmid with the inserted gene was analysed using the same *EcoRI* or *SalI* endonucleases to demonstrate the full size of the linearised plasmid or both enzymes to show the inserted fragment (**Figure 4.3**).

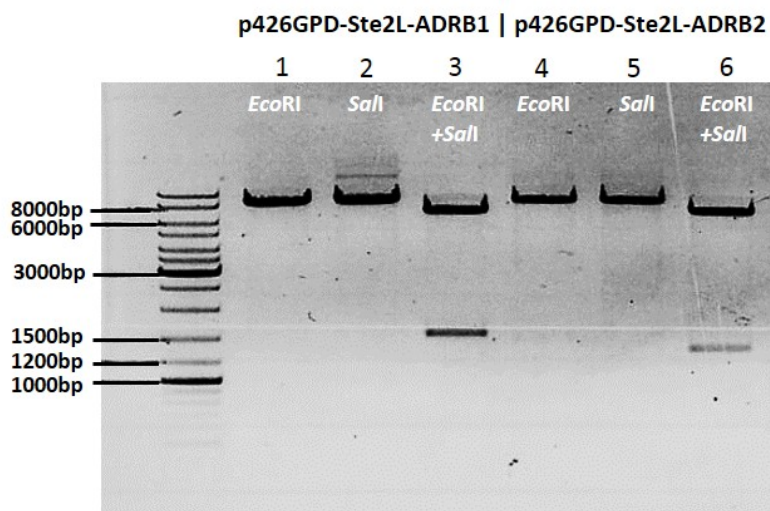


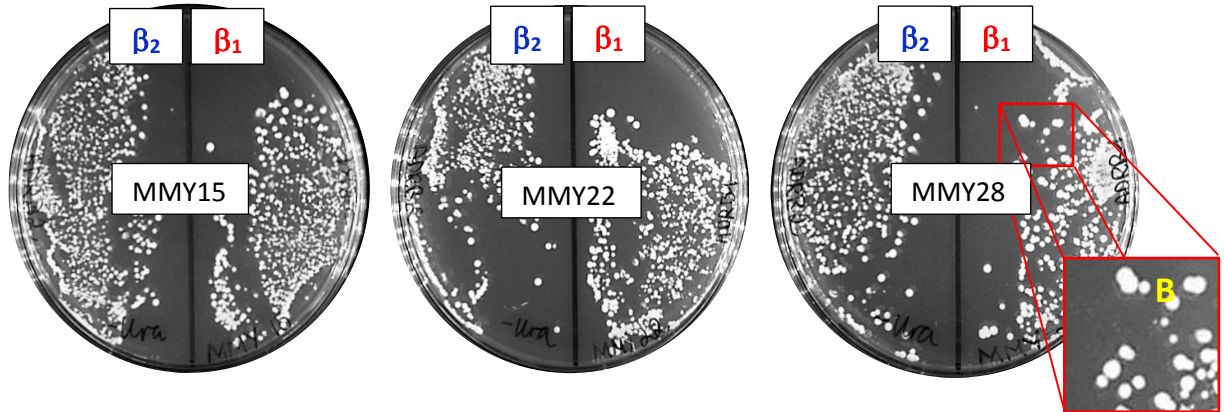
Figure 4.3 Construction of the p426GPD-Ste2L-ADRB1 and p426GPD-Ste2L-ADRB2. [A] The endonuclease restriction analyses were performed with *EcoRI* (lanes 2 and 5), *SalI* (lanes 3 and 6) which show the linearised vector of around 8,000bp, or both the enzymes (lanes 4 and 7) which show a fragment of approximately 1,500bp in case of the ADRB1 gene in lane 4, or 1,200bp in the case of the ADRB2 gene in lane 7.

4.2.2. The transformation of MMY 12-28 strains with p426GPD episomal plasmids

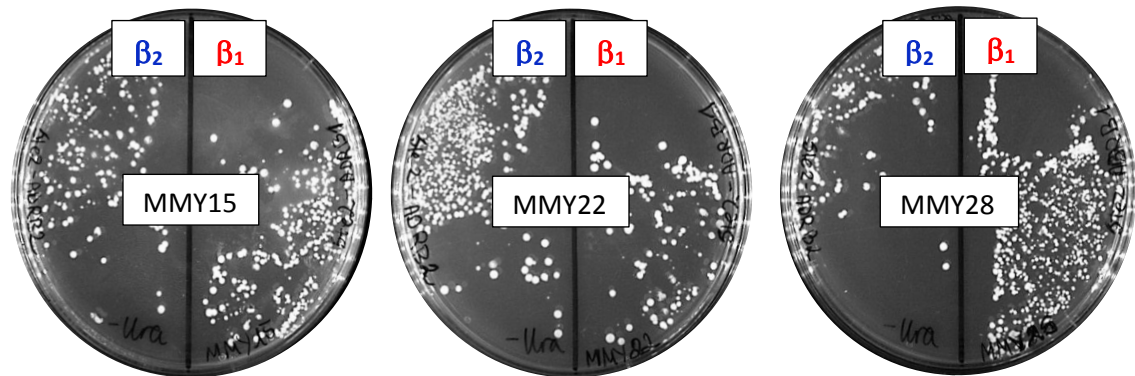
The MMY yeast grew on WHAUL+His-Ura plates (supplemented with histidine because the receptors are not stimulated) in 48h when transformed with p426GPD-ADRB1/ -ADRB2 and p426GPD-Ste2L-ADRB1/ -ADRB2 plasmids but an additional 48h were required for p426GPD-MF α -ADRB1/ -ADRB2 transformants to grow. In addition, the colonies of variable size and irregular shape formed in the later transformant group as shown in **Figure 4.4**, insert C. In contrast, the 'no leader' and 'Ste2 leader' plasmid containing colonies appeared consistent in size and round in shape, insert B. This phenomenon was observed across all MMY strains; transformation of strains MMY 15, 22, and 28 are shown in **Figure 4.4**.

Both MMY15 and MMY28 carry a chG α_s , however during the generation of MMY strains two colonies of G α_s stain were observed to have different coupling properties to mammalian GPCRs and therefore were designated as separate strains – MMY15 and MMY28.

p426GPD-ADRB1/ADRB2



p426GPD-Ste2-ADRB1/ADRB2



p426GPD-MF α -ADRB1/ADRB2

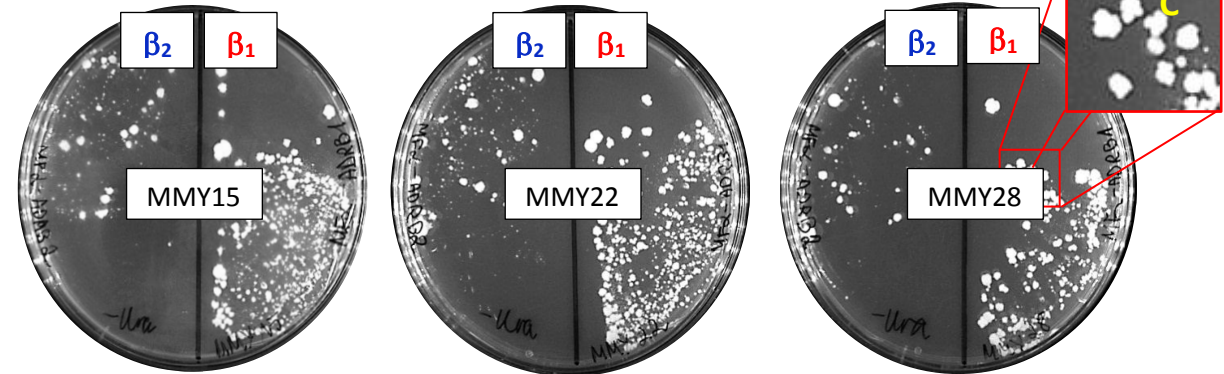


Figure 4.4 MMY yeast transformation result. p426GPD-ADRB1/ADRB2 transformed MMY15 (Gs), 22 (Go) and 28 (Gs) strains shown in the top row of the main panel, p426GPD-Ste2-ADRB1/ADRB2 transformed yeast in the middle row, and p426GPD-MF α -ADRB1/ADRB2 in the bottom row. The same number of cells was plated on each half of the plate during the same transformation experiment. The standard and Ste2 vector transformed cells formed round, uniformly sized colonies (**insert B**). The MF α vector transformants took an additional 48h to form comparably sized colonies, which appeared to be irregular in shape (**insert C**), variable in size and lower in overall number. The growth was reduced even further in cells transformed with p426GPD-MF α -ADRB2.

4.2.3. Overview of the pre-screening strategy for the identification of functional colonies

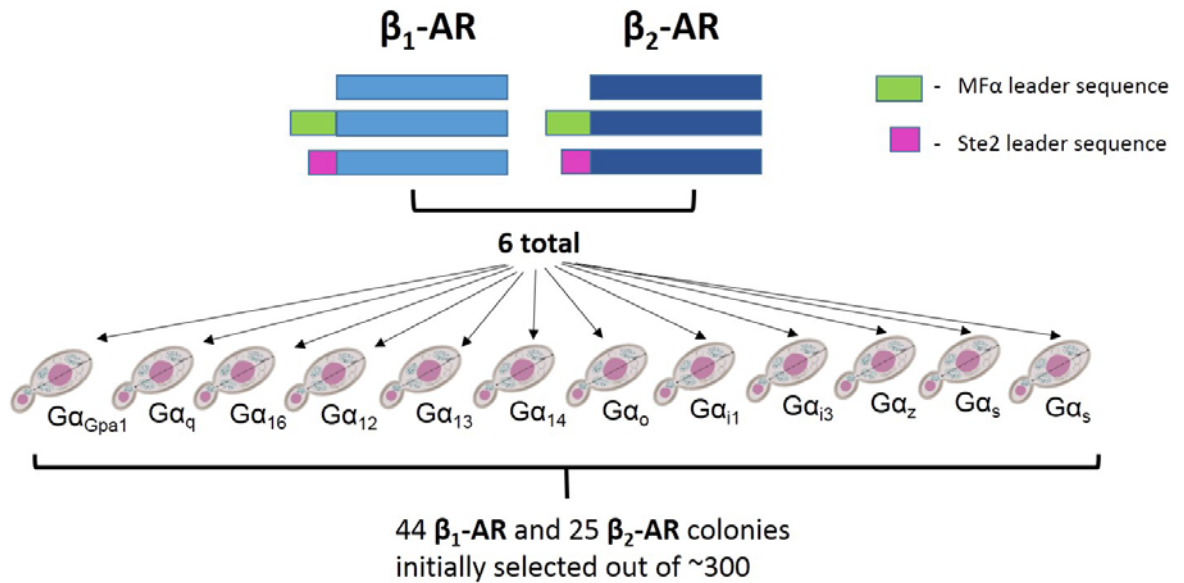
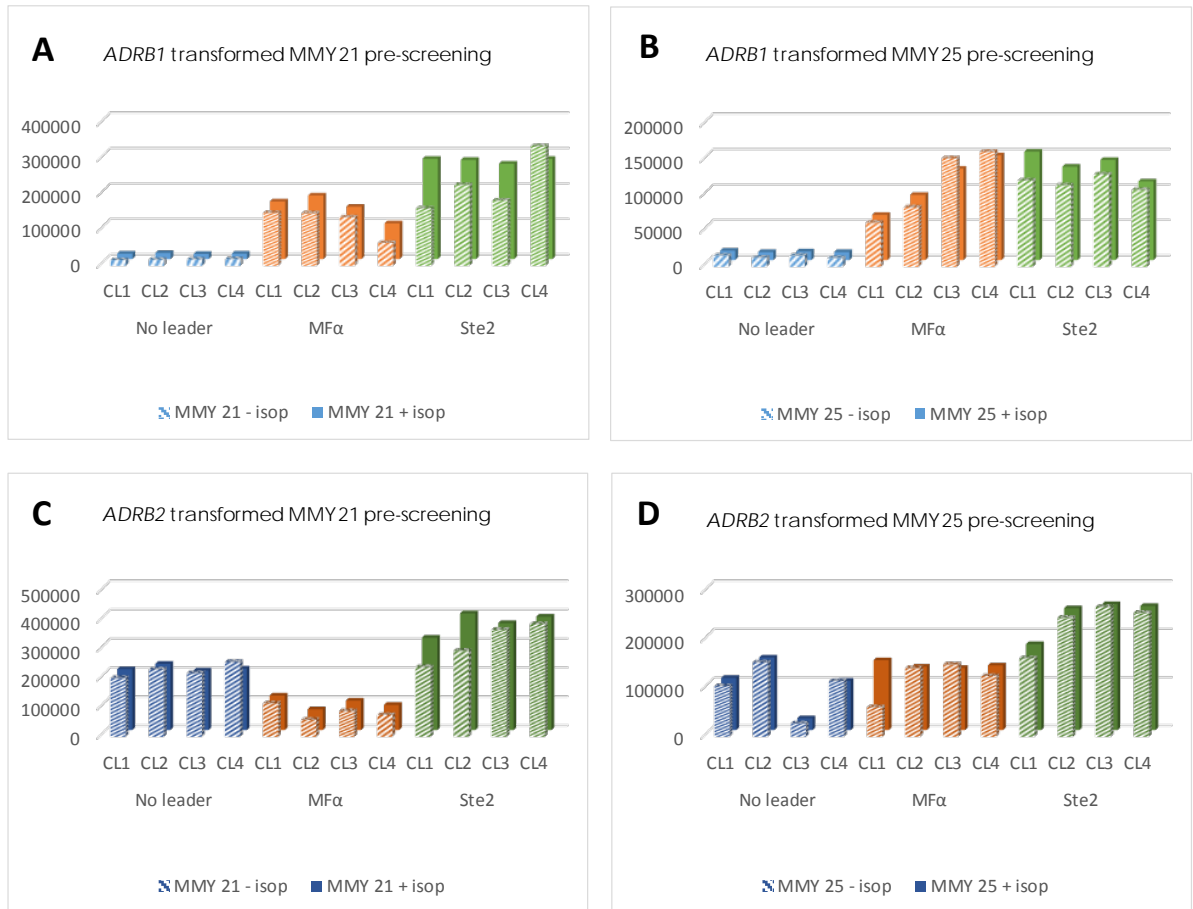


Figure 4.5 The overview of colony selection strategy for the identification of functional expression of β_1 -AR and β_2 -AR in p426GPD vectors.



Each of the 6 plasmid constructs was transformed into 12 MMY strains, generating 72 populations of transformed yeast. Because of the instability of the *ura3-1* nutrient selection marker and low transformation efficiency, transformed colonies may or may not contain the desired plasmid at variable copy number. For this reason, four to eight colonies from each transformation population were screened based on their ability to elicit a response upon high concentration of known beta-adrenergic agonist isoprenaline (or isoproterenol). Because not all chG α s were expected to demonstrate positive coupling with the receptor and in turn respond to agonist stimulation due to their different chG α protein, the functional screening was the most straightforward strategy to select colonies that had been correctly transformed and were capable of coupling with the β -adrenoceptors. The example in **Figure 4.6** shows a typical profile of colonies that show positive growth induction and hence RFU signal when stimulated with 100 μ M isoprenaline as compared with background growth with no agonist present. MMY21 colonies transformed with β_1 -AR (**Figure 4.6 [A]**) and with β_2 -AR [**C**] are compared with MMY25 colonies also transformed with β_1 -AR [**B**] and β_2 -AR [**D**] gene carrying plasmids. A variation in total RFUs could be observed in isoprenaline stimulated and negative control groups represented by solid and hatched bars respectively. The differences of RFUs between these two groups were analysed based on duplicate raw data and taken as an indication of potential functional coupling. Although this is only a sample of all data collected, it accurately represents all data

collected. Using this approach a population of 69 colonies were selected as *potentially* functionally coupling. As can be seen from **Table 4.7 [A]**, nearly two-thirds of all colonies were carrying the ADRB1 plasmid. The majority of those were transformed with p426GPD-MF α -ADRB1 while ADRB2 colonies were mostly transformed with ‘no leader’ plasmid p426GPD (**Table 4.7 [B]**).



Legend:

Pattern

-  - Induced growth
-  - Background growth

Colour




-  - p426GPD-ADRB1/ADRB2 (no leader sequence)
-  - p426GPD-MF α -ADRB1/ADRB2
-  - p426GPD-Ste2-ADRB1/ADRB2

Figure 4.6 An example of a pre-screening experiment.

The transformants carrying episomal ADRB1 gene constructs [**A** and **B**] or ADRB2 gene constructs [**C** and **D**] are shown. For illustration of the example MMY21 [**A** and **C**] and MMY25 [**B** and **D**] colony pre-screening results are shown. Relative fluorescence units (RFU) are on the Y axis; on the X axis the values of isoprenaline-stimulated growth are shown in solid colour, and background growth in hatched colour. The screening experiments were carried out in duplicates. Results of one replicate are shown. The different colours represent the type of vector, as shown in the legend. As summarised in **Table 4.7.B**, the majority of selected ADRB1 transformants carried the MF α construct (orange boxes in [**A**], while “no leader” constructs were more frequently selected for ADRB2 transformants (blue boxes in [**B**]).

A

MMY strain	ADRB1			ADRB2		
	No leader	MF α	Ste2	No leader	MF α	Ste2
12	-	3	1	1	-	-
14	-	4	1	1	-	-
15	2	3	1	-	-	-
16	-	2	1	2	-	1
19	-	-	1	1	-	1
20	-	3	3	1	3	2
21	1	6	2	1	-	2
22	-	-	-	2	1	-
23	-	2	-	-	-	-
24	-	1	-	-	-	-
25	-	-	2	-	1	-
28	2	3	-	2	1	2
Total	5	27	12	11	6	8

B

Summary of colonies responding to 100 μ M of isoprenaline

Vector	ADRB1	ADRB2
No leader	5	11
Mfa	27	6
Ste2	12	8
Total	44	25

Table 4.7 Distribution of colonies pre-selected as potentially functional according to the strain and plasmid construct. All 69 colonies that were selected in the pre-screening experiments for further testing with a full range of isoprenaline are grouped in table **A** according to the MMY strain, plasmid and receptor. In table **B** the same colonies are summarised according to the receptor and plasmid type – no leader, MF α , or Ste2.

4.2.4. Episomal plasmid screening results

The 69 colonies obtained in the pre-screening process were further investigated using isoprenaline in serial 3-fold dilutions ranging from 1.69x10⁻⁹ to 1x10⁻⁴M. The full curve experiments revealed that the majority of colonies showing potential coupling did not show a concentration-dependent response to isoprenaline. Based on the initial experiment with fresh transformants, 14 were selected and frozen with glycerol added at -80°C for long term storage. The experiments with isoprenaline dilutions were repeated on those colonies that had undergone a freeze-thaw cycle to obtain 3 independent experimental repeats. The conditions were kept consistent throughout the experiments and the results for ADRB1 and ADRB2 transformants are depicted in **Figures 4.9** and **4.10**, respectively.

The episomally-expressed ADRB1 was found to couple weakly to native yeast Gpa1, G α_q , G α_{14} and G α_s strains, summarised in **Table 4.8**. The most reproducible results were generated in the G α_s strain MMY15 (**Figure 4.9 [C]**), however, the alternative strain MMY28 transformed with the same plasmid did not match the results observed in the MMY15. The highest pEC₅₀ was obtained from the G α_{14} strain clone 18B1 (pEC₅₀=5.28, \pm 0.33, r^2 =0.58), but the standard error is high and the fit value is low. The G α_q strain MMY21 and Gpa1 strain MMY12 yeast clones have a relatively low standard error and closely fitting curves (**Figure 4.9 [B]** and **Table 4.8**).

The ADRB2 transformants retained virtually no activity after the freeze-thaw cycle, which was initially observed in the first screening experiments with fresh colonies, as is demonstrated in **Figure 4.10** – the left hand panels A, C, E, G show the average of 3 repeats while the right hand panels B, D, F, H are the results of the initial experiment on which basis the colonies were frozen for further experimentation.

One common observation was that the RFU readings in the control wells with no isoprenaline very frequently were higher than the readings of the wells with the lowest isoprenaline concentrations. For this reason much of the curve on the graphs appear in the negative scale, since the background RFU has been subtracted. This is mostly observed in colonies with transformed β_2 -AR plasmids. At first it was thought to be an artefact of the well's position on the plate, however, no significant evaporation in column 12 was observed across different experiments. Nevertheless, this observation does not change the main conclusion of this work, which is that none of the yeast colonies transformed with the episomal plasmids showed a significant β_2 -AR mediated responsiveness to the isoprenaline that would be robust and reproducible.

Experiments were performed over the period of 48h; readings were taken at several intervals, including 24h and 48h, which were later used for data analysis. It was observed, that often 24h were not sufficient to produce RFUs indicative of a response to isoprenaline and after an additional 24h, the signal improved.

Table 4.8 Summary of episomal colony screening results. The colonies marked in blue carrying ADRB2 gene; failed to produce any response to isoprenaline after the freeze-thaw cycle and hence

<i>Sample</i>	<i>pEC₅₀</i>	<i>SEM</i>	<i>r²</i>	<i>Receptor</i>	<i>Strain</i>	<i>Plasmid</i>	<i>Chimeric Ga</i>
3B2	N/A	-	0.06	β_2 -AR	MMY 16	Standard	G α_{16}
4B2	N/A	-	0.08	β_2 -AR	MMY 19	Standard	G α_{12}
5B2	N/A	-	-	β_2 -AR	MMY 20	Standard	G α_{13}
6B2	N/A	-	0.04	β_2 -AR	MMY 21	Standard	G α_{14}
13B1	5.07	0.30	0.63	β_1 -AR	MMY 12	MF α	Gpa1
14B1	4.27	0.70	0.33	β_1 -AR	MMY 12	MF α	Gpa1
16B1	4.89	0.25	0.71	β_1 -AR	MMY 14	MF α	G α_q
18B1	5.28	0.33	0.58	β_1 -AR	MMY 21	MF α	G α_{14}
19B1	4.91	0.52	0.37	β_1 -AR	MMY 21	MF α	G α_{14}
26B1	4.93	0.34	0.57	β_1 -AR	MMY 14	MF α	G α_q
57B1	5.07	0.23	0.74	β_1 -AR	MMY 15	MF α	G α_s
59B1	N/A	-		β_1 -AR	MMY 28	MF α	G α_s
61B1	4.16	1.10	0.19	β_1 -AR	MMY 28	MF α	G α_s
62B1	4.64	0.15	0.88	β_1 -AR	MMY 15	Ste2	G α_s

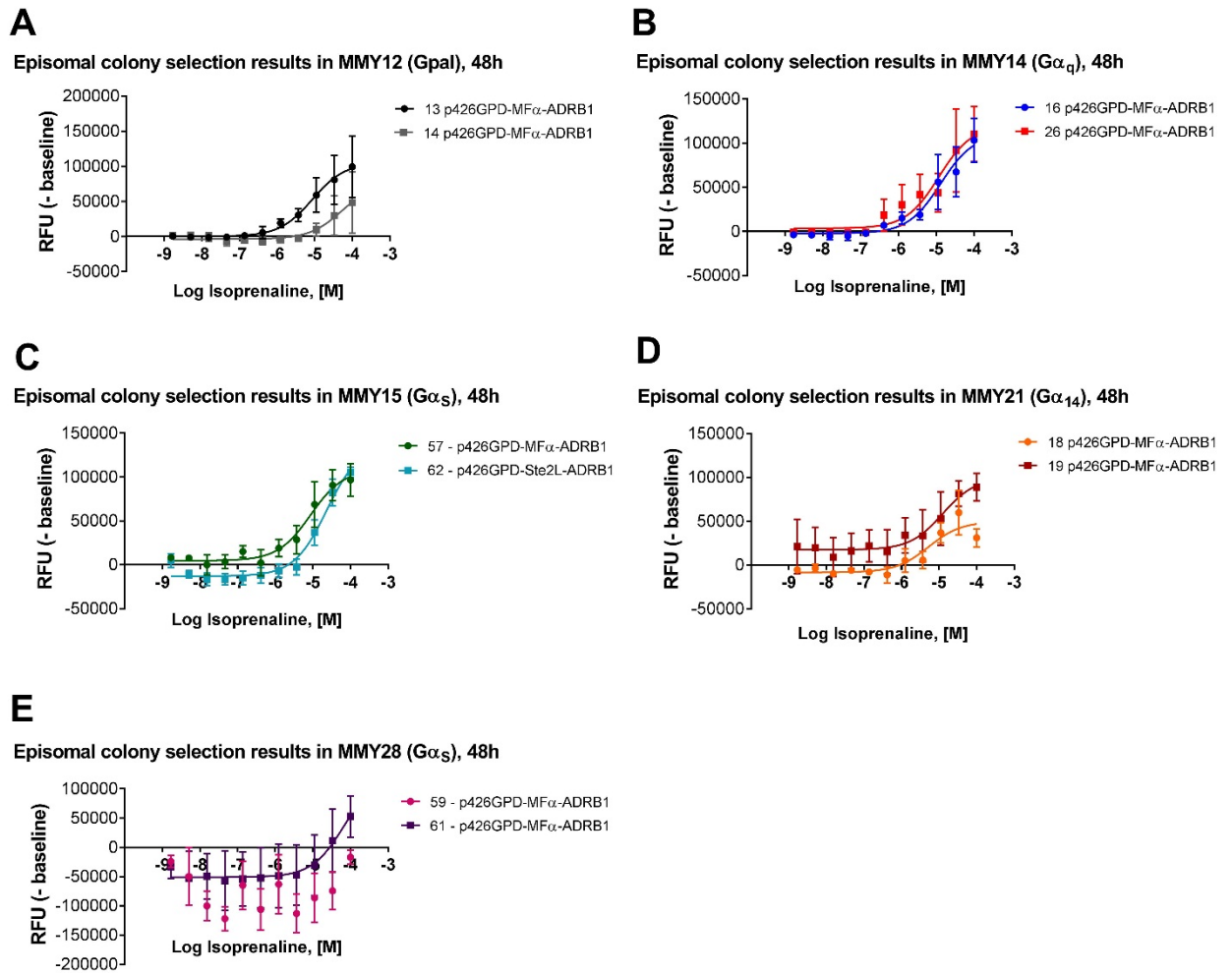


Figure 4.9 The β_1 -AR expressing MMY strain responses to the isoprenaline stimulation. Response to increasing concentrations of β -AR agonist isoprenaline was detected in five different MMY strains transformed with an episomal vector construct: [A] – MMY12 (Gpa1), [B] – MMY14 (G α_q), [C] – MMY 15 (G α_s), [D] – MMY21 (G α_{14}), [E] – MMY28 (G α_s). Only the colonies which showed concentration-response relationship upon full range of isoprenaline concentrations were frozen and tested again to obtain n=3. As shown in this figure only 10 colonies out of initially selected 44 ADRB1 expressing colonies (**Table 4.7**) were frozen.

Freshly picked

After freeze-thaw

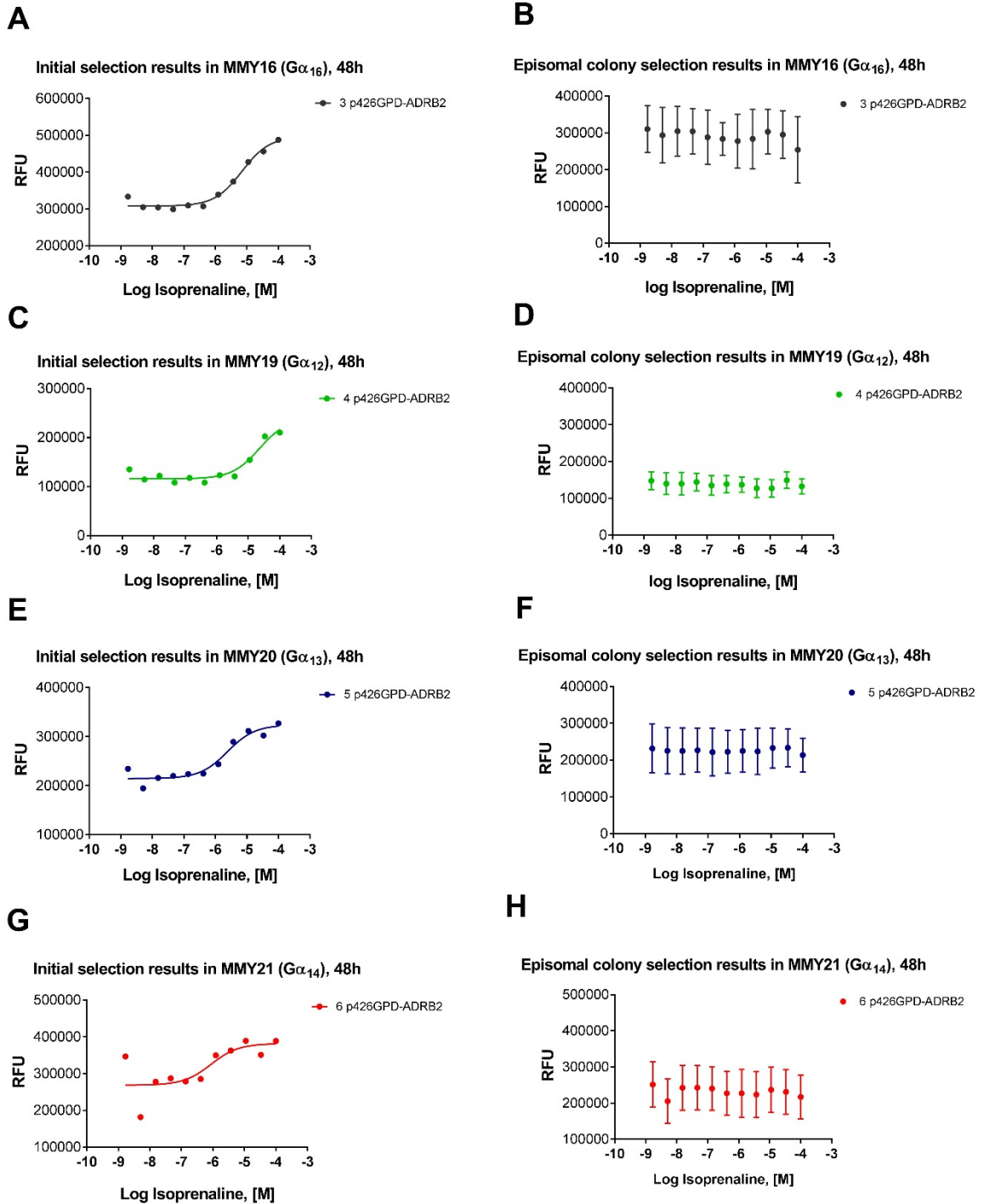


Figure 4.10 The β_2 -AR expressing MMY strain responses to isoprenaline stimulation. Response to increasing concentrations of β_2 -AR agonist isoprenaline was detected in four different MMY strains transformed with the p426GPD-ADRB2 vector: [A] and [B] – MMY16 ($G\alpha_{16}$), [C] and [D] – MMY19 ($G\alpha_{12}$), [E] and [F] – MMY20 ($G\alpha_{13}$), [G] and [H] – MMY21 ($G\alpha_{14}$). The initial screening results are presented on the left hand-side. However, when the assay was repeated after freeze-thaw cycle ($n=3$), the isoprenaline-stimulated growth could not be replicated in the same colonies as shown on the right hand-side.

4.2.5. Summary of episomal plasmid screening results

The purpose of testing the episomal plasmid system was to evaluate it as a tool for selecting the best coupling strain for a particular receptor. The episomal plasmids are maintained at high copy number and are easy to transform into yeast. The three different p426GPD constructs were designed for each receptor containing either one of the leader signal sequences – MF α or Ste2 – as well as no leader sequence. The native yeast leader sequences facilitate the target protein transportation to the cell membrane, and because GPCRs normally reside in the cell membrane it seemed it would be beneficial for its expression in the recombinant host. The first observation of leader sequence dependent effects was observed at the transformation level as shown in **Figure 4.4** Inserts **B** and **C** show the difference in colony shape and uneven size which can be attributed to the MF α leader sequence as neither the ‘no leader’ nor the Ste2 leader plasmids display this phenotype. Together with reduced overall number of colonies this could be a sign that the cells are stressed due the burden of recombinant protein expression.

The second observation of plasmid construct dependent effects was made after the pre-screening experiments which concluded that there was a preference for a particular plasmid construct. As summarised in **Table 4.7.B**, the majority of β_1 -AR expressing colonies selected as potentially coupling carried the MF α sequence in the construct. However, β_2 -AR expressing colonies that were selected carried the ‘standard’ plasmid construct with no leader sequence. This could be linked to that fact that significantly fewer β_2 -AR colonies grew when transformed with the MF α plasmid construct.

The pre-screening experiments identified 69 colonies which potentially demonstrated functional receptor expression. To follow this up, they were then tested with a range of isoprenaline to evaluate whether they actually responded to ligand stimulation. The samples then were narrowed down to 14 colonies (summarised in **Table 4.8**) which were archived at -80°C. To evaluate whether cells can retain the episomal plasmid and demonstrate the same functionality, a fresh plate was streaked out from a frozen glycerol stock and the experiments were carried out on two different days to generate the 3 independent repeats. This is important because episomal plasmids are known for mitotic instability [74], which would make the system unstable in the long term. However, we did not see a uniform effect of the freeze-thawing because the β_1 -AR transformants were able to demonstrate comparable functionality while β_2 -AR completely lost any function. Further investigation is needed to understand this receptor dependent effect.

Although episomal plasmids were a useful tool for identification of potentially coupling MMY strains for the β_1 -AR there was overall insufficient robustness for both receptors. It was anticipated that, the integrative plasmids may provide to be more useful in evaluating the β_2 -AR functionality in this yeast

assay. Furthermore, the integrative plasmids were expected to show less variability between the different transformation colonies as they carry one copy of the plasmid in the genome. It was therefore decided to pursue the use of integrative vectors for all future studies.

4.3. Integrative p306GPD plasmids for the expression of β_1 -AR and β_2 -AR

The integrative p306GPD series vectors have some similarities to the above - described episomal vectors, such as the GPD promoter and CYC1 terminator elements that regulate the gene expression, as well as the *URA3* selection marker. However, these vectors are not able to replicate independently and therefore have to be integrated at the *URA3* locus by homologous recombination. For this reason the yeast transformation procedure requires an additional step, which is unfavourable for screening a greater number of plasmid-strain combinations. Another key difference is that the gene is maintained at a significantly lower copy number in the cell which is expected to result in a lower protein expression level when compared to expression of p426GPD transformed yeast.

4.3.1. The construction of the p306GPD-(MF α)-ADRB1 and p306GPD-(MF α)-ADRB2 plasmids

Based on the episomal plasmid screening results, it was anticipated that the p306GPD-MF α -ADRB1 /-ADRB2 would be the best plasmid construct for the expression of both receptors. However, for the purpose of comparing both the expression level and functional expression level the 'standard' plasmids were also constructed. The Ste2L leader sequence did not appear to significantly improve the expression of either β_1 -AR or β_2 -AR therefore was omitted from the comparison in the integrative plasmid system.

The 'standard' p306GPD-ADRB1 /-ADRB2

The ADRB1 and ADRB2 fragments were obtained from the p426GPD-ADRB1 /-ADRB2 plasmids and inserted into the 5266bp long p306GPD vector at the *SpeI* restriction site at the 5' end and the *SalI* and the 3' end of the gene of interest. Both of the endonucleases were used in the enzymatic digestion analysis to confirm the correct insertion of the gene fragments (**Figure 4.11**).

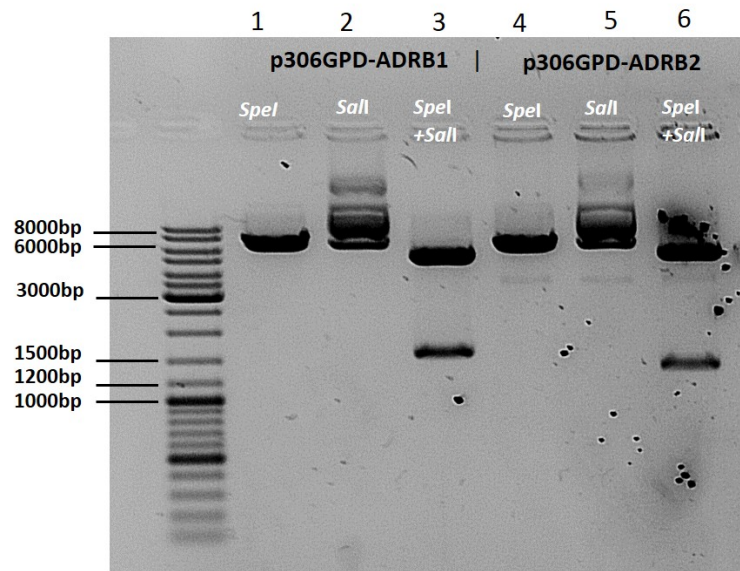


Figure 4.11 Construction of the p306GPD-ADRB1 and p306GPD-ADRB2. The endonuclease restriction analyses were performed with *SpeI* (lanes 2 and 5), *Sall* (lanes 3 and 6) which show the linearised vector of around 6500-6700bp, or both the enzymes (lanes 4 and 7) which show a fragment of approximately 1500bp in case of ADRB1 gene in lane 4, or 1200bp ADRB2 gene in lane 7. These sizes are consistent with predictions.

The p306GPD-MF α -ADRB1 /-ADRB2 plasmids

Similarly to the previous plasmids, the ADRB1 and ADRB2 genes along with the MF α leader sequence were cut out from the p426GPD-MF α plasmids and inserted into the MCR of the p306GPD vector at the *SpeI* site at the 5' end of the gene and *HindIII* at the 3' end (**Figure 4.12**).

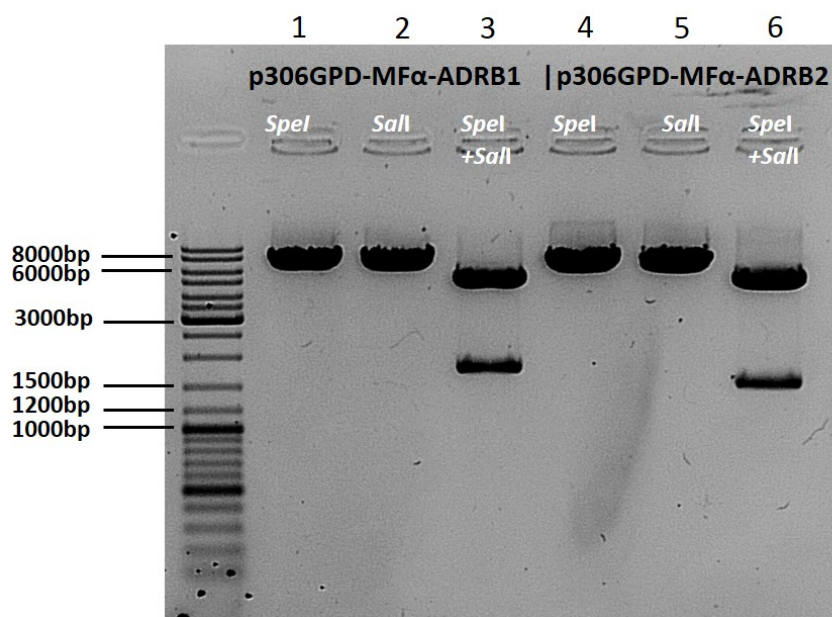


Figure 4.12 Construction of the p306GPD-MF α -ADRB1 and p306GPD-MF α -ADRB2. The endonuclease restriction analyses were performed with *SpeI* (lanes 2 and 5), *Sall* (lanes 3 and 6) which show the linearised vector of around 6,500-6,700bp, or both the enzymes (lanes 4 and 7) which show a fragment of approximately 1,500bp in case of ADRB1 gene in lane 4, or 1,200bp for the ADRB2 gene in lane 7.

4.3.2. The transformation of MMY12-24 yeast with the p306GPD plasmids and the functional colony selection

To build on the findings of episomal plasmid screening for functional β_1 -AR and β_2 -AR expression in the MMY yeast, the p306GPD-MF α -ADRB1 and p306GPD-MF α -ADRB2 plasmids were deemed to have the highest likelihood of success of producing functional expression. The p306GPD-ADRB1 and p306GPD-ADRB2 were transformed only into MMY15, to make a direct comparison with the leader sequence MF α -containing plasmid, as well as the episomal p426GPD plasmids in both functional assays and western blots.

As with the episomal plasmids, the MMY strains with the integrated p306GPD plasmids appeared after 48h following transformation (**Figure 4.13**). The irregular shape of the colonies observed in the p426GPD-MF α transformed yeast (**Figure 4.4**, insert **C**) was observed in a few colonies transformed with the p306GPD-MF α plasmid, but were far fewer in number as compared to the episomally transformed yeast. Generally, the transformations worked well, however, the MMY25 transformed yeast did not produce any colonies and MMY28 was not tested, because it was previously shown that the other version of the G α_s strain, MMY15, was more favourable for the functional expression of β_1 -AR.

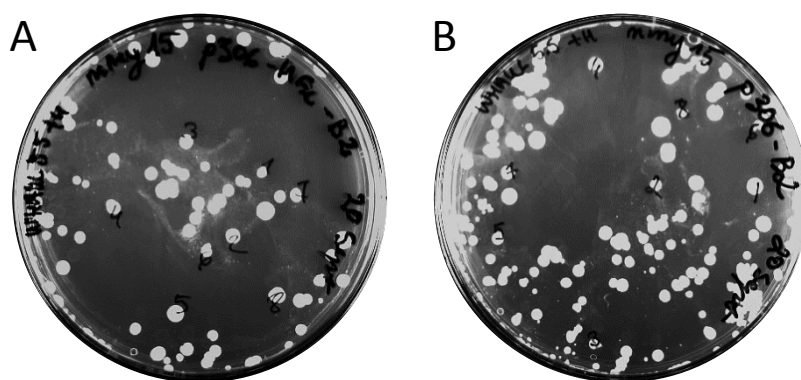


Figure 4.13 Transformation of the MMY15 with p306GPD vectors. The G α_s strain was transformed with the p306GPD-MF α -ADRB2 vector [**A**], and the p306GPD-ADRB2 vector with no leader sequence [**B**]. Unlike the episomal vectors, the p306GPD vectors have to integrate into the genome at the *URA3* locus in order to be maintained and allow the cells to survive on a plate lacking uracil.

Because of a lower number of transformants to screen, the pre-selection step was not employed. Instead, 4-8 colonies from each transformed MMY strain were tested with serial 3-fold dilutions of a known β -AR agonist, isoprenaline. The complete data set for the β_1 -AR and β_2 -AR expressing yeast was collected in 4 individual experiments, using two different instruments on two different sites. In order to demonstrate the variation of responses, the RFU were not normalised and were instead plotted as RFU values from which the background RFU of a well containing only solvent was subtracted. Furthermore, because of different signal windows between the instruments, and indeed between experiments, the RFU scale was matched for all data within the same experiment. This was necessary

in order to distinguish which of the MMY strains demonstrated functional coupling with β -AR. For example, in **Figure 4.14 [A]**, the MMY12 colonies expressing β_1 -AR gave very high RFUs of approximately 4×10^6 , which is nearly two orders of magnitude (80 times to be precise) higher than the signal which was obtained from screening MMY14 and MMY24 colonies presented in **[B]** and **[J]** respectively. The experiment for MMY15 presented in **[C]** of the same figure gave RFUs of 1×10^5 which are between the ranges of the two experiments described above. This is likely to be a technical artefact because of several observations. The first is that the colonies for screening experiments are grown in 96-well plates, and because of the small volume of culture, their OD_{600} readings tend to be lower than would be observed in a larger culture. As a consequence, when the cells are diluted into the assay mixture, the final OD_{600} and carry-over histidine might be higher than intended, which boosts the cell number and the generated RFU. The second observation is that if the receptor is unable to functionally couple to the $chG\alpha$ in a particular strain, then even at higher cell inoculation numbers the response to the agonist is not observed. This is particularly evident in the strains expressing β_2 -AR in **Figure 4.15** which responded to isoprenaline in fewer strains than β_1 -AR.

It was concluded that β_1 -AR shows functional coupling in MMY strains 12 (Gpa1), 14 ($G\alpha_q$), 15 ($G\alpha_s$), 16 ($G\alpha_{16}$), 21 ($G\alpha_{14}$), 22($G\alpha_o$), 23 ($G\alpha_{i1}$), and 24 ($G\alpha_{i3}$). The MMY20 ($G\alpha_{i3}$) transformant showed a very weak response to isoprenaline compared to other strains. The β_2 -AR responded to isoprenaline stimulation only in 5 MMY strains - 14 ($G\alpha_q$), 15 ($G\alpha_s$), 16 ($G\alpha_{16}$), 21 ($G\alpha_{14}$), 23 ($G\alpha_{i1}$). This was an important achievement of project's milestone as it allowed for further pharmacological investigation of these receptors in the yeast as discussed in Chapter 5.

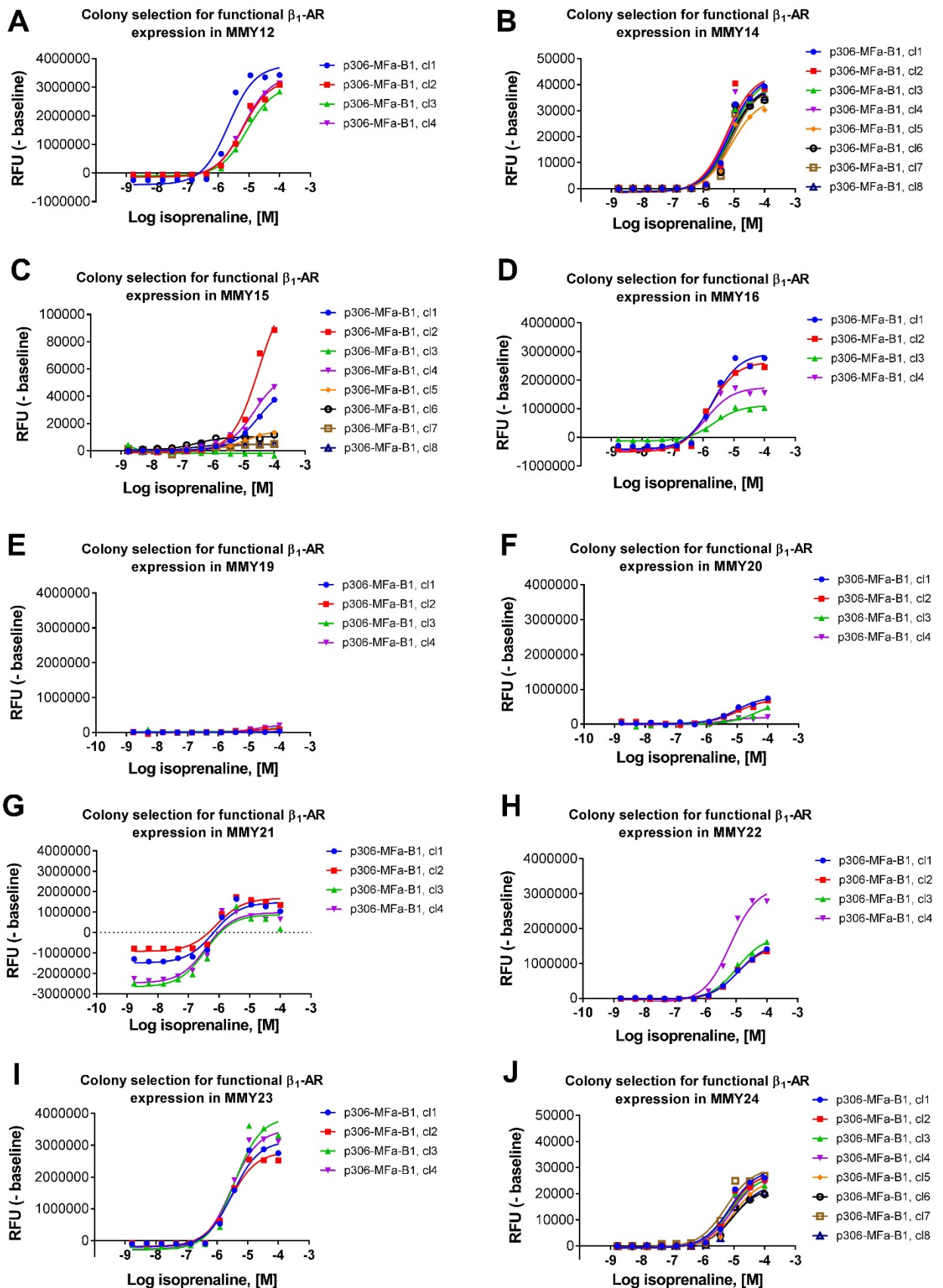


Figure 4.14 The β_1 -AR expressing MMY strain responses to the isoprenaline stimulation. Response to increasing concentrations of β -AR agonist isoprenaline was detected in ten different MMY strains transformed with the integrating p306GPD-MFa-ADRB1 vector: [A] – MMY12 ($G_{\alpha 1}$), [B] – MMY14 ($G_{\alpha 4}$), [C] – MMY 15 ($G_{\alpha 5}$), [D] – MMY16 ($G_{\alpha 16}$), [E] – MMY19 ($G_{\alpha 12}$), [F] – MMY20 ($G_{\alpha 13}$), [G] – MMY21 ($G_{\alpha 14}$), [H] – MMY22 ($G_{\alpha 0}$), [I] – MMY23 ($G_{\alpha 11}$), [J] – MMY24 ($G_{\alpha 13}$). The differences in the RFU scale arise from different days and/or instruments used for screening. The scale of RFU for each strain reflects the level of signal produced in comparison to other strains tested on the same experiment. n=1

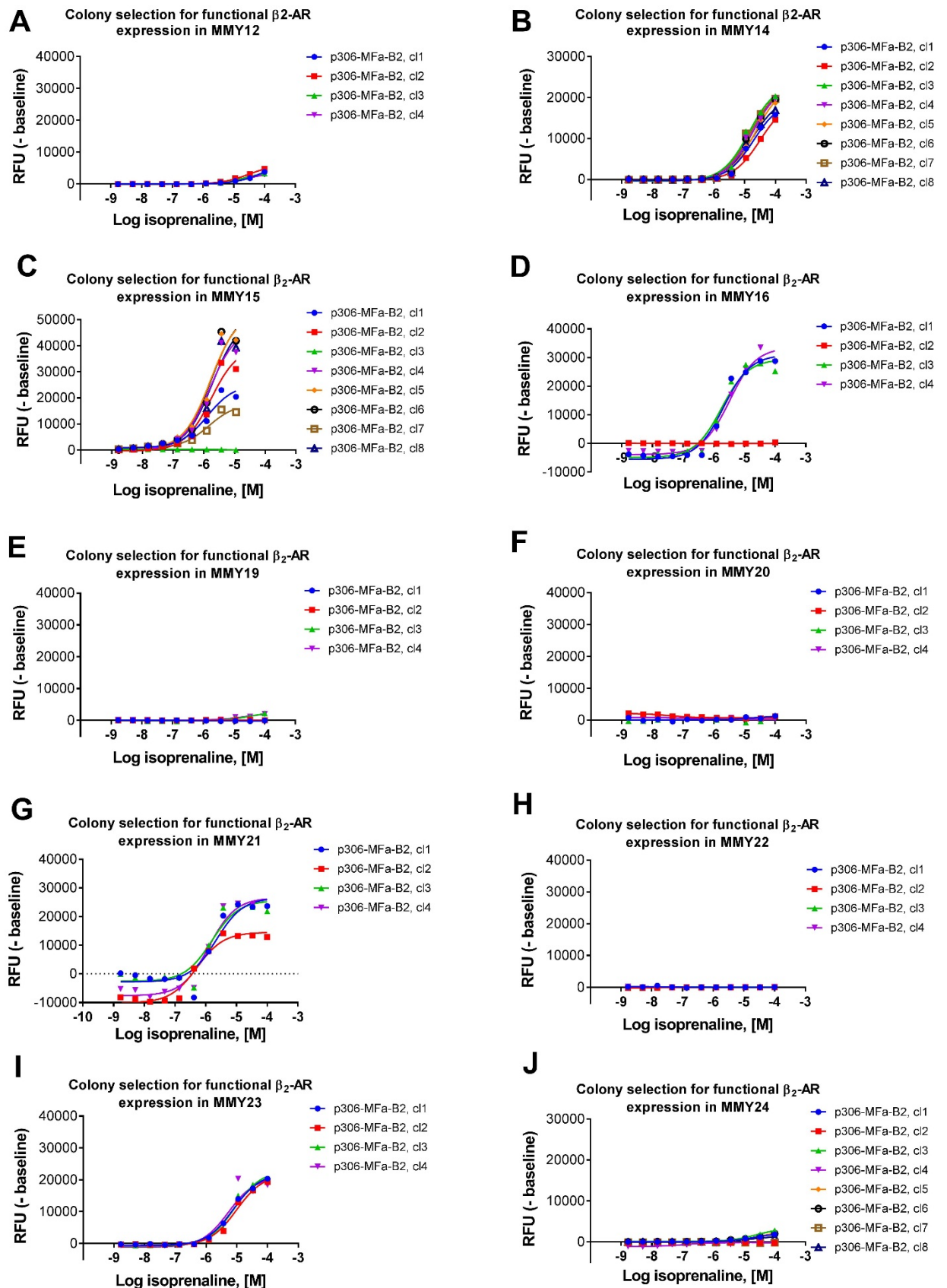


Figure 4.15 The β_2 -AR expressing MMY strain responses to the isoprenaline stimulation. Response to increasing concentrations of β -AR agonist isoprenaline was detected in ten different MMY strains transformed with the integrating p306GPD-MFa-ADRB1 vector: [A] – MMY12 ($G\alpha_{1p}$), [B] – MMY14 ($G\alpha_q$), [C] – MMY 15 ($G\alpha_s$), [D] – MMY16 ($G\alpha_{16}$), [E] – MMY19 ($G\alpha_{12}$), [F] – MMY20 ($G\alpha_{13}$), [G] – MMY21 ($G\alpha_{14}$), [H] – MMY22 ($G\alpha_o$), [I] – MMY23 ($G\alpha_{i1}$), [J] – MMY24 ($G\alpha_{i3}$). n=1

4.3.3. Summary of integrated plasmid screening results

The purposes of transforming the yeast strains with integrated plasmids after preliminary functional expression was assessed in the episomal expression system was to improve the expression of the β_2 -AR receptor and to compare the two different systems. **This was achieved.**

The responses in MMY12, 14, 15 and 21 observed in the p426GPD-MF α -ADRB1 transformed yeast were largely replicated in the p306GPD-MF α -ADRB1 transformed yeast, with additional strains MMY16, MMY20, MMY23 and MMY24 showing functional coupling with this receptor. The signal window, however, appears to be much larger when the plasmids have been integrated. This is important when testing other compounds with lower levels of efficacy, which may not appear if the signal is low with the full agonist stimulation.

The MMY21 strain appears to have higher unspecific background growth in the no compound well, which is something that has been observed before in the results of episomal plasmid screening, but seems to only have affected this strain. This effect was observed with transformed β_1 -AR and β_2 -AR.

The β_2 -AR was for the first time observed to functionally couple in MMY strains and, as predicted, the construct with the MF α leader sequence was suitable for this purpose. The no leader p306GPD-ADRB2 plasmid was tested in MMY15 to test whether it was essential. No functional response to isoprenaline was detected in 8 colonies tested with this plasmid (data not shown).

4.4. Western blot analysis of protein expression patterns of the β_1 -AR and β_2 -AR

The functional expression differences between the episomal vs integrative plasmids, with and without any leader sequences raised many questions about what is happening in the cell in terms of protein expression and localisation:

- Is the protein expressed regardless of whether the leader sequence is present or not?
- Do the protein levels differ between p426GPD (episomal) and p306GPD (integrating) plasmid expression?

4.4.1. β_1 -AR expression in the MMY15 (G α S) strain

To make a direct comparison between the expression level and pattern in different plasmid transformed yeast, and the functional assay data, various plasmid constructs were transformed into MMY15 host strain. As previously shown (**Figure 4.9** and **Figure 4.14**) functional coupling was observed when either episomal or integrated plasmids were transformed, but the constructs required the MF α leader sequence.

The selection of colonies freshly transformed with p426GPD-ADRB1 and p426GPD-MF-ADRB1 were assessed by functional assay output was performed first (**Figure 4.16 [C]**), however the rate of selecting a positive colony was low, as demonstrated previously in section 4.2.3 – only 14 functional colonies expressing β_1 -AR and β_2 -AR were selected from around 300 screened p426GPD plasmid transformed yeast. The same colonies were then examined on a western blot (**Figure 4.16 [A]**). The anti- β_1 AR antibody unfortunately exhibited inconsistency in unspecific background detection between the different batches. This made the interpretation of the results difficult and limited. To provide some clearance, a colony previously deemed functional was tested on the western blot presented in **Figure 4.16 [A]**, lane 10. Coincidentally, only lane 10 shows a presence of a double band of around 22-24kDa, which is consistent with previous western blot of a functional colony with the same construct (insert **[B]**). The other lanes presented the pattern identical to negative control lane 2, indicating that no β_1 -AR specific band is present. This is largely in agreement with the functional data in **[A]** – colony 62 was the only that demonstrated some functional signal, albeit only after 44h of incubation. Prolonged incubation performed on some of other colonies did not improve the signal (data not shown).

The expression pattern of p306GPD transformed MMY15 was assessed similarly (**Figure 4.17**). However, more functional colonies were picked from the same number of total colonies screened as for the episomal p426GPD plasmids. The functional assay result is presented in **Figure 4.17 [C]** shows that four out of 5 colonies carrying p306GPD-MF α -ADRB1 plasmid showed a response to isoprenaline at variable E_{max} levels. Four colonies with this plasmid were analysed on the western blot presented in **Figure 4.17 [A]**, along with four colonies carrying p306GPD-ADRB1 plasmid construct with no leader sequence. Again, there is a lot of unspecific bands, however, all colonies that show functional expression in the FD-glu assay experiment appear to have a double band at 22-24kDa, consistent with the p426GPD-MF-ADRB1 CL62 presented in **Figure 4.16 [A]**. This band, although smaller than expected size for a GPCR, has been observed previously with a batch of the same antibody which gave less unspecific background (insert **[B]**).

β_1 -AR expression in p426GPD vectors

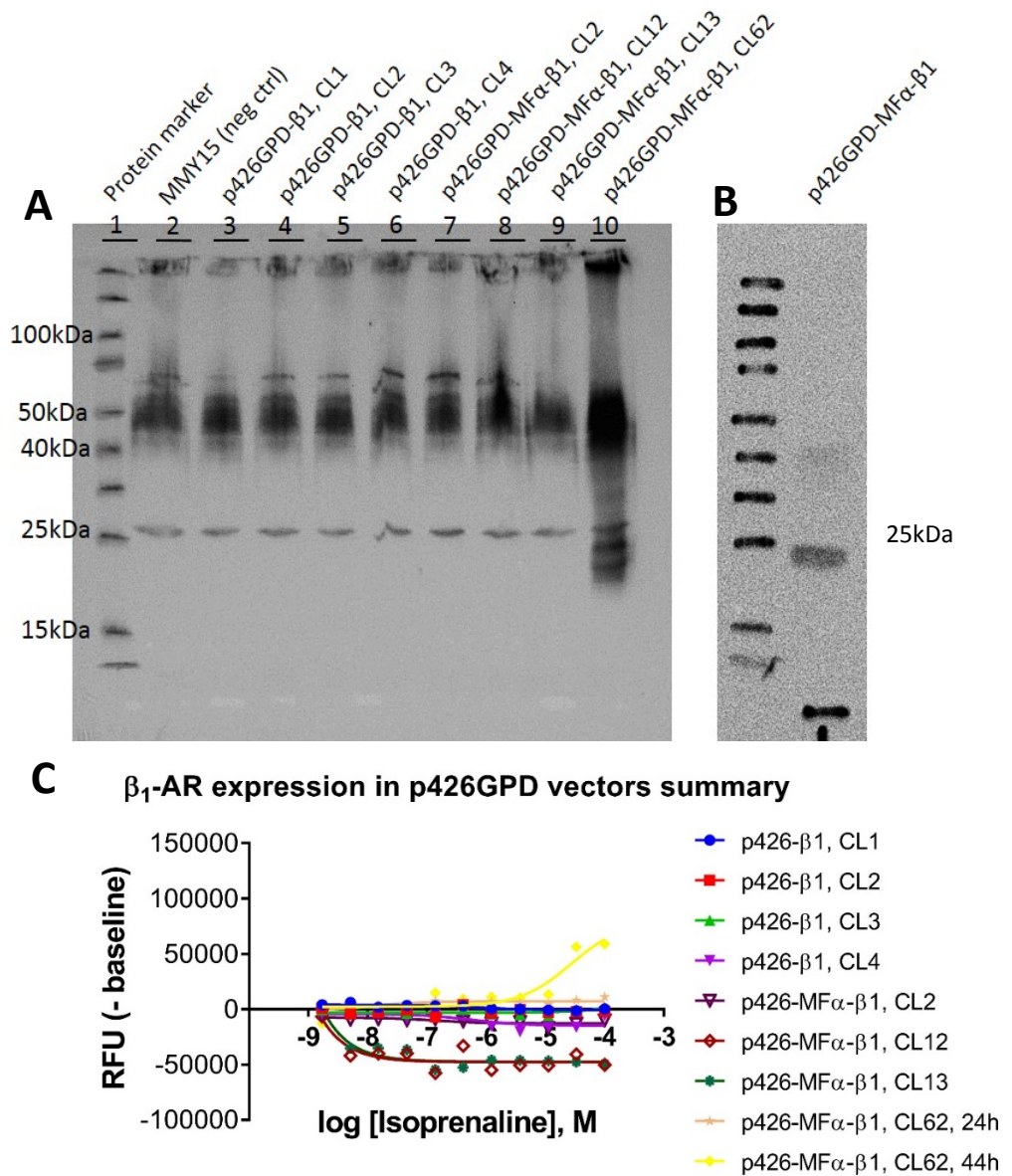


Figure 4.16 β_1 -AR protein expression in p426GPD vectors comparison with the functional data obtained from the FD-glu assay. [A] An equal number of p426GPD and p426GPD-MF α transformed colonies were analysed on a western blot using anti- β_1 AR antibody but no β_1 -AR specific band is thought to be present with the exception of possibly the double band of 22-24kDa in lane 10. [B] This size is consistent with a previous result. [C] None of the colonies were found to show functional expression as assessed by isoprenaline induced FD-glu signal.

β_1 -AR expression in p306GPD vectors

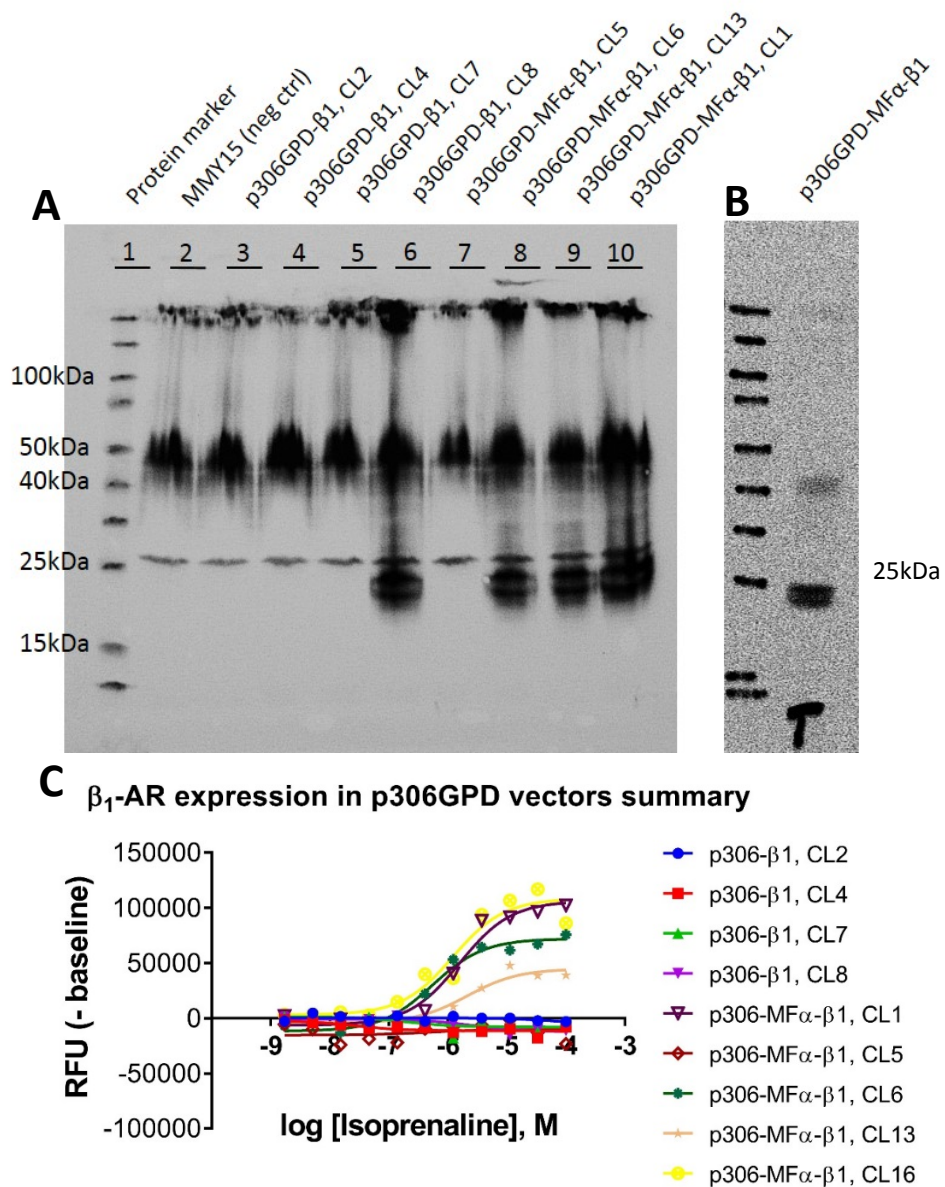


Figure 4.17 β_1 -AR protein expression in p306GPD vectors comparison with the functional data obtained from the FD-glu assay. [A] An equal number of p306GPD and p306GPD-MF α transformed colonies were analysed on a western blot using the same anti- β_1 AR antibody. Bands of previously observed size of 22-24kDa were detected in lanes 6, 8, 9, and 10. [B] This size is consistent with a previous result. [C] The same colonies showed functional coupling in MMY upon stimulation with isoprenaline. Although various levels of E_{max} were observed, the intensity of the mentioned bands does not look higher or lower between the different colonies.

4.4.2. β_2 -AR expression in the MMY15 ($G\alpha_s$) strain

The expression of β_2 -AR was too investigated in both episomal and integrated plasmid constructs, despite the fact that no functional colonies could be detected in the episomal plasmid screening. This was to investigate whether the protein is expressed in non-functional colonies. For this work, p426GPD-ADRB2, p426GPD-MF α -ADRB2, p306GPD-ADRB2 and p306GPD-MF α -ADRB2 were freshly transformed into MMY15 to eliminate any effects of potential plasmid loss. As previously observed, the number of p426GPD-MF α -ADRB2 transformed colonies was much smaller than that of p426GPD-ADRB2 (**Figure 4.18**). From each plate, 4 colonies were tested in the functional assay (**Figure 4.19 [B]**) before extracting membranes for western blot [**A**].

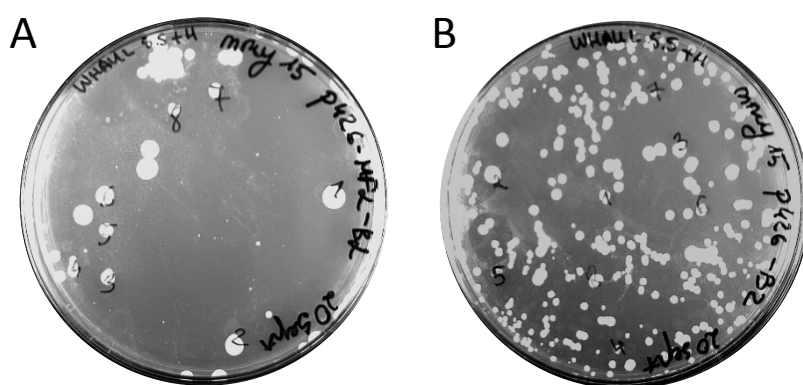


Figure 4.18 Transformation of MMY15 with p426GPD vectors. The $G\alpha_s$ strain was transformed with the p426GPD-MF α -ADRB2 vector [**A**], and the p426GPD-ADRB2 vector with no leader sequence [**B**].

Interestingly, 3 of the 4 p426GPD-ADRB2 colonies showed a weak response to isoprenaline which echoes the observation in the initial testing of episomal β_2 -AR functional expression presented in **Figure 4.10**. The same colonies – blue, red and green – showed a double band of around 39-41kDa and a lower band of approximately 21kDa on the western blot (lanes 3, 4, 5 respectively). No functional response was found in the yeast transformed with the MF α leader sequence version of the plasmid, nor could any bands be detected on the western blot, suggesting that the lack of functional response is because there is no protein expression. Together with the consistently low number of transformed colonies, the results would suggest that cells that take up the plasmid do not survive long after the transformation to produce any visible colonies, and the ones that do appear on the plate are false positive colonies.

The observation is slightly different in the p306GPD transformed yeast. The colony distribution is much more similar between p306GPD-ADRB2 and p306GPD-MF α -ADRB2 transformed colonies (**Figure 4.13**). However, colonies with the MF α leader sequence show the response to isoprenaline, while the no leader colonies do not (**Figure 4.20 [B]**). The same colonies that show response – green, purple and pink – also produced bands of 39kDa and 21kDa on the western blot ([**A**]).

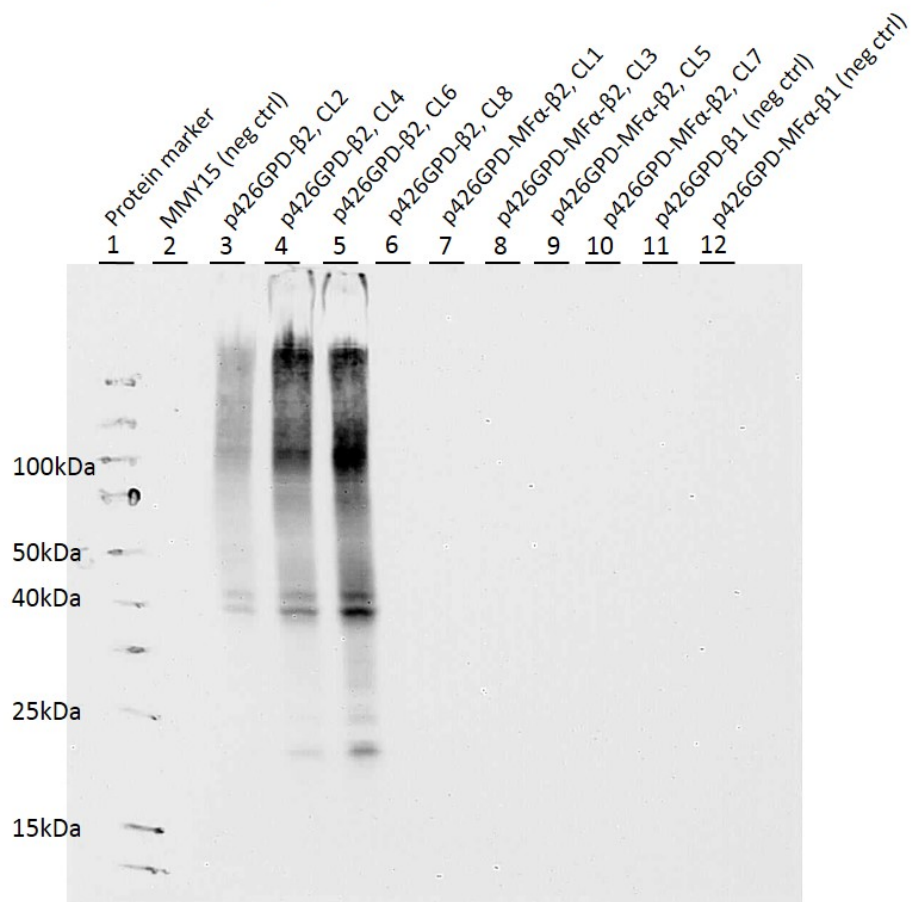
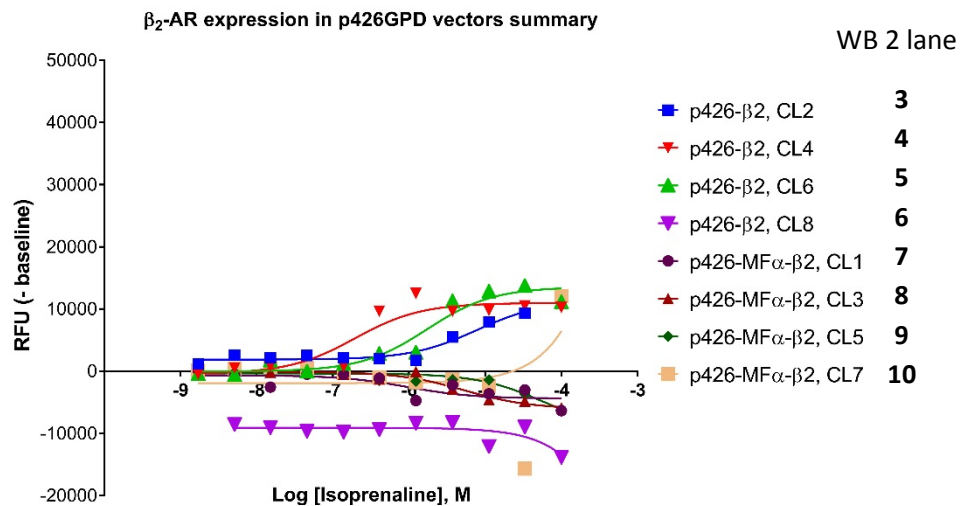
A **β_2 -AR expression in p426GPD vectors****B**

Figure 4.19 β_2 -AR protein expression in p306GPD vectors comparison with the functional FD-glu assay results. [A] The initial functional FD-glu assay has revealed that p426GPD-ADRB2 colonies 2, 4, and 6 have responded to isoprenaline stimulation. None of the colonies with the MF α leader sequence have responded. This is with an agreement with previous colony screening results presented in Figure 4.10. [B] The western blot analysis shows that the same p426GPD-ADRB2 colonies presented a double band at 39-41kDa and a smaller band of around 21kDa. The negative controls, including untransformed MMY15, and β_1 -AR transformed yeast did not show an unspecific bands.

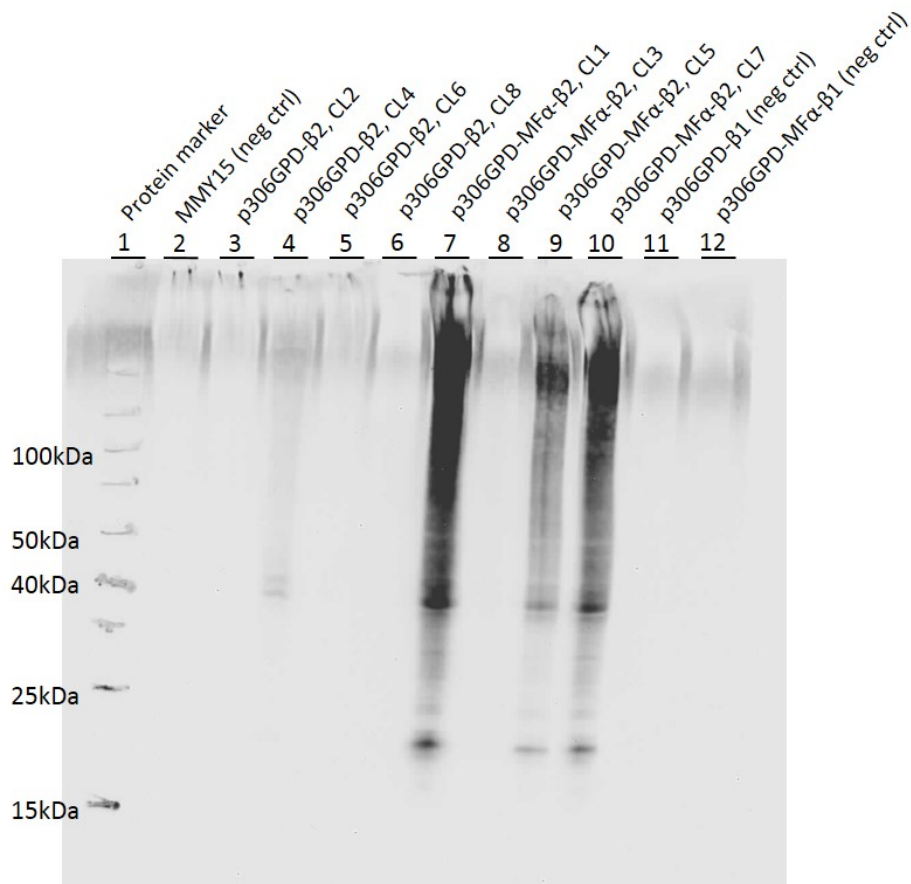
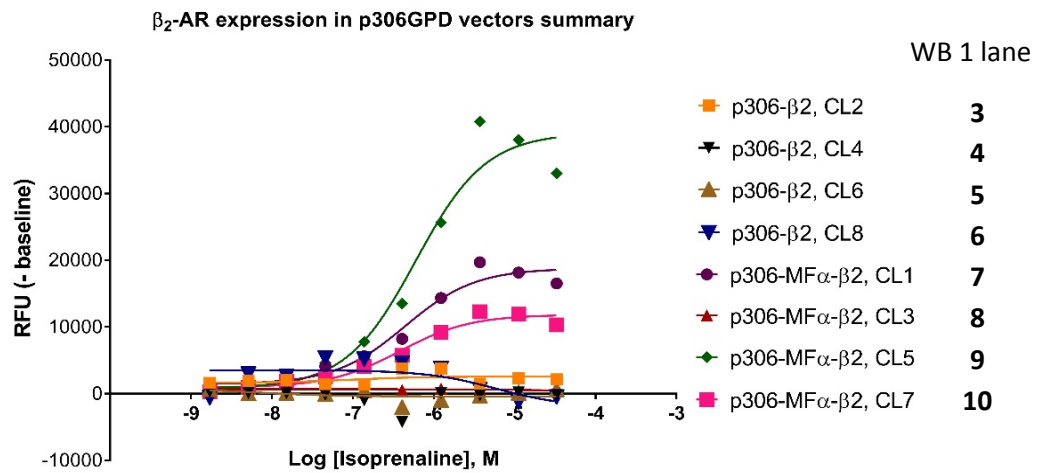
A **β_2 -AR expression in p306GPD vectors****B**

Figure 4.20 β_2 -AR protein expression in p306GPD vectors comparison with the functional FD-glu assay results. [A] As before four colonies transformed with p306GPD and p306GPD-MF α construct were assessed by the functional FD-glu assay. Contrary to p426GPD constructs, the leader sequence appears to be required for functional expression. [B] Western blot analysis show that the same functional colonies 1, 5, and 7 of the p306GPD-MF α construct displayed a band of around 39kDa and a smaller at around 21kDa. There is a faint band in lane 4 (p306GPD-ADRB2, CL 4) but no functional signal was detected in [B]. The same quantities of total membrane protein were loaded on the gel. The negative control lanes are clear of any unspecific bands.

4.4.3. Summary of western blot analysis of β_1 -AR and β_2 -AR expression in MMY yeast

The western blot performed in this study can provide a limited information on the relationship between the level of protein expression and the functional response. The first limitation is that western blots of the total membranes cannot inform us on how much of this protein is correctly folded and in what cellular compartment it resides. The only clear pattern the experiments show is that when the colonies show a functional response there is also a band pattern on the western blot that is not observed in the negative controls. When there is no functional response, most of the colonies analysed did not show any specific bands on the western blot, with the exception of p306GPD-ADRB2 CL4 which showed weakly detected bands at 40-42kDa.

In the colonies that present bands on a western blot and a functional signal assay no correlation between the level of signal intensities can be drawn. If there was a direct correlation, p306GPD-MF α -ADRB2 CL5, WB lane 9 in **Figure 4.20 B** would have the strongest band signal on the western blot, but instead it's p306GPD-MF α -ADRB2 CL1 in lane 7. However, there still must be a threshold of protein expression required for a functional response as indicated by the faint bands of colony p306GPD-ADRB2 CL4, which produced no functional response.

It is difficult to interpret why there is difference in functional response and western blot of β_2 -AR expressing colonies depending whether it is expressed in the p426GPD or p306GPD plasmid in that MF α only seemed to bring an improvement in the integrating plasmid system. There is also slightly different band pattern - the colonies expressing β_2 -AR in p426GPD plasmid appear to have clear bands at 39kDa and 41kDa while those expressed in p306GPD MF α plasmid do not appear to have the 41kDa band or it is very faint. The p306GPD-ADRB2 CL4 colony (non-functional) which has no MF α sequence appear to have both bands. One of possible explanation is that the 41kDa band represents a hyperglycosylated protein while the 39kDa is the non-glycosylated form.

The functional expression of β_1 -AR has a clearer preference for constructs with MF α leader sequence as demonstrated in section 4.2.4, although it was more difficult to demonstrate this on the western blot partly because of antibody quality issues. There too appears to be two bands of similar size, however it is a smaller band that would be expected for β_1 -AR (50kDa as estimated by Abcam).

Chapter 5 – The pharmacological characterisation of adrenoceptors β_1 and β_2 in yeast

5.1. Introduction

The adrenoceptors β_1 and β_2 have been well characterised in other recombinant hosts but scarcely in *Saccharomyces cerevisiae*. We have taken the opportunity of having obtained functional expression of these receptors in the MMY yeast and tested them against a panel of known agonists and antagonists listed in **Table 5.1**. The aims of this work were to: 1) characterise the activity of the ligands at these GPCRs coupled to chGas proteins using MMY strains that represent different signalling pathways; 2) compare the values of previously obtained pEC₅₀ and pIC₅₀ from other assays; 2) bench-mark the yeast assay against the others for the same signalling pathway.

5.2. Ligand selection and experimental set-up

The IUPHAR international database hosts a comprehensive collection of information on the adrenoceptors including lists of known agonists and antagonists. This information source was used to select the ligands for this study. Those that were available on the GSK's UK based compound library were used and are listed in the **Table 5.1**. The third column notes the interaction also retrieved from the IUPHAR.

Initially, the interacting strains were identified by their response to a full agonist isoprenaline (isoproterenol). The agonist assay data have also been normalised to this ligand where the baseline (bottom) of isoprenaline is 0% response and its maximal response (top) is the 100%. The top and bottom values were obtained from the three parameter non-linear regression curve fit on GraphPad Prism V7.03. Nine MMY strains were identified to respond to isoprenaline when β_1 -AR was present, as shown in **Chapter 4** – MMY12 (Gpa1), MMY14 (G α_q), MMY15 (G α_s), MMY16 (G α_{16}), MMY20 (G α_{13}), MMY21 (G α_{14}), MMY22 (G α_o), MMY23 (G α_{i1}), and MMY24 (G α_{i3}). For the β_2 -AR five strains were identified as responsive to receptor-pathway coupling - MMY14 (G α_q), MMY15 (G α_s), MMY16 (G α_{16}), MMY21 (G α_{14}), and MMY23 (G α_{i1}).

For the antagonist assays the receptors were stimulated with 2.5 μ M of isoprenaline to demonstrate the inhibition of growth by antagonist action. Antagonism data were normalised against control compound carvedilol (C30) in the same way as agonist data were normalised against isoprenaline.

Each assay was carried out for 24h; readings were taken at 18h and 24h. The data presented in this chapter are the mean of three independent experiments read at 24h; the error bars represent S.E.M.

Table 5.1 List of β_1 -AR and β_2 -AR agonists and antagonists used in this study. The list was compiled based on the information available on the IUPHAR database.

Agonists

Compound ID	Generic name	Receptor interaction (from IUPHAR)
C21	orciprenaline	β_2 agonist
C22	xamoterol	β_1 partial agonist
C25	dobutamine	β_1 and β_2 partial agonist
C31	procaterol	β_2 agonist
C33	zinterol	β_2 agonist
C34	fenoterol	β_2 agonist
C36	terbutaline	β_2 partial agonist
C39	mirabegron	β_1 and β_2 agonist
C40	indacaterol	β_1 and β_2 agonist
C42	isoprenaline	β_1 and β_2 full agonist
C46	pindolol	β_1 and β_2 partial agonist

Antagonists

Compound ID	Generic name	Receptor interaction (from IUPHAR)
C20	levobetaxolol	β_1 and β_2 antagonist
C23	labetalol	β_1 and β_2 antagonist
C24	metoprolol	β_1 and β_2 antagonist
C26	nadolol	β_1 and β_2 antagonist
C27	propranolol	β_1 and β_2 antagonist
C28	alprenolol	β_2 antagonist
C29	sotalol	β_1 and β_2 antagonist
C30	carvedilol	β_1 and β_2 antagonist
C35	levobunolol	β_1 and β_2 antagonist
C37	esmolol	β_1 antagonist
C38	propafenone	β_1 and β_2 antagonist
C41	atenolol	β_1 and β_2 antagonist
C43	acebutolol	β_1 antagonist
C44	practolol	β_1 antagonist
C48	bupranolol	β_1 and β_2 antagonist
C49	betaxolol	β_1 and β_2 antagonist

5.3. Pharmacological characterisation of the β_1 -AR in MMY strains

5.3.1. Agonist assay

The compound testing results presented in **Figure 5.2** give an overview of agonist activity in the nine MMY strains expressing β_1 -AR. The Gpa1, $G\alpha_q$, $G\alpha_s$, $G\alpha_{16}$, $G\alpha_{i1}$, and $G\alpha_{i3}$ strains at the first glance look the most similar to each other in terms of order of agonist potency and maximum efficacy. The **Table 5.3** in which both these parameters are listed reiterates this observed pattern. There are some differences between these strains too, for example C22 – xamoterol – appears to have partial agonist activity in $G\alpha_s$, $G\alpha_{16}$, and $G\alpha_{i1}$ but no agonism in Gpa1 or $G\alpha_q$ strains.

The remaining strains $G\alpha_{13}$, $G\alpha_{14}$, and $G\alpha_o$ demonstrate much more distinct profiles. In the $G\alpha_{13}$ strain most of agonist show a very weak or no agonism on the receptor (**Figure 5.2**). Orciprenaline (C21) and fenoterol (C34) have comparable efficacy to isoprenaline (C42), terbutaline (C36) has a slightly lower and dobutamine (C25) appears to have a much higher E_{max} compared to isoprenaline albeit large error bars and low potency (**Figure 5.4**). Other compounds C22, C31, C33, C39, and C46 do not appear to have any effect on the β_1 -AR in this strain contrary to the observation in other strains. Another interesting aspect about this strain is that several listed antagonists show an ability to inhibit baseline yeast growth which could be interpreted as inverse agonism. They are highlighted in orange in **Table 5.3**. These are compounds C27, C35, C37, C43 and C48; they have no other activity in other strains, similarly to C30 shown **Figure 5.4**. Carvedilol (C30) is the most potent out of these with $pEC_{50}=6.5$. Compounds C23 and C38 show very small agonist activity in the $G\alpha_{14}$ strain (C23 shown in **Figure 5.4**) but are inhibiting growth in the $G\alpha_{13}$ strain. Indacaterol (C40), a potent agonist in most strains, not only has no activity as an agonist in this strain, but also shows some inhibition of growth in $G\alpha_{13}$ similar to the mentioned antagonists (**Figure 5.4**). Overall, many compounds show no ability to induce growth or sometimes even inhibit it.

Another MMY strain which stands out is MMY21 ($G\alpha_{14}$) in which almost the opposite effects are observed. For example, C22, C28, C31, C46 show 55-84% of E_{max} , (**Table 5.3**) whereas in other strains it is less than 14-31%. Xamoterol (C22) is listed as partial β_1 -AR agonist, as it appears to be in $G\alpha_s$, $G\alpha_{16}$ and $G\alpha_{i1}$, however in this strain it is approximately three times more efficacious; this is well illustrated in **Figure 5.4**. Alprenonol (C28) is listed as β_2 -AR antagonist in the IUPHAR database and has some activity as an antagonists in β_1 -AR, but again, $G\alpha_{14}$ is an exception – the ligand appears to have partial agonist activity (**Figure 5.4**). Pindolol (C46) also shows higher efficacy in this strain compared to others is listed as partial β_1 -AR and β_2 -AR agonist. Often agonists that show activity in most of the strains appear to be most potent in $G\alpha_{14}$, for example C36, C39, C42, C42. The $G\alpha_o$ similarly to $G\alpha_{13}$ appears to

poorly respond to most agonist stimulation, although order of potencies is similar to those observed in $G\alpha_q$ and Gpa1 strains.

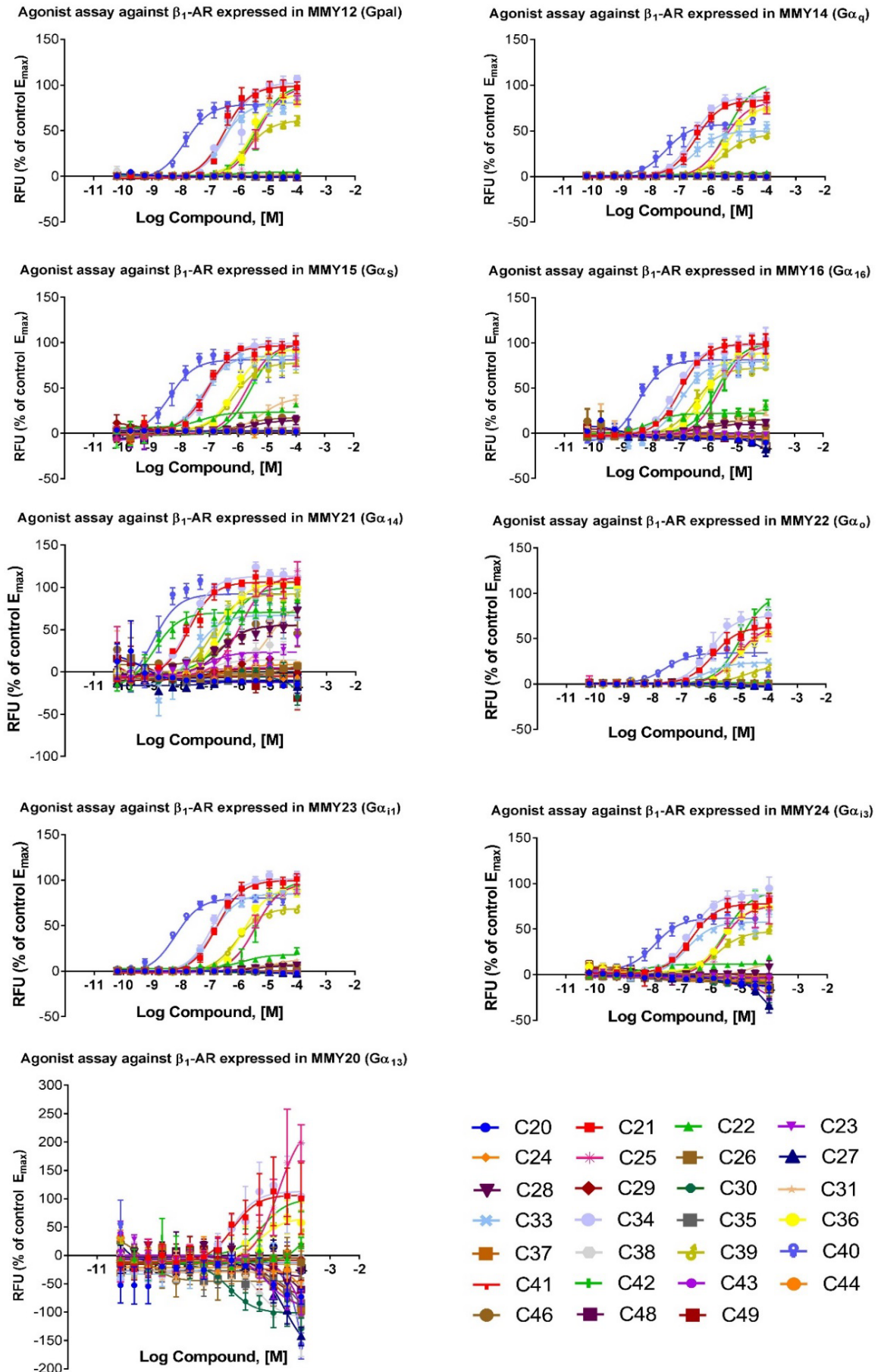


Figure 5.2 The summary of agonist assay results in β_1 -AR expressing MMY strains. Responses were normalised against full agonist isoprenaline. n=3

Table 5.3 Summary of pEC₅₀ and E_{max} values of β₁-AR agonist assay in MMY strains. The data is presented as a mean of 3 independent experiments and was obtained from GraphPad Prism three parameter non-linear fit analysis. E_{max} values are colour coded as follows: green >80%, light green 50-80%, orange <80% which indicates inverse agonism. Some data could not be fitted because the compound produced no response and hence empty cells.

Agonist assay	Gpa1		Gq		Gs		G16		G13		G14		Go		G11		G13	
	E _{max}	pEC ₅₀	E _{max}	pEC ₅₀	E _{max}	pEC ₅₀	E _{max}	pEC ₅₀	E _{max}	pEC ₅₀	E _{max}	pEC ₅₀	E _{max}	pEC ₅₀	E _{max}	pEC ₅₀	E _{max}	pEC ₅₀
C20 levobetaxolol	-0.2 (±0.4)	8.9	-0.2 (±0.2)	5.5	2.3 (±0.1)	10.2	-6.3 (±1.6)	8.9			-11.6 (±3.4)	9.3	-3.1 (±0.9)	4.8	-2.8 (±0.4)	4.9	-12.9 (±2.1)	5.6
C21 orciprenaline	98.8 (±3.3)	6.5	83.7 (±1.9)	6.4	96.5 (±2.4)	7.0	99.15 (±2.0)	7.0	106.7 (±16.2)	6.3	106.4 (±2.2)	7.7	63.0 (±2.9)	5.9	99.7 (±1.8)	6.8	77.8 (±1.8)	6.7
C22 xamoterol	4.8 (±0.3)	6.1	3.1 (±0.3)	7.3	23.3 (±1.2)	7.3	22.3 (±1.3)	8.0			70.3 (±3.0)	8.9	1.4 (±0.1)	7.1	18.2 (±1.3)	5.9	11.4 (±0.8)	8.5
C23 labetalol	-0.8 (±0.2)	5.6	-0.5 (±0.2)	5.5			-0.5 (±0.5)	8.1	-92.3 (±12.9)	5.2	23.5 (±2.6)	7.1	-2.8 (±0.9)	5.0	-2.1 (±0.3)	5.3	-3.2 (±0.8)	8.6
C24 metoprolol	-1.0 (±0.5)	4.4	-0.4 (±0.3)	4.5	1.6 (±0.8)	6.3	-4.8 (±0.5)	6.2							-1.3 (±0.3)	4.7	-5.9 (±1.0)	7.2
C25 dobutamine	98.2 (±4.5)	5.4	82.0 (±3.0)	5.5	99.0 (±4.4)	5.7	98.0 (±3.8)	5.6	238.8 (±47.4)	4.8	112.9 (±6.7)	6.0	64.9 (±3.4)	5.1	96.9 (±3.3)	5.4	75.8 (±4.7)	5.6
C26 nadolol	0.2 (±0.1)	9.0			2.8 (±0.6)	8.7	-2.6 (±1.3)	9.2	-4.9 (±9.8)	5.8	12.3 (±21.5)	4.4	-1.4 (±40.6)	3.2	0.0 (±0.1)	7.8	-11.6 (±5.5)	4.4
C27 propranolol	-0.8 (±0.2)	5.5	-0.7 (±0.2)	5.1	2.7 (±0.2)	9.9	-33.1 (±18.8)	4.0	-176.7 (±25.3)	4.6	-10.0 (±1.8)	6.8	-3.7 (±1.0)	4.8	-3.8 (±0.8)	4.6	-65.6 (±21.2)	4.0
C28 alprenolol			0.7 (±0.1)	8.3	14.3 (±1.4)	5.6	10.0 (±1.0)	6.5	-37.8 (±17.3)	5.4	55.5 (±3.2)	6.6	-1.0 (±1.3)	4.4	6.1 (±0.6)	5.4	0.8 (±1.1)	9.2
C29 sotalol	0.4 (±0.1)	5.5	0.4 (±0.1)	6.0	2.5 (±0.9)	9.5	-3.0 (±0.4)	7.1	-8.9 (±5.2)	7.8	3.6 (±1.7)	7.2	1.4 (±0.8)	4.6			-2.7 (±0.5)	9.2
C30 carvedilol	-1.1 (±0.1)	6.6	-0.4 (±0.2)	6.8	3.1 (±0.5)	5.3	-11.5 (±16.2)	4.1	-101.8 (±9.2)	6.5			-3.2 (±0.5)	6.7	-2.4 (±0.3)	6.4	-9.6 (±2.5)	6.4
C31 procaterol	3.8 (±0.7)	4.7	2.5 (±0.3)	5.0	39.5 (±2.7)	5.2	31.2 (±8.9)	4.8	-29.7 (±4.3)	11.1	83.9 (±16.4)	5.0	1.1 (±0.2)	6.8	13.2 (±0.8)	4.9	14.4 (±3.2)	4.7
C33 zinterol	80.7 (±2.3)	6.6	49.9 (±2.1)	6.5	85.5 (±2.9)	7.2	79.2 (±3.4)	7.0	-14.2 (±7.5)	7.3	66.9 (±5.8)	7.5	23.6 (±0.7)	6.1	85.1 (±1.0)	6.9	57.6 (±1.8)	6.9
C34 fenoterol	102.6 (±3.6)	6.3	87.4 (±2.2)	6.5	99.5 (±2.6)	7.0	97.5 (±3.1)	7.1	112.8 (±19.5)	6.4	113.2 (±2.2)	7.8	74.9 (±3.4)	6.0	101.7 (±2.1)	6.9	87.9 (±2.4)	6.7
C35 levobunolol	-1.1 (±0.4)	4.6	-0.3 (±0.3)	4.6	2.4 (±0.5)	9.0	-6.2 (±3.0)	4.5	-127.9 (±100.2)	4.1	10.1 (±1.0)	8.4	-2.0 (±1.1)	4.4	-2.4 (±0.8)	4.4	-5.6 (±0.8)	8.8
C36 terbutaline	91.6 (±3.6)	5.6	78.8 (±2.2)	5.3	92.6 (±2.8)	6.1	89.5 (±2.1)	6.1	66.4 (±14.3)	5.4	105.6 (±2.6)	6.6	61.8 (±3.6)	5.0	92.5 (±2.1)	5.8	77.6 (±3.1)	5.6
C37 esmolol	-1.2 (±0.3)	4.7	0.0 (±0.2)	5.5	2.8 (±0.6)	9.1	-10.9 (±3.4)	4.5	-101.7 (±27.3)	4.8	-2.3 (±1.2)	7.9	-2.5 (±0.6)	5.0	-2.9 (±0.9)	4.4	-7.6 (±1.2)	8.6
C38 propafenone			-0.3 (±0.1)	6.9	8.4 (±2.0)	4.7			-110.4 (±14.8)	5.6	14.3 (±4.6)	7.0	-3.7 (±0.7)	6.2	-1.0 (±0.3)	6.3	-34.8 (±24.0)	4.2
C39 mirabegron	61.6 (±1.8)	5.7	46.0 (±1.6)	5.5	77.8 (±3.0)	6.2	72.6 (±2.0)	6.4			92.2 (±2.4)	6.9	20.6 (±1.7)	4.7	69.1 (±1.0)	6.1	47.4 (±2.6)	5.8
C40 indacaterol	78.9 (±2.0)	7.9	57.1 (±2.1)	7.5	81.9 (±3.8)	8.4	81.4 (±2.8)	8.4			92.2 (±4.5)	9.0	34.2 (±2.6)	7.6	80.3 (±1.7)	8.2	61.9 (±2.7)	7.9
C41 atenolol			0.3 (±0.1)	9.6	2.6 (±0.6)	9.3	-3.0 (±0.5)	8.2	-4.5 (±6.4)	6.7			0.9 (±0.3)	5.6	0.1 (±0.1)	7.0	-5.8 (±1.1)	8.5
C42 isoprenaline	100.0 (±4.5)	5.4	103.0 (±2.8)	5.4	99.6 (±4.2)	5.6	100.0 (±4.2)	5.7	100.0 (±19.6)	5.3	100.0 (±2.6)	6.5	100.0 (±4.3)	5.0	100.0 (±4.3)	5.4	91.2 (±3.9)	5.5
C43 acebutolol			-1.0 (±0.4)	4.4	2.9 (±1.3)	9.1	-32.6 (±42.4)	3.6	-265.4 (±337.5)	3.7	4.8 (±2.1)	7.3	-3.7 (±2.8)	4.2			-33.1 (±9.1)	4.4
C44 practolol	0.3 (±0.1)	8.3	0.7 (±0.1)	7.0	2.5 (±0.6)	8.8	-4.0 (±0.3)	8.8	-15.8 (±9.6)	6.7	8.7 (±2.2)	6.1	0.9 (±0.3)	6.2	0.3 (±0.1)	6.9	-1.8 (±1.1)	8.0
C46 pindolol	1.3 (±0.2)	6.3	1.8 (±0.1)	6.0	17.0 (±1.4)	5.9	14.8 (±2.9)	6.1	-45.7 (±7.8)	9.4	54.8 (±5.7)	6.5			7.5 (±0.4)	5.5	-0.3 (±1.0)	8.2
C48 bupranolol	-1.1 (±0.2)	5.8	0.0 (±0.2)	5.7	2.7 (±0.7)	9.0	-6.1 (±0.8)	8.0	-83.9 (±76.1)	4.3	-4.8 (±1.3)	8.4	-2.9 (±0.8)	4.9	-2.9 (±0.7)	4.6	-3.7 (±1.5)	8.2
C49 betaxolol	-0.8 (±0.2)	5.7	-0.3 (±0.1)	5.8	2.9 (±1.2)	9.0	-5.4 (±1.1)	8.6	-73.7 (±23.4)	5.1	-12.4 (±3.0)	8.9	-2.0 (±0.6)	5.0	-2.5 (±0.4)	4.8	-11.4 (±2.1)	6.2

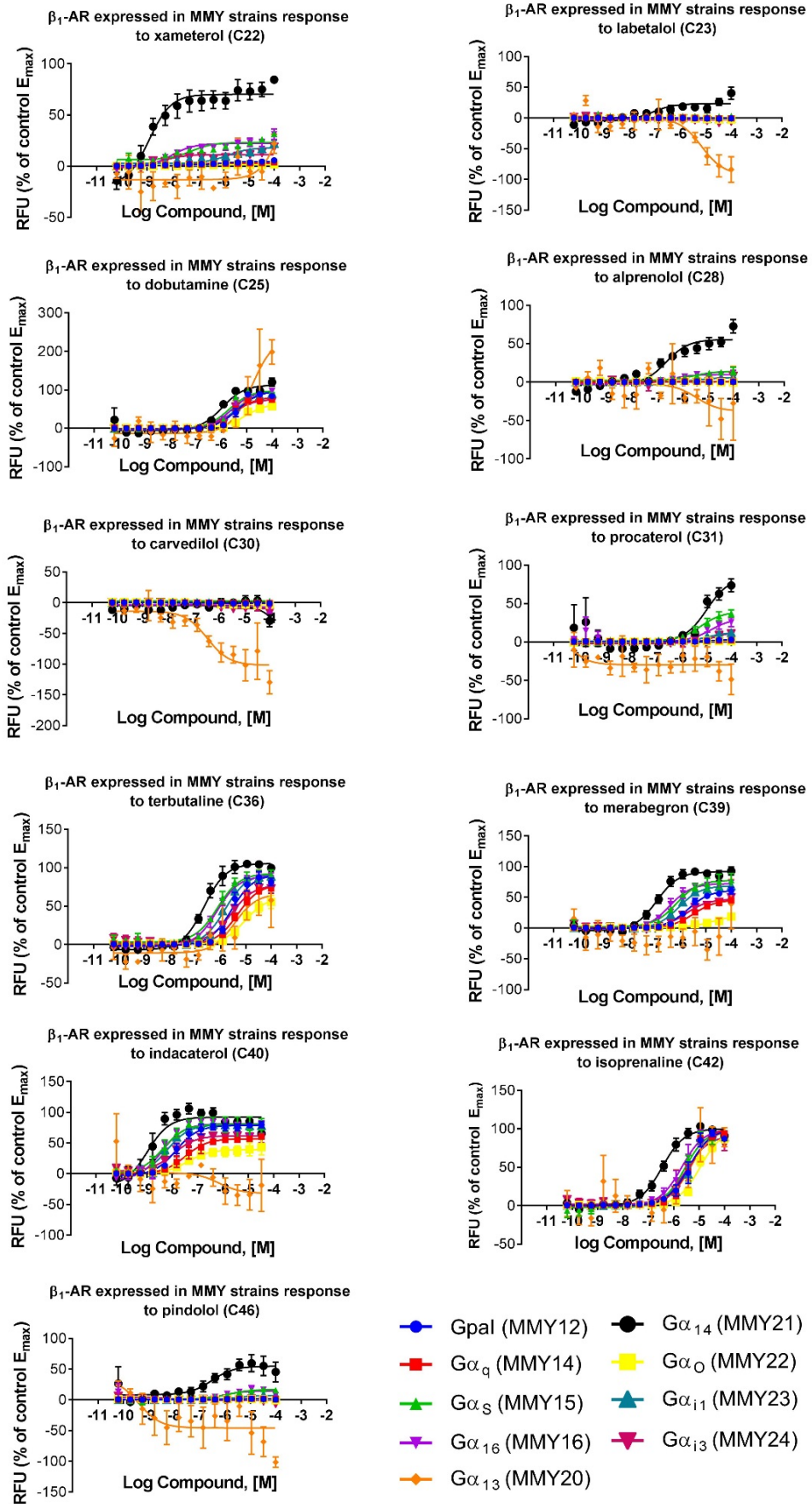


Figure 5.4 Selected compound response on the β_1 -AR presented in all strains. This graph illustrates some responses that were different in particular strains. n=3

5.3.2. Antagonist assay

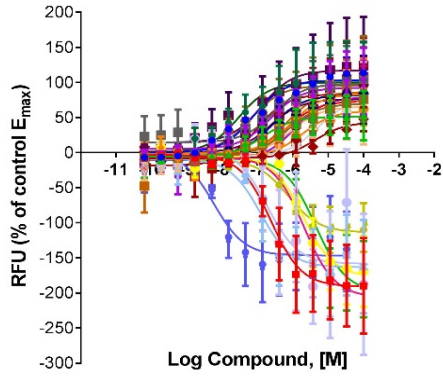
The antagonist assay using β_1 -AR expressed in the same MMY strains is presented in **Figure 5.5** and the pIC_{50} and E_{max} values in **Table 5.6**. The raw values were normalised against carvedilol (C30) and therefore any agonist activity appears on the negative Y axis.

Based on the overview in **Figure 5.5** the antagonism of the β_1 -AR in different strains appears more uniform than agonism. Some of the individual compounds are shown in **Figure 5.7** and are discussed below.

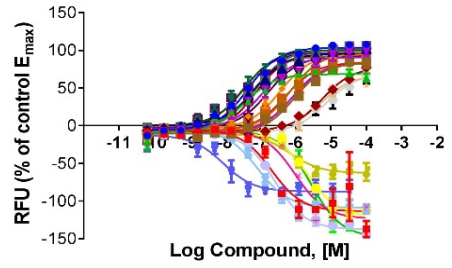
The first compound presented is xamoterol (C22) which as discussed in the agonist section has strong agonist activity in $G\alpha_{14}$. However, when tested in an antagonist assay it exhibited antagonistic activity in $G\alpha_q$, $Gpa1$, $G\alpha_{i3}$, $G\alpha_o$ but not in $G\alpha_s$, $G\alpha_{16}$, $G\alpha_{13}$, $G\alpha_{14}$ or $G\alpha_{i1}$ strains. Procaterol (C31) demonstrates variable potencies and efficacies. It is most potent in $G\alpha_{16}$ although E_{max} is lower than in $Gpa1$, $G\alpha_q$, $G\alpha_{i1}$ and $G\alpha_o$ strains. Very low or no antagonistic effect in $G\alpha_s$, $G\alpha_{13}$, $G\alpha_{14}$, $G\alpha_{i3}$. Indacaterol (C40) mirrors the activity that was seen in the agonist assay – agonistic effect of various degrees in all strains but $G\alpha_{13}$ and $G\alpha_{14}$. Very weak or no antagonist activity in $G\alpha_{13}$ was also produced by majority of compounds listed as antagonists – C24, C26, C28, C29, C41, C44, C48, and C49. Antagonist C20, C23, C27, C35, C37, C46 although produced comparable inhibition on $G\alpha_{13}$ strain when compared with others, showed lower potencies in this strain (**Table 5.6**). Other compounds not mentioned in this paragraph had either comparable antagonism to that of control compound carvedilol or only agonistic affect that was observed in the agonist assay, including isoprenaline. Individual graphs of all compounds not shown in **Figure 5.7** can be found in the **appendix D**.

The agonist in this panel of compounds produced agonism (induction of growth), which is expected. However, the level of induction was different between the strains. This can be explained by strain background growth and because agonist assay results were normalised against an agonist, all other compound responses are relative to agonist and therefore do not appear so different as when they were normalised to an antagonist carvedilol.

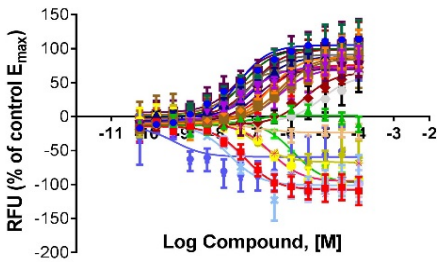
Antagonist assay against β_1 -AR expressed in MMY12 (G α_i)



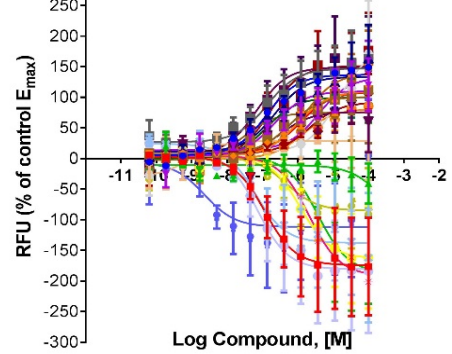
Antagonist assay against β_1 -AR expressed in MMY14 (G α_q)



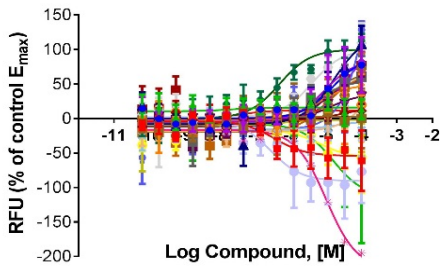
Antagonist assay against β_1 -AR expressed in MMY15 (G α_s)



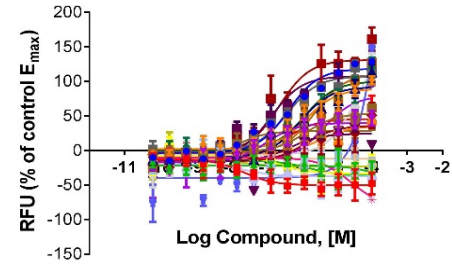
Antagonist assay against β_1 -AR expressed in MMY16 (G α_{16})



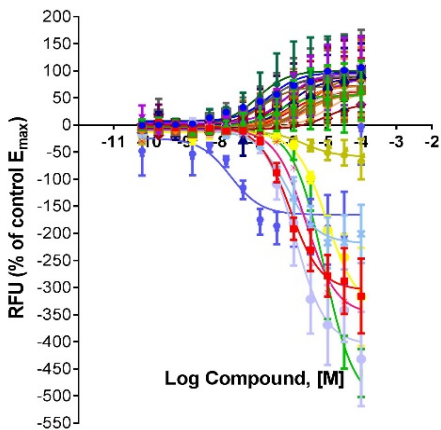
Antagonist assay against β_1 -AR expressed in MMY20 (G α_{13})



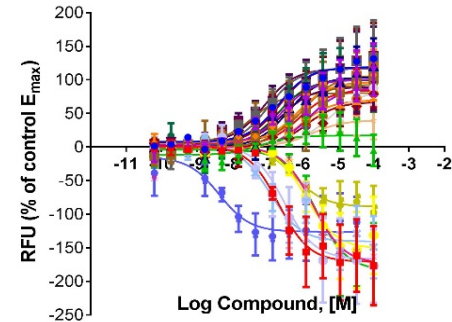
Antagonist assay against β_1 -AR expressed in MMY21 (G α_{14})



Antagonist assay against β_1 -AR expressed in MMY20 (G α_o)



Antagonist assay against β_1 -AR expressed in MMY23 (G α_{11})



Antagonist assay against β_1 -AR expressed in MMY24 (G α_{13})

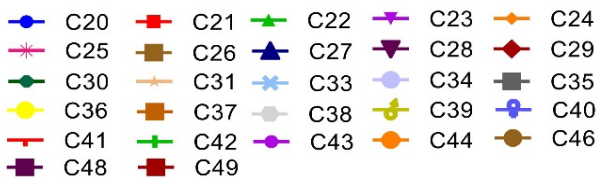
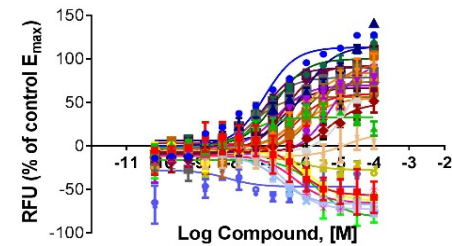


Figure 5.5 The summary of antagonist assay results in β_1 -AR expressing MMY strains. The data was normalised against antagonist carvedilol. n=3

Table 5.6 Summary of pIC₅₀ and E_{max} values of β_1 -AR antagonist assay in MMY strains. The data are presented as a mean of 3 independent experiments and was obtained from GraphPad Prism three parameter non-linear fit analysis. E_{max} values are colour coded as follows: green <49%, light pink 50-80%, dark pink >80% inhibition of control antagonist carvedilol. Some data could not be fitted because the compound produced no response and hence empty cells.

Antagonist assay	Gpal		Gq		Gs		G16		G13		G14		Go		G11		G13	
	E _{max}	pIC ₅₀	E _{max}	pIC ₅₀	E _{max}	pIC ₅₀	E _{max}	pIC ₅₀	E _{max}	pIC ₅₀	E _{max}	pIC ₅₀	E _{max}	pIC ₅₀	E _{max}	pIC ₅₀	E _{max}	pIC ₅₀
C20 levobetaxolol	103 (±13.2)	7.1	103.6 (±3.0)	7.3	105.3 (±7.3)	7.4	136.9 (±11.3)	6.9	91.4 (±31.3)	4.8	118.1 (±6.9)	6.4	96.9 (±17.4)	6.6	118.8 (±12.4)	6.7	113.2 (±5.5)	7.1
C21 orciprenaline	-190.9 (±17.0)	6.6	-113.4 (±7.3)	6.7	-107.7 (±4.7)	7.2	-174.3 (±20.0)	6.9	-54.3 (±10.1)	6.5	-50.6 (±4.2)	7.6	-305 (±16.3)	6.0	-171 (±15.0)	6.7	-57.0 (±8.6)	6.2
C22 xamoterol	51.3 (±7.5)	6.8	68.6 (±2.1)	7.5	1.6 (±3.1)	7.2	-99.1 (±379.1)	3.7	15.8 (±5.8)	7.7	-44.7 (±138.0)	3.9	54.7 (±17.2)	6.4	17.2 (±7.1)	7.2	33.0 (±2.5)	7.6
C23 labetalol	92.5 (±11.3)	6.6	90.8 (±2.6)	6.9	72.8 (±4.3)	7.1	109.9 (±10.8)	6.7	86.0 (±23.3)	5.0	39.4 (±5.4)	7.0	96.0 (±18.7)	6.1	100.5 (±9.8)	6.6	69.7 (±2.5)	6.8
C24 metoprolol	83.9 (±10.7)	6.1	94.9 (±2.5)	6.4	88.1 (±6.3)	6.5	109.8 (±8.7)	6.0	49.3 (±13.6)	5.2	89.2 (±7.4)	5.9	72.2 (±16.0)	5.9	97.0 (±9.5)	6.1	84.7 (±4.9)	6.0
C25 dobutamine	-206.2 (±18.3)	5.7	-123.4 (±4.8)	6.0	-95.5 (±6.8)	6.5	-191.7 (±27.2)	5.7	-218.2 (±24.7)	5.0	-81.7 (±25.5)	4.6	-349.5 (±17.1)	5.6	-173.6 (±17.7)	5.7	-65.4 (±4.6)	6.2
C26 nadolol	69.6 (±8.2)	6.1	83.4 (±2.6)	6.0	85.2 (±5.9)	6.2	100.9 (±8.7)	6.2	2.7 (±7.6)	7.4	53.5 (±6.1)	5.9	58.2 (±14.6)	5.7	93.0 (±8.8)	6.2	74.3 (±5.7)	6.1
C27 propranolol	81.7 (±10.9)	6.6	95.4 (±1.8)	7.2	87.6 (±5.7)	6.9	133.7 (±5.7)	6.7	122.5 (±12.5)	4.8	91.8 (±27.1)	6.0	84.9 (±6.5)	6.1	104.1 (±18.0)	6.4	114.3 (±11.5)	6.0
C28 alprenolol	76.0 (±9.4)	6.7	92.5 (±3.3)	6.8	70.4 (±6.0)	6.9	76.0 (±11.7)	6.5	35.8 (±18.4)	4.9	24.2 (±5.7)	6.3	72.6 (±17.0)	5.9	89.2 (±10.4)	6.6	66.7 (±3.5)	6.7
C29 sotalol	43.5 (±8.4)	5.4	77.6 (±2.8)	5.3	65.3 (±4.4)	5.5	92.1 (±9.7)	5.7	15.4 (±17.0)	4.6	35.9 (±8.8)	5.9	40.0 (±12.1)	5.0	67.0 (±8.1)	5.9	49.1 (±6.5)	5.3
C30 carvedilol	100.0 (±12.9)	7.5	100.0 (±2.7)	7.4	100.0 (±7.5)	7.3	100.0 (±8.8)	6.9	100.0 (±8.0)	6.3	100.0 (±6.4)	5.9	100.0 (±17.9)	6.9	100.0 (±13.2)	6.7	100.0 (±4.3)	6.8
C31 procaterol	65.7 (±16.6)	6.0	67.4 (±4.3)	5.3	-23.8 (±2.9)	6.8	28.9 (±8.7)	9.0	145.8 (±809.6)	3.5	-12.2 (±2.9)	9.2	62.1 (±20.1)	5.0	39.8 (±7.9)	5.7	14.4 (±15.3)	4.8
C33 zinterol	-163.3 (±15.3)	6.9	-108.5 (±2.6)	7.1	-101.1 (±6.0)	7.7	-137.8 (±21.9)	7.2	-3.3 (±31.4)	4.7			-218.4 (±14.9)	6.1	-140.5 (±10.2)	6.9	-67.1 (±3.2)	6.7
C34 fenoterol	-158.3 (±26.3)	6.7	-137.2 (±2.5)	6.6	-106.3 (±4.4)	7.3	-180.6 (±23.3)	7.1	-90.7 (±12.5)	6.6	-37.8 (±5.6)	7.6	-405.2 (±26.9)	5.9	-166.9 (±17.8)	6.5	-72.8 (±2.7)	6.5
C35 levobunolol	98.5 (±14.5)	6.6	100.9 (±2.0)	7.1	91.2 (±5.8)	7.1	147.1 (±13.2)	6.9	54.9 (±16.8)	5.3	107.1 (±4.9)	6.4	89.6 (±20.3)	6.6	116.9 (±12.2)	7.0	78.7 (±3.9)	7.2
C36 terbutaline	-177.2 (±15.9)	5.7	-120.9 (±3.7)	5.7	-94.7 (±7.3)	6.5	-163.3 (±22.6)	5.9	-58.0 (±18.0)	5.2	-33.6 (±5.7)	6.6	-341.9 (±31.4)	5.0	-151.4 (±16.1)	5.9	-63.3 (±3.6)	5.8
C37 esmolol	86.6 (±12.9)	6.2	97.3 (±3.2)	6.2	87.7 (±8.1)	6.2	139.9 (±13.5)	5.8	67.1 (±17.3)	5.0	111.3 (±7.5)	5.6	91.4 (±20.1)	5.4	106.7 (±11.8)	6.0	94.8 (±5.9)	5.6
C38 propafenone	77.1 (±11.7)	5.3	69.4 (±6.7)	5.1	60.7 (±15.7)	5.1	181.9 (±40.5)	4.9	100.5 (±15.6)	5.4	172.5 (±42.2)	4.4	67.0 (±9.3)	5.7	83.5 (±9.0)	5.2	122.1 (±19.3)	4.6
C39 mirabegron	-113.7 (±9.9)	6.1	-62.8 (±3.3)	6.2	-67.2 (±7.3)	6.9	-85.1 (±19.3)	6.3	-2.1 (±9.1)	6.3	-23.4 (±3.9)	7.6	-58.5 (±9.5)	5.6	-88.8 (±8.8)	6.3	-27.5 (±4.4)	6.2
C40 indacaterol	-146.7 (±14.4)	8.2	-87.3 (±3.6)	8.0	-59.3 (±9.3)	9.2	-111.7 (±19.8)	8.6	867.4 (±12.5)	3.3			-165.6 (±16.8)	7.7	-126.1 (±11.1)	8.4	-46.9 (±5.9)	8.1
C41 atenolol	73.3 (±9.1)	6.2	83.8 (±3.1)	6.3	75.8 (±8.6)	6.6	108.8 (±11.4)	5.9	11.7 (±2.8)	7.5	45.4 (±8.0)	6.5	61.9 (±14.2)	5.9	84.8 (±9.2)	6.1	59.8 (±4.8)	6.2
C42 isoprenaline	-199.1 (±19.9)	5.4	-148.1 (±4.7)	5.6	-98.5 (±8.3)	5.8	-187.1 (±25.7)	5.4	-114.3 (±39.2)	4.8	-37.0 (±6.4)	5.8	-515.2 (±22.3)	5.1	-183.5 (±17.7)	5.6	-82.0 (±6.5)	5.6
C43 acebutolol	79.3 (±11.5)	5.9	83.9 (±2.6)	6.1	70.3 (±8.0)	6.3	133.1 (±16.9)	5.4	112.2 (±31.2)	4.4	79.1 (±12.8)	5.4	87.5 (±20.8)	5.3	88.4 (±9.3)	5.8	95.7 (±8.7)	5.2
C44 practolol	59.7 (±8.0)	5.7	84.8 (±2.0)	6.1	70.3 (±7.5)	6.2	81.0 (±9.3)	5.8			35.3 (±7.7)	5.5	58.2 (±14.1)	5.6	69.6 (±8.1)	6.1	54.8 (±4.6)	6.0
C46 pindolol	95.7 (±13.0)	7.2	92.6 (±1.6)	7.3	69.5 (±7.2)	7.5	75.01 (±10.9)	7.5	69.9 (±28.0)	4.9	28.0 (±3.7)	8.0	71.8 (±16.9)	6.8	80.3 (±11.1)	7.4	56.2 (±3.7)	7.5
C48 bupranolol	117.2 (±18.1)	6.9	96.7 (±2.1)	7.5	99.9 (±8.5)	7.4	149.2 (±14.6)	7.2	60.4 (±19.5)	5.1	107.4 (±5.9)	6.9	87.1 (±16.9)	6.7	116.5 (±11.0)	7.1	90.0 (±3.0)	7.1
C49 betaxolol	83.5 (±13.3)	7.0	95.5 (±2.3)	7.2	98.8 (±7.7)	7.0	151.5 (±13.9)	6.8			130.8 (±9.2)	6.6	88.5 (±17.8)	6.3	119.2 (±12.3)	6.7	92.2 (±4.4)	6.5

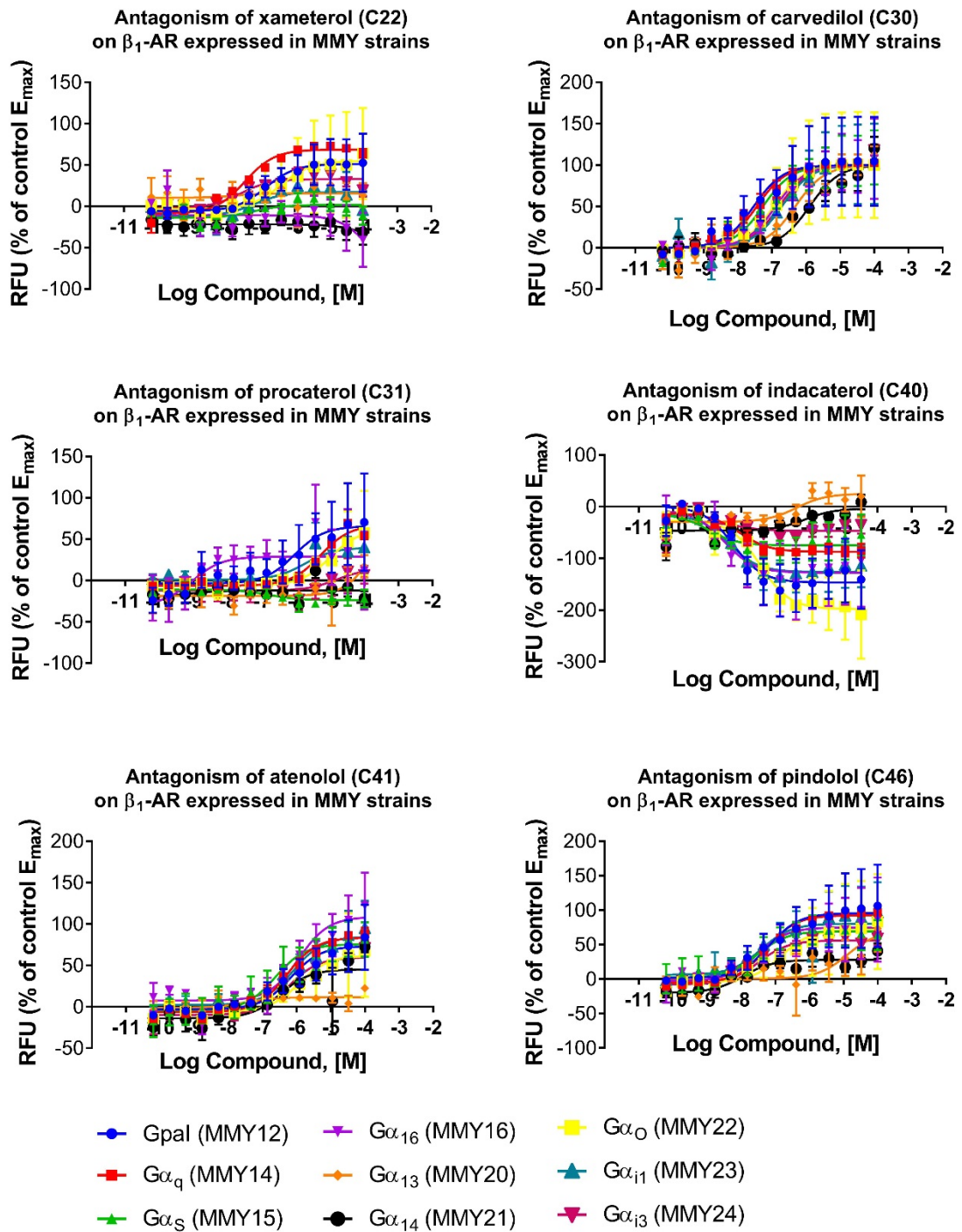


Figure 5.7 Selected compound antagonism on the β_1 -AR presented in all strains. The majority of antagonist compounds showed the same level of inhibition of growth in MMY strains expressing the β_1 -AR similar to control compound carvedilol, and therefore are not shown in this graph. Xameterol (C22) and pindolol (C46) are listed as partial agonists and procaterol (C31) as β_2 -AR antagonist but have demonstrated some antagonistic activity on this receptor.

5.4. Pharmacological characterisation of the β_2 -AR in MMY strains

5.4.1. Agonist assay

As mentioned in the introduction, only 5 MMY strains showed response to isoprenaline in the initial strain screening experiments. The agonist assay result overview is presented in **Figure 5.8**. The agonist responses in $G\alpha_s$, $G\alpha_{16}$ and $G\alpha_{14}$ strains look the most similar, while in $G\alpha_q$ and $G\alpha_{i1}$ appear to have lower efficacy with the exception of isoprenaline against which the interacting strains were selected.

Indeed, most of listed β_2 -AR agonists and partial agonists – C21, C25, C31, C33, C34, C36, and C40 show a much lower efficacy in $G\alpha_q$ and $G\alpha_{i1}$ (**Table 5.9** and **Figure 5.10**). The exception to this are C39 and C46 which are listed as partial β_2 -AR agonists but show no activity on this receptor in the tested strains.

Interestingly, idacaterol (C40) as well as showing partial agonism in $G\alpha_q$ and $G\alpha_{i1}$ do not fit the sigmoidal curve of three-parameter fit very well, but does fit a biphasic sigmoid curve as noted in dashed line in **Figure 5.10**.

As shown in β_1 -AR results, carvedilol (C30), and to lower extent C38 and C49, demonstrate the ability to inhibit baseline yeast growth in $G\alpha_{16}$ strain, characteristic of inverse agonist. However this effect appears to be lower than that seen in the β_1 -AR transformed yeast.

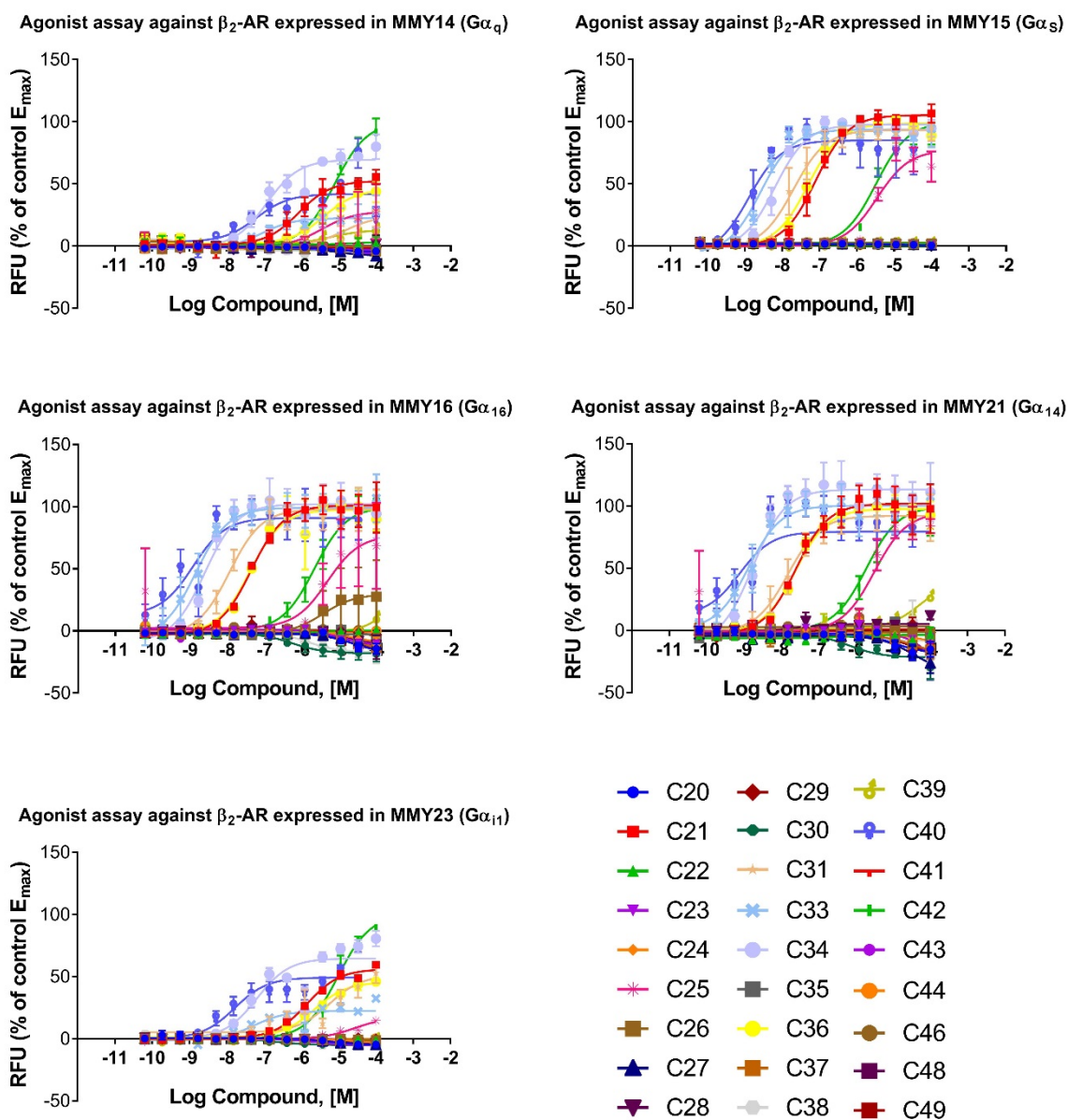


Figure 5.8 The summary of agonist assay results in β_2 -AR expressing MMY strains. As described in Chapter 4, 5 MMY strains showed response to isoprenaline – MMY 14 ($G\alpha_q$), MMY15 ($G\alpha_s$), MMY16 ($G\alpha_{16}$), MMY21 ($G\alpha_{14}$), and MMY23 ($G\alpha_{11}$). Responses were normalised against full agonist isoprenaline. n=3

Table 5.9 Summary of pEC₅₀ and E_{max} values of β₁-AR agonist assay in MMY strains. The data is presented as a mean of 3 independent experiments and was obtained from GraphPad Prism three parameter non-linear fit analysis. E_{max} values are colour coded as follows: green >80%, light green 50-80%, orange <80% which indicates inverse agonism. Some data could not be fitted because the compound produced no response and hence empty cells.

Agonist assay	Gq		Gs		G16		G14		Gi1	
	E _{max}	pEC ₅₀	E _{max}	pEC ₅₀	E _{max}	pEC ₅₀	E _{max}	pEC ₅₀	E _{max}	pEC ₅₀
C20 levobetaxolol	-4.7 (±0.9)	5.3	0.2 (±0.7)	4.6	-18.2 (±3.1)	4.6	-18.8 (±4.2)	5.0	-5.1 (±1.3)	5.3
C21 orciprenaline	52.4 (±2.8)	6.1	105.3 (±2.1)	7.1	101.0 (±3.4)	7.4	102.0 (±3.8)	7.6	56.0 (±1.3)	5.8
C22 xamoterol	3.3 (±4.9)	4.7	2.1 (±0.6)	4.2	0.6 (±0.8)	5.7	-3.5 (±1.5)	6.3		
C23 labetalol	-3.0 (±0.8)	5.9	0.9 (±0.4)	5.3	-12.2 (±2.5)	4.9			-5.3 (±0.8)	5.7
C24 metoprolol			1.2 (±0.2)	5.2	-10.4 (±4.0)	4.6	-13.2 (±11.7)	4.1	-5.3 (±2.1)	4.1
C25 dobutamine	27.8 (±7.9)	5.4	77.3 (±5.2)	5.5	77.1 (±15.3)	5.3	95.1 (±9.3)	5.5	17.5 (±2.7)	4.6
C26 nadolol			1.7 (±0.1)	5.9	29.6 (±9.7)	5.4	-1.2 (±1.0)	6.0	-1.0 (±0.2)	6.2
C27 propranolol	-7.9 (±1.5)	5.2	0.6 (±0.3)	5.2	-12.6 (±4.2)	4.7	-33.7 (±8.3)	4.5	-5.7 (±0.9)	5.2
C28 alprenolol			1.0 (±0.4)	5.2	-16.0 (±11.6)	4.4	5.1 (±1.1)	7.5	-3.8 (±0.6)	5.2
C29 sotalol	-1.6 (±0.3)	5.8	1.9 (±0.1)	9.2			0.3 (±0.8)	7.7		
C30 carvedilol	-2.8 (±0.9)	7.2	-0.3 (±0.3)	6.7	-18.1 (±1.7)	6.3	-21.7 (±2.2)	6.2	-5.0 (±0.5)	6.7
C31 procaferol	24.3 (±4.9)	4.9	93.3 (±3.0)	7.7	98.0 (±3.2)	7.9	92.2 (±3.5)	7.8	51.2 (±5.8)	5.2
C33 zinterol	22.5 (±2.8)	7.1	93.8 (±2.5)	8.6	99.1 (±3.9)	8.8	100.4 (±4.0)	8.9	22.4 (±1.8)	7.3
C34 fenoterol	69.4 (±3.5)	6.9	97.9 (±1.9)	8.2	102.0 (±4.0)	8.6	113.4 (±4.1)	8.8	64.7 (±4.0)	7.2
C35 levobunolol	-3.4 (±1.4)	4.9	1.6 (±0.1)	7.4	-2.7 (±0.4)	9.3			-6.7 (±2.7)	4.2
C36 terbutaline	45.5 (±3.6)	5.4	98.7 (±2.5)	7.3	97.6 (±4.1)	7.4	97.8 (±2.4)	7.6	45.6 (±1.6)	5.7
C37 esmolol	-2.4 (±0.6)	8.7	0.9 (±0.3)	5.0	-20.1 (±5.4)	4.3	-19.6 (±8.2)	4.5	-5.6 (±1.1)	5.0
C38 propafenone	-3.7 (±0.7)	8.8	0.7 (±0.2)	6.2	-17.2 (±1.9)	5.9	-8.3 (±3.5)	6.2	-5.4 (±0.7)	6.4
C39 mirabegron	12.9 (±6.1)	5.2	2.4 (±0.6)	5.0			41.2 (±10.7)	4.3	-2.7 (±0.5)	6.1
C40 indacaterol	41.8 (±12.1)	7.2	85.0 (±4.5)	8.9	90.9 (±5.1)	8.9	79.4 (±5.1)	9.1	49.3 (±3.1)	7.8
C41 atenolol	-2.2 (±0.7)	9.7			0.0 (±0.4)	7.3	0.9 (±0.8)	9.3		
C42 isoprenaline	100.0 (±5.30)	5.1	100.0 (±3.8)	5.5	100.0 (±4.5)	5.7	100.0 (±4.5)	5.7	100.0 (±3.7)	5.0
C43 acebutolol	-7.6 (±3.3)	4.7	0.1 (±1.0)	4.4	-32.5 (±25.0)	3.8	-85.1 (±137.9)	3.5	-10.0 (±7.5)	4.0
C44 practolol	-0.5 (±0.6)	9.4	1.7 (±0.1)	6.0	-1.1 (±0.6)	8.0	0.7 (±1.0)	6.6	-0.2 (±0.2)	7.2
C46 pindolol	-3.3 (±1.1)	6.1	2.6 (±0.3)	9.2			3.3 (±1.2)	7.4	-8.2 (±4.7)	4.0
C48 bupranolol	-1.7 (±0.7)	9.1	1.0 (±0.3)	5.7	-13.1 (±2.9)	-4.6			-5.0 (±0.8)	5.1
C49 betaxolol	-3.0 (±0.5)	9.0	0.9 (±0.3)	5.3	-16.0 (±2.6)	-4.8	-19.8 (±4.6)	4.7	-5.3 (±0.9)	5.3

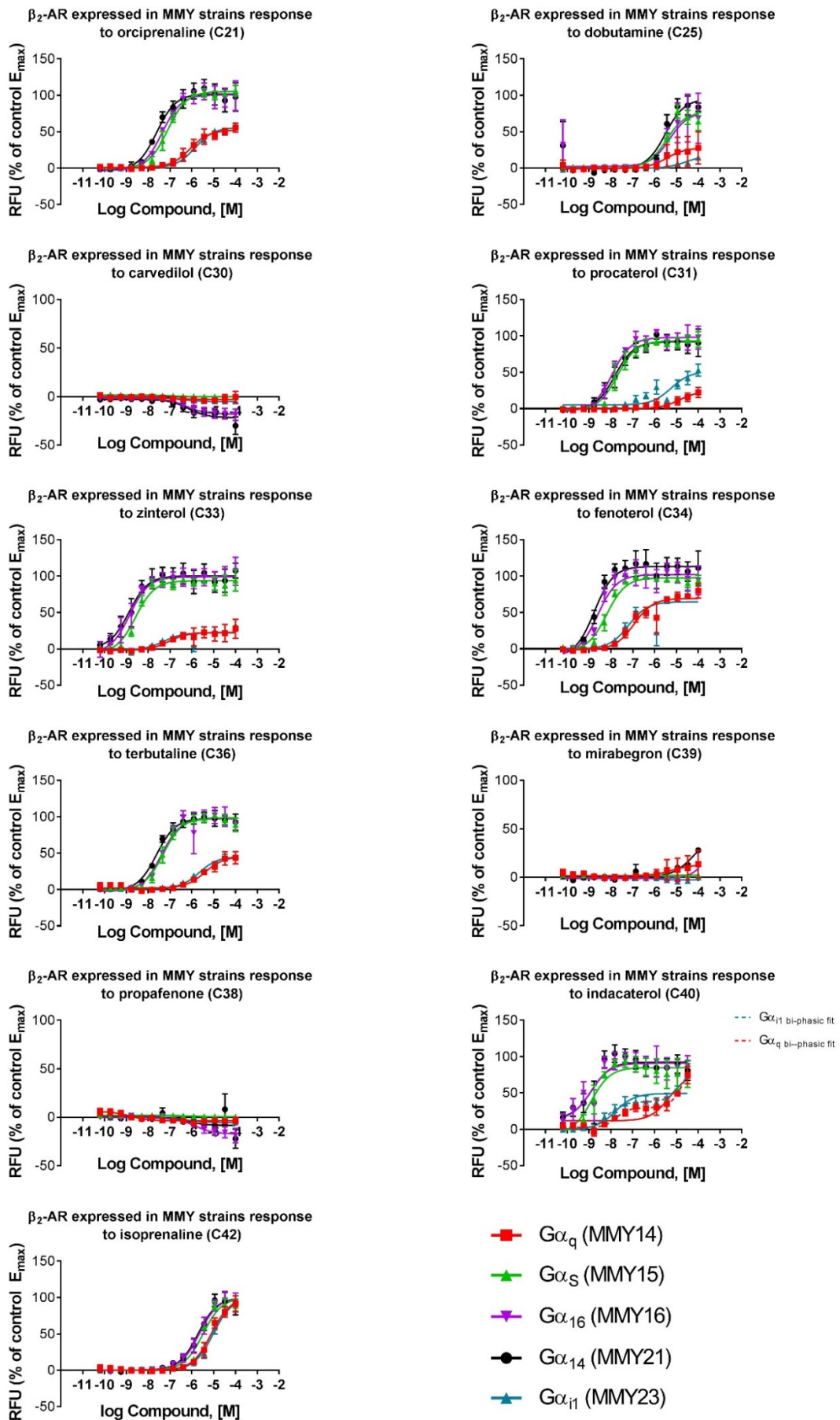


Figure 5.10 Selected agonist responses on β_2 -AR expressing strains. The examples clearly illustrate that much weaker responses were observed in $G\alpha_q$ (red) and $G\alpha_{i1}$ (teal) strains. Carvedilol and propafenone showed weak inverse agonist activity.

5.4.2. Antagonist assay

The antagonist assay against MMY strains expressing β_2 -AR was set up in the same way as for the β_1 -AR and normalised against carvedilol (C30). The agonist again appear on the negative Y axis. The overview presented in **Figure 5.11** does not show the differences in antagonist activity between the strains, but the agonists appear much more efficacious in the $G\alpha_q$ strain; again, this could be an artefact of the strain background.

To get a clearer view of antagonist activity the data of individual ligands in the different MMY strains was plotted as before. Selected results are presented in **Figure 5.13**. The ligands not presented in this figure either demonstrate agonist activity comparable to that shown in the agonist assay or are antagonists which have an activity in all tested strains comparable to the control compound carvedilol (shown in **Figure 5.13**).

One compound that stands out from this data set, as well as other assays discussed in this chapter is xamoterol (C22). It has been described as β_1 -AR partial agonist with no activity on the β_2 -AR, and indeed in the agonist assay did not show activity on the β_2 -AR. However, when tested with isoprenaline for the antagonist assay it does appear to have some agonistic effect, albeit low potency, in $G\alpha_s$ and to lesser extent $G\alpha_{16}$ and $G\alpha_{14}$, but appear so have slightly inhibitory effect in $G\alpha_q$ and $G\alpha_{i1}$. The summary of the effects of C22 in different assays is presented in **Figure 5.14**.

Compounds C27, C28, and 48 results in $G\alpha_q$, $G\alpha_s$ and $G\alpha_{i1}$ strains do not fit the sigmoidal curve very well.

Compound C39 (mirabegron) appears to have strong antagonistic effect in $G\alpha_q$ and $G\alpha_{i1}$ strains and weaker in $G\alpha_s$ and $G\alpha_{16}$ strains; it did not show significant activity as an agonist on β_2 -AR. This is in agreement with mirabegron's therapeutic use as selective β_3 -AR agonists.

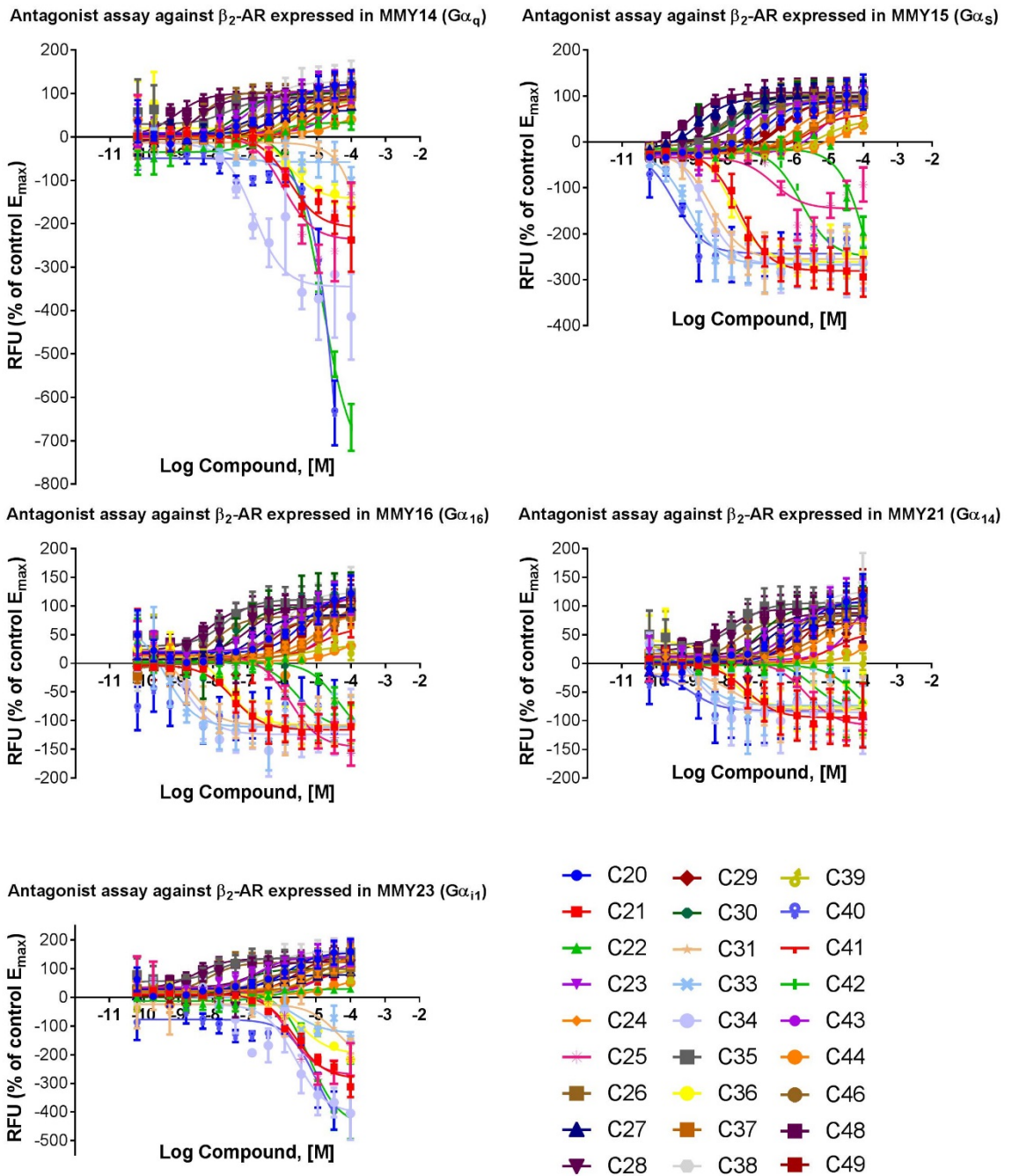


Figure 5.11 The summary of antagonist assay results in β_2 -AR expressing MMY strains. Responses were normalised against carvedilol. Agonist responses therefore appear on the negative scale. n=3

Table 5.12 Summary of pIC₅₀ and E_{max} values of β₂-AR antagonist assay in MMY strains. The data are presented as a mean of 3 independent experiments and was obtained from GraphPad Prism three parameter non-linear fit analysis. E_{max} values are colour coded as follows: green <-49%, light pink 50-80%, dark pink >80% inhibition of control antagonist carvedilol. Some data could not be fitted because the compound produced no response and hence empty cells.

Antagonist assay	Gq		Gs		G16		G14		Gi1	
	E _{max}	pIC ₅₀	E _{max}	pIC ₅₀	E _{max}	pIC ₅₀	E _{max}	pIC ₅₀	E _{max}	pIC ₅₀
C20 levetaxolol	122.1 (±13.4)	5.9	90.0 (±8.0)	6.8	120.9 (±15.1)	5.4	108.6 (±11.4)	5.9	156.4 (±15.3)	5.8
C21 orciprenaline	-209.4 (±17.0)	5.8	-280.7 (±12.3)	7.6	-116.1 (±8.0)	7.4	-94.6 (±12.5)	7.4	-284.3 (±11.8)	5.6
C22 xamoterol	33.1 (±8.5)	6.5	-602.0 (±498.5)	3.7	-136.2 (±52.9)	4.4	-104.5 (±45.4)	4.2	29.7 (±8.8)	6.2
C23 labetalol	107.5 (±9.5)	7.0	87.7 (±5.9)	7.5	111.7 (±11.6)	5.9	107.0 (±12.4)	6.0	142.0 (±12.2)	6.7
C24 metoprolol	103.3 (±14.9)	5.5	78.7 (±6.2)	6.0	87.3 (±13.7)	5.1	77.0 (±9.3)	5.2	132.0 (±14.1)	5.4
C25 dobutamine	-237.2 (±21.7)	6.0	-145.1 (±13.5)	6.6	-146.7 (±12.2)	5.8	-108.3 (±11.6)	5.7	-272.0 (±22.1)	5.8
C26 nadolol	89.9 (±7.1)	6.7	95.3 (±6.7)	7.0	78.9 (±4.5)	6.5	85.9 (±8.1)	6.3	99.6 (±7.7)	6.6
C27 propranolol	60.5 (±5.9)	7.2	96.0 (±6.3)	8.7	84.4 (±5.4)	6.8	83.4 (±6.7)	6.7	78.7 (±5.0)	6.5
C28 alprenolol	91.9 (±7.4)	8.5	98.63 (±9.7)	7.4	98.1 (±10.8)	7.0	88.2 (±11.6)	6.9	125.2 (±14.6)	6.8
C29 sotalol	85.9 (±7.4)	6.3	91.0 (±6.7)	6.4	80.8 (±8.3)	6.3	70.8 (±6.9)	6.3	100.0 (±7.2)	6.5
C30 carvedilol	100.0 (±5.0)	7.3	100.0 (±8.7)	7.7	100.0 (±11.2)	7.3	100.0 (±7.2)	7.0	100.0 (±4.3)	7.3
C31 procatrol			-255.0 (±14.0)	8.4	-108.0 (±9.3)	8.7	-80.7 (±11.1)	7.8	-234.8 (±124.1)	4.3
C33 zinterol	-57.7 (±10.4)	7.9	-266.2 (±12.5)	9.1	-111.2 (±12.1)	9.4	-73.3 (±13.8)	8.8	-124.8 (±24.9)	5.6
C34 fenoterol	-345.1 (±31.4)	6.8	-267.6 (±13.6)	8.6	-124.3 (±10.3)	8.8	-85.3 (±14.4)	8.9	-404.5 (±23.3)	5.6
C35 levobunolol	88.5 (±6.7)	7.6	84.1 (±3.5)	8.2	111.4 (±9.7)	7.7	105.6 (±10.5)	7.6	137.8 (±12.0)	7.9
C36 terbutaline	-143.4 (±19.4)	5.9	-261.2 (±12.6)	7.8	-107.7 (±9.2)	7.6	-76.2 (±11.1)	8.0	-196.4 (±18.3)	5.5
C37 esmolol	97.6 (±12.3)	5.3	86.9 (±6.0)	5.4	105.9 (±16.5)	4.8	96.7 (±16.7)	5.1	159.0 (±24.8)	4.8
C38 propafenone	127.2 (±12.8)	6.7	105.1 (±7.6)	6.4	123.1 (±10.4)	6.1	125.0 (±12.8)	5.9	160.6 (±12.9)	6.6
C39 mirabegron	82.3 (±14.1)	5.7	46.1 (±7.1)	5.1	30.6 (±14.3)	5.2	0.2 (±4.9)	9.3	94.1 (±14.9)	5.5
C40 indacaterol	-2375.0 (±1871.0)	4.0	-243.1 (±12.5)	9.5			-82.6 (±14.5)	9.0	-508.8 (±97.9)	5.0
C41 atenolol	80.3 (±13.1)	5.1	60.1 (±6.7)	5.5	61.7 (±20.5)	4.9	53.4 (±14.2)	4.9	99.9 (±16.7)	5.0
C42 isoprenaline	-763.1 (±24.2)	4.8	-250.7 (±12.6)	5.8	-114.0 (±11.5)	5.6	-81.5 (±18.2)	5.5	-449.5 (±38.2)	5.2
C43 acebutolol	168.5 (±70.4)	4.2	90.7 (±8.1)	5.2	122.3 (±23.6)	4.5	164.1 (±52.8)	4.1	132.5 (±17.9)	4.8
C44 practolol	58.2 (±54.8)	4.3	45.0 (±11.7)	4.8	47.4 (±62.5)	4.2			70.8 (±52.1)	4.4
C46 pindolol	105.1 (±7.3)	8.4	103.2 (±7.5)	7.9	81.8 (±7.4)	8.0	75.5 (±8.8)	7.7	122.5 (±12.4)	8.2
C48 bupranolol	101 (±7.0)	9.1	107.7 (±6.6)	9.0	101.7 (±7.5)	8.1	95.5 (±8.4)	8.0	135.7 (±10.1)	8.5
C49 betaxolol	112.8 (±10.1)	5.6	89.7 (±6.3)	6.4	117.4 (±11.8)	5.3	119.2 (±13.4)	5.4	144.6 (±13.7)	5.6

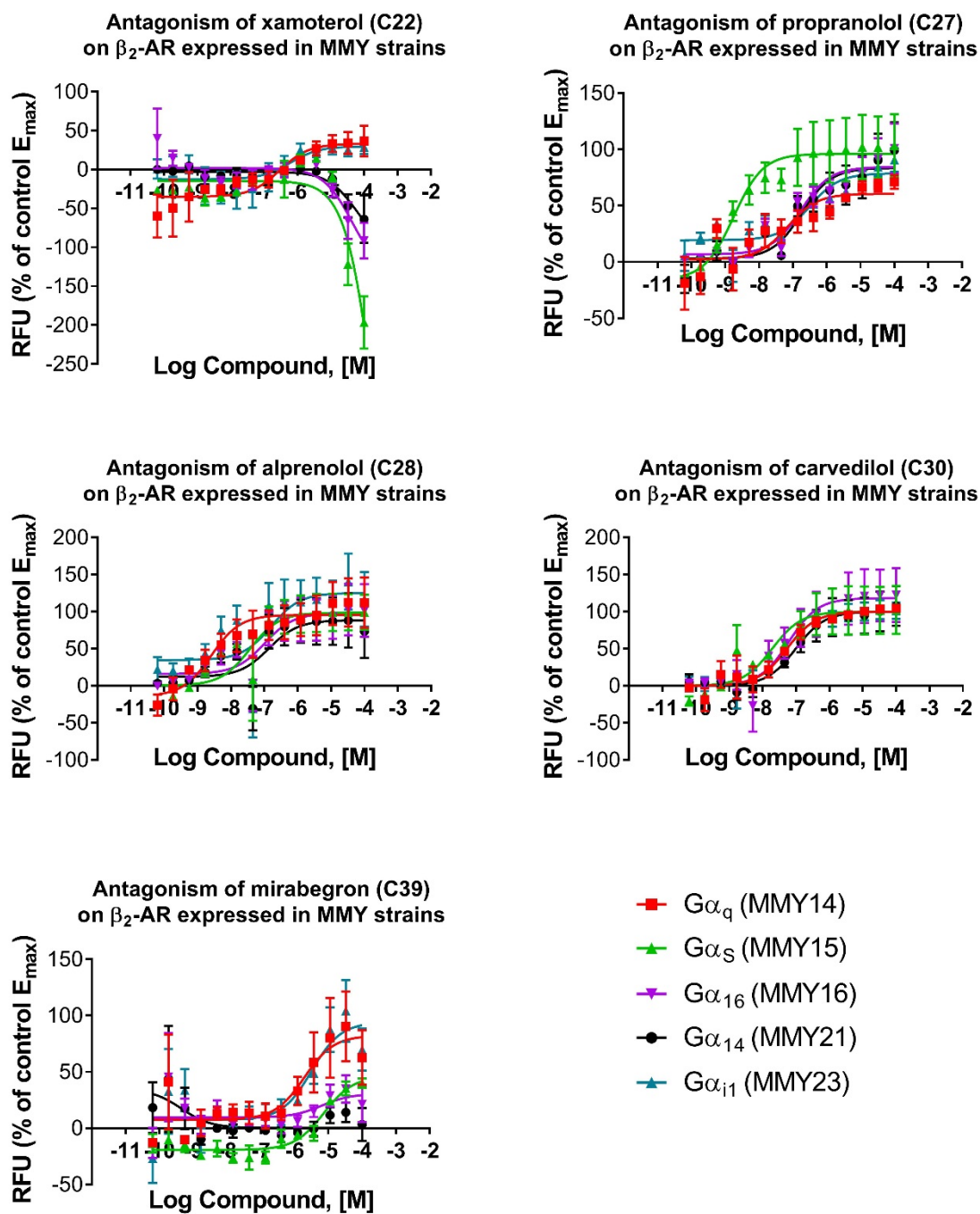


Figure 5.13 Selected antagonist responses on β_2 -AR expressing strains. Propranolol and alprenolol show markedly increased potencies in $G\alpha_s$ and $G\alpha_q$ strains respectively (see also **Table 5.12**). Mirabegron, which is primarily β_3 -AR agonist exhibit antagonistic properties on β_2 -AR.

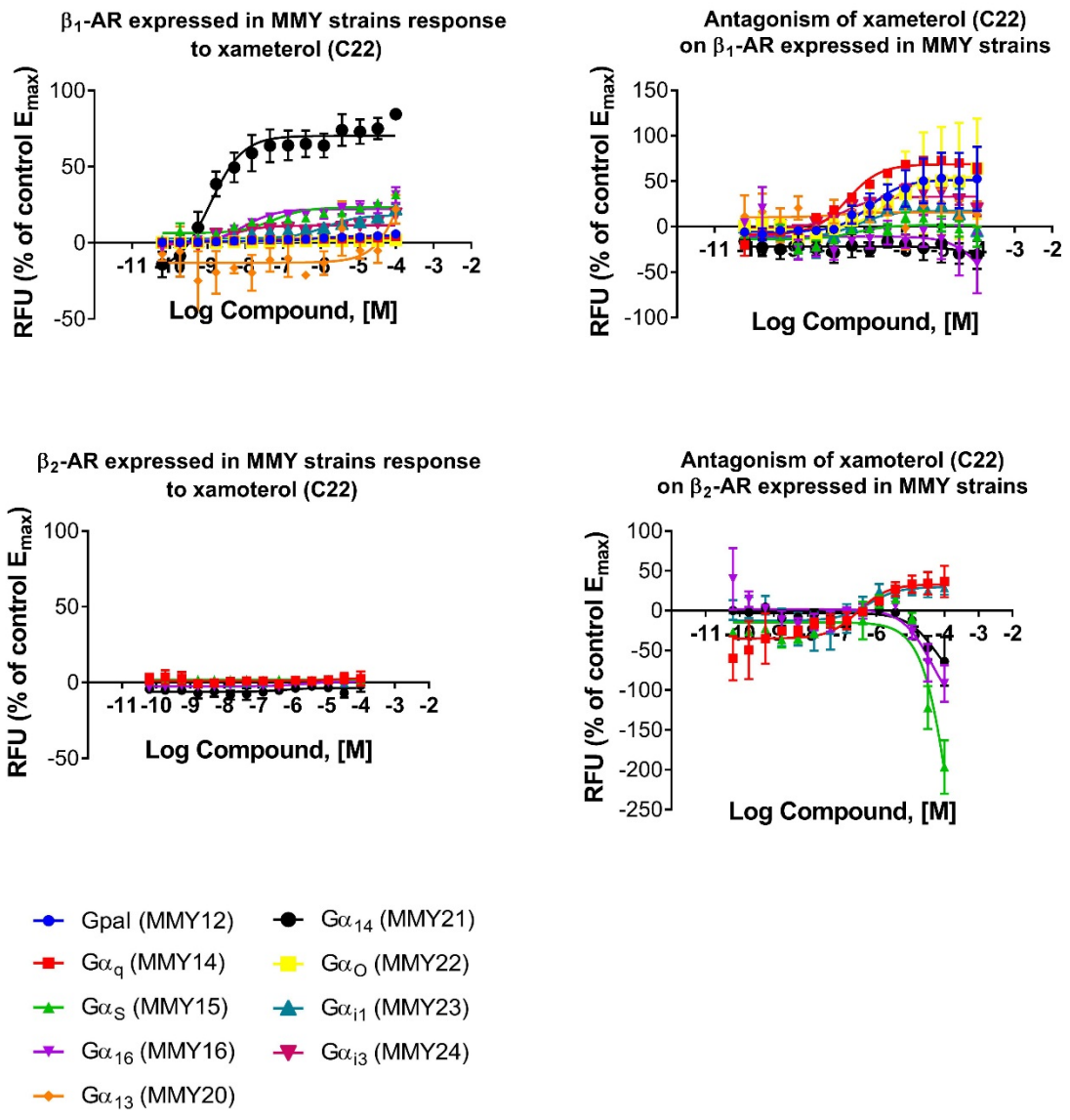


Figure 5.14 Summary of xameterol (22) pharmacology on β -adrenoceptors in yeast. As an agonist xameterol only showed marked activity on β_1 -AR in the G α_{14} strain. It has also displayed antagonist effect on both receptors at various degrees in MMY strains.

5.5. Comparison of signalling pathways for β_1 -AR and β_2 -AR in yeast

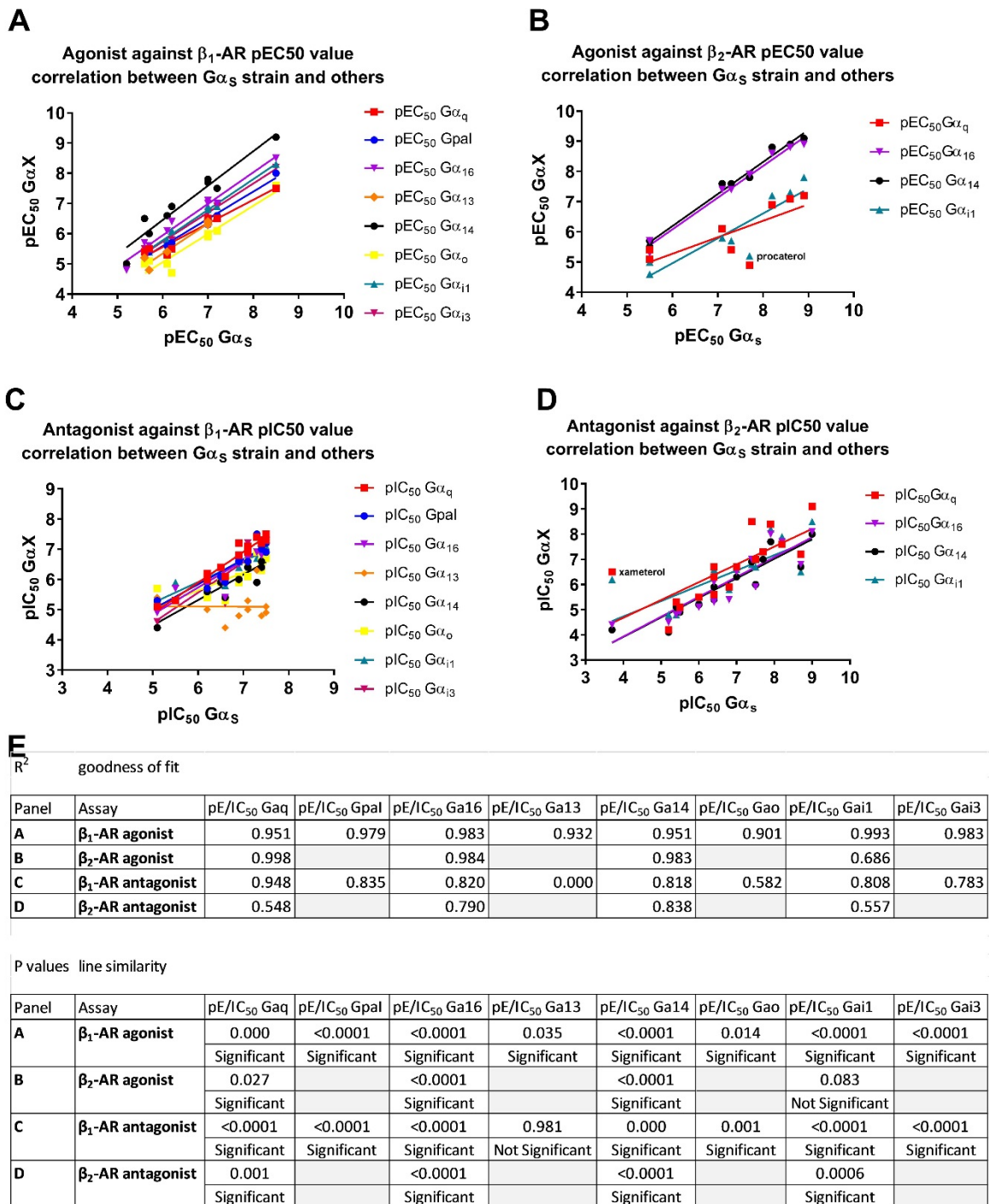


Figure 5.15 Correlation plots of pEC₅₀ and pIC values between those obtained in $G\alpha_s$ strain and other $chG\alpha$ strains. The comparisons were carried out for agonist β_1 -AR [A] and β_2 -AR [B] data, and antagonist β_1 -AR [C] and β_2 -AR [D] data to show if there is significant shift in coupling between the strains or particular ligands-outliers, which are noted on the scatter plots. Agonist values $\geq 20\%$ E_{max} and antagonist values $\geq 50\%$ E_{max} were used. Linear regression plots represent the fit between data points; R² and P values shown in [E].

To better illustrate the trends observed in data presented in sections 5.3 and 5.4 correlation analyses were performed and presented in Figure 5.15. The pEC₅₀ and pIC₅₀ values of agonist and antagonist

responses in $G\alpha_5$ strain were compared to data generated in other strains. Only agonist values of $\geq 20\%$ E_{max} and antagonist of $\geq 50\%$ E_{max} were compared to avoid any insignificant outliers. The lines represent linear regression analysis which compare the goodness of fit between the data points in the set and compare the slopes.

The agonist values on β_1 -AR expressed in MMY strains correlate significantly with each other – correlation r^2 values between 0.90-0.99 (**Table 5.16 [A]**), P values indicate the data is not picked randomly, meaning that the correlation is significant. Linear regression analysis show the goodness of fit is above R^2 0.90 (Figure 5.16 [E]) and that although the slopes are not significantly different, there is approximately 1.5 log difference between MMY21 ($G\alpha_{14}$) and MMY20 ($G\alpha_{13}$) data values, well reflecting the trend that was observed in **Figure 5.2** where the $G\alpha_{14}$ strain demonstrated the strongest coupling across all compounds tested.

The β_2 -AR agonist data in $G\alpha_{16}$ and $G\alpha_{14}$ correlate strongly with the data in $G\alpha_5$, but $G\alpha_q$ and $G\alpha_{i1}$ correlated poorly (**Table 5.16 [C]**). The goodness of fit of these two strains data is poor too as indicated by P values in **Figure 5.15 [E]** and similarly in **Table 5.16 [C]**, however this could be explained by an outlier – procaterol. The pEC_{50} values differ by approximately 0.5-2 log between the well correlating $G\alpha_{16}$ and $G\alpha_{14}$ and the $G\alpha_q$ and $G\alpha_{i1}$ strains as indicated by linear regression plots (**Figure 5.15 [B]**). This observation reflects the pattern shown in **Figure 5.10** where 7 agonists appeared to have lower potencies and efficacies in the two strains with lower correlation while the control agonist isoprenaline had the same effect in all strains.

As for antagonist analysis, significant correlation of antagonists on β_1 -AR in most strains was found. Only the $G\alpha_{13}$ data did not correlate with $G\alpha_5$ which can be clearly seen by the linear regression plot and the associated parameters. This agrees with a previous observation that antagonists on this strain produced either lower efficacies or lower potencies in comparison with the values produced in other strains (**Table 5.6**). Antagonists on β_2 -AR also correlated according to the correlation coefficient r^2 . The slope of $G\alpha_q$ and $G\alpha_{i1}$ strain data was slightly different to other strains as observed on agonist values in the same strains; however, this is likely to be an artefact produced by xameterol outlier data.

In summary the correlation analysis echoes the patterns that were observed in data presented earlier in this chapter. The most notable observation is the poor correlation of antagonist $G\alpha_{13}$ strain data on β_1 -AR as compared with other strain data, however, as shown in Figure 5.2 and 5.5 the coupling in this strain to β_1 -AR was overall low therefore lack of correlation is not significant. As for β_2 -AR several log differences in agonist pEC_{50} values produced in $G\alpha_5$, $G\alpha_{16}$ and $G\alpha_{14}$ and those in $G\alpha_q$ and $G\alpha_{i1}$, which indicate lower coupling efficiencies in these two strains. Procaterol on agonist data and xameterol on antagonist data correlation (**Figure 5.15 [B]** and **[D]**) point out that these compounds may be exhibiting

bias agonism towards coupling to particular strains which is an interesting point for further investigation.

Table 5.16 Pearson's correlation analysis of pEC₅₀ and pIC₅₀ values. The values obtained from Gα_s strain experiment data were compared to those obtained in other chGα strains. This data complements the scatter plots presented in **Figure 5.15**. The analyses were obtained for agonist β₁-AR [A] and β₂-AR [C] data, and antagonist β₁-AR [B] and β₂-AR [D] data. The Pearson R² coefficient indicate whether there is correlation, two-tailed P values indicate whether the correlation is significant or random. Analyses were obtained from GraphPad Prism 7.

β ₁ -AR Agonist	pEC50 GaS vs. pEC50 Gaq	pEC50 GaS vs. pEC50 Gpal	pEC50 GaS vs. pEC50 Ga16	pEC50 GaS vs. pEC50 Ga13	pEC50 GaS vs. pEC50 Ga14	pEC50 GaS vs. pEC50 Gao	pEC50 GaS vs. pEC50 Gai1	pEC50 GaS vs. pEC50 Gai3
Pearson r								
R squared	0.9422	0.979	0.9739	0.933	0.9334	0.9069	0.9929	0.9805
P (two-tailed)	<0.0001	<0.0001	<0.0001	0.0075	<0.0001	0.0003	<0.0001	<0.0001
P value summary	****	****	****	**	****	***	****	****
Significant? (alpha = 0.05)	Yes	Yes	Yes	Yes	Yes	Yes	Yes	Yes
Number of XY Pairs	7	8	8	4	8	5	8	7

β ₁ -AR Antagonist	pIC50 GaS vs. pIC50 Gaq	pIC50 GaS vs. pIC50 Gpal	pIC50 GaS vs. pIC50 Ga16	pIC50 GaS vs. pIC50 Ga13	pIC50 GaS vs. pIC50 Ga14	pIC50 GaS vs. pIC50 Gao	pIC50 GaS vs. pIC50 Gai1	pIC50 GaS vs. pIC50 Gai3
Pearson r								
R squared	0.9475	0.8353	0.8198	0.0001	0.8184	0.5815	0.8084	0.7833
P (two-tailed)	<0.0001	<0.0001	<0.0001	0.9807	0.0001	0.0009	<0.0001	<0.0001
P value summary	****	****	****	ns	***	***	****	****
Significant? (alpha = 0.05)	Yes	Yes	Yes	No	Yes	Yes	Yes	Yes
Number of XY Pairs	16	15	16	10	11	15	16	16

β ₂ -AR Agonist	pEC50 Gas vs. pEC50Gaq	pEC50 Gas vs. pEC50Ga16	pEC50 Gas vs. pEC50 Ga14	pEC50 Gas vs. pEC50 Gai1
Pearson r				
R squared	0.562	0.9839	0.9828	0.7919
P (two-tailed)	0.0322	<0.0001	<0.0001	0.0031
P value summary	*	****	****	**
Significant? (alpha = 0.05)	Yes	Yes	Yes	Yes
Number of XY Pairs	3	8	8	5

β ₂ -AR Antagonist	pIC50 Gas vs. pIC50Gaq	pIC50 Gas vs. pIC50Ga16	pIC50 Gas vs. pIC50 Ga14	pIC50 Gas vs. pIC50 Gai1
Pearson r				
R squared	0.5478	0.7903	0.8384	0.5572
P (two-tailed)	0.0007	<0.0001	<0.0001	0.0006
P value summary	***	****	****	***
Significant? (alpha = 0.05)	Yes	Yes	Yes	Yes
Number of XY Pairs	17	17	17	17

5.6. Comparison of the functional yeast assay for GPCRs against other assays in a high-throughput screening setting

Another interesting question to ask of from the available data was how well the values obtained in yeast compared to other high-throughput screening mammalian cell-based assays and between these assays themselves. Because β -adrenoceptors are well known drug targets, a substantial amount of data were available in the internal GSK database. For this analysis values for compounds described in this chapter, as well as an additional 19 GSK proprietary compounds were used. The data for full-curve pEC_{50} and pIC_{50} values for agonists and antagonists respectively were retrieved from the data-base and grouped according to the assay's identifiers (**Figure 5.17**). Interestingly all the previous screening data were obtained from assays that fell largely in the two categories – cAMP measured by enzyme fragment complementation (EFC) and immunoassay for cAMP detection by fluorophore-conjugated antibody and subsequent time-resolved fluorescence energy transfer (TR-FRET) measurement (**Figure 1.2**). According to the information available on assay providers' literature, the assays noted as LANCE (Perkin Elmer) cAMP in **[A]** and **[C]**, HTRF cAMP (also a TR-FRET assay [75]) **[E]** measure cAMP from a cell lysate, while EFC cAMP (DiscoverX) **[B]**, **[F]**, **[G]** measure cAMP in an intact engineered cell line [15, 16]. All assays use the CHO-K1 stably transfected cell line which overexpresses β -adrenoceptor and the second messenger cAMP is used to monitor ligand induced coupling or inhibition of $G\alpha_s$ and $G\alpha_i$ pathways. The two DiscoverX assays in **[B]** and **[F]** are based on the EFC cAMP luminescence measurement and the differences likely to lie within the protocols. The other DiscoverX EFC in **[G]** assay measures the activation of the β -arrestin pathway, not the production of cAMP.

The analysis showed variable correlations between the yeast agonist and antagonist data obtained in the $G\alpha_s$ strain and CHO assays. For β_1 -AR receptor agonist cAMP LANCE assay in **Figure 5.17 [A]** showed weak correlation and stronger correlation with the antagonist EFC assay **[D]**, although due to small sample size, correlation was deemed insignificant (**Table 5.18**). A few more assays were available for comparison of β_2 -AR yeast data also generated in the $G\alpha_s$ strain. Moderate correlation was observed in 5 out of 7 assays with the following r^2 coefficient rank: Human Antagonist - EFC – pKi **[D]** > Agonism β -arrestin EFC – PathHunter **[G]** > Agonist cAMP LANCE TR-FRET **[A]** > DiscoverX HitHunter cAMP EFC **[F]** > Antagonist cAMP LANCE TR-FRET **[C]** in **Table 5.18**; P values indicate that the correlation is significant. A correlation matrix between the CHO cAMP assays was also performed; statistical parameters are presented in **Table 5.19**. It is perhaps not surprising that the correlation of CHO assays is stronger than that with the yeast assay data since all CHO assays compared used the same cell background and measured the same cAMP second messenger, which is different from the growth measured in yeast. The major differences between these assays are the assay protocols and the type of reporter (fluorescence vs luminescence) used. Even within this set of data some variation in the r^2

values was observed. For example, HTRF cAMP agonist assay correlated weaker with DiscoverX cAMP EFC (cell based assay, likely to be cAMP Hunter assay) as shown in **Table 5.19**.

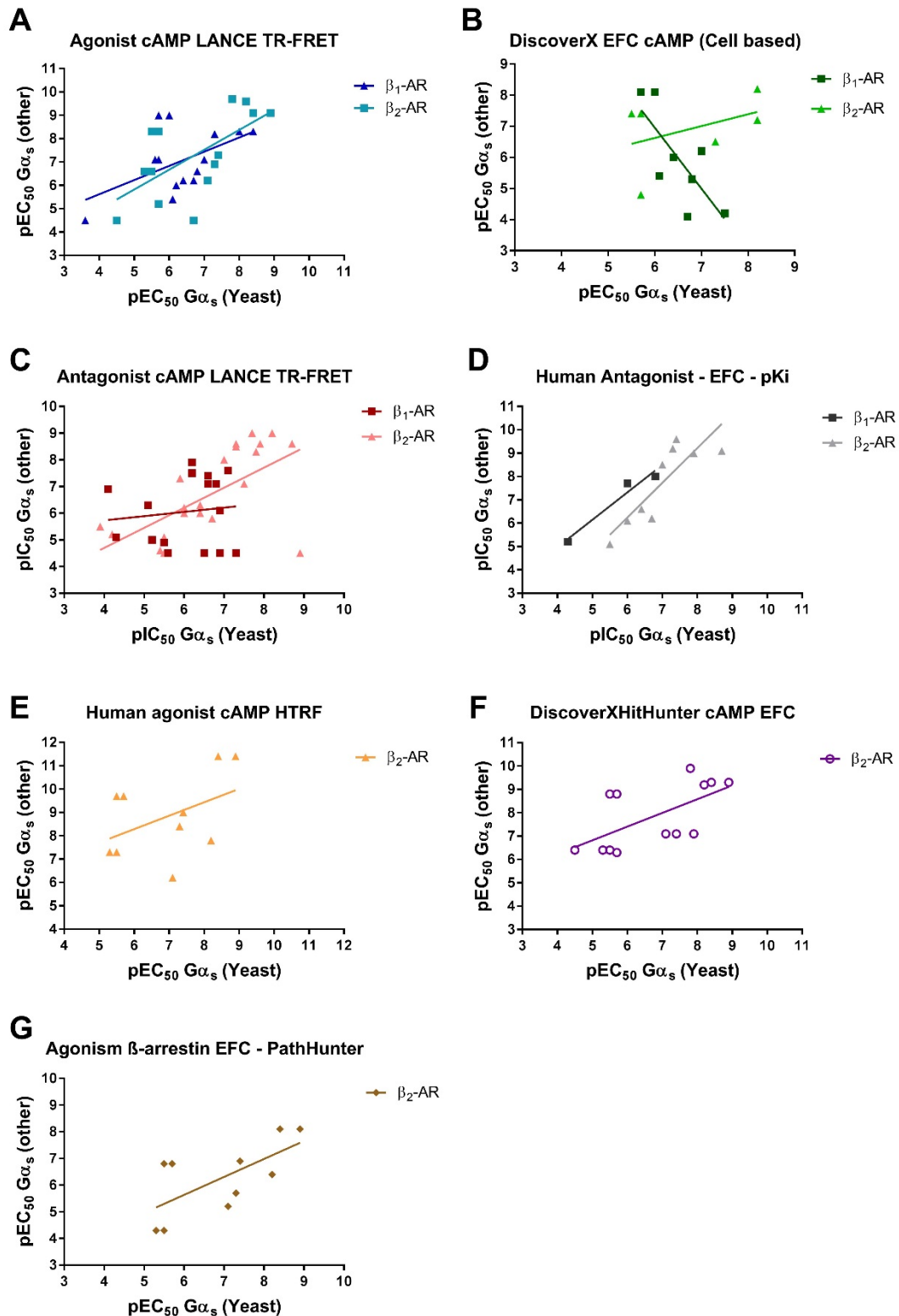


Figure 5.17 Yeast Gα_s agonist and antagonist assay correlation comparison with various cAMP assays in CHO cell background. Several cAMP assays were found in GSK databases from previous screening experiments. All assays detected change in cellular cAMP by antibody detection or enzyme fragment complementation (EFC). Upon detection of cAMP the signal is detected – either FRET (fluorescence) or luminescence respectively.

	A	B	C	D
β 1-AR assay correlation comparison	Agonist cAMP LANCE TR-FRET	DiscoverX EFC cAMP (Cell based)	Antagonist cAMP LANCE TR-FRET	Human Antagonist - EFC pKi
Pearson r				
R squared	0.3056	0.1795	0.0143	0.952
P value				
P (two-tailed)	0.0326	0.2955	0.6591	0.1407
P value summary	*	ns	ns	ns
Significant? (alpha = 0.05)	Yes	No	No	No
Number of XY Pairs	15	8	16	3

	A	B	C	D	E	F	G
β 2-AR assay correlation comparison	Agonist cAMP LANCE TR-FRET	DiscoverX EFC cAMP (Cell based)	Antagonist cAMP LANCE TR-FRET	Human Antagonist - EFC pKi	Human agonist cAMP HTRF	DiscoverX HitHunter cAMP EFC	Agonism β -arrestin EFC - PathHunter
Pearson r							
R squared	0.4119	0.1755	0.3562	0.7373	0.1953	0.3829	0.4377
P value							
P (two-tailed)	0.0134	0.4084	0.0016	0.003	0.2009	0.0242	0.0372
P value summary	*	ns	**	**	ns	*	*
Significant? (alpha = 0.05)	Yes	No	Yes	Yes	No	Yes	Yes
Number of XY Pairs	14	6	25	9	10	13	10

Table 5.18 Yeast $G\alpha$ s agonist and antagonist assay comparison with various cAMP assays in CHO cell background – correlation parameter analysis. The Pearson r^2 value indicates the correlation between the assays where 1 is perfect correlation and 0 is no correlation. The two-tailed test P values indicate whether the probability of the correlation is significant. The letters above the tables indicate the scatter plots presented in **Figure 5.17**.

β_1 -AR Assay Pearson's r^2	Agonist cAMP LANCE TR-FRET	DiscoverX EFC cAMP (Cell based)	Human Antagonist - EFC pKi	Antagonist cAMP LANCE TR-FRET
Agonist cAMP LANCE TR-FRET		0.885		
DiscoverX EFC cAMP (Cell based)	0.885			
Human Antagonist - EFC pKi				
Antagonist cAMP LANCE TR-FRET				

P=0.019

β_2 -AR Assay Pearson's r^2	Human agonist cAMP HTRF	DiscoverX HitHunter cAMP EFC	Agonist cAMP LANCE TR-FRET	DiscoverX EFC cAMP (Cell based)	Agonism β -arrestin EFC - PathHunter	Human Antagonist - EFC - pKi	Antagonist cAMP LANCE TR-FRET
Human agonist cAMP HTRF		0.891	0.978	0.547	0.898		
DiscoverX HitHunter cAMP EFC	0.891		0.932	0.993	0.902		-0.976
Agonist cAMP LANCE TR-FRET	0.978	0.932		0.992	0.913		-0.897
DiscoverX EFC cAMP (Cell based)	0.547	0.993	0.992		0.989		
Agonism β -arrestin EFC - PathHunter	0.898	0.902	0.913	0.989			
Human Antagonist - EFC - pKi							0.990
Antagonist cAMP LANCE TR-FRET		-0.976	-0.897			0.990	

β_2 -AR Assay correlation P values	Human agonist cAMP HTRF	DiscoverX HitHunter cAMP EFC	Agonist cAMP LANCE TR-FRET	DiscoverX EFC cAMP (Cell based)	Agonism β -arrestin EFC - PathHunter	Human Antagonist - EFC - pKi	Antagonist cAMP LANCE TR-FRET
Human agonist cAMP HTRF		0.00298	0.00001	0.45297	0.00042		
DiscoverX HitHunter cAMP EFC	0.00298		0.00001	0.00661	0.00221		0.13911
Agonist cAMP LANCE TR-FRET	0.00001	0.00001		0.00084	0.00058		0.03929
DiscoverX EFC cAMP (Cell based)	0.45297	0.00661	0.00084		0.01115		
Agonism β -arrestin EFC - PathHunter	0.00042	0.00221	0.00058	0.01115			
Human Antagonist - EFC - pKi							0.00000
Antagonist cAMP LANCE TR-FRET		0.13911	0.03929			0.00000	

Table 5.19 Correlation matrix analysis of CHO cAMP assay produced pEC₅₀ and pIC₅₀ on β_1 -AR and β_2 -AR collected from GSK database. Pearson's correlation r^2 coefficients were compared. Correlation was significant if P<0.05.

5.7. Chapter summary

The pharmacological characterisations of β -adrenoceptor functional coupling to a range of chimeric $G\alpha$ s are presented in this chapter. For the initial identification of β -adrenoceptor coupling to the chG α s a full agonist isoprenaline was used (Figures 4.14 and 4.15). Although it is possible that for some β -AR-G-protein interactions isoprenaline was not optimal for inducing full agonism, many studies use this compound as a gold standard for β -adrenoceptor agonism. Furthermore, isoprenaline stimulated β_1 -AR was able to couple to Gpa1, $G\alpha_{13}$, $G\alpha_o$ and $G\alpha_{i3}$, but the β_2 -AR did not show such response, suggesting that isoprenaline was a good choice for the experimental design.

Overall a range of pharmacological responses were observed including full agonism (isoprenaline, oricprenaline), partial agonism (xamoterol, pindolol), inverse agonism (carvedilol) and antagonism (propranolol, propafenone). The pharmacological profiles largely agree with the data observed in mammalian assay data; however there are some previously uncharacterised interactions too.

It is unusual in an industrial setting to be able to characterise such a diversity of G coupling in a uniform cell background and other assay variables, therefore this makes a valuable comparison of individual compounds' ability to induce or inhibit receptor's coupling to a range of $G\alpha$ s. As was shown by correlation analysis even the same cellular messenger can be measured by different reporters and under different assay conditions. Further details of the protocols are needed to say exactly what purpose the different assays served, although it is likely that the changes in assay methods were influenced by other non-biological factors such as newer and improved assays becoming available on the market, change in supplier or other requirements for a particular screening programme. The only significant protocol aspect that is currently unknown is whether the protocol included forskolin-induced cAMP stimulation which would indicate whether $G\alpha_s$ or $G\alpha_i$ pathway was targeted.

Chapter 6 – The engineering of *Saccharomyces cerevisiae* strains

6.1. Introduction

In this chapter the objectives and strategies for further engineering of *Saccharomyces cerevisiae* are outlined. The chapter is divided into two major parts, in which two different strategies are described. The first strategy concerns the deletion of the selectable marker, the *URA3* gene. The parental strain W303-1A, from which the MMY strains were engineered, possesses *ura3-1* marker gene which is only a point mutation resulting substitution from glycine to glutamate. It is thought to cause selection of false positive colonies when transforming the MMY strains. Because uracil selection is relied upon for the uptake of p426GPD and p306GPD and selection of positive colonies, it was important to look into improving this selection strategy. As an interim solution, the MMY strains were subjected to several rounds of counter-selection agent 5-fluoroorotic acid (5-FOA) to enforce the Ura⁻ phenotype. Later, a complete deletion of the *ura3-1* gene was attempted in MMY11 from which other MMY strains were originally constructed. This was done with the aim to construct a new set of MMY strains that would be less prone to false positive colony formation.

The second part describes the strategy for introducing a cholesterol synthesis pathway and consequential disruption of the ergosterol synthesis pathway in the MMY strains. This strategy was devised based on three published studies [56-58] that all target *ERG5* and *ERG6* genes in the ergosterol synthesis pathway and introduce *DHCR7* and *DHCR24* genes of the cholesterol synthesis pathway. Described in detail are the engineering of plasmids and attempts at integration of these plasmids into the MMY11 strain genome. The application of cholesterol-producing yeast can be very broad but is of an interest in membrane protein research, and in particular GPCR studies. With emerging details on how cholesterol influences β_2 -AR signalling a greater need for understanding the role of lipids in cell signalling has been hypothesised. Because a lot of membrane research is carried out in recombinant hosts, such as yeast [37, 59], the aim of this work was to address the need of studying the GPCRs, and other membrane proteins, in a more native-like membrane environment.

6.2. The engineering of *ura3Δ* MMY11 strain

Throughout this project and in the past at GSK, it was observed that negative control cells with no plasmid were able to grow on uracil depleted medium. Therefore a question was raised whether these strains are truly *Ura⁻*, or perhaps they are mixed *Ura⁻* and *Ura⁺* populations of cells. To answer these questions, selection on uracil-depleted medium and the counter-selective agent 5-FOA were performed to show that based on the cells' ability to grow on both types of medium, the population is mixed (6.2.1). Furthermore, a genetic investigation showed that two versions of the gene – full length and truncated *URA3* – can be detected in the genomic DNA of MMY strains (6.2.2). Following this discovery, it was decided to delete the full length gene to test the hypothesis that the full length gene is the source of the reversion to *Ura⁺* phenotype. The strategy and the preliminary results of this work are detailed in section 6.2.3.

6.2.1. *Saccharomyces cerevisiae* strain MMY12-28 counter-selection with 5-FOA

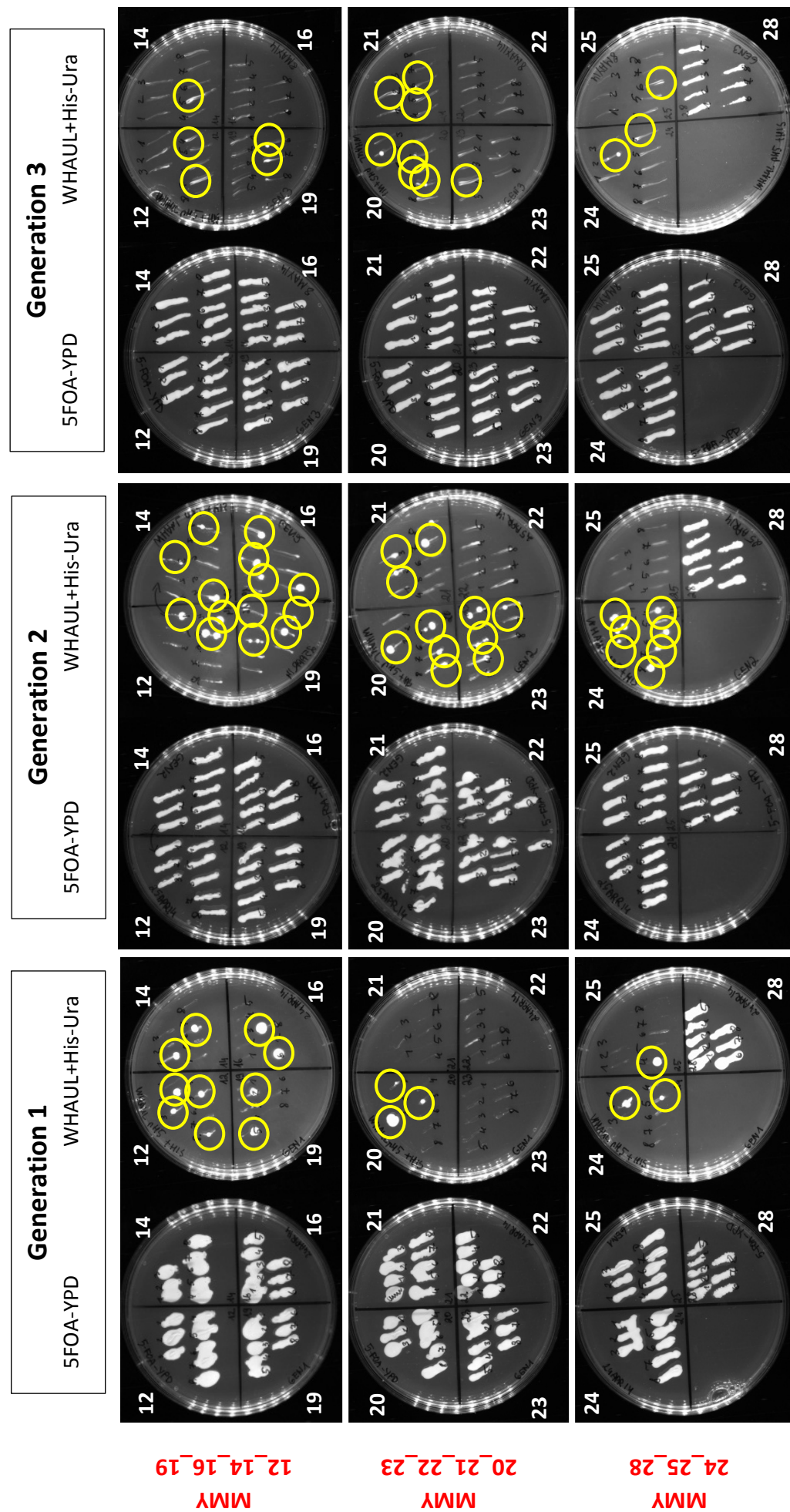
The counter-selective agent 5 fluoroorotic acid (5-FOA) was used to select MMY12-28 strain clones exhibiting a *Ura⁻* phenotype. Eight colonies of each MMY strain were picked from stock YPD plates and streaked as a single line on 5-FOA/YPD and WHAUL+His-Ura (–Ura plates for short) plates. All plates were incubated at 30°C until growth was apparent after 24h. With the exception of MMY28, colonies on –Ura plate did not show any signs of grow after 24h, however, after an extended period of incubation, round colonies started to emerge on some of the streaked lines. As shown in **Figure 6.2**, such growth and reversion to *Ura⁺* phenotype was noted out of 8 colonies streaked on uracil depleted medium plates. For example, the MMY12 in the first generation selection produced growth on 4 out of 8 streaks (**Figure 6.2**, first panel). Two colonies on the same line were counted as 1 reversion (for example MMY12, 20, and 23 on the second generation shown in the middle panel), because all colonies on the same line originated from a single clonal cell. These results formed generation 1 selection. To enhance selective pressure, generations 2 and 3 were produced, however, this time the colonies were picked not from the original YPD stock, but from the plate of the preceding generation. Similar results were observed in generation 2 and 3 selection, as in generation 1. The reversion to *Ura⁺* phenotype became apparent after 48-72h incubation. Results are summarised in **Table 6.1**.

MMY strains	G α sub-unit	Number of reverted colonies out of 8			Colonies that did NOT revert
		Generation 1	Generation 2	Generation 3	
12	Gpa1	4	2	2	1, 6
14	Gpa1-Gq	2	4	1	2, 4, 7
16	Gpa1-G16	2	4	0	2, 4, 5
19	Gpa1-G12	2	4	2	1, 4, 8
20	Gpa1-G13	0	4	4	4
21	Gpa1-G14	0	4	3	1, 4
22	Gpa1-Go	0	0	0	all
23	Gpa1-Gi1	0	4	1	2, 5, 7, 8
24	Gpa1-Gi3	2	7	2	none
25	Gpa1-Gz	1	0	1	1, 2, 3, 5, 7, 8
28	Gpa1-Gs	8	8	8	none

Table 6.1 Summary of 5-FOA selection results. Each MMY strain produced a variable number of reverted colonies, which had to transform to Ura⁺ phenotype in order to grow in uracil depleted media. The exception to that, however are MMY22, highlighted in green, which despite repeated selective pressure did not produce any revertants, and MMY28, in red, which in contrast was able to adapt very quickly to both selective pressures. Colonies that did not revert at all within the 3 selective generations are noted in the last column. Highlighted in green are those strains in which at least half of all colonies did not revert. Similarly, in red are those strains for which all colonies reverted at least once.

Overall, with the exception of MMY22, all strains produced at least one Ura⁺ reverted colony when nutrient selective pressure was applied. MMY28 grew exceptionally well in all three generation on both 5-FOA and –Ura plates, requiring only 24 hours to grow. All eight colonies of MMY24 reverted at least once in three generation selection and although the reversion was not as prominent as for MMY28, the high instability made it difficult to select which colony should be archived in –80°C freezer. Overall this shows that there is significant genetic variation in the *URA3* locus amongst the MMY strains.

Figure 6.2 Selection for Ura⁻ phenotype with 5-FOA. Images of culture plates show the results of 5-FOA selection. Each plate is divided into four sections to accommodate all 11 MMY strains onto 3 plates for each selection group. Cell growth is compared on two different selection media – 5-FOA-YPD on the left side of each panel and WHAUL + His – Ura – Ura on the right side. The former allows only Ura⁻ phenotypes to survive, and the latter does the opposite – identifies cells with a functional *URA3* gene. Highlighted in yellow circles are the colonies of cells with reverted Ura⁺ genotypes in each of three generations.



6.2.2. Design of genomic PCR test for the detection of *trURA3* and *flURA3* genotypes

The instability of Ura⁻ phenotype amongst the different MMY strains prompted an investigation of the genomic *ura3* locus for possible causes. To predict what might be expected of genomic PCR, a set of primers were first optimised using a p140 vector (**Table 2.7**) which carried a truncated *URA3* gene and p426GPD vector with a full length *URA3*.

The reason for selecting the p140 vector was because it was used to engineer the MMY strains. The genes *FAR1*, *SST2*, and *STE2* were deleted using a plasmid which had a *URA3* marker for the selection of successful deletion events by cultivation on uracil-depleted media, as the original W303-1A strain has a mutant *URA3* gene as described previously [76, 77]. To restore the Ura⁻ phenotype, these *URA3* genes were deleted using a vector derived from pUC19 in which *URA3* with additional restriction sites *EcoRV* and *StuI* was ligated at *SalI* site. After digestion with *EcoRV* and *StuI* a 247 bp fragment from the middle coding region of *URA3* was released, leaving 5' and 3' ends intact. The re-ligated disrupted gene can replace the genomic *URA3* genes. Successful deletion events were confirmed using 5-FOA which kills Ura⁺ phenotype carrying cells [78]. So it was hypothesised that the ~250 bp smaller *URA3* gene (*trURA3*) band would be detected in the MMY genome. The full *URA3* gene (*flURA3*), like the wild type found on the expression plasmids p426GPD and p306GPD, was also expected to be found if the endogenous mutated gene was the cause of the reverted Ura⁺ phenotype.

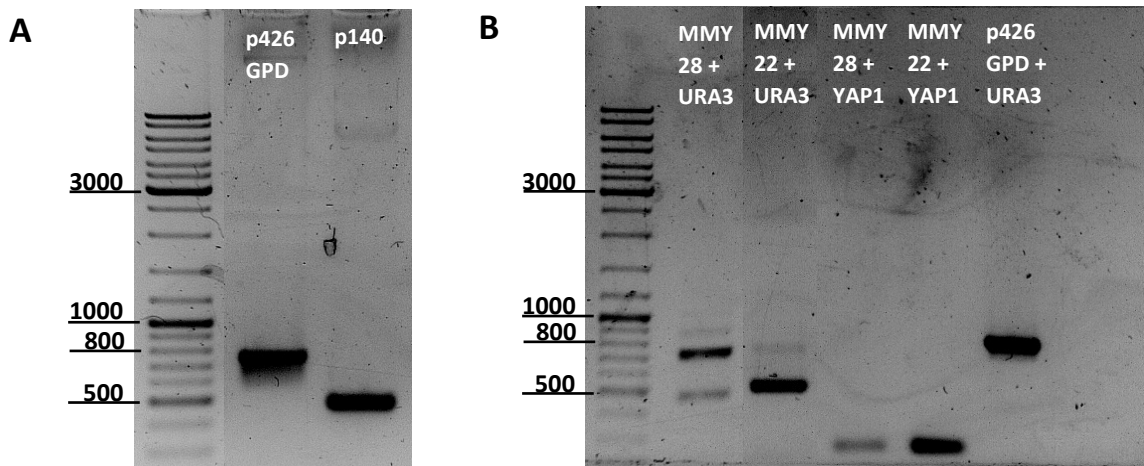


Figure 6.3 Optimisation of primers for *URA3* detection. The primers 1_URA3 and 2_URA3 were designed to amplify both *flURA3* and *trURA3* from gDNA. [A] Primer optimisation on p426GPD vector carrying *flURA3* and p140 with *trURA3* showed the later to produce a band 200bp shorter than *flURA3*. [B] Both full length and truncated *URA3* were detected in gDNA of MMY28 which phenotypically showed to be able to switch between Ura⁺ and Ura⁻ phenotypes. MMY22 gDNA showed only the truncated gene version present; it was also unable to demonstrate Ura⁺ phenotype. *YAP1* primers were used as a positive control for gDNA quality.

Indeed when the primers were optimised using the plasmid-borne *URA3* genes, two different PCR product sizes were observed (**Figure 6.3 A**). The 1_URA3 and 2_URA3 primers were designed to anneal at the far 5' and the far 3' end of the reading frame, so that the pair would amplify most of the reading frame and that would also amplify the gene if it was truncated in the middle section.

The next challenge was to test the primers with the genomic DNA. The genomic DNA was extracted from the MMY22 and MMY28 based on the different phenotypic behaviour of these strains described in 6.2.1 (**Table 6.1**). Interestingly, the PCR detected both full length and truncated gene versions in both MMY22 and MMY28 but the dominant gene in MMY28 was flURA3, while in MMY22 the dominant band was of the trURA3 gene, with a very faint band of flURA3. This result can be related back to the fact that MMY22 was unable to revert under the selective pressure of 5-FOA and displayed strictly Ura⁻ phenotype. In contrary, MMY28 has displayed a very adaptive phenotype.

6.2.3. The deletion of the full length *URA3* gene

In order to eliminate any possibility of the *ura3* (original mutation in the W303-1A strain) reverting to the wild type, methods for a complete gene deletion were investigated. The strategy used by Brachmann *et al* in the paper describing a set of *S. cerevisiae* deletion strains [79] where a *URA3* deletion cassette was designed to include flanking regions of upstream from the 5' and downstream from the 3' ends. This cassette when integrated in the *URA3* locus, deletes the reading frame completely. The pJL164 vector used in this study is deposited in the ATCC collection and therefore was available to be purchased (**Table 2.7**). The deletion fragment was released from the vector by *SpeI* + *XhoI* digestion and was used to transform MMY11 using standard methods. The integration event was enforced by the 5-FOA selective pressure [79]. However, a very large number of colonies were observed following transformations. An additional step involving growing the cells for approximately one generation in a liquid 5-FOA/YPD was included (see section 2.2.1.3) to increase the stringency of the selective pressure. Even then, a large number of colonies growing on 5-FOA/YPD medium were also able to grow on -Ura+Trp (tryptophan required for MMY11 only because it is Trp⁻) medium. Approximately 40 colonies which passed the phenotypic screening were analysed by PCR with the primers described in the previous section until one colony was identified displaying only the trURA3 gene (**Figure 6.4**).

This colony named MMY11_ura3Δ was incapable of forming any colonies on uracil deficient plates even when large numbers were plated on several occasions. These observations together with the PCR test indicate that this train is truly *ura3Δ*.

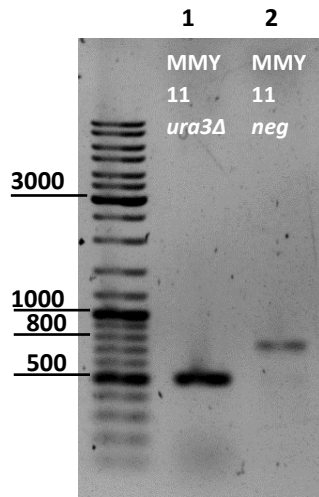


Figure 6.4 The detection of *flURA3Δ* by genomic PCR. A colony screen was performed during which one colony in lane 1 was as identified carrying only *trURA3*. In contrast the colony in the lane 2 demonstrated the presence of *flURA3*.

The *ura3* gene deletion was attempted in MMY11 first, because it was soon apparent that deleting the gene in all 11 progeny strains (MMY12-28) simultaneously would not be feasible. Instead, introducing the chimeric Gpa1-Gα proteins was expected to be a more straight-forward process.

6.3. The engineering of cholesterol biosynthesis pathway in *S. cerevisiae* MMY strains

Sterols play a vital role in the normal plasma membrane physiology in eukaryotic cells. They create a microenvironment for the membrane proteins. The details of how sterols actually bring about their function are only starting to emerge and a lot is still unknown. What is known is that some functions are more structure dependent than others in the membrane, for example, the substitution of ergosterol in yeast with a mammalian cholesterol or plant campesterol was adequate for function of Tat2p and Ste2p but not Pdr12p or Can1p [56, 58]. Indeed, it is common for human membrane proteins, such as GPCRs, ABCs, transmembrane ATPases and others to have cholesterol binding sites which play a role in their function. Not surprisingly, putting those receptors in an environment that does not contain cholesterol, be it a foreign yeast membrane or a solubilising agent, can alter their pharmacological activity or render them completely inactive. There is also evidence that upon recombinant protein production in a non-native host, such as yeast, protein becomes inactive because it fails to be inserted in the right environment and is sent to be degraded reducing overall production yields.

Three independent published studies attempted to replace ergosterol, a native sterol in yeast membranes, with the cholesterol that is found in mammalian membranes by genetically engineering the yeast. Two genes were identified as key in achieving this – *DHCR7* and *DHCR24*, and their competing counterparts – *ERG5* and *ERG6*. [56-58]. The cholesterol synthesis pathway enzymes 7-

dehydrosterol reductase and 24-dehydrosterol reductase – gene products of *DHCR7* and *DHCR24* respectively – saturate the sterol intermediates at positions C-7 and C-24 [80-83] in cholesterol but not ergosterol in synthesis, while Erg5 introduces double bond at position C-22 and Erg6p adds methyl group at position C-24 in ergosterol synthesis therefore also competes with Dhrc24 for the substrate (summarised in **Figure 6.5**).

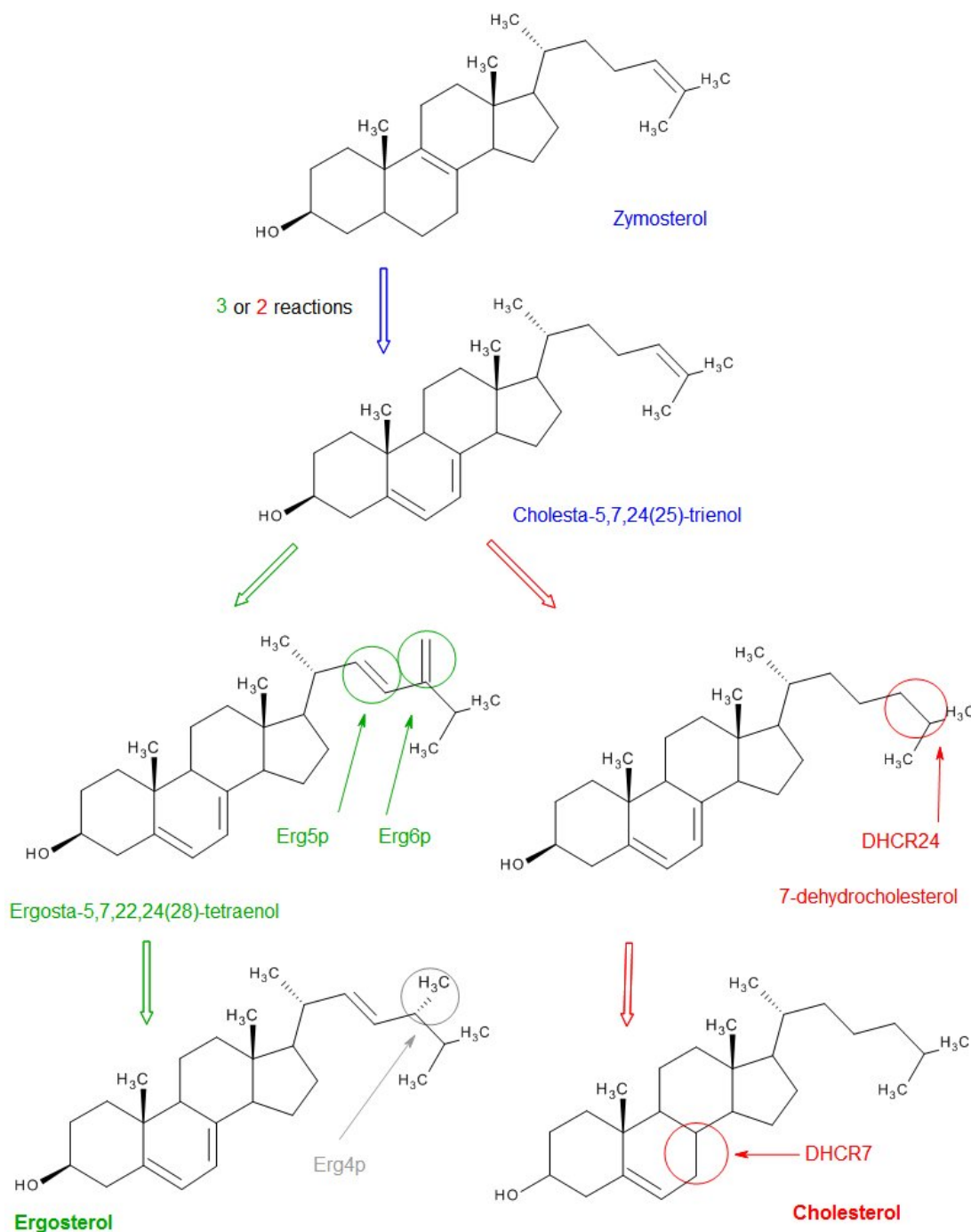


Figure 6.5 The summary of key enzymes and their substrates for shifting the sterol synthesis from ergosterol to cholesterol in yeast. The sterol intermediates and enzymes marked in green are involved in ergosterol synthesis while the ones marked in red are for cholesterol synthesis. The diagram is simplified to show only key enzymes relevant to this engineering strategy.

This subchapter describes the strategy for the integration of *DHCR24* and *DHCR7* genes (6.3.1), followed by a detail account of how the plasmids were constructed (6.3.2). The first attempt to integrate the *erg5Δ::DHCR24* is described in section 6.3.3 and future work is summarised in section 6.3.4.

6.3.1. The design of *erg5Δ::DHCR24* and *erg6Δ::DHCR7* integration cassettes

Human *DHCR* genes containing cassettes were used to disrupt *S. cerevisiae* *ERG5/6* genes in the study reported by Marioka *et al.* *DHCR7* was used to replace *ERG6* and *DHCR24* replaced *ERG5*. Firstly, *DHCR7/24* genes were inserted in between a *GAPDH* promoter and *CYC1* terminator in pRS416 vector, then the promoter-gene-terminator sequence fragments were amplified with PCR primers to include flanking regions of *ERG5/6* loci. Resulting fragments were inserted in pAUR135 plasmids containing aureobasidin A (*AUR1-C*) selection gene in between *ERG* gene promoter region and a region containing the initiation codon. *AUR1-C* is recyclable marker which can be removed once the plasmid is integrated into the genome by growing cells on galactose containing medium [58]. The pAUR135 vector aureobasidin A selection described in this study was used as a platform for our engineering strategy because a lot of selection markers were unavailable to use due to the heavily-engineered nature of the MMY strains. However, some modification to the construct were made.

It was reported that copies of *DHCR7* and *DHCR24* genes obtained from the cDNA of zebrafish *Danio rerio* (Genbank NM_201330 and BC086711 respectively), and codon optimised for *S. cerevisiae*, produced better results than *Xenopus laevis* or human gene products [56]. The *DHCR7* and *DCH24* genes in this work have also originated from *D. rerio* and were codon optimised for the expression in yeast by GenScript who synthesised the gene.

GPD promoters were used in all three studies, *AOX1* terminator for *P. pastoris* expression plasmids and *CYC1-term* for *S. cerevisiae* [56-58], which controlled the transcription of the recombinant genes. However, since the *GPD* promoter was already used for the expression of chimeric Gpa1-Gα proteins and the recombinant GPCRs, we wanted to avoid overburdening the cell's translational machinery. Therefore a possibility of utilising the endogenous promoters was explored. It has been previously demonstrated that the deletion of other ergosterol biosynthesis pathway genes resulted in an accumulation of intermediates and the subsequent transcriptional activation at the locus of the deleted gene [84, 85]. It was hypothesised that lack of Erg5 and Erg6 would activate the transcription of *DHCR24* and *DHCR7*.

Figure 6.6 outlines the design of the cholesterol gene integration and simultaneous ergosterol gene deletion in MMY 11 strain. As described in Marioka *et al.*, marker recycling requires colony selection

on galactose after the initial selection for integration on aureobasidin A (AbA). The growth on galactose medium results in transcriptional activation on the Gal10 promoter, which on the integrated plasmid induces the overexpression of GIN11M86 sequences that inhibit cell growth [86]. This can result in two scenarios: in the first, the genetic rearrangement reverts the genomic locus to the original structure removing the pAUR vector completely, in the second, a desired deletion results.

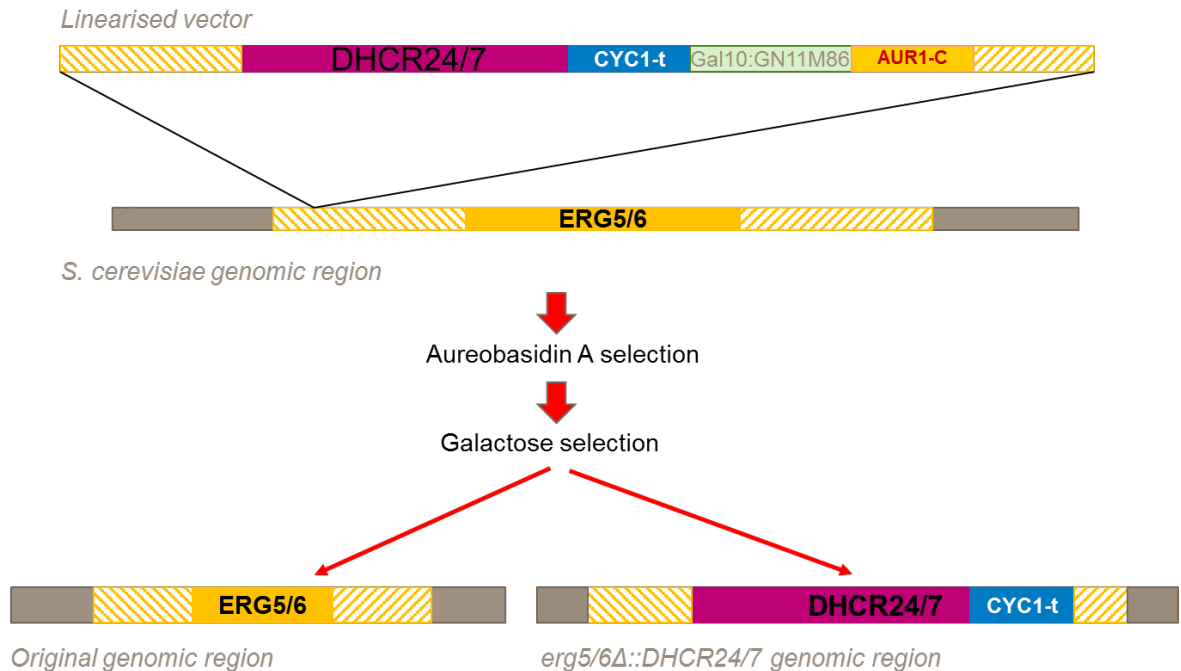


Figure 6.6 An overview of the strategy for cholesterol pathway engineering in MMY yeast. The deletion cassettes present in the pAUR135 vector first have to be integrated upstream of the reading frame of ERG5/6 upon the selection pressure of aureobasidin A. The subsequent selection on galactose induces the expression of toxic sequences under the transcriptional regulation of GAL10 promoter which promotes the cell to ‘loop out’ this element along with the AUR1-C gene. This allows the marker to be recycled. Because of the flanking 5’ and 3’ ERG5/6 sequences present upstream and downstream of the DHCR24/-7-cyc1t construct it is able to replace the ERG5/6 reading frame; alternatively this can be removed along with the selection marker, returning the genetic loci to the original structure.

6.3.2. The engineering of pAUR135-erg5-DHCR24-erg5-cys1t and pAUR135-erg6-DHCR7-erg6-cys1t plasmids

In order to obtain the plasmids for the integration of cholesterol genes *DHCR7* and *DHCR24*, two intermediate plasmids had to be made first. The p426GPD vector was selected as the backbone for the insertions of the deletion cassette elements because it was readily available and is episomally maintained at a high copy number, which is required for the recovery of the plasmid back from the yeast when the yeast gap repair is attempted.

p426GPD-ERG5 and p426-ERG6

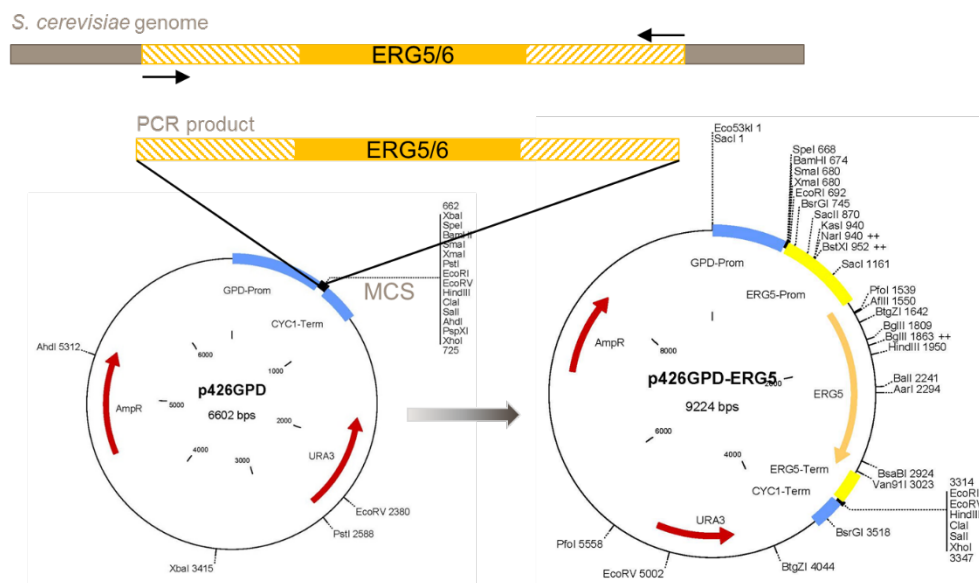


Figure 6.7 The schematic representation of the construction of p426GPD-ERG5. Both *ERG5* and *ERG6* genomic regions were amplified by PCR and then inserted into intermediate vector p426GPD.

In order to integrate the deletion cassette, it had to have a sequence homologous to the genomic *ERG5/6* loci. Therefore the first step was to amplify the genomic loci and insert it into the intermediate plasmid as depicted in **Figure 6.7**. The amplification was designed so that the sequence upstream from the 5' of the reading frame was modified as little as possible in the hope that the features of the transcription machinery binding would be preserved.

For the *ERG5* PCR amplification and subsequent insertion this was relatively easy because the *EcoRI* restriction sites were conveniently located 740bp upstream from the ATG codon and 265bp downstream from the 3' of the reading frame. The PCR product was digested with *EcoRI* and inserted

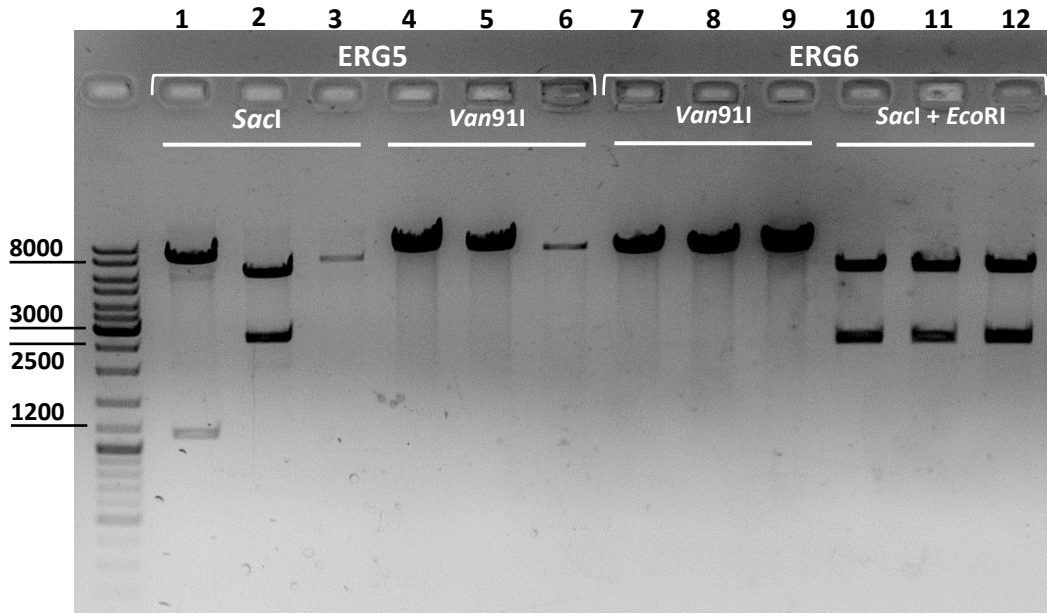


Figure 6.8 The restriction digestion analysis of p426GPD-ERG5 and p426-ERG6 vectors. The *ERG5* inserted at the correct orientation was predicted to appear as 1160bp + 8064bp bands when digested with *SacI*. The clone in lane 2 appears to have the predicted sizes, while clones in lanes 1 and 3 do not, despite all three having the *ERG5* gene inserted, as indicated by *Van91I* digestion in lanes 4-6. The *ERG6* insertion was less equivocal because two different restriction sites were used and as a result all 3 colonies chosen for the analysis displayed the expected digestion pattern.

by conventional ligation methods. The *ERG6* genomic locus did not have such suitable restriction sites, therefore the primers were designed to add *SacI* at the 5' end and *EcoRI* at the 3' end. These restriction sites were chosen because they were compatible with the ligation strategy both in relation to the vector backbone and the PCR-amplified DNA fragment.

The correct plasmid ligations were confirmed using several restriction enzymes. For the *ERG5* insertion, *SacI* was used to select the plasmid clones in which the fragment was inserted at the correct orientation. *Van91I* was also used to indicate that the fragment contained *ERG5* or *ERG6* reading frame; this enzyme does not cut within the p426GPD vector. And finally, *SacI* and *EcoRI* digestion of the p426-ERG6 colonies demonstrated that digestion with these enzymes cut out a fragment of the same size as the PCR product. Out of tested plasmid clones, 1 showed the correct ligation of p426GPD-ERG5 and 3 colonies of p426-ERG6 (**Figure 6.8**).

p426GPD-erg5-DHCR24-cys1t-erg5

The second engineering step relied on the yeast DNA repair machinery to ligate the *DHCR24* gene into p426GPD-ERG5, replacing the reading frame of *ERG5* with that of *DHCR24* (**Figure 6.9**). The *DHCR24*

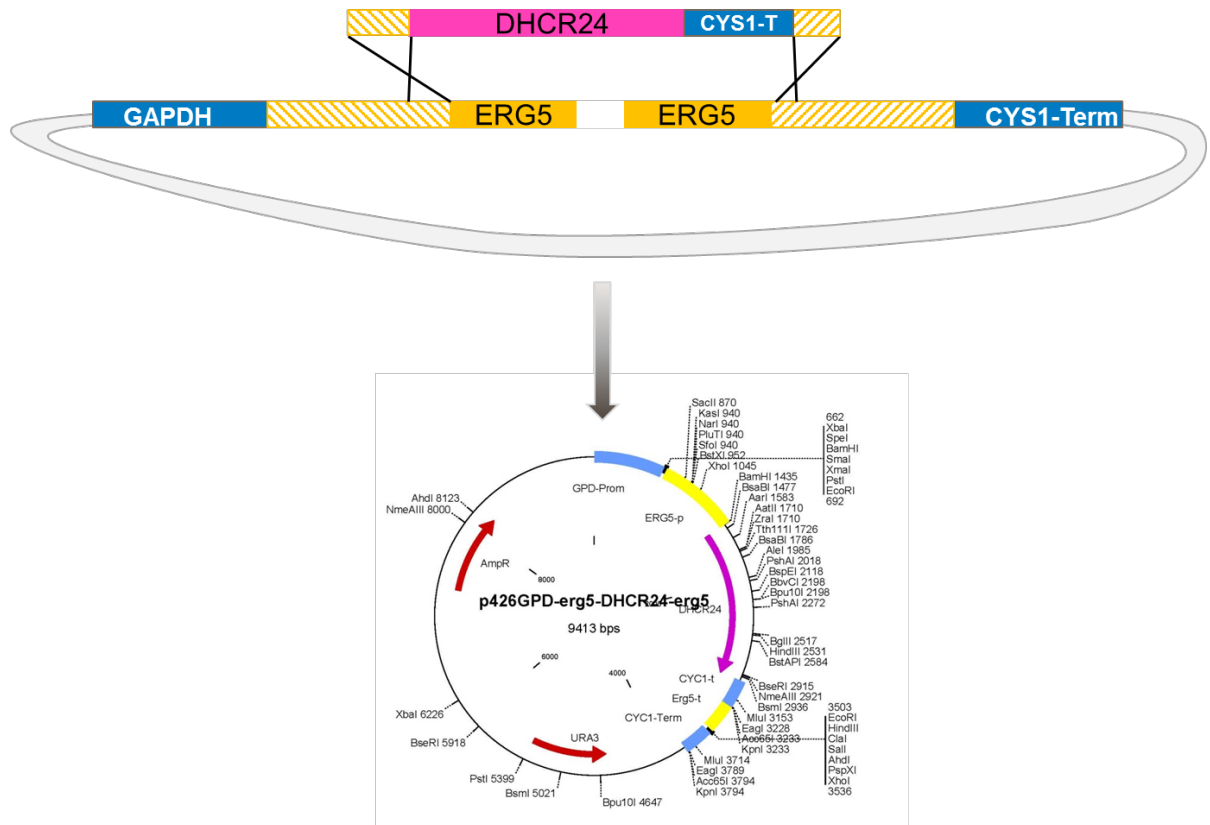


Figure 6.9 Schematic representation of the 'gap repair' cloning of the p426GPD-erg5-DHCR24-cys1t-erg5 and p426-erg6-DHCR7-cys1t-erg6 vectors. The homologous *ERG5/6* sequences on the synthesised *DHCR24/7* fragments and the p426GPD-*ERG5/6* vector allowed the ligation where the *ERG5/6* reading frame is replaced by *DHCR24/7*.

gene from *Danio rerio* (the zebrafish) was synthesised by GenScript, optimising the codon for use in *S. cerevisiae*. The synthesised fragment also included the 273bp 5' flanking sequence upstream from the *ERG5* reading frame, and 100bp downstream from the end of the reading frame. These homologous sequences were required to ligate the desired plasmid in yeast by gap repair mechanism (more details in Materials and Methods section). The *cys1* terminator sequence is located between the *DHCR24* 3' end and the 100bp of the homologous *ERG5* sequence.

The original p426GPD-*ERG5* and p426GPD-erg5-DHCR24-cys1t-erg5 did not differ much in size, therefore differences in restriction sites were utilised to select successful ligations. It was predicted, that in the presence of *ERG5* gene the *HindIII* digestion would result in two fragments of 1376bp + 7848bp but if the *DHCR24* has successfully replaced the *ERG5* reading frame the plasmid would be linearised only once. As shown in **Figure 6.10**, both negative and positive ligation patterns are observed and clone in lane 2 was determined to be successfully ligated p426GPD-erg5-DHCR24-cys1t-erg5 plasmid.

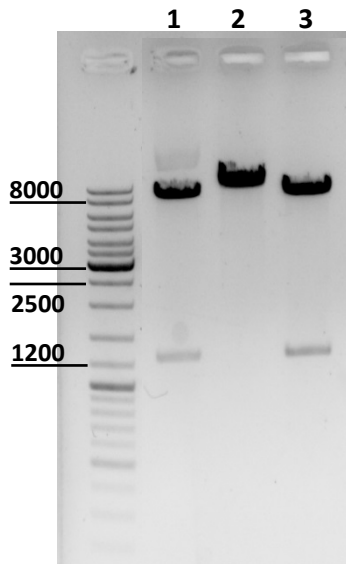


Figure 6.10 The selection of successfully ligated p426GPD-erg5-DHCR24-cys1t-erg5. Following ligation 3, colonies were digested with *HindII* which cuts *ERG5* containing vector into two fragments as can be seen in lanes 1 and 3, while *DHCR24* containing vectors would be linearised only once like in lane 2.

p426GPD-erg6-DHCR7-cys1t-erg6

A similar design and strategy for cloning was planned for the p426GPD-erg5-DHCR24-cys1t-erg5 plasmid. However, no colonies could be generated following the yeast gap repair. Instead, Gibson Assembly was used. This method relies on homologous overlapping sequences present on the fragments to be ligated together [87]. Therefore, the synthesised erg6-DHCR7-cys1t-erg6 fragment could be ligated into p426-ERG6 where the sequences overlap (essentially by the same mechanism as the gap repair).

Four colonies were selected for analysis with *BamHI*, *HindIII*, and *PvuII* enzymes which cut the *DHCR7* and *ERG6* gene-containing plasmids differently:

1) *BamHI*:

1586 + 7374 bp if *DHCR7* present;
8420 bp if *ERG6* present.

2) *HindIII*:

1103 + 7857 bp if *DHCR7* present;
8420 bp if *ERG6* present.

3) *PvuII*:

603 + 1361 + 5274 + 1722 bp if *DHCR7* present;
5274 + 3146 bp if *ERG6* present.

Shown in **Figure 6.11** are the restriction digestion analysis which indicate that 3 out of 4 colonies had a successful ligation.

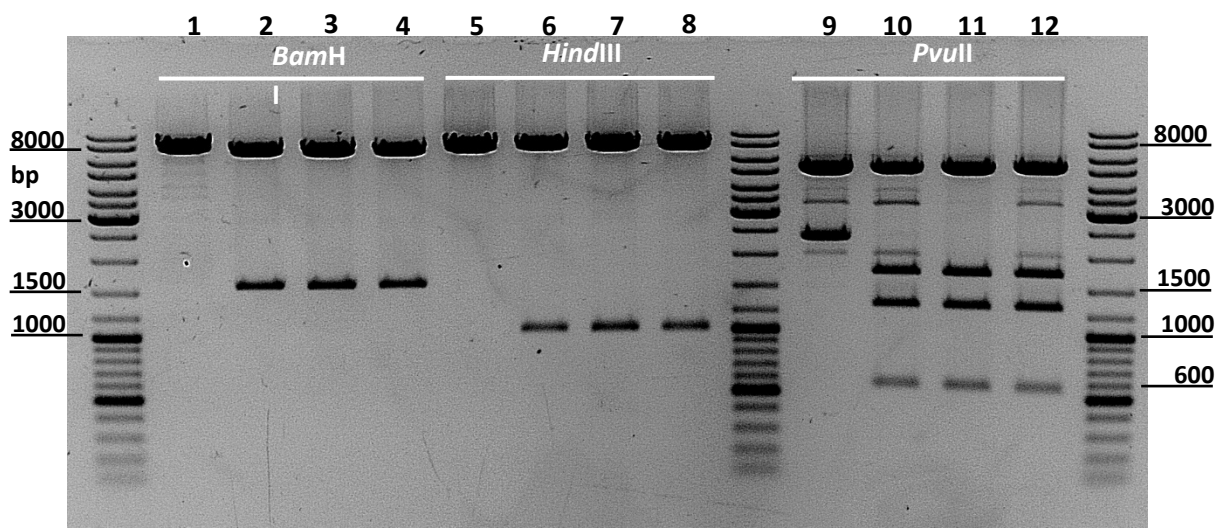


Figure 6.11 The selection of successfully ligated p426-erg6-DHCR7-cys1t-erg6. Based on the digestion patterns of *Bam*HI, *Hind*III and *Pvu*II 3 vectors were deemed to have the correct DHCR7 fragment ligated into the p426-ERG6.

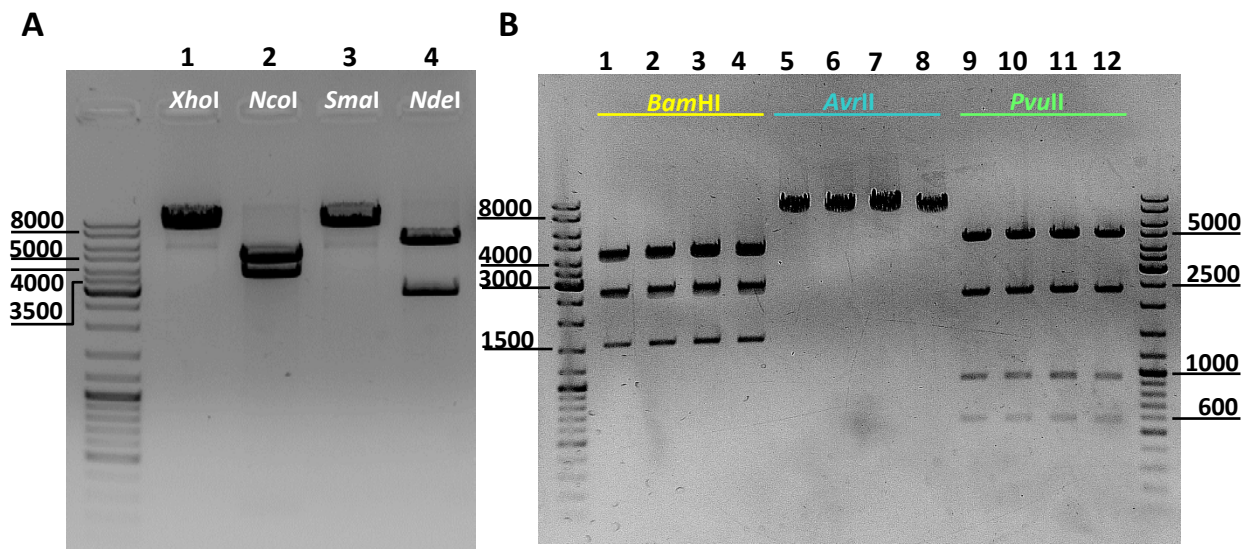
pAUR135-erg5-DHCR24-cys1t-erg5 and pAUR135-erg6-DHCR7-cys1t-erg6

The last step in engineering these plasmids was achieved by a standard ligation method where the deletion cassette was inserted into the pAUR135 vector. The erg5-DHCR24-cys1t-erg5 cassette was inserted at the *Eco*RI restriction site and the erg6-DHCR7-cys1t-erg6 at the *Sac*I and *Eco*RI sites.

One colony of pAUR135-erg5-DHCR24-cys1t-erg5 was analysed by restriction digestion with *Xho*I, *Nco*I, *Sma*I and *Nde*I, all of which confirmed the expected digestion pattern (**Figure 6.12 [A]**). The later has also indicated that the fragment was inserted at the right orientation, since the same restriction site was used for 5' and 3' end digestion.

For the selection of pAUR135-erg6-DHCR7-cys1t-erg6, 4 plasmids were selected and digested with *Bam*HI, *Avr*II or *Pvu*II. All 4 plasmids showed the correct digestion pattern (**Figure 6.12 [B]**).

The digestion pattern predictions are summarised in **Figure 6.12 [C]**.



C

Enzyme	Predicted pAUR135-erg5-DHCR24-cys1t-erg5 sizes
<i>XhoI</i>	8885bp
<i>NcoI</i>	4804 + 3820 + 261bp
<i>SmaI</i>	8885bp
<i>NdeI</i>	6103 + 2782bp if correct 8430 + 455bp if reverse

Enzyme	Predicted pAUR135-erg6-DHCR7-cys1t-erg6 sizes
<i>BamHI</i>	4608 + 2869 + 1586 + 54bp
<i>AvrII</i>	9117bp
<i>PvuII</i>	5116 + 2364 + 1034 + 603bp

Figure 6.12 The selection of successfully ligated pAUR135-erg5-DHCR24-cys1t-erg5 and pAUR135-erg6-DHCR7-cys1t-erg6. [A] Digestion pattern of pAUR135-erg5-DHCR24-cys1t-erg5 vector. [B] Digestion pattern and selection of the pAUR135-erg6-DHCR7-cys1t-erg6 vector. [C] Summary of each vectors' expected digestion pattern.

6.3.3. The selection of the MMY11 *erg5*Δ::DHCR24 strain

The pAUR135-*erg5*-DHCR24-*cys1t-erg5* was designed to integrate within the upstream flanking region, where the promoter would be expected to be. For this, the plasmid was linearised at *AvrII* unique restriction site. Following standard yeast transformation protocol MMY11_ura3Δ colonies growing on AbA were picked for PCR analysis. Primers 39 and 40 (Table 2.6) were designed to anneal at 884bp upstream from the *ERG5* reading frame and 323bp downstream from the end of the reading frame. These positions were outside the PCR amplified region inserted in the transformation plasmid therefore would only amplify the genomic region. However, it was predicted that upon the insertion of the transformation plasmid the PCR product would be 10049bp instead of the 2784bp which was observed during primer optimisation. This size difference was utilised for positive integration selection. As demonstrated in Figure 6.13, both size fragments were observed in 10 out of 17 screened colonies. It is unclear whether the lower band has resulted from a mixed population in the sample or as a non-specific PCR product. It was noted that the intensity of the top band in relation to the lower band differed between the test samples. The sample in lane 14 was clearly negative with only the lower size band. Other samples did not show any bands or they are very faint. This could be due to the quality of the gDNA sample. Based on the intensity of the top band, colonies represented in lanes 1, 2 and 13 we selected for the next step involving the galactose-induced selection.

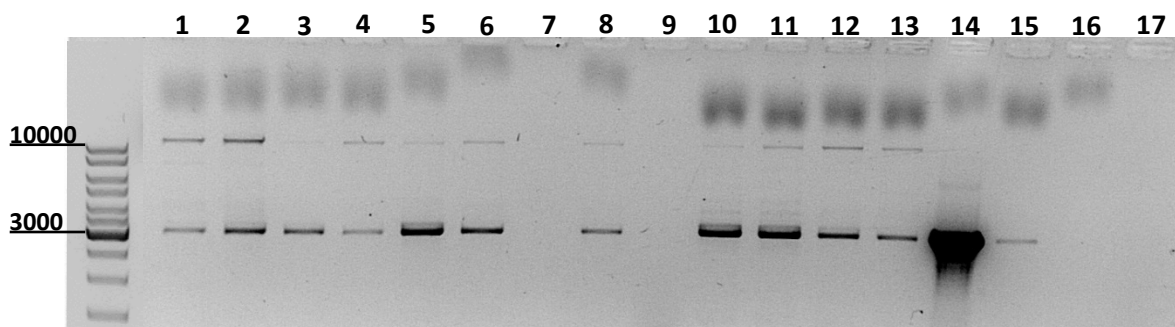


Figure 6.13 PCR screening of the integration of pAUR135-*erg5*-DHCR24-*cys1t-erg5* into MMY11_ura3Δ. The primers 39 + 40 were designed to amplify the genomic locus of *ERG5* which appears as a band of approximately 3,000bp in the untransformed strain, and was expected to appear as a 10,000bp band upon a successful integration of the vector. Colonies represented in lanes 1, 2, 4-6, 8, 10-13 appear to have both the band characteristic of the wild type locus and that containing the vector. Samples in lanes 3, 14, and 15 indicate that no integration took place and samples in lanes 7, 9, 16, 17 are inconclusive.

Several WHAUL+His+Ura+Trp + galactose plates (WHAUL+gal for short) were inoculated with selected colonies to induce the looping out of the selection marker *AUR1C* cassette. 10 colonies were picked for PCR screening which is depicted in Figure 6.14 [A]. The pAUR135 vector was designed so that the *GAL10*-prom induced expression of toxic GIN11M86 sequences to drive the cell's genetic

rearrangement to the original locus or the *erg5Δ::DHCR24* version (outlined in **Figure 6.6**). The same primers 39 and 40 can amplify either of those regions, however, distinction by PCR alone is difficult because of less than 200bp size difference between the two resulting loci. The solution to this was to digest the PCR products with two enzymes – *XhoI* and *HindIII* – which were predicted to cut the fragment differently depending on whether *ERG5* or *DHCR24* was present. As shown in **Figure 6.14 [B]**, two colonies in lanes 1, 8 and 5, 12 appeared to have the digestion pattern predicted to appear if *DHCR24* is present.

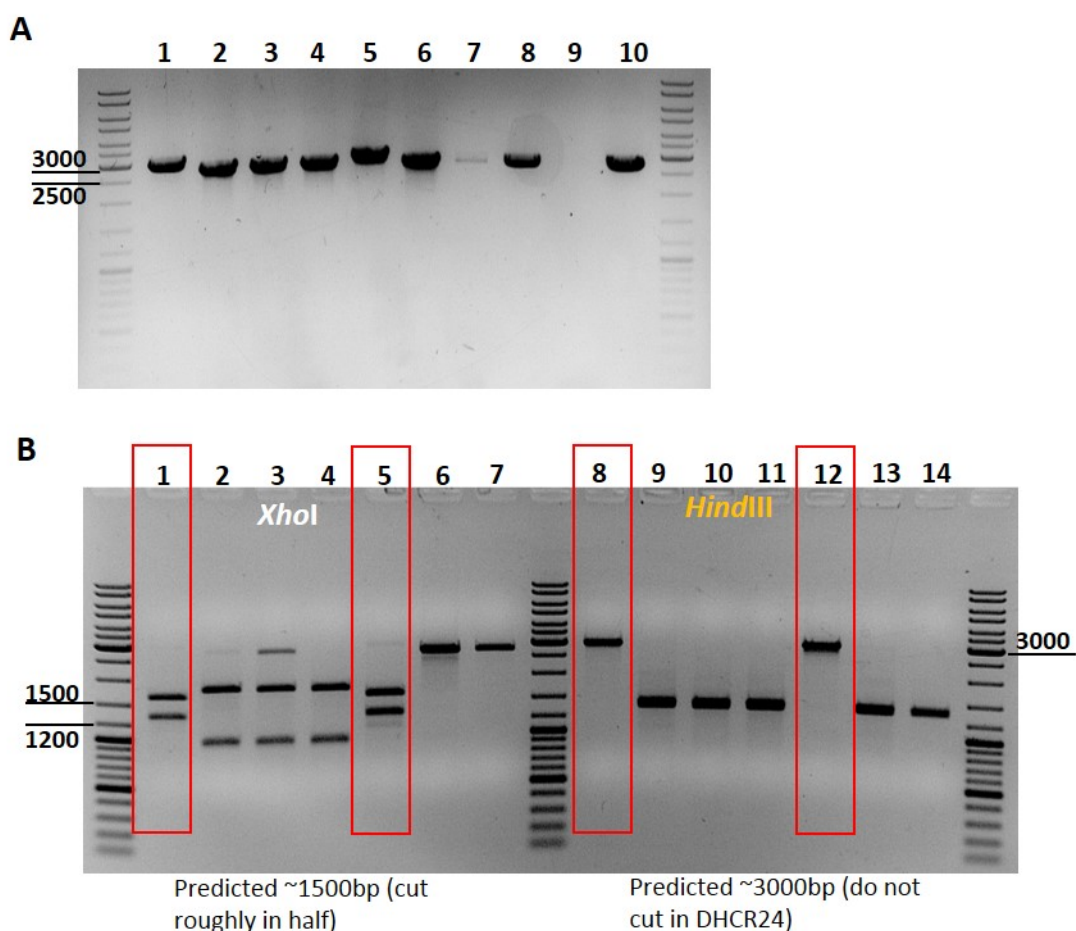


Figure 6.14 The selection of *MMY11 erg5Δ::DHCR24* colonies. **[A]** The initial PCR screening of galactose selected colonies showed bands of very similar sizes, therefore further analysis by restriction digestion, shown in **[B]**, had to be performed. The predicted digestion pattern allowed the selection of two colonies which are believed to have the desired genomic locus structure, in which *ERG5* reading frame has been deleted and replaced with *DHCR24*.

6.3.4. Future work

The integration of the *DHCR7* gene was also attempted several times, and although the integration of the AUR135-*erg6*-*DHCR7*-*cys1t*-*erg6* could be detected, following the galactose selection all colonies appeared to have reverted to the original locus structure. Given the number of attempts to integrate, it may be necessary to redesign the deletion cassette.

The success of the engineering strategy would eventually have to be confirmed by analysing the sterol composition of engineered yeast, as was described in the original studies. Even the intermediate strain MMY11 *erg5*Δ::*DHCR24* is expected to produce ergosterol/cholesterol intermediates. A mass spectrometry method therefore needs to be optimised for the detection of ergosterol, cholesterol and their intermediates.

Chapter 7 – Discussion and future work

The results presented in this thesis were carried out in yeast engineered for the functional investigation of GPCR pharmacology. The aim of this study was to optimise the functional expression of adrenergic receptors that had previously been difficult to express and/or characterise pharmacologically in these yeast strains. Further understanding of the host's response to protein expression was sought after along this process. The sections below discuss the findings presented in Chapters 3, 4, 5, and 6.

7.1. MMY yeast are a powerful tool for GPCR drug discovery

Throughout this thesis a few examples of compound screening experiments have been presented in Chapter 3 and 5. It's quick and inexpensive set up makes it very attractive for screening programmes where the aim is to identify potential interacting (in an agonistic or antagonistic manner) compounds for further development and characterisation. However, as any assay it does require some optimisation. At GSK, where these yeast were engineered, parameters such as concentration of 3-AT, incubation time, inoculation density, substrate concentration have been recognised to make a difference on the signal window. The data presented in Chapter 3 illustrates this with some examples. The variation of 3-AT concentration, as already discussed, has proved to be a useful in controlling unspecific background growth and as was shown in **Figures 3.3, 3.4 and 3.9** where the level of control needed depended greatly on the receptor. What is interesting is that 3-AT concentration did not have a uniform effect on all tested compounds in terms of efficacy. For example, compound 9 retained E_{max} of approximately 6×10^6 at 2mM and 10mM of 3-AT, while compound 11 dropped from 5×10^6 to 3×10^6 RFUs. Similarly, inverse agonists 4, 8 and 21 were able to inhibit growth regardless of overall high unspecific growth (**Figure 3.9 [B]**). Therefore particular caution has to be taken when interpreting efficacy of a ligand. When a screening assay is set up for a new receptor, a reference known agonist is included along with a no compound control to determine a signal window. Another useful control could be a known partial agonist acting on the same signalling pathway as the reference agonist. By tuning the 3-AT concentration to match the curve profiles of both full and partial agonists the assay conditions can be optimised to better represent the efficacies of test compounds.

Another novel observation arising from the data presented in Chapter 3 is the variation between different instruments, especially in terms of their dynamic range (**Figure 3.6 and 3.7**). Each instrument manufacturer have their unique features but generally the fluorophore excitation is achieved by either a monochromator which generates any desired wavelength or by the light passing through a filter. Generally, the optical filter based fluorescence readers are considered to be more sensitive because the filter eliminates wavelengths other than the selected one; a filter at a different wavelength is

required for emission. Four different fluorescence readers were used in this thesis project – three described in Chapter and the fourth one – Spectrafluor Plus (Tecan) – used for generating Chapter 5 data. Out of these Gemini (Molecular Devices) is a dual monochromator based reader while the other three are filter-based readers. The Gemini instrument produced a lowest magnitude of RFUs in a range of 10^3 RFU, while the filter-based readers generated between 10^4 - 10^6 RFUs (including SpectraFluor Plus instrument). The magnitude of the signal window produced by background fluorescence and the agonist stimulation produced fluorescence were also different. For this work instrument dependent settings were not optimised, however, this is something that should be considered if the signal window is not satisfactory. For example, the α_{2B} strain YIG153 has demonstrated consistently to have a higher background growth produced signal, however, as demonstrated in **Figure 3.7** some strength of that signal may be masked by instrument settings.

7.2. A comparison of episomal and integrative plasmid functional expression systems – which is better?

The results presented in Chapter 4 describe a detailed comparison of two systems for recombinant gene introduction into yeast and the resulting protein translations. For the functional expression of the β -adrenoceptors the p306GPD vector provided several benefits. Firstly, the positive colony selection process was more robust and unambiguous and overall a lot more positive colonies could be selected. Secondly, the signal window on the functional FD-glu assay was wider and less variable between the different colonies of the same strain-vector combination (**Figures 4.15** and **4.16**). Together with a lower frequency of positive colony selection, smaller signal window and three combinations of vector constructs (with/without leader sequence) made the selection process quite laborious. Although the episomal vectors do not need to be linearised prior transformation, which is considered to speed up the process, in retrospective it did not provide a great advantage over the integrative vectors which had to be linearised. However the most disappointing property of p426GPD transformed colonies was the disappearance of functional signal in β_2 -AR transformed yeast. This prompted the decision not to carry out any compound profiling experiments with these constructs and move on to the integrative system.

Despite early reports of generation instability of the 2μ vectors [74, 88] they are still widely used for expression of GPCRs in yeast. Successful reports of functional GPCR studies in MMY strains transformed with high copy number producing 2μ vectors have also been reported [2, 47, 48, 50, 89-91]. Although the study investigating adenosine A_1 reported lower agonist efficacy in $G\alpha_o$ when compared to data produced in Chinese hamster ovary (CHO) cells [47]. The authors argue that the yeast pheromone signalling pathway has a lower signal amplification which explains a weaker coupling

of lower efficacy ligands. Other reasons thought to influence the results are sub-optimal design of chimeric G α proteins, different compartmentalisation and/or lack of other signalling components [47]. However, the receptors in these studies were expressed in an episomal expression system and no apparent leader sequences were added to their constructs. It could be argued that the lack of sensitivity of the yeast system they experienced could have been alleviated with additional optimisation of the expression vector, as it has in the work presented here. The episomal expression in p426 vector was suboptimal for the β_1 -AR and β_2 -AR functional expression in the same yeast strains as used in their studies.

Based on the published evidence and the ones presented in this thesis it is difficult to say that the integrative system is better for functional expression of GPCRs in MMY yeast over the episomal or vice versa. The cellular responses that made the functional expression of the adrenoceptors more robust in p306GPD transformed yeast remains unknown, although it has been shown in the literature that high copy number does not always correlate with increased expression yields [92]. It is possible that the high copy number of the gene and hence increased expression burden to the cell is the driving force for plasmid loss, and the genomic integration not only reduces that burden but is also unlikely to be removed from the genome. In theory the CEN-ARS which are episomal vectors, such as p41X and p31X [79, 93], maintained at lower copy number (1-2 per cell) would alleviate the translational burden if that is an issue.

7.3. Protein expression level and functional expression of the β -adrenoceptors

The comparison of different expression vectors in the search of an ideal construct for functional expression of the β -adrenoceptors has also created a platform for investigating cellular responses to GPCR production. As mentioned in the previous section, by introducing a single gene copy via p306GPD vector construct for both receptors a functional expression has improved, which posed a question whether protein expression levels differed. The western blot experiments described in section 4.4 attempted to answer this question. However, no correlation between the relative protein quantity and functional signal strength could be drawn based on presented results. However, it is not to say that there is no correlation at all. The total membrane western blot does not give an information about the folding status of detected proteins – it is possible that expression via high copy number vector results in more misfolded protein. Nor does this method indicate which membranes these proteins are associated with. The yeast Gpa1 (a G α subunit) and the Ste4-Ste18 (G $\beta\gamma$) complex are located on the plasma membrane when the signalling takes place therefore the receptor would be expected to be predominantly located there as well. The mating factor α (MF α) secretion signal would be also expected to enhance receptor's functional expression and trafficking to the plasma membrane.

A more detailed investigation into these theories could be achieved by separating the membrane fractions and combining with radio-labelled ligand studies, which are often used to quantify and confirm receptor folding status [38]. There are various well established methods such as membrane fraction separation on sucrose gradient or biotinylation of the cell surface and a subsequent plasma membrane isolation with the help of an antibody. Yeast microscopy is another method of visually assessing the receptor's location by either tagging it with a fluorescent protein, such as mCherry, yeast enhanced or conventional GFP [49, 90, 94], or by fluorophore conjugated antibodies. The microscopy was attempted on MMY15 expressing functional untagged β -adrenoceptors, however, the antibodies available did not provide sufficient sensitivity to give any conclusive results. A small tag, such as FLAG tag or poly-histidine tag would provide minimal interference with the receptors signalling yet giving an array of antibodies and protocols for protein detection on a western blot, microscopy or cell fractionation.

In regards to the detected band sizes the β_2 -AR signal on the western blot is somewhat more conclusive than the β_1 -AR signal. The expected size of β_2 -AR is 46-48kDa for a monomer and around 68kDa for a dimer when expressed in mammalian cells (Abcam, cat# ab182136, cat# ab137494, cat# ab61778). The detected top bands in yeast were around 39-41kDa which is not largely different to the expected size, or the size of β_2 -AR and other GPCRs expressed in yeast [11, 94, 95] and mammalian cells [96]. The presence of a double band in p426GPD-MF α expressed plasmid compared to a single 39kDa band in p306GPD-MF α plasmid is an interesting observation. A post-translational modification such as glycosylation has been described in the literature to results in similar size difference between the bands [95, 97, 98] and although is not essential for the native GPCR Ste2, the role of glycosylation on the β -adrenoceptors might be to aid the receptor's localisation to plasma membrane [99]. The glycosylation can be cleaved off with Peptide -N-Glycosidase F or Endoglycosidase H enzymes which would reduce the size of the protein if the glycosylation is responsible for shift in the size [97, 98]. The same double size bands were observed on β_1 -AR western blots, although almost twice smaller than the β_2 -AR protein sizes. This reduction in size likely indicates protein degradation. Whether these bands actually represent the receptor could be confirmed by protein sequence. However, overall it would be beneficial to add an already mentioned Flag, poly-histidine or biotin tag for further investigation as the tested antibodies have provided limitations to further investigation.

7.4. Fixing the uracil selection marker deletion in the MMY yeast strains

Despite the inconclusive band sizes one pattern observed from the western blot analysis was quite clear – the non-functional colonies picked for analysis showed no presence of the β -adrenoceptor at the protein level. During the functional colony selection of p426GPD episomally transformed yeast

described in section 4.4 a large number of colonies picked for pre-screening and later full-curve analysis did not show any response to isoprenaline, despite being picked from a selection plate after the transformation. Some of these colonies were still able to grow on the selection medium when first selected and also when grown in a larger volumes for membrane isolation. The lack of expression could be due to many reasons: transcription inhibition, poor translation or rapid degradation due to missfolding. However, we also had concerns about the auxotrophy of uracil marker (*ura3-1*) and therefore made further investigation as described in sub-chapter 6.1.

Several so called 'Designer strains' were engineered based on two most popular *S. cerevisiae* genetic backgrounds – S288C and W303-1a [79, 100]. In these strains the coding sequences of the auxotrophic markers were completely deleted. The rationale for this was that point mutations, small internal deletions and Ty insertions on auxotrophic marker genes leave large fragments of sequences homologous to the wild type sequences located on transformation vectors. This can result in the repair of the auxotrophy rather than an integration of the desired gene carried out on a vector or PCR generated fragment. The way to circumvent this issues is to delete those homologous sequences on the genome so that there is no way for the exogenous markers to cross over to the original locus.

The Ura⁻ phenotype of the W303-1A strain from which the MMY yeast were engineered is brought about by a point mutation (*ura3-1*) therefore it is highly likely that the 'false-positive' selected yeast colonies the recombination took place and the phenotype reverted to Ura⁺. However, even without the introduction of the exogenous *URA3* gene colonies were able to display Ura⁺ phenotype (**Figure 6.2**), questioning the reliability of that point mutation.

Furthermore, some 426GPD transformed yeast colonies did show functional expression but failed to retain it after freeze-thaw cycle (**Figure 4.10**), suggesting that these cells did initially uptake the plasmid but the marker repair did not take place, because the cells also struggled to grow in the selection medium upon presumed plasmid loss. As further investigated by PCR showed that two distinct population of cells existed – fl*URA3* and tr*URA3* – and that the strains displaying a full length gene, presumably the original *ura3-1* locus, were more likely to revert to Ura⁺ phenotype than the ones carrying a truncated gene fragment resulting from marker recycling (section 6.2.2, **Figures 6.2** and **6.3**). Whether reversion to Ura⁺ phenotype was due to reverted point-mutation or repair by homologous recombination upon transformation with *URA3* carrying vector, the observations pointed towards the problem with the full length *ura3-1* gene. To test this theory and potentially resolve this 'false-positive' colony selection issue the same strategy described in 'Designer strain' engineering studies was employed [79, 100]. The pJL164 vector designed to generate *ura3Δ0* allele was transformed into MMY11 which lacks the chimeric Gα proteins. The remake of MMY12-28 strains from MMY *ura3Δ0* could potentially make the selection process for functional GPCR expression much quicker and is

expected to result in smaller number of transformation colonies which would be the result of reduced 'false-positive' background.

7.5. Pharmacology of β_1 -AR and β_2 -AR – the Devil is in the (structural) details

The yeast assay for functional GPCR studies was designed to produce the best coupling interactions between the mammalian receptor and the chG α as discussed in section 1.3.6 and reviewed in [1]. A high signal induction upon ligand stimulation, or inverse relationship for inhibition by antagonists and inverse agonists, is a desirable feature for high-throughput screening of compound libraries in an industrial setting. As demonstrated in Chapters 3, 4 and 5 this can be achieved in yeast by optimising assay conditions or expression vector design. However, since the design of this assay a lot more details have emerged about the mechanism of synthetic ligand-induced GPCR signalling, such as β -arrestin signalling, bias agonism and allosteric modulation. Therefore a question to ask is how the yeast assay can be used to investigate a more complex pharmacology. A few published studies have already demonstrated that ligand bias can be observed in the yeast assay and confirmed in mammalian cell assays [48, 49]. The data presented in Chapter 5 can perhaps be used to gain more understanding of interactions between the receptor and the G α subunit.

The recently proposed kinetics of GPCR pharmacology suggest that binding of a ligand promotes association with the G α_s protein, for which cytoplasmic ends of H3, H5 and H6 form a pocket for G α_s N terminus interaction. The engagement in coupling is required to stabilise the receptor and increases its affinity for the ligand [65]. From the results presented in Chapter 5 it was clear that most agonists, with the exception of isoprenaline, have stronger β_2 -AR coupling with G α_s , G α_{14} , and G α_{16} strains and weaker with G α_q and G α_{i1} . As the differences were fairly consistent it suggests that the pocket formed by the active receptor conformation is suboptimal for all necessary contacts with the 5 α helix of chG α to completely stabilise the interaction and efficient GDP exchange to GTP on the chG α subunit. A receptor-G protein interactions in the presence of various ligands could be investigated by modelling techniques. Particularly interesting experiments would be with outliers, such as procaterol and xamoterol, presented in **Figure 5.15**. By comparing models of receptor-ligand complex coupling to mammalian G α , yeast Gpa1 and chG α can potentially inform on which residues bring about the specificity of ligand-induced interactions and explain any observed pharmacological differences.

7.6. Thesis summary

This following objectives were achieved:

- Assay parameters were described in well coupling α_{2A} and α_{2B} adrenoceptors. Receptor dependent variables and technical parameter optimisation was established (Chapter 3).
- A systematic comparison between different expression vector designs was performed and identified that the addition of the mating factor α (MF- α) leader sequence to the amino-terminus of the β_1 - and β_2 -adrenoceptors was required to produce and retain a pharmacological response in the yeast assay (Chapter 4).
- A pharmacological characterisation of the β -adrenoceptors was performed. To gain more insight into the signalling mechanisms and coupling interaction of these receptors a more detailed modelling studies could be performed (Chapter 5).
- Strategies were designed to further engineer the host to produce cholesterol instead of the yeast ergosterol which is hypothesised to provide a more native-like environment for the G protein coupled receptors and increase the number of pharmacological targets that can be tested in the yeast system (Chapter 6).

References

1. Dowell, S.J. and A.J. Brown, *Yeast assays for G-protein-coupled receptors*. Receptors Channels, 2002. **8**(5-6): p. 343-52.
2. Brown, A.J., et al., *Functional coupling of mammalian receptors to the yeast mating pathway using novel yeast/mammalian G protein alpha-subunit chimeras*. Yeast, 2000. **16**(1): p. 11-22.
3. Palczewski, K., et al., *Crystal structure of rhodopsin: A G protein-coupled receptor*. Science, 2000. **289**(5480): p. 739-45.
4. Cherezov, V., et al., *High-resolution crystal structure of an engineered human beta2-adrenergic G protein-coupled receptor*. Science, 2007. **318**(5854): p. 1258-65.
5. Lefkowitz, R.J., et al., *β -Adrenergic receptors and rhodopsin: shedding new light on an old subject*. Trends in Pharmacological Sciences, 1986. **7**(0): p. 444-448.
6. Rang, H.P., Dale, M.M., Ritter, J.M., Flower, R.J., Henderson, G., *Rang and Dale's Pharmacology*. 2012: Elsevier Churchill Livingstone.
7. Ritter, S.L. and R.A. Hall, *Fine-tuning of GPCR activity by receptor-interacting proteins*. Nat Rev Mol Cell Biol, 2009. **10**(12): p. 819-30.
8. Yalow, R.S. and S.A. Berson, *Assay of plasma insulin in human subjects by immunological methods*. Nature, 1959. **184** (Suppl 21): p. 1648-9.
9. Leach, K., Valant, C., Sexton, P.M., Christopoulos, A., *Measurement of Ligan-G protein-coupled Receptor Interactions*. G Protein-Coupled Receptors, ed. D.R. Poyner, Wheatley, M. 2010: A John Wiley and Sons, Ltd.
10. Sridharan, R., et al., *Fluorescent approaches for understanding interactions of ligands with G protein coupled receptors*. Biochim Biophys Acta, 2014. **1838**(1 Pt A): p. 15-33.
11. Zhang, R., et al., *Biochemical and mass spectrometric characterization of the human CB2 cannabinoid receptor expressed in Pichia pastoris--importance of correct processing of the N-terminus*. Protein Expr Purif, 2007. **55**(2): p. 225-35.
12. Sander, P., et al., *Heterologous expression of the human D2S dopamine receptor in protease-deficient Saccharomyces cerevisiae strains*. Eur J Biochem, 1994. **226**(2): p. 697-705.
13. Blocker, K.M., et al., *Recombinant G Protein-Coupled Receptor Expression in Saccharomyces cerevisiae for Protein Characterization*. Methods in Enzymology, 2015. **556**: p. 165-183.
14. Gregory, K.J., Sexton, P.M., Christopoulos, A., Hick, C.A., *Second messenger assays for G protein-coupled receptors: cAMP, Ca²⁺, inositol phosphates, ERK1/2*. G Protein-Coupled Receptors, ed. D.R. Poyner, Wheatley, M. 2010: John Wiley and Sons, Ltd.
15. Gauthier, N., Blouin, J., Caron, M., Roby, P., Beaudet, L., Padros, J., *Application Note: Time-resolved fluorescence resonance energy transfer*. 2010, PerkinElmer, Inc.
16. DiscoverX, *User Manual cAMP Hunter GaS and Gai cell line*. DiscoverX.
17. Versele, M., K. Lemaire, and J.M. Thevelein, *Sex and sugar in yeast: two distinct GPCR systems*. EMBO Rep, 2001. **2**(7): p. 574-9.
18. Feldmann, H., *Yeast: Molecular and Cell Biology*. 2nd ed. 2012, Weinheim, Germany: Wiley-Blackwell.
19. Schrick, K., B. Garvik, and L.H. Hartwell, *Mating in Saccharomyces cerevisiae: the role of the pheromone signal transduction pathway in the chemotropic response to pheromone*. Genetics, 1997. **147**(1): p. 19-32.
20. *MF(ALPHA)1/YPL187W Summary*, in *Saccharomyces genome database*. 2012.
21. *MF(ALPHA)2/YGL089C*, in *Saccharomyces genome database*. 2012.
22. *MFA1/YDR461W Summary*, in *Saccharomyces genome database* 2012.
23. *MFA2/YNL145W Summary* in *Saccharomyces genome database*. 2012.
24. Bardwell, L., *A walk-through of the yeast mating pheromone response pathway*. Peptides, 2005. **26**(2): p. 339-50.

25. Price, L.A., et al., *Functional coupling of a mammalian somatostatin receptor to the yeast pheromone response pathway*. Mol Cell Biol, 1995. **15**(11): p. 6188-95.
26. Lambright, D.G., et al., *The 2.0 Å crystal structure of a heterotrimeric G protein*. Nature, 1996. **379**(6563): p. 311-9.
27. Chang, F. and I. Herskowitz, *Identification of a gene necessary for cell cycle arrest by a negative growth factor of yeast: FAR1 is an inhibitor of a G1 cyclin, CLN2*. Cell, 1990. **63**(5): p. 999-1011.
28. Butty, A.C., et al., *The role of Far1p in linking the heterotrimeric G protein to polarity establishment proteins during yeast mating*. Science, 1998. **282**(5393): p. 1511-6.
29. Alvaro, C.G. and J. Thorner, *Heterotrimeric G Protein-coupled Receptor Signaling in Yeast Mating Pheromone Response*. J Biol Chem, 2016. **291**(15): p. 7788-95.
30. Alvaro, C.G., et al., *Specific alpha-arrestins negatively regulate Saccharomyces cerevisiae pheromone response by down-modulating the G-protein-coupled receptor Ste2*. Mol Cell Biol, 2014. **34**(14): p. 2660-81.
31. Alvaro, C.G., A. Aindow, and J. Thorner, *Differential Phosphorylation Provides a Switch to Control How alpha-Arrestin Rod1 Down-regulates Mating Pheromone Response in Saccharomyces cerevisiae*. Genetics, 2016. **203**(1): p. 299-317.
32. Bardwell, L., *A walk-through of the yeast mating pheromone response pathway*. Peptides, 2004. **25**(9): p. 1465-76.
33. Kang, Y.S., et al., *Effects of expression of mammalian G alpha and hybrid mammalian-yeast G alpha proteins on the yeast pheromone response signal transduction pathway*. Mol Cell Biol, 1990. **10**(6): p. 2582-90.
34. Goffeau, A., et al., *Life with 6000 genes*. Science, 1996. **274**(5287): p. 546, 563-7.
35. Hino, T., et al., *G-protein-coupled receptor inactivation by an allosteric inverse-agonist antibody*. Nature, 2012. **482**(7384): p. 237-40.
36. Marth, J.D. and P.K. Grewal, *Mammalian glycosylation in immunity*. Nat Rev Immunol, 2008. **8**(11): p. 874-87.
37. Byrne, B., *Pichia pastoris as an expression host for membrane protein structural biology*. Curr Opin Struct Biol, 2015. **32**: p. 9-17.
38. Andre, N., et al., *Enhancing functional production of G protein-coupled receptors in Pichia pastoris to levels required for structural studies via a single expression screen*. Protein Sci, 2006. **15**(5): p. 1115-26.
39. King, K., et al., *Control of yeast mating signal transduction by a mammalian beta 2-adrenergic receptor and Gs alpha subunit*. Science, 1990. **250**(4977): p. 121-3.
40. Ficca, A.G., L. Testa, and G.P. Tocchini Valentini, *The human beta 2-adrenergic receptor expressed in Schizosaccharomyces pombe retains its pharmacological properties*. FEBS Lett, 1995. **377**(2): p. 140-4.
41. King, K., Dohlman, H., Caron, M., Lefkowitz, R.J., *EP0548165 (A1) - EXPRESSION OF G PROTEIN COUPLED RECEPTORS IN YEAST.*, E.P. Office, Editor. 1993.
42. Gerasimov, A.S., et al., *[Biosynthesis and purification of human beta2-adrenergic receptor expressed in methylotrophic yeast Pichia pastoris]*. Mol Biol (Mosk), 2012. **46**(2): p. 308-16.
43. Brown, A.J., et al., *Pharmacology of GPR55 in yeast and identification of GSK494581A as a mixed-activity glycine transporter subtype 1 inhibitor and GPR55 agonist*. J Pharmacol Exp Ther, 2011. **337**(1): p. 236-46.
44. Brown, A.J., et al., *Pharmacological properties of acid N-thiazolylamide FFA2 agonists*. Pharmacol Res Perspect, 2015. **3**(3): p. e00141.
45. Brown, A.J., et al., *The Orphan G protein-coupled receptors GPR41 and GPR43 are activated by propionate and other short chain carboxylic acids*. J Biol Chem, 2003. **278**(13): p. 11312-9.
46. Dowell, S.J. and A.J. Brown, *Yeast assays for G protein-coupled receptors*. Methods Mol Biol, 2009. **552**: p. 213-29.
47. Stewart, G.D., et al., *Determination of adenosine A1 receptor agonist and antagonist pharmacology using Saccharomyces cerevisiae: implications for ligand screening and functional selectivity*. J Pharmacol Exp Ther, 2009. **331**(1): p. 277-86.

48. Stewart, G.D., P.M. Sexton, and A. Christopoulos, *Detection of novel functional selectivity at M3 muscarinic acetylcholine receptors using a Saccharomyces cerevisiae platform*. ACS Chem Biol, 2010. **5**(4): p. 365-75.
49. Weston, C., et al., *Investigating G protein signalling bias at the glucagon-like peptide-1 receptor in yeast*. Br J Pharmacol, 2014. **171**(15): p. 3651-65.
50. Weston, C., et al., *Receptor activity-modifying protein-directed G protein signaling specificity for the calcitonin gene-related peptide family of receptors*. J Biol Chem, 2016. **291**(49): p. 25763.
51. Prasanna, X., D. Sengupta, and A. Chattopadhyay, *Cholesterol-dependent Conformational Plasticity in GPCR Dimers*. Sci Rep, 2016. **6**: p. 31858.
52. Soubias, O., et al., *The role of membrane curvature elastic stress for function of rhodopsin-like G protein-coupled receptors*. Biochimie, 2014. **107 Pt A**: p. 28-32.
53. Prasanna, X., A. Chattopadhyay, and D. Sengupta, *Cholesterol modulates the dimer interface of the beta(2)-adrenergic receptor via cholesterol occupancy sites*. Biophys J, 2014. **106**(6): p. 1290-300.
54. Pluhackova, K., et al., *Dynamic Cholesterol-Conditioned Dimerization of the G Protein Coupled Chemokine Receptor Type 4*. PLoS Comput Biol, 2016. **12**(11): p. e1005169.
55. Rasmussen, S.G., et al., *Crystal structure of the beta2 adrenergic receptor-Gs protein complex*. Nature, 2011. **477**(7366): p. 549-55.
56. Souza, C.M., et al., *A stable yeast strain efficiently producing cholesterol instead of ergosterol is functional for tryptophan uptake, but not weak organic acid resistance*. Metab Eng, 2011. **13**(5): p. 555-69.
57. Hirz, M., et al., *A novel cholesterol-producing Pichia pastoris strain is an ideal host for functional expression of human Na,K-ATPase alpha3beta1 isoform*. Appl Microbiol Biotechnol, 2013. **97**(21): p. 9465-78.
58. Morioka, S., et al., *Effect of sterol composition on the activity of the yeast G-protein-coupled receptor Ste2*. Appl Microbiol Biotechnol, 2013. **97**(9): p. 4013-20.
59. Routledge, S.J., et al., *The synthesis of recombinant membrane proteins in yeast for structural studies*. Methods, 2016. **95**: p. 26-37.
60. Black, J.W., et al., *An operational model of pharmacological agonism: the effect of E/[A] curve shape on agonist dissociation constant estimation*. Br J Pharmacol, 1985. **84**(2): p. 561-71.
61. Kenakin, T., et al., *A simple method for quantifying functional selectivity and agonist bias*. ACS Chem Neurosci, 2012. **3**(3): p. 193-203.
62. Ballesteros, J., Weinstein, H., *Integrated methods for the construction of three-dimensional models and computational probing of structure-function relations in G protein-coupled receptors*. Methods in Neurosciences, 1995. **25**: p. 366-428.
63. Warne, T., et al., *The structural basis for agonist and partial agonist action on a beta(1)-adrenergic receptor*. Nature, 2011. **469**(7329): p. 241-4.
64. Warne, T., et al., *Crystal structures of a stabilized beta1-adrenoceptor bound to the biased agonists bucindolol and carvedilol*. Structure, 2012. **20**(5): p. 841-9.
65. Gregorio, G.G., et al., *Single-molecule analysis of ligand efficacy in beta2AR-G-protein activation*. Nature, 2017. **547**(7661): p. 68-73.
66. EMBL, *Transformation heat-shock competent E. coli cells*.
67. (ATCC), A.T.C.C., *p426 GPD (ATCC® 87361™)*.
68. Amberg, D.C., Burke, D.J., Strathern, J.N., 2. "Quick and dirty" plasmid transformation of yeast colonies, in *Methods in Yeast Genetics*. 2005. p. 113 - 115.
69. Joung, J.K., E.I. Ramm, and C.O. Pabo, *A bacterial two-hybrid selection system for studying protein-DNA and protein-protein interactions*. Proc Natl Acad Sci U S A, 2000. **97**(13): p. 7382-7.
70. Bylund DB, B.R., Eikenburg DC, Hieble JP, Hills R, Minneman KP, Parra S. , *Ligand ID: 102 - Yohimbine*. 2013, IUPHAR/BPS Guide to PHARMACOLOGY.
71. Bylund DB, B.R., Eikenburg DC, Hieble JP, Hills R, Minneman KP, Parra S. , *Ligand Id: 520 - Brimonidine*. 2013, IUPHAR/BPS Guide to PHARMACOLOGY.

72. Roberts, C.J., et al., *Signaling and circuitry of multiple MAPK pathways revealed by a matrix of global gene expression profiles*. *Science*, 2000. **287**(5454): p. 873-80.
73. Mumberg, D., R. Muller, and M. Funk, *Yeast vectors for the controlled expression of heterologous proteins in different genetic backgrounds*. *Gene*, 1995. **156**(1): p. 119-22.
74. Christianson, T.W., et al., *Multifunctional yeast high-copy-number shuttle vectors*. *Gene*, 1992. **110**(1): p. 119-22.
75. Degorce, F., et al., *HTRF: A technology tailored for drug discovery - a review of theoretical aspects and recent applications*. *Curr Chem Genomics*, 2009. **3**: p. 22-32.
76. Rothstein, R.J., *One-step gene disruption in yeast*. *Methods Enzymol*, 1983. **101**: p. 202-11.
77. Thomas, B.J. and R. Rothstein, *Elevated recombination rates in transcriptionally active DNA*. *Cell*, 1989. **56**(4): p. 619-30.
78. Boeke, J.D., F. LaCroute, and G.R. Fink, *A positive selection for mutants lacking orotidine-5'-phosphate decarboxylase activity in yeast: 5-fluoro-orotic acid resistance*. *Mol Gen Genet*, 1984. **197**(2): p. 345-6.
79. Brachmann, C.B., et al., *Designer deletion strains derived from *Saccharomyces cerevisiae* S288C: a useful set of strains and plasmids for PCR-mediated gene disruption and other applications*. *Yeast*, 1998. **14**(2): p. 115-32.
80. database, G.C.-H.G. *DHCR7*. [cited 2017 27/06]; Available from: <http://www.genecards.org/cgi-bin/carddisp.pl?gene=DHCR7>.
81. Moebius, F.F., et al., *Molecular cloning and expression of the human delta7-sterol reductase*. *Proc Natl Acad Sci U S A*, 1998. **95**(4): p. 1899-902.
82. database, G.C.-H.G. *DHCR24*. [cited 2017 27/06]; Available from: <http://www.genecards.org/cgi-bin/carddisp.pl?gene=DHCR24&keywords=DHCR24>.
83. Waterham, H.R., et al., *Mutations in the 3beta-hydroxysterol Delta24-reductase gene cause desmosterolosis, an autosomal recessive disorder of cholesterol biosynthesis*. *Am J Hum Genet*, 2001. **69**(4): p. 685-94.
84. Smith, S.J., J.H. Crowley, and L.W. Parks, *Transcriptional regulation by ergosterol in the yeast *Saccharomyces cerevisiae**. *Mol Cell Biol*, 1996. **16**(10): p. 5427-32.
85. Kennedy, M.A., R. Barbuch, and M. Bard, *Transcriptional regulation of the squalene synthase gene (*ERG9*) in the yeast *Saccharomyces cerevisiae**. *Biochim Biophys Acta*, 1999. **1445**(1): p. 110-22.
86. Aritomi, K., et al., *Self-cloning yeast strains containing novel *FAS2* mutations produce a higher amount of ethyl caproate in Japanese sake*. *Bioscience Biotechnology and Biochemistry*, 2004. **68**(1): p. 206-214.
87. NEB. *Gibson Assembly*. [cited 2017 25/06]; Available from: <https://www.neb.com/applications/cloning-and-synthetic-biology/dna-assembly-and-cloning/gibson-assembly>.
88. Elliott, S., et al., *Secretion of glycosylated human erythropoietin from yeast directed by the alpha-factor leader region*. *Gene*, 1989. **79**(1): p. 167-80.
89. Stewart, G.D., P.M. Sexton, and A. Christopoulos, *Prediction of functionally selective allosteric interactions at an M3 muscarinic acetylcholine receptor mutant using *Saccharomyces cerevisiae**. *Mol Pharmacol*, 2010. **78**(2): p. 205-14.
90. Knight, A., et al., *Discovery of Novel Adenosine Receptor Agonists That Exhibit Subtype Selectivity*. *J Med Chem*, 2016. **59**(3): p. 947-64.
91. Liu, R., et al., *A yeast screening method to decipher the interaction between the adenosine A2B receptor and the C-terminus of different G protein alpha-subunits*. *Purinergic Signal*, 2014. **10**(3): p. 441-53.
92. Aw, R. and K.M. Polizzi, *Can too many copies spoil the broth?* *Microb Cell Fact*, 2013. **12**: p. 128.
93. Sikorski, R.S. and P. Hieter, *A system of shuttle vectors and yeast host strains designed for efficient manipulation of DNA in *Saccharomyces cerevisiae**. *Genetics*, 1989. **122**(1): p. 19-27.
94. Blocker, K.M., et al., *Recombinant G protein-coupled receptor expression in *Saccharomyces cerevisiae* for protein characterization*. *Methods Enzymol*, 2015. **556**: p. 165-83.

95. Claes, K., et al., *Modular Integrated Secretory System Engineering in Pichia pastoris To Enhance G-Protein Coupled Receptor Expression*. ACS Synth Biol, 2016. **5**(10): p. 1070-1075.
96. Warne, T., J. Chirnside, and G.F. Schertler, *Expression and purification of truncated, non-glycosylated turkey beta-adrenergic receptors for crystallization*. Biochim Biophys Acta, 2003. **1610**(1): p. 133-40.
97. Shukla, A.K., et al., *Heterologous expression and comparative characterization of the human neuromedin U subtype II receptor using the methylotrophic yeast Pichia pastoris and mammalian cells*. Int J Biochem Cell Biol, 2007. **39**(5): p. 931-42.
98. Weiss, H.M., et al., *Comparative biochemical and pharmacological characterization of the mouse 5HT5A 5-hydroxytryptamine receptor and the human beta2-adrenergic receptor produced in the methylotrophic yeast Pichia pastoris*. Biochem J, 1998. **330 (Pt 3)**: p. 1137-47.
99. Montesana, P.E. and J.B. Konopka, *Mutational analysis of the role of N-glycosylation in alpha-factor receptor function*. Biochemistry, 2001. **40**(32): p. 9685-94.
100. Replogle, K., L. Hovland, and D.H. Rivier, *Designer deletion and prototrophic strains derived from Saccharomyces cerevisiae strain W303-1a*. Yeast, 1999. **15**(11): p. 1141-9.

Appendix A – Ga protein sequence alignment

8/10/2017

www.ebi.ac.uk/Tools/services/rest/clustalo/result/clustalo-l20170810-122502-0948-66000732-oy/aln-clustal

CLUSTAL O(1.2.4) multiple sequence alignment

```
Gs|P63092|GNAS2_HUMAN      -----MGCLGNSKT----- EDQRNEEKAQREANKKIEKQLQKDKQV
sp|P08539|GPA1_YEAST      -----MGCTVSTQTIGDE----- SDPFLQNKRANDVIEQSLQLEKQR
G12|Q03113|GNA12_HUMAN    MS-----GVVRTLSRCLLPAAEAGGARERRRAGSGARDAEREARRSRDIDALLARERRA
G13|Q14344|GNA13_HUMAN    MADFLPSRSVLSVCFPGCLL----- TSGEAEQQRKSEIDKCLSRKTY
Gz|P19086|GNAZ_HUMAN      -----MGCRQ-----SSEEKAAARRSRRIDRHLRSESQR
Go|P09471|GNAO_HUMAN      -----MGCTL-----SAEERAALERSKAIEKNLKEDGIS
G12|P63096|GNAI1_HUMAN    -----MGCTL-----SAEDKAAVERSKMIDRNLRDEGEK
G13|P08754|GNAI3_HUMAN    -----MGCTL-----SAEDKAAVERSKMIDRNLRDEGEK
G16|P30679|GNA15_HUMAN    -----MARSLTWRCPPWCL----- TEDEKAAARVDQIEINRILLEKQKKQ
Gq|P50148|GNAQ_HUMAN      -----MTLESI---MACCL-----S EEAKEARRINDEIERQLRRDKRD
G14|O95837|GNA14_HUMAN    -----MA---GCCCL-----SAEEKESQRISAEIERQLRRDKKD
      . . * : * :

Gs|P63092|GNAS2_HUMAN      YRATHRLLLLGAGESGKSTIVKQMRILHVNGFN GEGGEDPQAARSNSDGEKATKVQDIK
sp|P08539|GPA1_YEAST      DKNEIKLLLLGAGESGKSTVLKQLKLLHQGGFSHQERLQYAQVIWADA-----
G12|Q03113|GNA12_HUMAN    VRLVKILLGAGESGKSTFLKQMRIIHGREFDQKALLEFRDTIFDNI-----
G13|Q14344|GNA13_HUMAN    VKRLVKILLGAGESGKSTFLKQMRIIHGQDFDQARAEFRPTIYSNV-----
Gz|P19086|GNAZ_HUMAN      QRREIKLLLLGTSNSGKSTIVKQMKIIHSGGFNL EACKEYKPLIINYA-----
Go|P09471|GNAO_HUMAN      AAKDVKLLLLGAGESGKSTIVKQMKIIHEDGFGS GEDVKYKPVVYSNT-----
G12|P63096|GNAI1_HUMAN    AAREVKLLLLGAGESGKSTIVKQMKIIHEAGYSE EECKQYKAVVYSNT-----
G13|P08754|GNAI3_HUMAN    AAKEVKLLLLGAGESGKSTIVKQMKIIHEDGYSE DECKQYKVVVYSNT-----
G16|P30679|GNA15_HUMAN    DRGELKLLLLGPGESGKSTFIKQMRIIHGAGYSE EERKGFRLVYQNI-----
Gq|P50148|GNAQ_HUMAN      ARRELKLLLLGTGESGKSTFIKQMRIIHGSGYSD EDKRGFTKLVYQNI-----
G14|O95837|GNA14_HUMAN    ARRELKLLLLGTGESGKSTFIKQMRIIHGSGYSD EDKRGFTKLVYQNI-----
      : : * * : * * : * :

Gs|P63092|GNAS2_HUMAN      NNLKEAIEIIVAAMSNLVPVELANPENQF----- RV
sp|P08539|GPA1_YEAST      ---IQSMKILIIQARKLGIQLDCDDPINNKDLFACKR ILLKAKALDYINASVAGGSDFLN
G12|Q03113|GNA12_HUMAN    ---LKGSRVLVDARDKLGIPWQYSENEKHGMFLMA -----
G13|Q14344|GNA13_HUMAN    ---IKGMRVLVDAREKLIHIPWGDNSNQGHDKMMS -----
Gz|P19086|GNAZ_HUMAN      ---IDSLTRIIRALAALRIDFHNPRDAYDAVQLFA -----
Go|P09471|GNAO_HUMAN      ---IQSLAAIVRAMDTLGI EYNGDKERKADAKMVCD -----
G12|P63096|GNAI1_HUMAN    ---IQSIIAIIIRAMGR LKIDFGDSARADDARQLFV -----
G13|P08754|GNAI3_HUMAN    ---IQSIIAIIIRAMGR LKIDFGAARADDARQLFV -----
G16|P30679|GNA15_HUMAN    ---FVSMRAMIEAMERLQ IPF SRPESKHHASLVMS -----
Gq|P50148|GNAQ_HUMAN      ---FTAMQAMIRAMDTL KIPYKYEHNKAHAQLVRE -----
G14|O95837|GNA14_HUMAN    ---FTAMQAMIRAMDTL RIQYVCEQNKENAQIIRE -----
      . : : *

Gs|P63092|GNAS2_HUMAN      DYIL-----
sp|P08539|GPA1_YEAST      DYVLKYSERYETRRRVQSTGRAKAAFD EEDGNISNVKSDTDRDAETVTQNEADARNSSRI
G12|Q03113|GNA12_HUMAN    -----F--ENKA-----
G13|Q14344|GNA13_HUMAN    -----F--DTRA-----
Gz|P19086|GNAZ_HUMAN      -----L--TGPA-----
Go|P09471|GNAO_HUMAN      -----V--VSRM-----
G12|P63096|GNAI1_HUMAN    -----L--AG-A-----
G13|P08754|GNAI3_HUMAN    -----L--AG-S-----
G16|P30679|GNA15_HUMAN    -----Q--D--P-----
Gq|P50148|GNAQ_HUMAN      -----V--D--V-----
G14|O95837|GNA14_HUMAN    -----V--E--V-----

Gs|P63092|GNAS2_HUMAN      -----SVMNVPDFDFPPEFYEHAKALWE-DEGVRACYERS
sp|P08539|GPA1_YEAST      NLQDICKDLNQE GDDQMFVRKTSREIQGQNRRL IHEDIAKAIKQLWNNDKGKQCFARS
G12|Q03113|GNA12_HUMAN    G-----L-----P-----VEPATFQLYVPALSALWR-DSGIREAFSRR
G13|Q14344|GNA13_HUMAN    P-----M-----AAQG-MVETRVFLQYLP AIRALWA-DSGIQNAYDRR
Gz|P19086|GNAZ_HUMAN      -----ESKG-----EITPELLGVMRRLWA-DPGAQACFSRS
Go|P09471|GNAO_HUMAN      -----EDTE-----PFSAE LLSAMMRLWG-DSGIQECFNRS
G12|P63096|GNAI1_HUMAN    -----AEEG-----FMTAELAGVIKRLWK-DSGVQACFNRS
G13|P08754|GNAI3_HUMAN    -----AEEG-----VMTPELAGVIKRLWR-DGGVQACFSRS
G16|P30679|GNA15_HUMAN    -----YKVT-----TFEKRYAAMQWLWR-DAGIRAYYERR
Gq|P50148|GNAQ_HUMAN      -----EKVS-----AFENPYVDAIKSLWN-DPGIQECYDRR
G14|O95837|GNA14_HUMAN    -----DKVS-----MLSREQVEAIKQLWQ-DPGIQECYDRR
      * * * : * *

Gs|P63092|GNAS2_HUMAN      NEYQLIDCAQYFLDKIDVIKQADYVPSDQDLLRCRVL TSGIFETKFQVDKVNFMFDVGG
```

<http://www.ebi.ac.uk/Tools/services/rest/clustalo/result/clustalo-l20170810-122502-0948-66000732-oy/aln-clustal>

sp|P08539|GPA1_YEAST
G12|Q03113|GNA12_HUMAN
G13|Q14344|GNA13_HUMAN
Gz|P19086|GNAZ_HUMAN
Go|P09471|GNAO_HUMAN
G12|P63096|GNAI1_HUMAN
G13|P08754|GNAI3_HUMAN
G16|P30679|GNA15_HUMAN
Gq|P50148|GNAQ_HUMAN
G14|O95837|GNA14_HUMAN

```
NEFQLEGSAAYYFDNIEKFASPNYVCTDEDILKGRIKTTGITETEFGNIGSSKFKVLVDAGG
SEFQLGESVKYFLDNLDRIQGLNYFPSKQDILLARKATKGIVEHDFVIKKIPFKMVDVGG
REFQLGESVKYFLDNLDKLGEPDYIPSSQDILLARRPTKGIHEYDFEIKNVPFKMVDVGG
SEYHLEDNAAYYLNDLERIAAADYIPTVEDILRSRDMTTGIVENKFTFKELTFKMDVDVGG
REYQLNDSAKYYLDSLDRIGAADYQPTQDILRTRVKTGTGIVETHFTFKNLHFRLLFDVGG
REYQLNDSAAYYLNLDRIAQPNYIPTQQDVLTRVKTGTGIVETHFTFKDLHFKMFDVGG
REYQLNDSASYLLNLDRIISQSNYIPTQQDVLTRVKTGTGIVETHFTFKDLYFKMFDVGG
REFHLLDSAVYYLSHLERITEEGYVPTAQDVLRSRMPPTTGINEYCFVSVQKTLRIVDVGG
REYQLSDSTKYLLNLDLRVADPAYLPTQQDVLRRVPTTGIEYFPDLQSVIFRMVDVGG
REYQLSDSAKYLLTDIDRIATPSFVPTQQDVLRRVPTTGIEYFPDLNIIFRMVDVGG
*::* . *:: : : . : : *:* * *.* * . . : : : . *.*
```

Gs|P63092|GNAS2_HUMAN
sp|P08539|GPA1_YEAST
G12|Q03113|GNA12_HUMAN
G13|Q14344|GNA13_HUMAN
Gz|P19086|GNAZ_HUMAN
Go|P09471|GNAO_HUMAN
G12|P63096|GNAI1_HUMAN
G13|P08754|GNAI3_HUMAN
G16|P30679|GNA15_HUMAN
Gq|P50148|GNAQ_HUMAN
G14|O95837|GNA14_HUMAN

```
QRDERRKWIQCFNDVTAIIFVVASSSYMMVIREDNQTNRLQEALNLFKSIWNNRWRRTIS
QRSERKKWIHCFEGITAVLFVLAMSEYDQMLFEDERVNRMHESIMLFDTLNLSKWFKDTTP
QRSQRQKWFQCFDGTISILFMVSSSEYDQVLMEDRRTNRLVESMNIIFETIVNNKLFNVNS
QRSERKRWFECFDSVTSILFLVSSSEFDQVLMEDRLNRLTESLNIFETIVNNRVFSNVS
QRSERKKWIHCFEGVTAIIFCVLSEYDQLKLYEDNQTSRMAESLRLFDSICNNWFINTS
QRSERKKWIHCFEDVTAIIFCVLSEYDQLKLYEDNQTSRMAESLRLFDSICNNWFIDTS
QRSERKKWIHCFEGVTAIIFCVLSEYDQLKLYEDNQTSRMAESLRLFDSICNNWFTDTS
QRSERKKWIHCFEGVTAIIFCVLSEYDQLKLYEDNQTSRMAESLRLFDSICNNWFTETS
QRSERKKWIHCFENVIALIYLASLSEYDQCLEENNQENRMKESLALFGTILELPWFKSTS
QRSERKKWIHCFENVTSIMFLVALSEYDQVLESDNENRMEESKALFRTIITYPWFQNSS
QRSERKKWIHCFESVTSIIFLVALSEYDQVLAECDNENRMEESKALFKTIITYPWFLNSS
*.:*:*:*.*.*.: : : : * : : : * .*: * : * : : :
```

Gs|P63092|GNAS2_HUMAN
sp|P08539|GPA1_YEAST
G12|Q03113|GNA12_HUMAN
G13|Q14344|GNA13_HUMAN
Gz|P19086|GNAZ_HUMAN
Go|P09471|GNAO_HUMAN
G12|P63096|GNAI1_HUMAN
G13|P08754|GNAI3_HUMAN
G16|P30679|GNA15_HUMAN
Gq|P50148|GNAQ_HUMAN
G14|O95837|GNA14_HUMAN

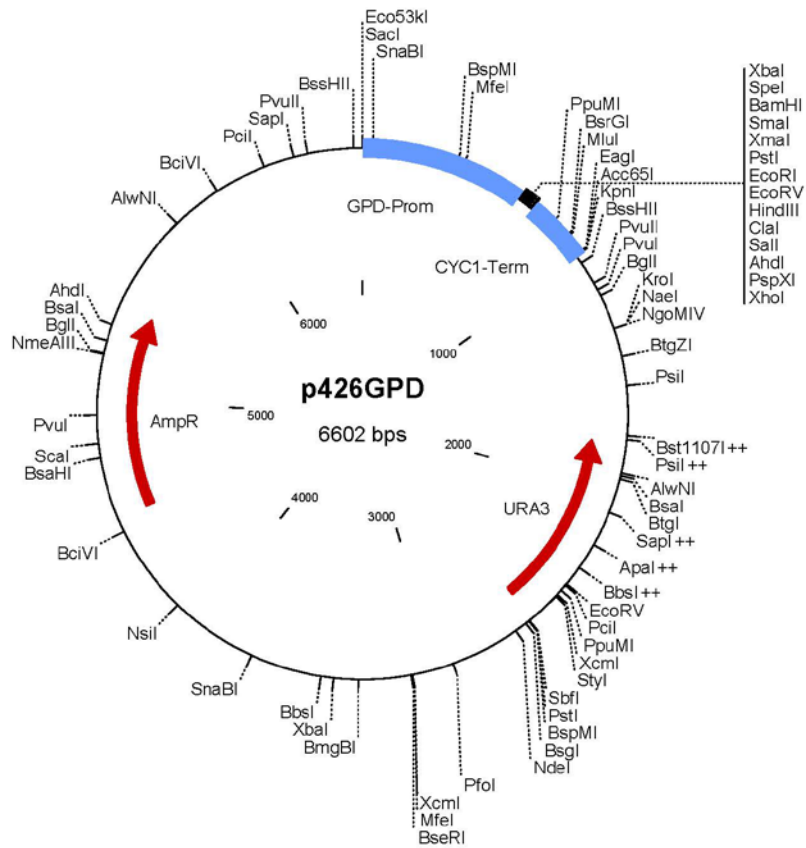
```
VILFLNKQDLLAEKVLGKSKIEDYFPEFARYTTPEDATPEPGEPRVTRAKYFIRDEFL
FILFLNKIDLFEEKVKS--MPIRKYFPDYQGRVGD AE-----AGLKYEKIFL
IILFLNKMDLLVEKVKT--VSIKKHFDPFRGDPHRL E-----DVQRYLVQCFD
IILFLNKTDLLEEKVQI--VSIKDYFLEFEGDPHCL R-----DVQKFLVECFR
LILFLNKKDLLAEKIRR--IPLTICFPEYKQNTYEE-----AA-VYIQRQFE
IILFLNKKDLFGEKIKK--SPLTICFPEYTGPNYED-----AA-AYIQAQFE
IILFLNKKDLFEEKIKK--SPLTICYPEYAGSNTYEE-----AA-AYIQCQFE
IILFLNKKDLFEEKIKR--SPLTICYPEYTGPNYEE-----AA-AYIQCQFE
VILFLNKTDILEEKIPT--SHLATYFSPFQGPQDAE-----AAKRFILDMYT
VILFLNKKDLLEEKIMY--SHLVDYFPEYDGPQRDAQ-----AAREFILKMFV
VILFLNKKDLLEEKIMY--SHLISYFPEYTGPKQDVR-----AARDFILKLYQ
.*.*.*.*.*.: *:* : : : : * : : : * .*: * : * : : :
```

Gs|P63092|GNAS2_HUMAN
sp|P08539|GPA1_YEAST
G12|Q03113|GNA12_HUMAN
G13|Q14344|GNA13_HUMAN
Gz|P19086|GNAZ_HUMAN
Go|P09471|GNAO_HUMAN
G12|P63096|GNAI1_HUMAN
G13|P08754|GNAI3_HUMAN
G16|P30679|GNA15_HUMAN
Gq|P50148|GNAQ_HUMAN
G14|O95837|GNA14_HUMAN

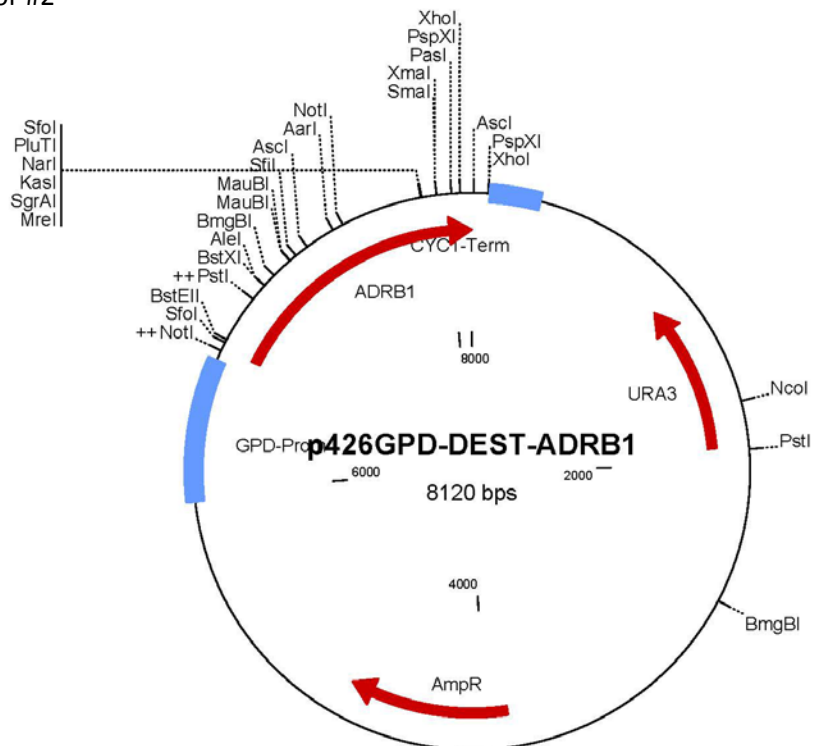
```
RISTA-----SGDGRHYCPHFTCAVDTENIRRVFNDCRDIQRMHLRQYELL
SLNK-----TNKPIYVKRTCATDTQTMK FVL SAVTDLIIQNLKKIGII
RKRR-----N-RSKPLFHHFTTAIDTENVRVVFHAVKDTILQENLKDIMLQ
NKRR-----DQQQKPLYHHFTTAINTENIRLVFRDVKDTILHDNLKQLMLQ
DLNR-----NKETKEIYSHFTCATDTSNIQVFVDAVTDVVIQNNLKYIGLC
SKNR-----SPNKEIYCHMTCATDTNNIQVVFDAVTDIIIANNLRGCGLY
DLNK-----RKDTKEIYTHFTCATDTKKNVQVFVDAVTDVVIKNNLKDCGLF
DLNR-----RKDTKEIYTHFTCATDTKKNVQVFVDAVTDVVIKNNLKEGLY
RMYTGCVDGPEGSKKGARSRRLLFSHYTCATDTQNIKRVFKDVRDVLARYLDEINLL
DLNP-----DSDKIYSHFTCATDTENIRVVFVAAVKDTILQLNLKEYNLV
DQNP-----DKEKVIYSHFTCATDTDNIRVVFVAAVKDTILQLNLREFNLV
: : : * * : * . : : * : * : * :
```

Appendix B – Vector and plasmid maps

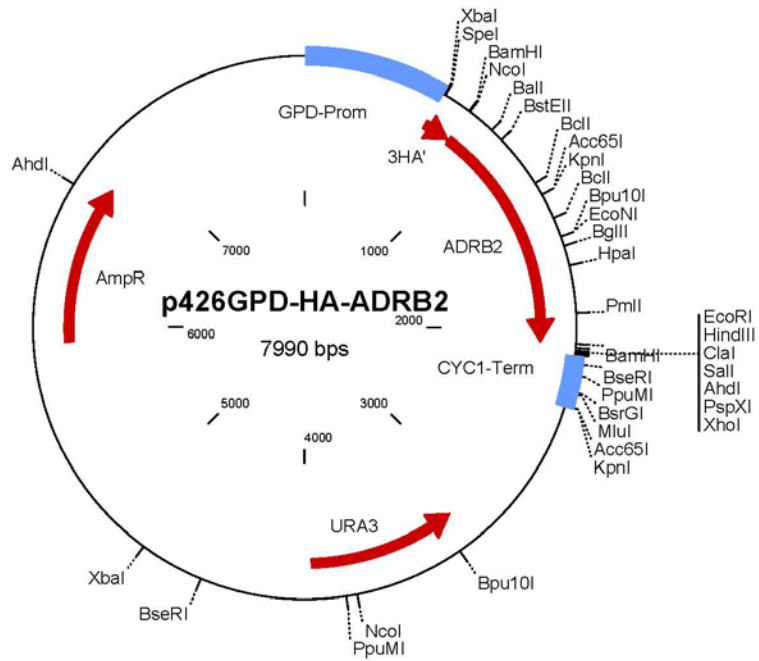
Vector #1



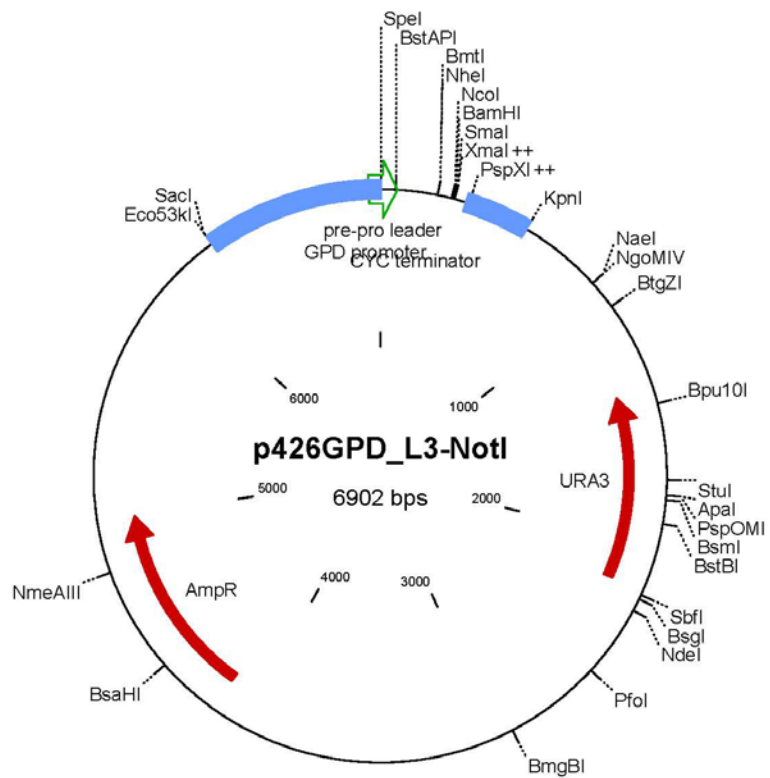
Vector #2



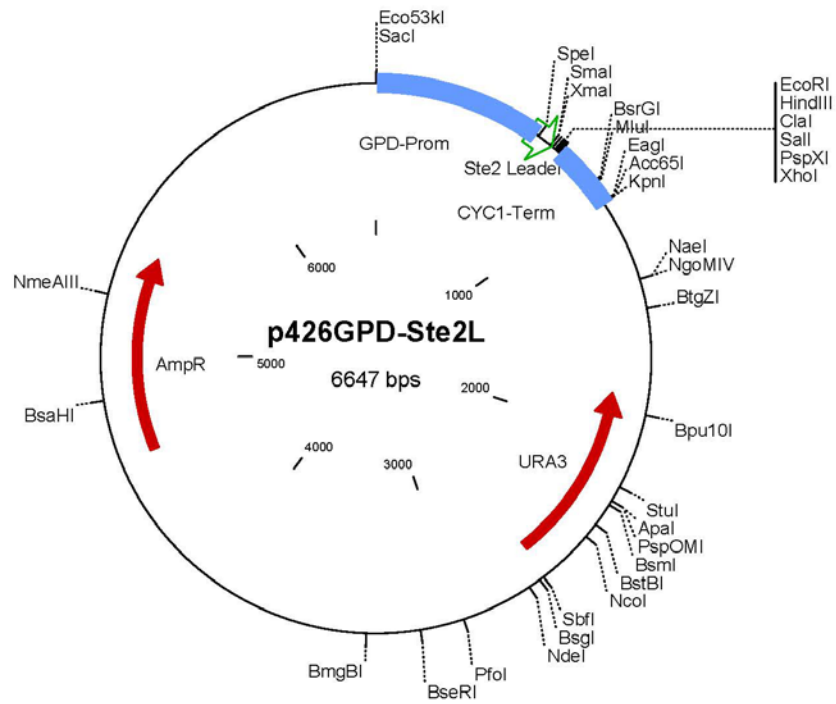
Vector #3



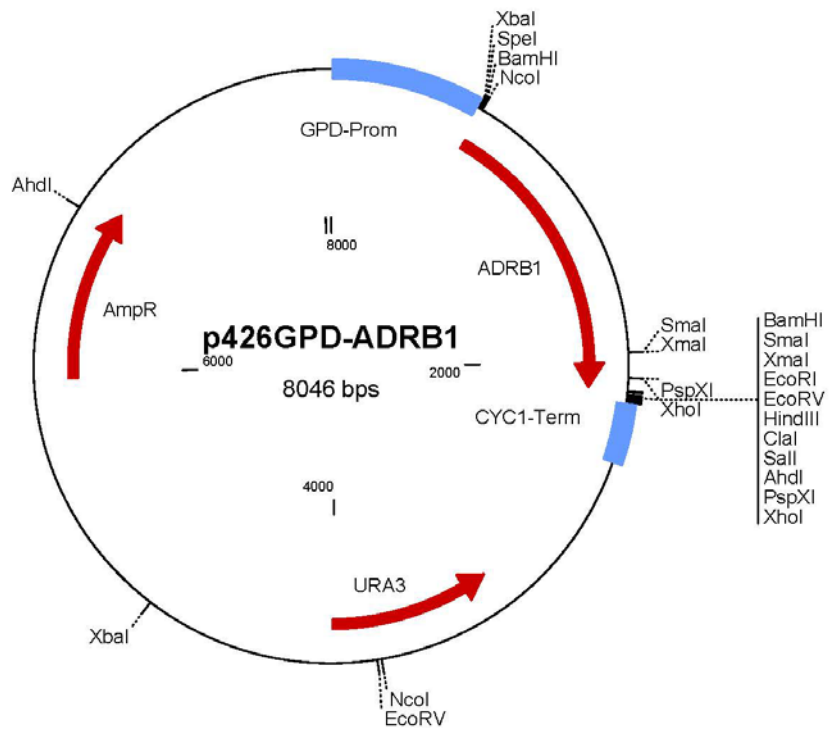
Vector #4



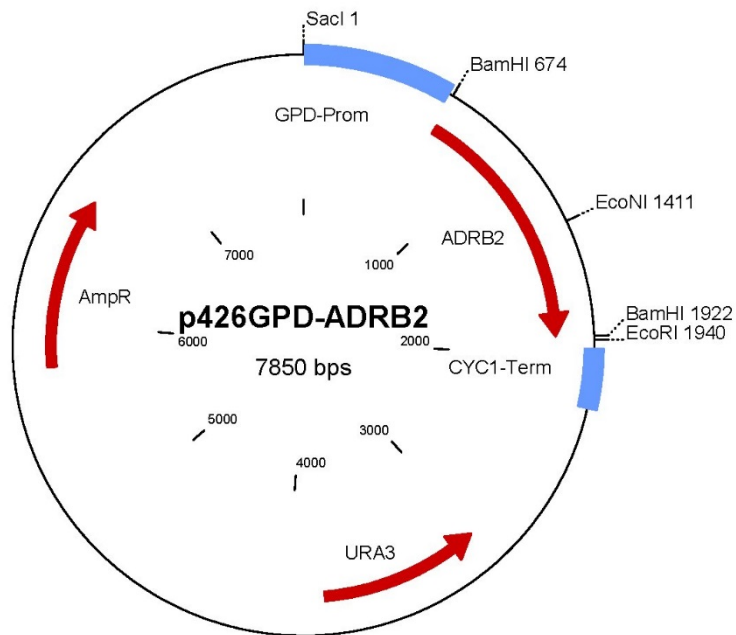
Vector #5



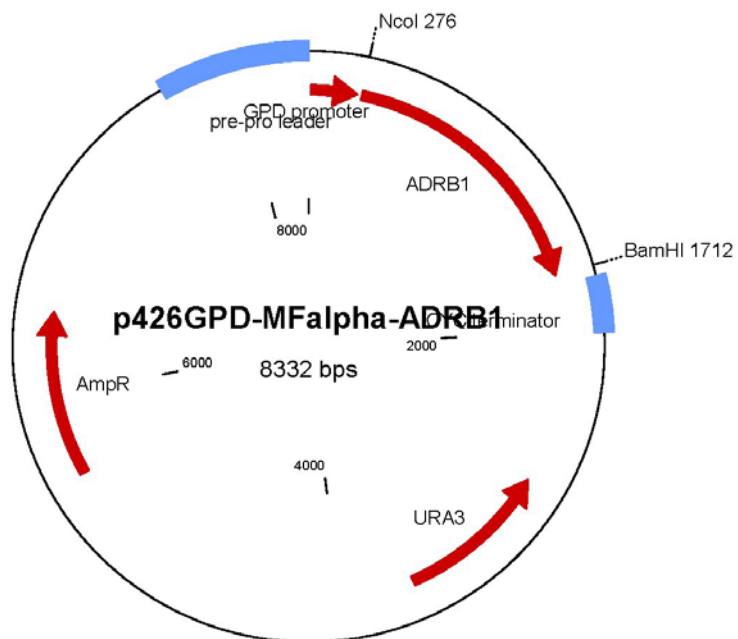
Vector #6



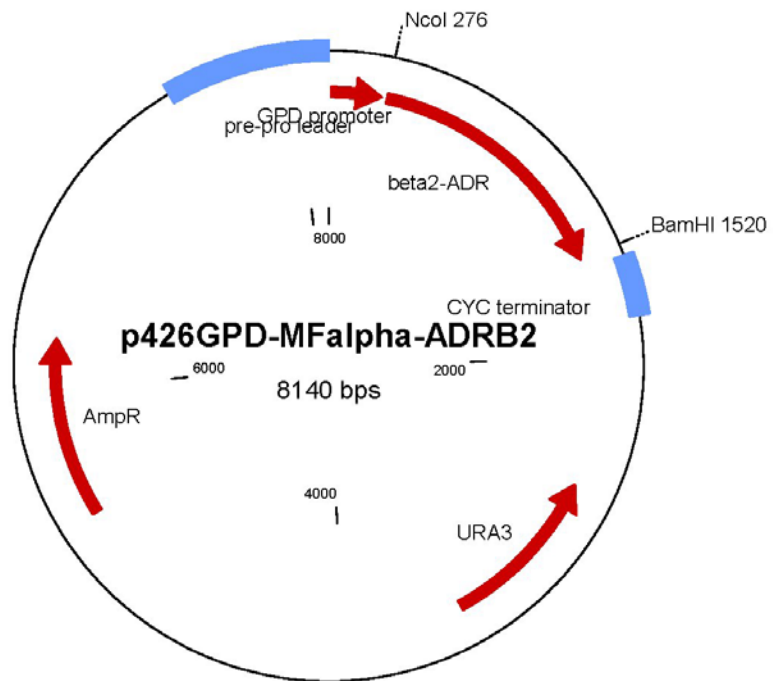
Vector #7



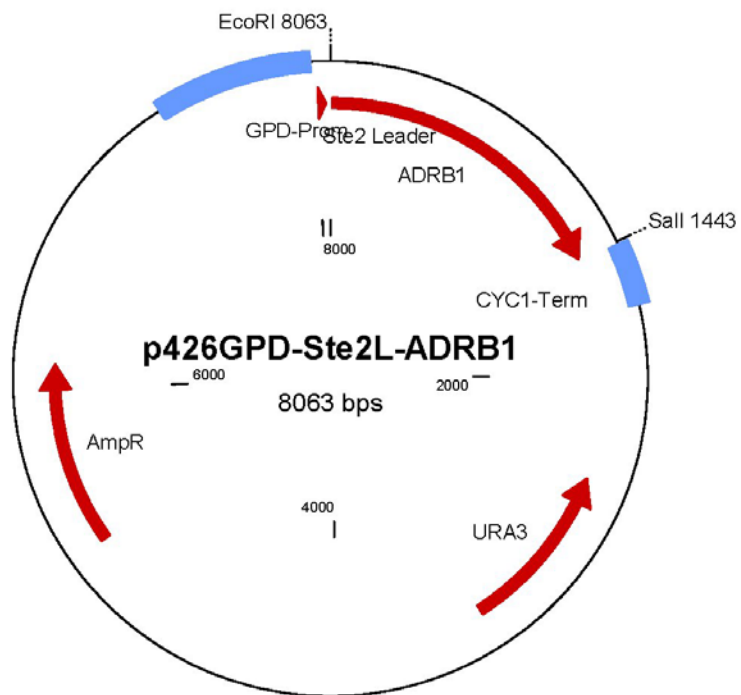
Vector #8



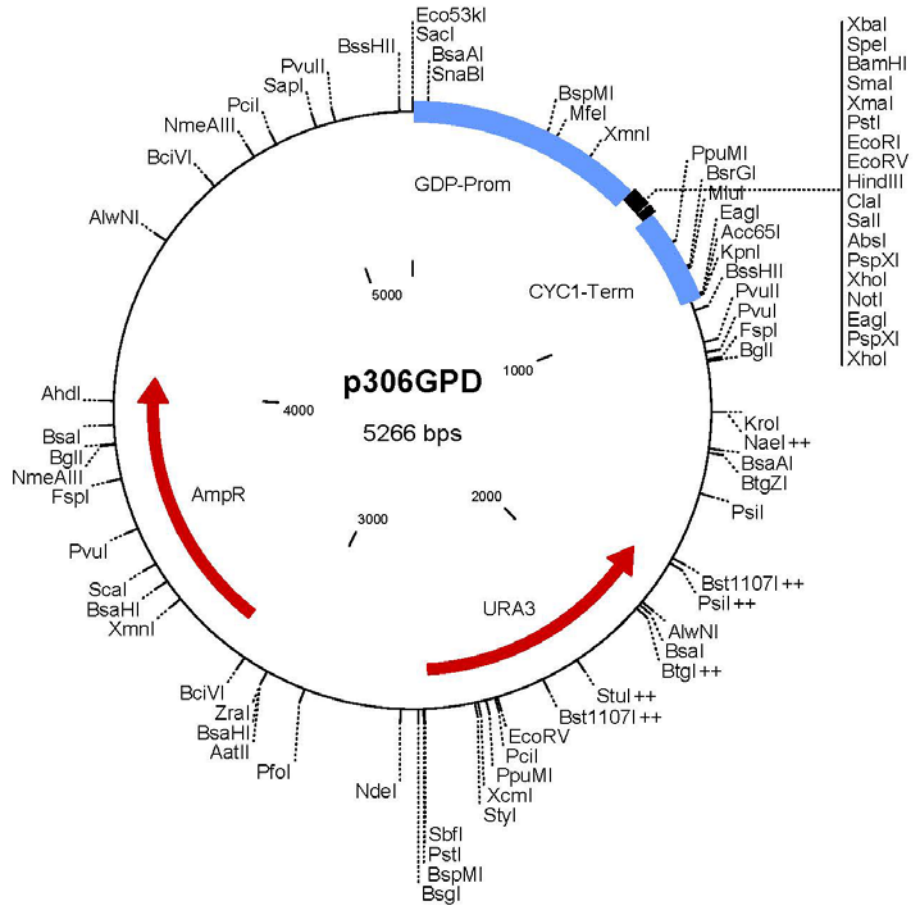
Vector #9



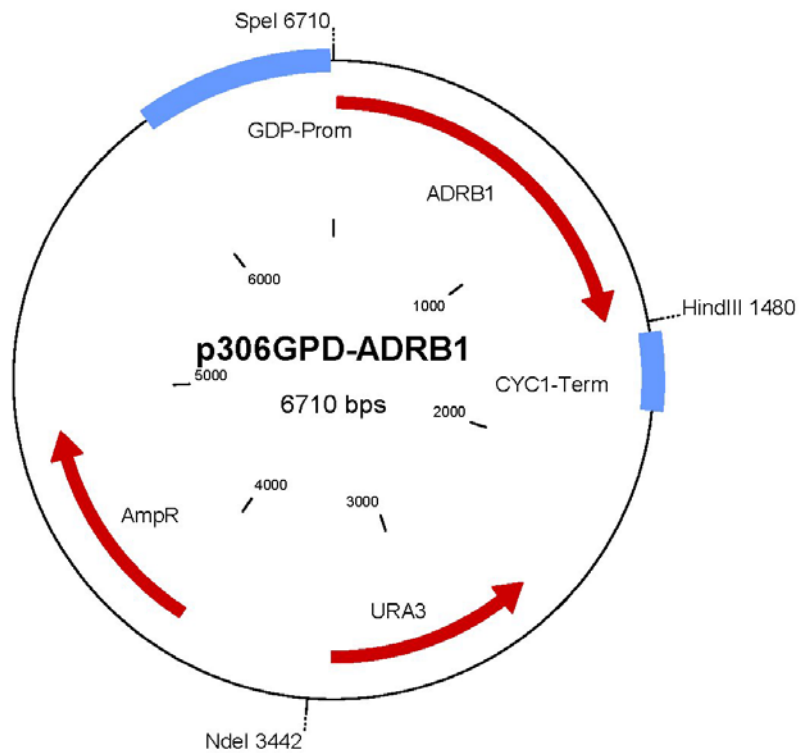
Vector #10



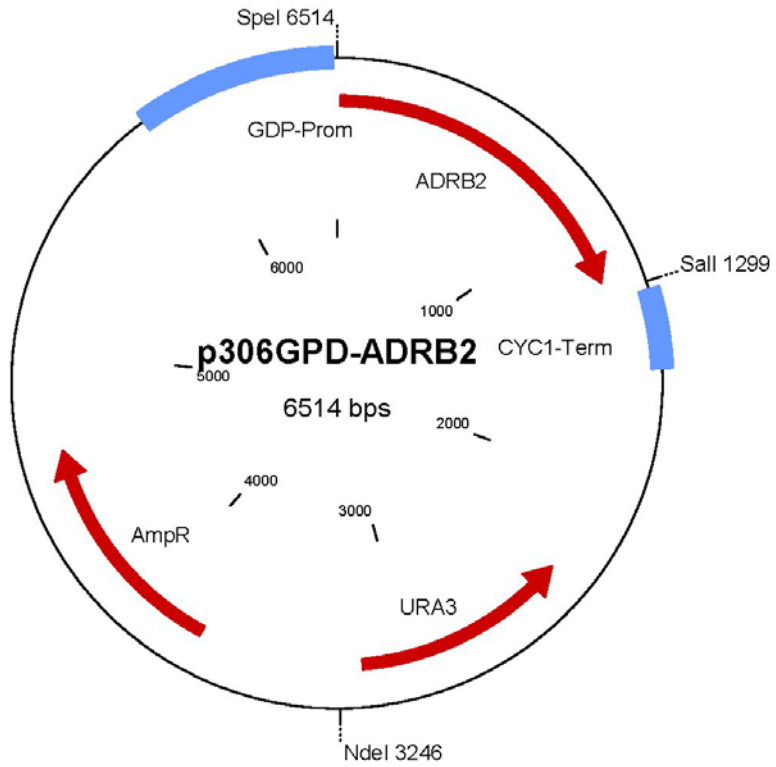
Vector #12



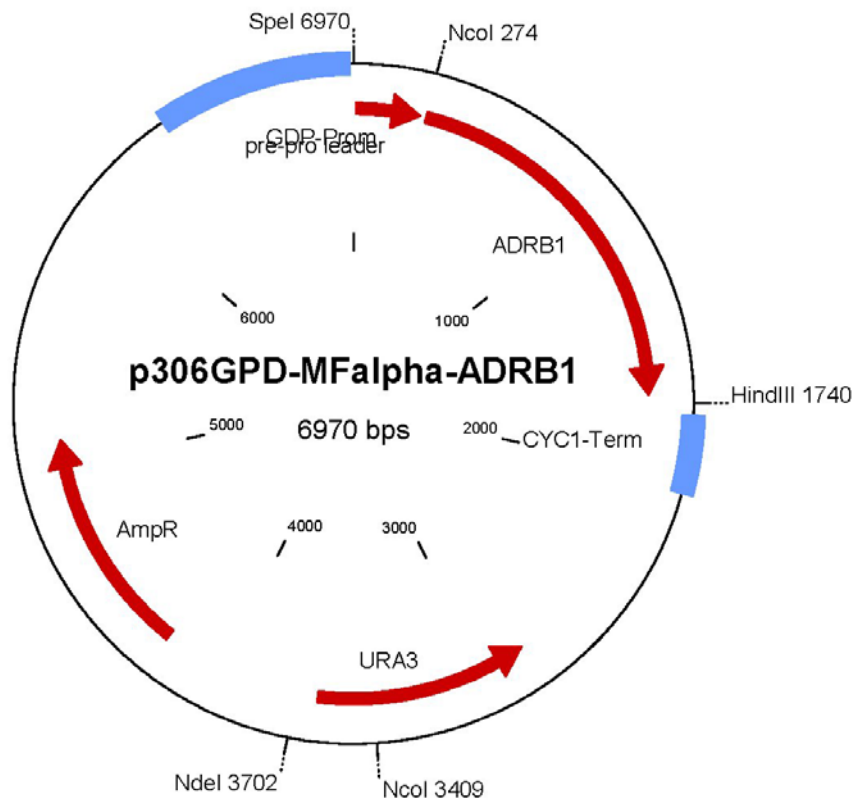
Vector #13



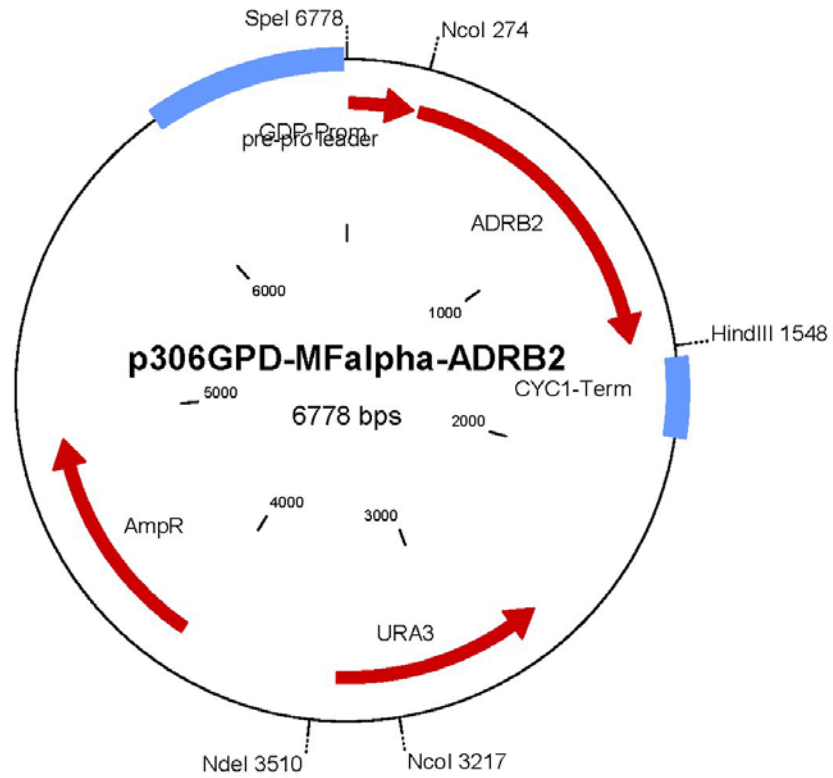
Vector #14



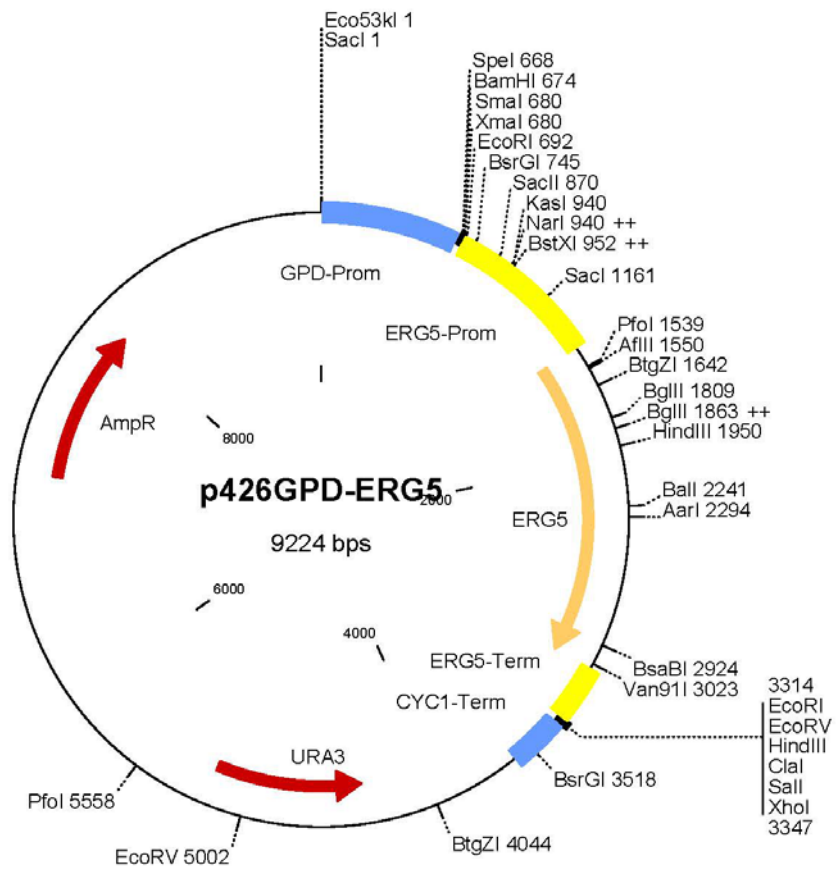
Vector #15



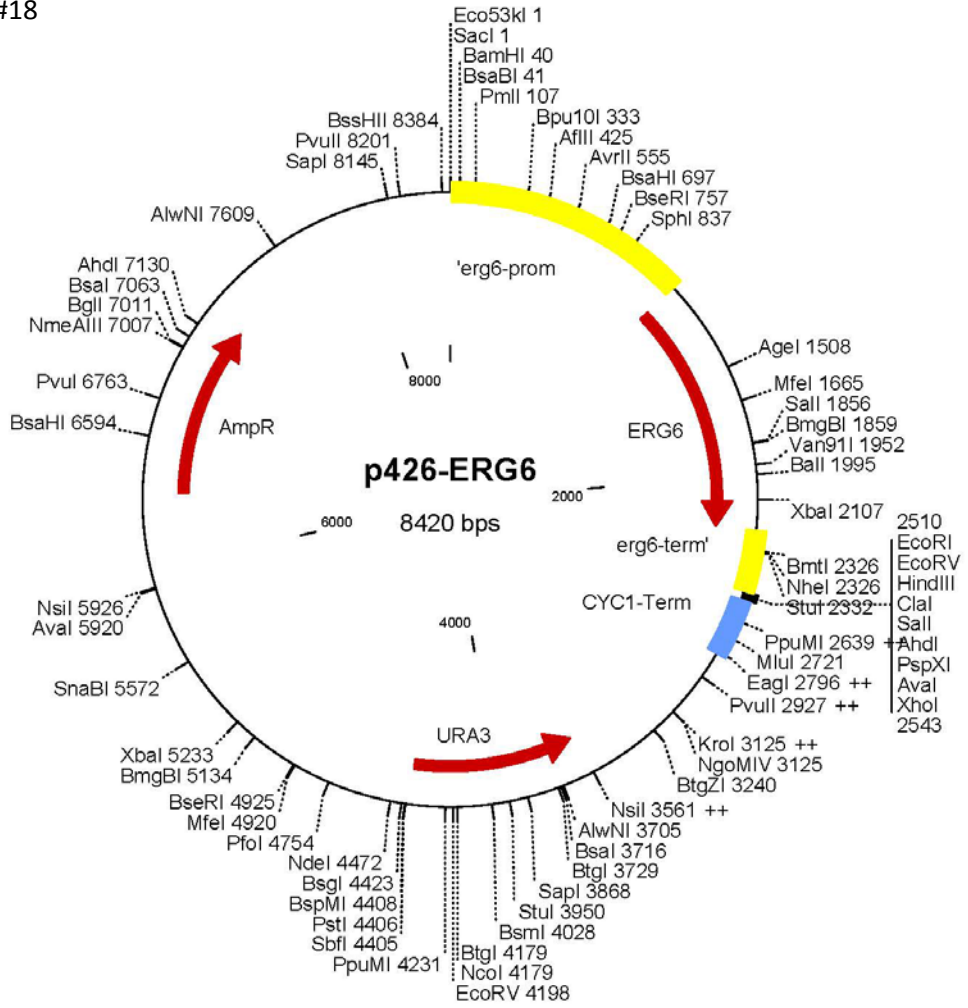
Vector #16



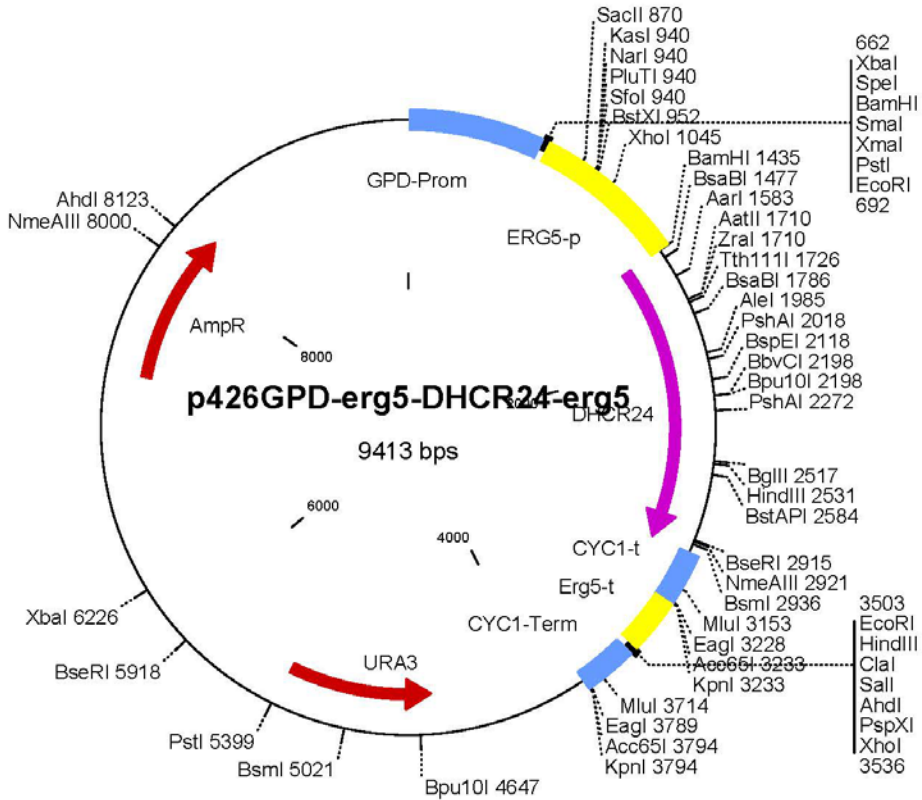
Vector #17



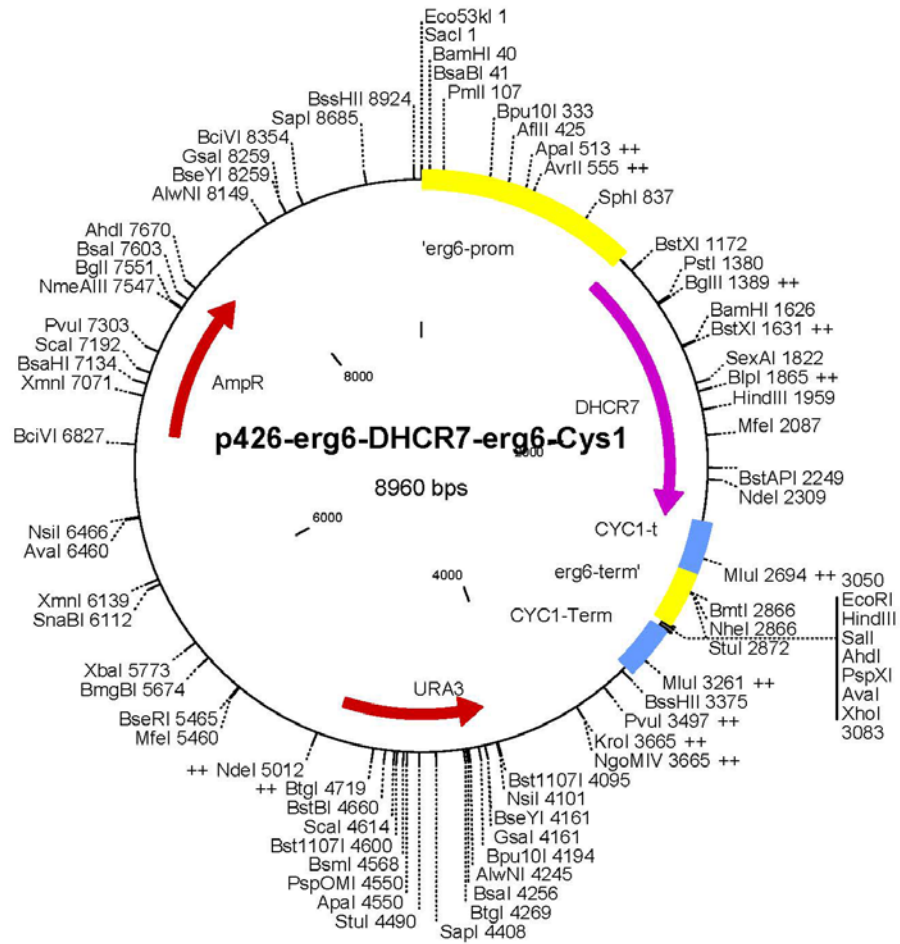
Vector #18



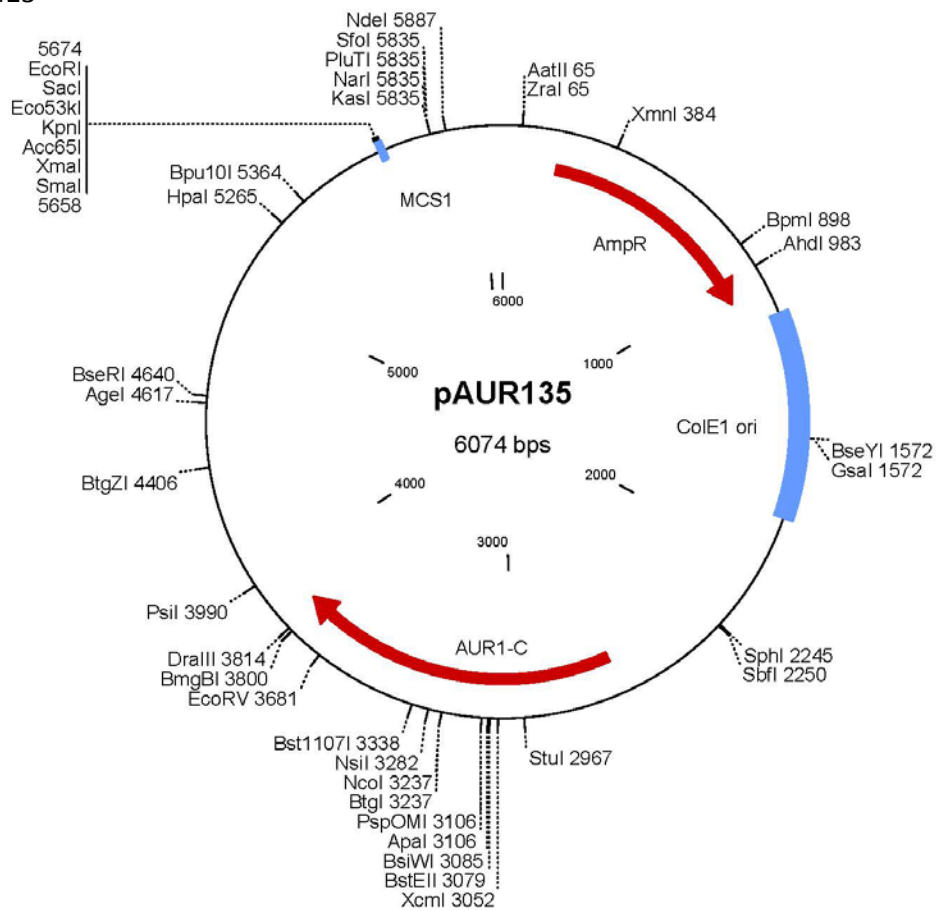
Vector #21



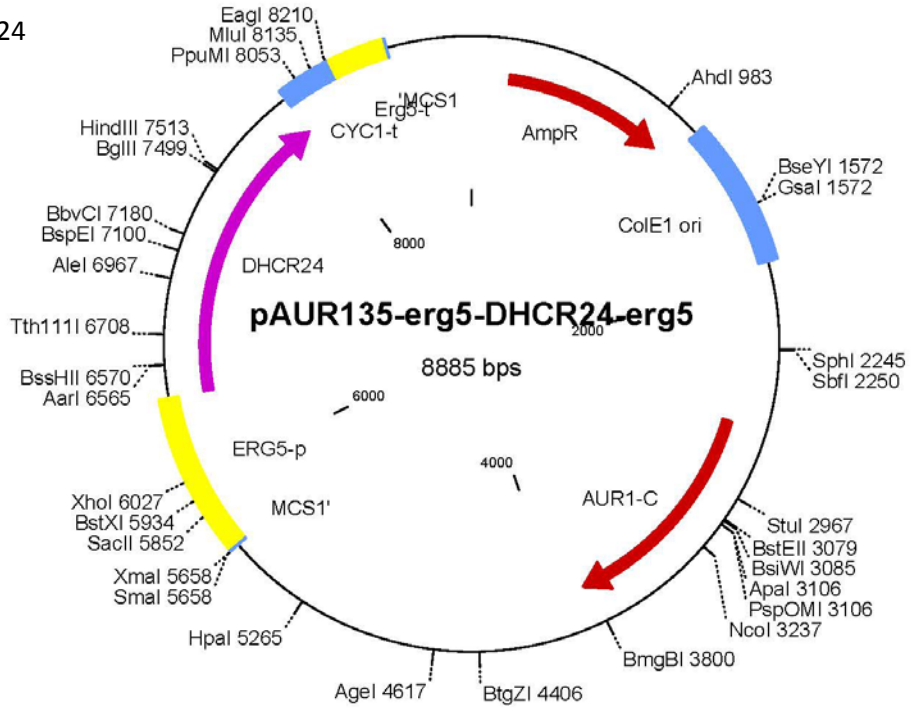
Vector #22



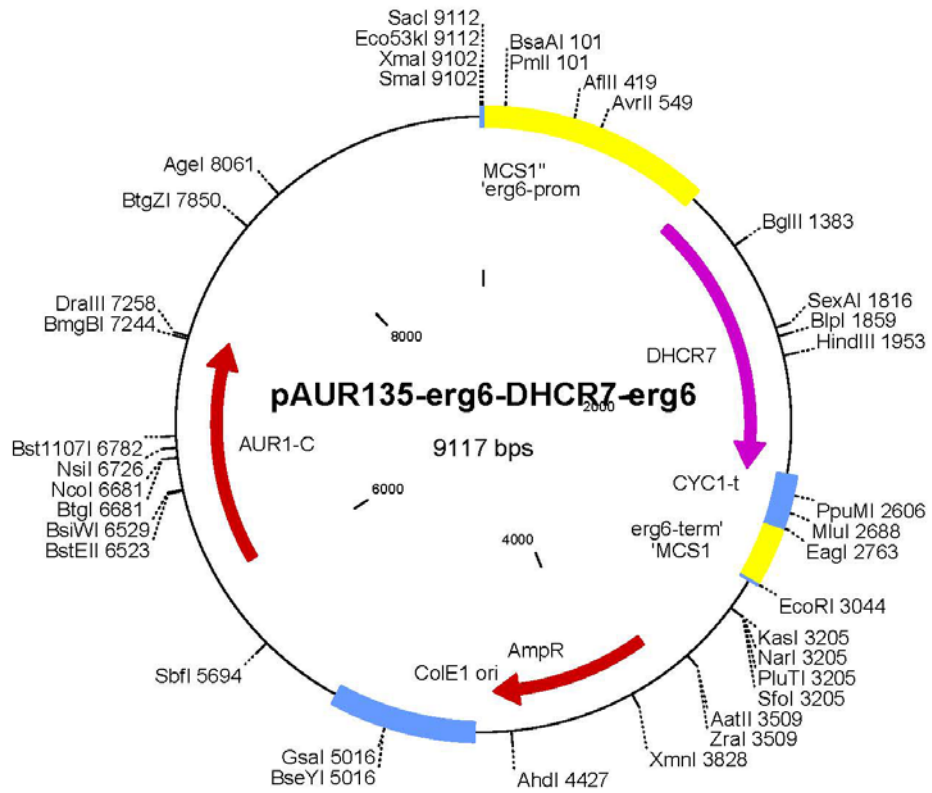
Vector #23



Vector #24

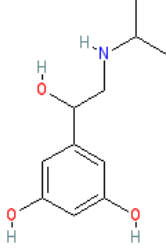
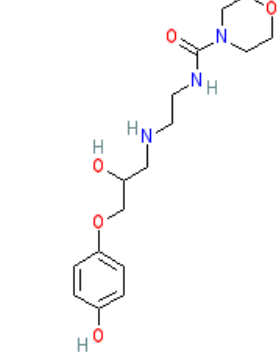
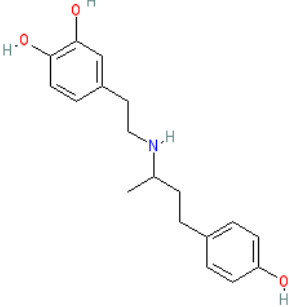
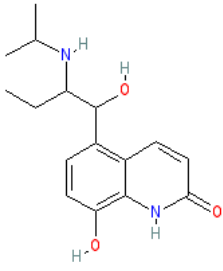


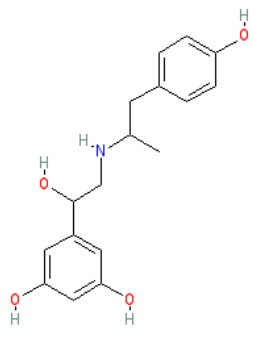
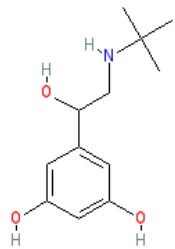
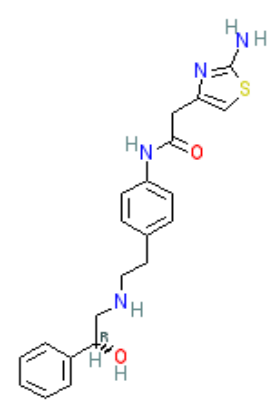
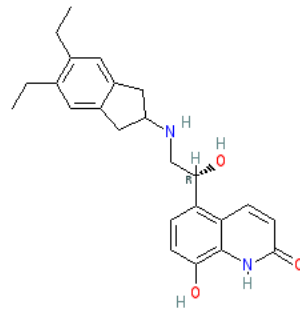
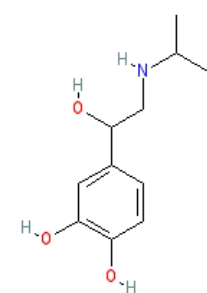
Vector #25

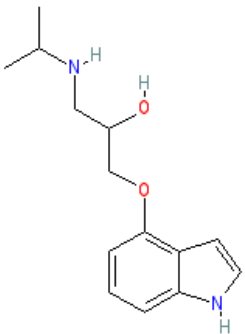


Appendix C – compound structures

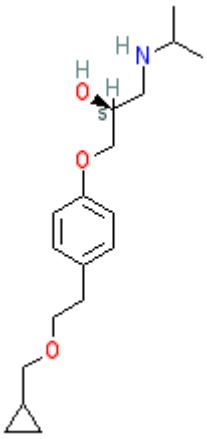
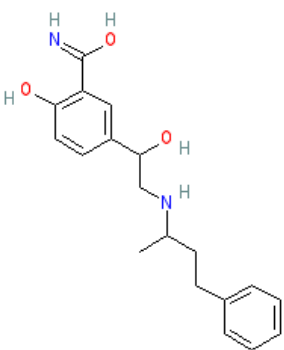
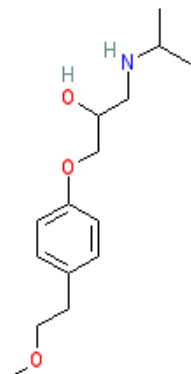
Agonists

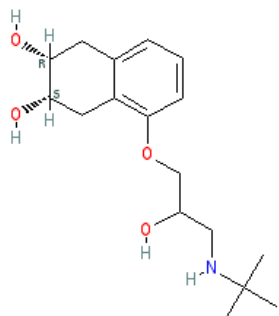
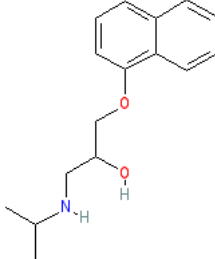
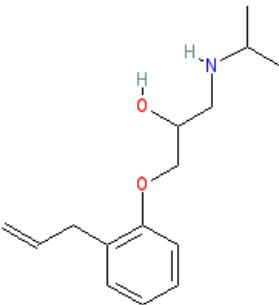
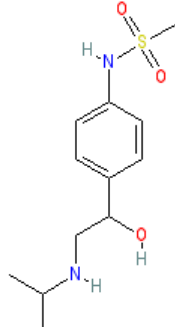
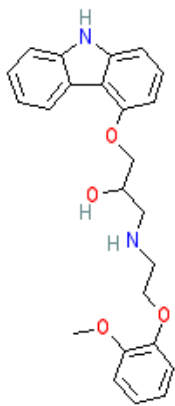
Compound ID	Generic name	Receptor interaction (from IUPHAR)	Structure
C21	orciprenaline	β_2 agonist	
C22	xamoterol	β_1 partial agonist	
C25	dobutamine	β_1 and β_2 partial agonist	
C31	procaterol	β_2 agonist	

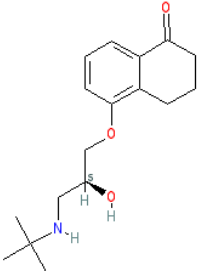
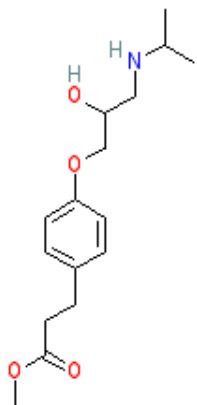
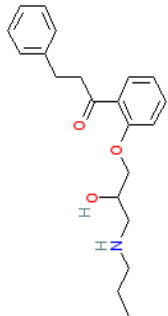
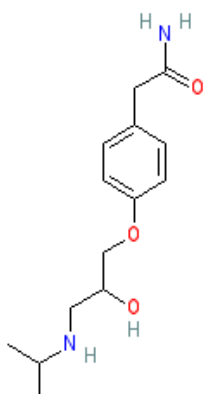
Compound ID	Generic name	Receptor interaction (from IUPHAR)	Structure
C34	fenoterol	β_2 agonist	
C36	terbutaline	β_2 partial agonist	
C39	mirabegron	β_1 and β_2 agonist	
C40	indacaterol	β_1 and β_2 agonist	
C42	isoprenaline	β_1 and β_2 full agonist	

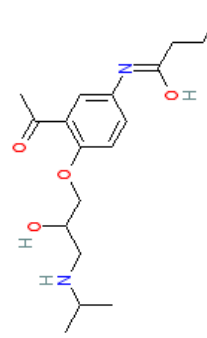
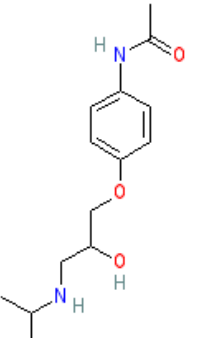
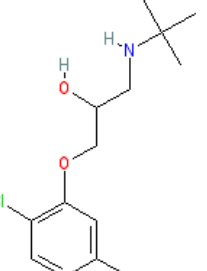
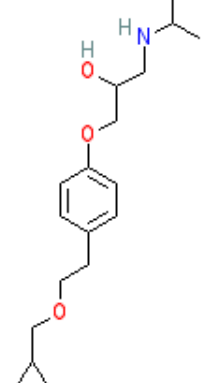
Compound ID	Generic name	Receptor interaction (from IUPHAR)	Structure
C46	pindolol	β_1 and β_2 partial agonist	

Antagonists

C20	levobetaxolol	β_1 and β_2 antagonist	
C23	labetalol	β_1 and β_2 antagonist	
C24	metoprolol	β_1 and β_2 antagonist	

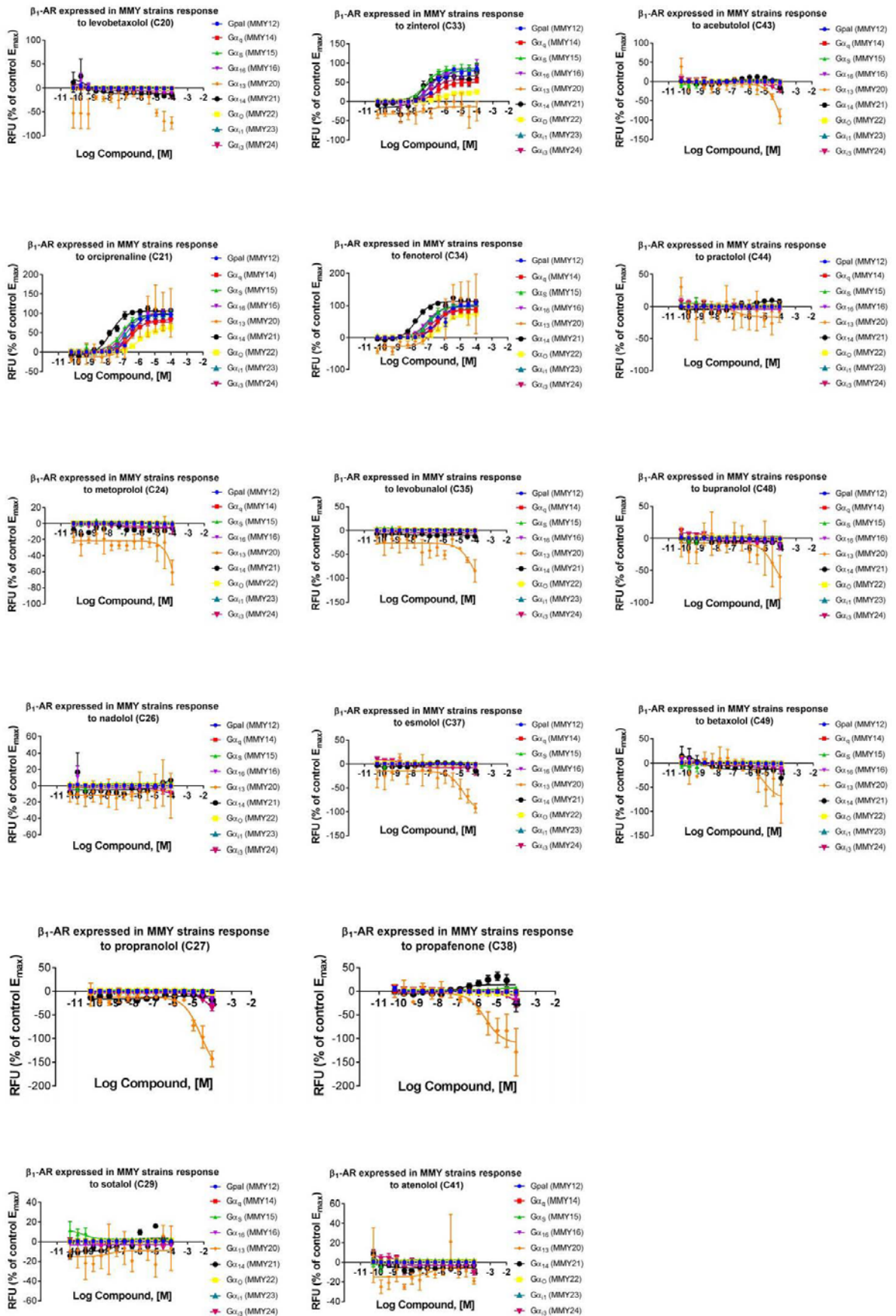
Compound ID	Generic name	Receptor interaction (from IUPHAR)	Structure
C26	nadolol	β_1 and β_2 antagonist	
C27	propranolol	β_1 and β_2 antagonist	
C28	alprenolol	β_2 antagonist	
C29	sotalol	β_1 and β_2 antagonist	
C30	carvedilol	β_1 and β_2 antagonist	

Compound ID	Generic name	Receptor interaction (from IUPHAR)	Structure
C35	levobunolol	β_1 and β_2 antagonist	 <p>The structure of levobunolol features a bicyclic core consisting of a benzene ring fused to a six-membered ring containing a ketone group. This core is linked via an ether oxygen to a chiral carbon atom. This carbon is also bonded to a hydrogen atom and a secondary amine group (N-H) which is substituted with a tert-butyl group. The stereochemistry at the chiral center is indicated with a wedge bond to the hydrogen atom and a dashed bond to the amine group.</p>
C37	esmolol	β_1 antagonist	 <p>The structure of esmolol consists of a central benzene ring. One para-substituted position of the benzene ring is connected to a propyl chain that terminates in a methyl ester group (-COOCH₃). The other para-substituted position is connected to a propyl chain that terminates in an isopropylamino group (-NHCH(CH₃)₂).</p>
C38	propafenone	β_1 and β_2 antagonist	 <p>The structure of propafenone features a central benzene ring. One position is substituted with a propyl chain ending in a secondary amine group (-NHCH₂CH₂CH₃). Another position is substituted with a propyl chain ending in a carbonyl group (-COCH₂CH₂Ph), where Ph represents a phenyl ring. A third position is substituted with an ether linkage (-OCH₂CH₂CH₂CH₂CH₂NHCH₂CH₂CH₃).</p>
C41	atenolol	β_1 and β_2 antagonist	 <p>The structure of atenolol consists of a central benzene ring. One para-substituted position is connected to a propyl chain that terminates in a primary amide group (-NH₂). The other para-substituted position is connected to a propyl chain that terminates in a secondary amine group (-NHCH(CH₃)₂).</p>

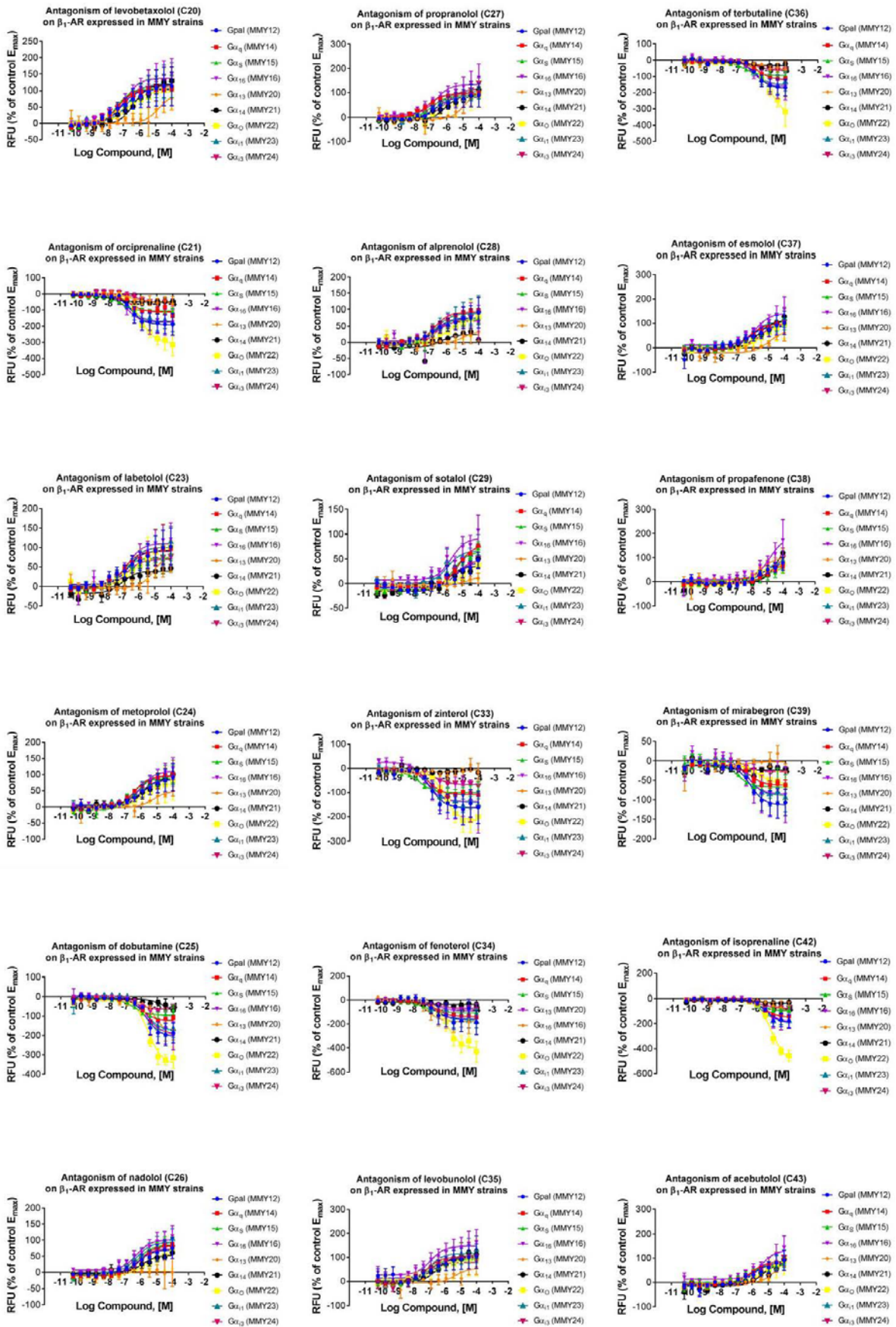
Compound ID	Generic name	Receptor interaction (from IUPHAR)	Structure
C43	acebutolol	β_1 antagonist	
C44	practolol	β_1 antagonist	
C48	bupranolol	β_1 and β_2 antagonist	
C49	betaxolol	β_1 and β_2 antagonist	

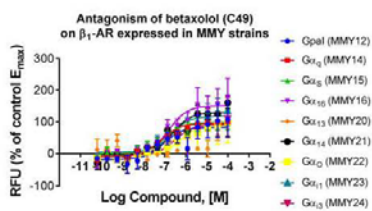
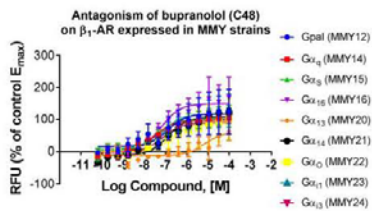
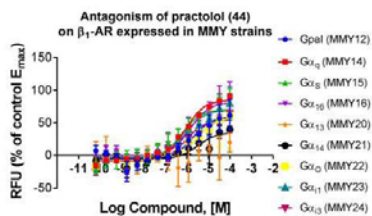
Appendix D – supplementary compound profiling data

β_1 -AR agonist responses in various strains

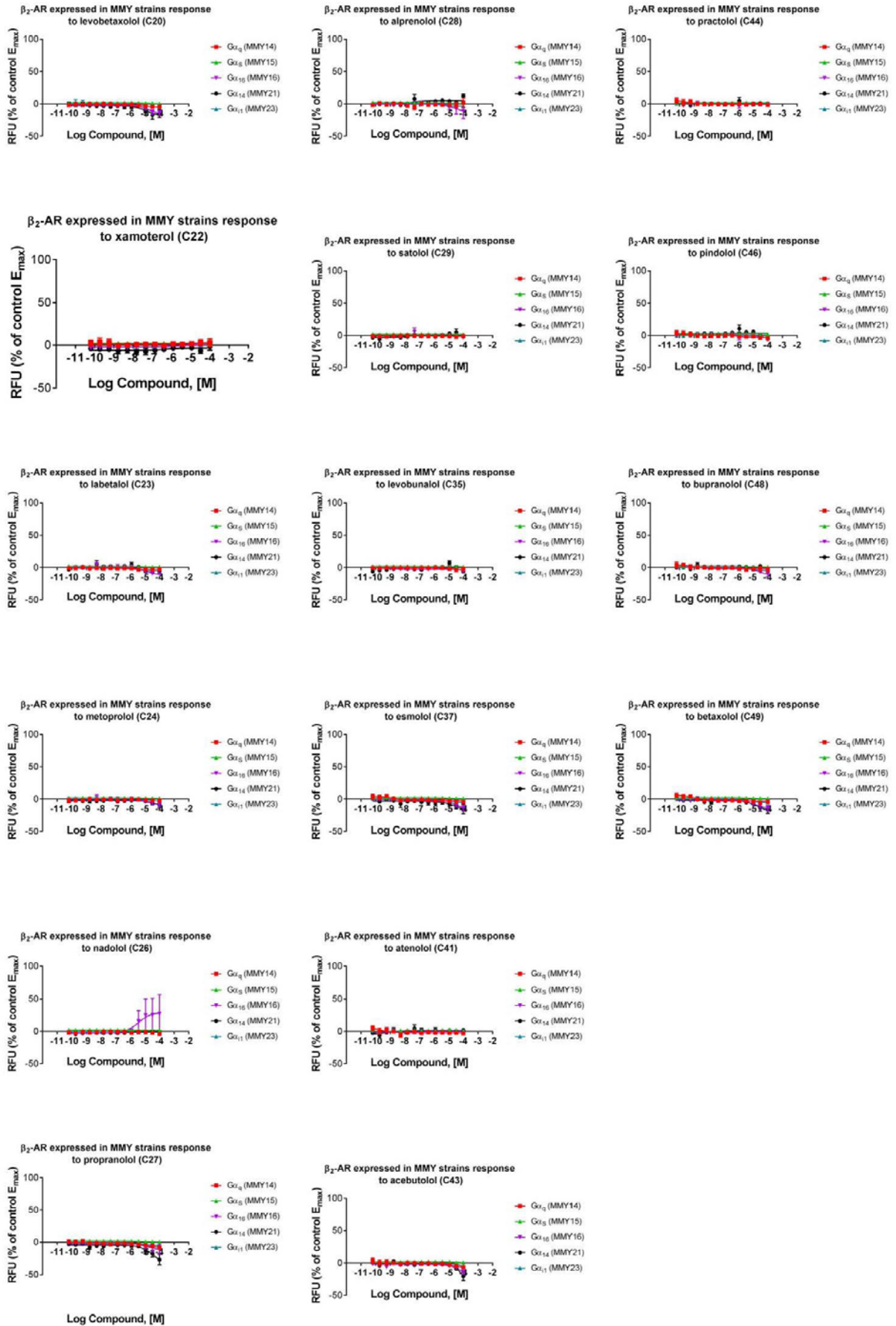


β_1 -AR antagonist responses in various strains

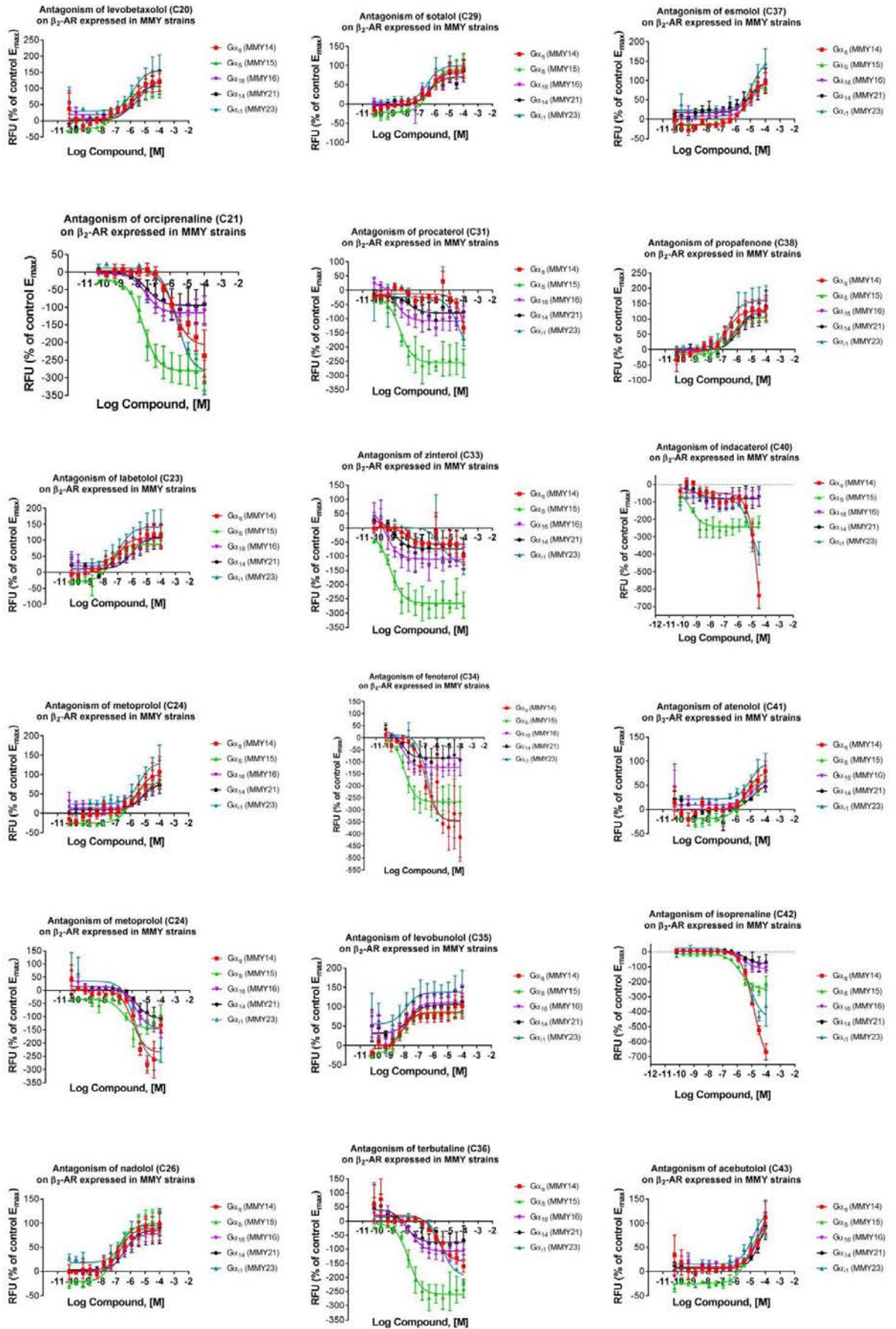


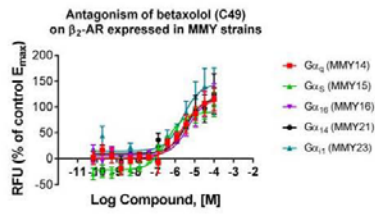
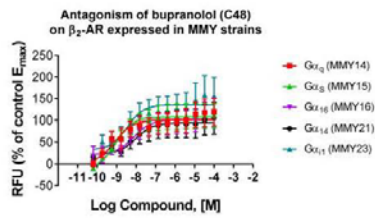
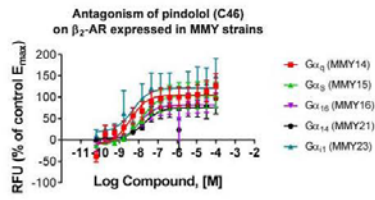
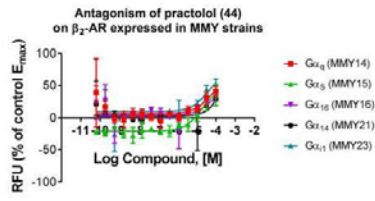


β_2 -AR agonist responses in various strains



β_2 -AR antagonist responses in various strains





Appendix E – Assay correlation data

The pEC₅₀ and pIC₅₀ (marked in red) values used for comparison between the Yeast GαS and CHO assays presented in Figure 5.17 and Table 5.18.

β₁-AR comparison

	Yeast assay in GαS	Agonist cAMP LANCE TR- FRET	DiscoverX EFC cAMP (Cell based)	Human Antagonist - EFC pKi	Antagonist cAMP LANCE TR-FRET
C1	6.0	9.0	8.1		
C2	4.3			5.2	5.1
C3	8.0	8.3			
C4	6.8	6.6	5.3		
C5	5.6	7.1			
C6	3.6	4.5			
C7	8.4	8.3			
C8	6.6				7.4
C9	6.2	6.0			
C10	6.7	6.2	4.1		
C11	5.8				
C12	5.6				4.5
C13	6.8			8.0	7.1
C14	6.6				7.1
C15	4.1				6.9
C16	6.5				4.5
C17	6.0			7.7	
C18					7.6
C19	6.5				
C20	7.4				
C21	7.0	7.1			
C22	7.3	8.2			
C23	7.1				7.6
C24	6.5				
C25	5.7	7.1			
C26	6.2				7.5
C27	6.9				4.5
C28	6.9				6.1
C29	5.5				4.9
C30	7.3				4.5
C31	5.2				5.0
C33	7.3				
C34	7.0		6.2		
C35	7.1				
C36	6.1	5.4	5.4		
C37	6.2				7.9
C38	5.1				6.3
C39	6.4	6.2	6.0		
C40	8.4	8.3			
C41	6.6				
C42	5.7	9.0	8.1		
C43	6.3				
C44	6.2				
C46	7.5		4.2		
C48	7.4				
C49	7.0				

β₂-AR comparison

	Yeast assay in Gαs	Human agonist cAMP HTRF	DiscoverX HitHunter cAMP EFC	Agonist cAMP LANCE TR- FRET	DiscoverX EFC cAMP (Cell based)	Agonism β- arrestin EFC - PathHunter	Human Antagonist - EFC - pKi	Antagonist cAMP LANCE TR-FRET
C1	5.7	9.7	8.8	8.3	7.4	6.8		
C2	6.7			4.5			6.2	5.8
C3	7.8		9.9	9.7				
C4	8.2		9.2	9.6	8.2			
C5	5.3	7.3	6.4	6.6		4.3		
C6	4.5		6.4	4.5				
C7	8.4	11.4	9.3	9.1		8.1		
C8	7							8
C9	7.4	9	7.1	7.3		6.9		
C10	5.7		6.3	5.2	4.8			
C11	6						6.1	6
C12	5.9							7.3
C13	7.3							8.5
C14	7.8							8.3
C15	4.2							5.2
C16	6							6.2
C17	7.3						9.2	8.6
C18	3.9							5.5
C19	7.7							9
C20	6.8							
C21	7.1	6.2	7.1	6.2		5.2		
C22							6.1	5.3
C23	7.5							7.1
C24	6							6.2
C25	5.5	7.3	6.4	6.6		4.3		
C26	7						8.5	
C27	8.7						9.1	8.6
C28	7.4						9.6	
C29	6.4						6.6	
C30	7.7							9
C31	7.7							
C33	8.6							
C34	8.2	7.8			7.2	6.4		
C35	8.2							9
C36	7.3	8.4		6.9	6.5	5.7		4.5
C37	5.4							4.6
C38	6.4							6.3
C39				6.2			5.5	5.3
C40	8.9	11.4	9.3	9.1		8.1		4.5
C41	5.5						5.1	5.1
C42	5.5	9.7	8.8	8.3	7.4	6.8		4.5
C43	5.2							5
C44								
C46	7.9		7.1				9	8.6
C48	9							
C49	6.4							6

Appendix F – Publications arising from this thesis